frontiers | Research Topics

Predictors for the aggressiveness of papillary thyroid carcinoma

Edited by
Yong Jiang, Emese Mezosi, An-Chen Qin and Eleonora Lori

Published in
Frontiers in Endocrinology

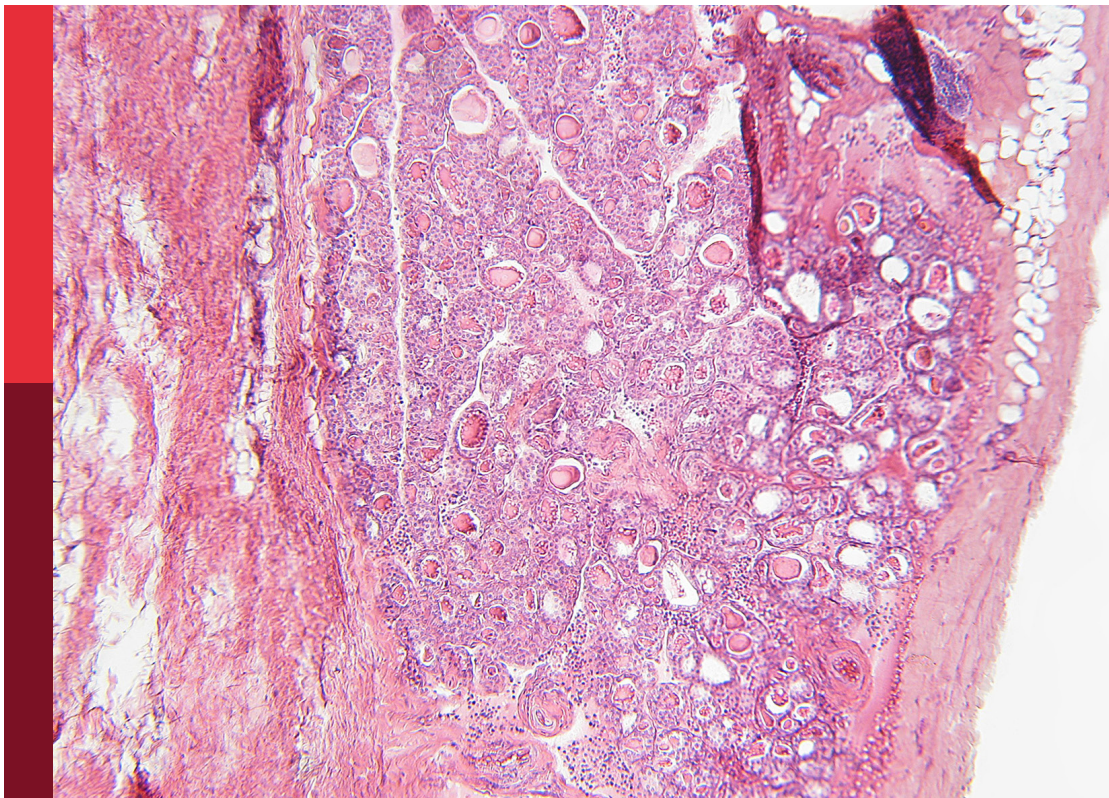

ISSN 1664-8714
ISBN 978-2-8325-4394-8
DOI 10.3389/978-2-8325-4394-8

About Frontiers

Frontiers is more than just an open access publisher of scholarly articles: it is a pioneering approach to the world of academia, radically improving the way scholarly research is managed. The grand vision of Frontiers is a world where all people have an equal opportunity to seek, share and generate knowledge. Frontiers provides immediate and permanent online open access to all its publications, but this alone is not enough to realize our grand goals.

Frontiers journal series

The Frontiers journal series is a multi-tier and interdisciplinary set of open-access, online journals, promising a paradigm shift from the current review, selection and dissemination processes in academic publishing. All Frontiers journals are driven by researchers for researchers; therefore, they constitute a service to the scholarly community. At the same time, the *Frontiers journal series* operates on a revolutionary invention, the tiered publishing system, initially addressing specific communities of scholars, and gradually climbing up to broader public understanding, thus serving the interests of the lay society, too.

Dedication to quality

Each Frontiers article is a landmark of the highest quality, thanks to genuinely collaborative interactions between authors and review editors, who include some of the world's best academicians. Research must be certified by peers before entering a stream of knowledge that may eventually reach the public - and shape society; therefore, Frontiers only applies the most rigorous and unbiased reviews. Frontiers revolutionizes research publishing by freely delivering the most outstanding research, evaluated with no bias from both the academic and social point of view. By applying the most advanced information technologies, Frontiers is catapulting scholarly publishing into a new generation.

What are Frontiers Research Topics?

Frontiers Research Topics are very popular trademarks of the *Frontiers journals series*: they are collections of at least ten articles, all centered on a particular subject. With their unique mix of varied contributions from Original Research to Review Articles, Frontiers Research Topics unify the most influential researchers, the latest key findings and historical advances in a hot research area.

Find out more on how to host your own Frontiers Research Topic or contribute to one as an author by contacting the Frontiers editorial office: frontiersin.org/about/contact

Predictors for the aggressiveness of papillary thyroid carcinoma

Topic editors

Yong Jiang — First People's Hospital of Changzhou, China

Emese Mezosi — University of Pécs, Hungary

An-Chen Qin — Affiliated Suzhou Hospital of Nanjing Medical University, China

Eleonora Lori — Sapienza University of Rome, Italy

Citation

Jiang, Y., Mezosi, E., Qin, A.-C., Lori, E., eds. (2024). *Predictors for the aggressiveness of papillary thyroid carcinoma*. Lausanne: Frontiers Media SA. doi: 10.3389/978-2-8325-4394-8

Table of contents

05 Editorial: Predictors for aggressiveness of papillary thyroid carcinoma
Emese Mezosi

07 LASSO-based machine learning models for the prediction of central lymph node metastasis in clinically negative patients with papillary thyroid carcinoma
Jia-Wei Feng, Jing Ye, Gao-Feng Qi, Li-Zhao Hong, Fei Wang, Sheng-Yong Liu and Yong Jiang

18 Relationship between serum NDRG3 and papillary thyroid carcinoma
Jiahao Wang, Jun Wang, Jinxing Quan, Juxiang Liu, Limin Tian and Changhong Dong

27 Central and lateral neck involvement in papillary thyroid carcinoma patients with or without thyroid capsular invasion: A multi-center analysis
Zheyu Yang, Yu Heng, Jian Zhou, Lei Tao and Wei Cai

40 Prelaryngeal and/or pretracheal lymph node metastasis could help to identify papillary thyroid carcinoma with intermediate risk from unilateral lobe cT1-2N0 papillary thyroid carcinoma
Bin Wang, Chun-Rong Zhu, Yuan Fei, Hong Liu, Xin-Min Yao and Jian Wu

51 Causal inference between aggressive extrathyroidal extension and survival in papillary thyroid cancer: a propensity score matching and weighting analysis
Ming Xu, Zihan Xi, Qiuyang Zhao, Wen Yang, Jie Tan, Pengfei Yi, Jun Zhou and Tao Huang

62 Nomogram prediction for cervical lymph node metastasis in multifocal papillary thyroid microcarcinoma
Wen-Hui Li, Wei-Ying Yu, Jia-Rui Du, Deng-Ke Teng, Yuan-Qiang Lin, Guo-Qing Sui and Hui Wang

72 Development and validation of a dynamic nomogram based on conventional ultrasound and contrast-enhanced ultrasound for stratifying the risk of central lymph node metastasis in papillary thyroid carcinoma preoperatively
Qiyang Chen, Yujiang Liu, Jinping Liu, Yuan Su, Linxue Qian and Xiangdong Hu

83 Multimodal predictive factors of metastasis in lymph nodes posterior to the right recurrent laryngeal nerve in papillary thyroid carcinoma
Yi Gong, Zhongkun Zuo, Kui Tang, Yan Xu, Rongsen Zhang, Qiang Peng and Chengcheng Niu

93 Assessing the role of central lymph node ratio in predicting recurrence in N1a low-to-intermediate risk papillary thyroid carcinoma
Teng Ma, Jian Cui, Peng Shi, Mei Liang, Wenxiao Song, Xueyan Zhang, Lulu Wang and Yafei Shi

103 A novel nomogram for identifying high-risk patients among active surveillance candidates with papillary thyroid microcarcinoma
Li Zhang, Peisong Wang, Kaixuan Li and Shuai Xue

frontiers | Frontiers in Endocrinology

TYPE Editorial
PUBLISHED 18 January 2024
DOI 10.3389/fendo.2024.1363836

OPEN ACCESS

EDITED AND REVIEWED BY
Claire Perks,
University of Bristol, United Kingdom

*CORRESPONDENCE
Emese Mezosi
mezosi.emese@pte.hu

RECEIVED 31 December 2023
ACCEPTED 05 January 2024
PUBLISHED 18 January 2024

CITATION
Mezosi E (2024) Editorial: Predictors for aggressiveness of papillary thyroid carcinoma. *Front. Endocrinol.* 15:1363836. doi: 10.3389/fendo.2024.1363836

Editorial: Predictors for aggressiveness of papillary thyroid carcinoma

Emese Mezosi*

I[st] Department of Internal Medicine, Clinical Center, University Medical School of Pecs, Pecs, Hungary

KEYWORDS

papillary thyroid cancer (PTC), aggressiveness, lymph node metastasis, predictive model, extrathyroidal extension (ETE)

Editorial on the Research Topic
Predictors for the aggressiveness of papillary thyroid carcinoma

Papillary thyroid cancer is the most common endocrine malignancy with a good prognosis in most cases. The increasing incidence of papillary thyroid cancer worldwide underlies the importance of early selection of those patients who have aggressive tumors and require more extended surgery and/or postoperative therapy. The preoperative risk stratification is not optimal due to the limitations of imaging methods and lack of information about the histological parameters and molecular background. The establishment of effective predictive models may help the decision-making in individual cases.

Feng et al. developed machine-learning models for predicting occult central lymph node metastasis (CLNM) based on clinicopathological and sonographic characteristics. The nine top-rank variables were tumor size, margin, extrathyroidal extension, gender, echogenic foci, shape, number, lateral lymph node metastasis, and chronic lymphocytic thyroiditis. Comparing eight machine learning models for the prediction of CLNM, the best performance was achieved by the Random Forest model. Prophylactic central lymph node dissection is recommended in high-risk patients.

Another paper in this Research Topic also dealt with the preoperative prediction of CLNM. They have combined conventional and contrast-enhanced ultrasound and developed and validated a web-based dynamic nomogram to stratify high-risk and low-risk groups which may help to refine surgical approach (Chen et al.).

Li et al. proposed a similar study to predict the risk of cervical lymph node metastasis in multifocal papillary microcarcinomas. Age, gender, the size of the tumor, and ultrasound characteristics were used to create a model that demonstrated a significant clinical benefit.

Zhang et al. further investigated the possible selection of high-risk patients with papillary microcarcinomas in a large dataset. Active surveillance has been accepted in a subgroup of PTMC (1). In their nomogram model, male sex younger age, larger tumor diameter, bilaterality, and multifocality were independent predictors of the high-risk group where surgery is recommended.

According to the current guideline, prophylactic central neck dissection is not routinely recommended for small (T1 or T2), noninvasive, cN0 PTC (1), however, the rate of CLNM was 36.4%~64.7% in clinically node-negative PTC. The decision about the type of surgery may be challenging in this group of patients. Wang et al. conducted a large retrospective

study to identify intermediate-risk patients with more than 5 metastatic central lymph nodes in T1-2 N0 PTC. They have found that if more than two metastatic prelaryngeal and/or pretracheal lymph nodes occurred, 71.2% of patients belonged to the intermediate-risk group where total thyroidectomy and ipsilateral CLN dissection should be performed.

Metastasis in lymph nodes posterior to the right recurrent laryngeal nerve (LN-prRLN) is a crucial component of the CLNMs, however, surgical removal is difficult, the complication rate is high, and the preoperative assessment is imperfect. The prediction of these CLMNs would be especially helpful for surgeons. Gong et al. investigated the possible prediction of this special localization CLNM in their retrospective study and demonstrated that patients with metastasis in LN-prRLN were younger with larger tumor size, CEUS centripetal perfusion pattern, the presence of CLNM detected by ultrasound and metastasis in LN anterior to the right recurrent laryngeal nerve were independent risk factors; complete CLN dissection is recommended in these cases.

The number of metastatic lymph nodes is influenced by the extent of LN dissection. Lymph node ratio (LNR) means the number of metastatic LNs divided by the total number of removed lymph nodes during surgery. This ratio has been used to estimate prognoses in several solid tumors. Ma et al. investigated the diagnostic efficacy of LNR to predict the risk of recurrence in N1a PTC patients. The optimal LNR cutoff values for structural and biochemical recurrence were 0.75 and 0.80, respectively. The authors recommended the evaluation of lateral neck lymphadenopathy and RAI treatment in those with LNR≥0.75.

The prediction of central and lateral neck lymph node involvement was the topic of a subsequent paper in PTC patients with thyroid capsular invasion (TCI) which includes both microscopic and macroscopic extrathyroidal extension. Patients with TCI were older and had larger tumor sizes, and the presence of bilateral disease and multifocality was more common. Interestingly, Hashimoto thyroiditis was more common in the no-TCI group. The occurrence of CLNM was significantly higher in the TCI than in the no-TCI group (77.1% vs. 34.2%). The involvement of lateral lymph nodes was evaluated in patients with CLNM and was much higher in patients with TCI, 29.3% vs. 16.4%. Nomogram models were constructed for the prediction of CLNM and LLNM in TCI and no-TCI patients to aid clinical decision-making in the management of PTC patients (Yang et al.).

The extrathyroidal extension (ETE) of the tumor as an important prognostic factor was the subject of investigation in the paper of Xu et al. who retrospectively evaluated an extremely large patient population, more the 100,000 PTC patients from the National Cancer Institute's SEER database. The role of ETE is a controversial issue; based on its limited impact on prognosis, minimal ETE has been removed from the staging system in the eighth edition of the AJCC. ETE was categorized into none, capsule, strap muscles, soft tissue, and other organs. ETE into soft tissues or other organs proved to be a bad prognostic factor for both overall survival and thyroid cancer-specific survival. Invasion into the strap muscles also impaired the overall survival of patients with age ≥55 years or >2 cm tumor size which should be taken into consideration in the treatment plans.

The work of Wang et al. is thematically different from the previous ones, the authors evaluated the diagnostic role of NDRG family member 3 as a serum tumor marker in patients with PTC, nodular goiter, and control subjects. NDRG3 is a downstream regulator of MYC which is a human proto-oncogene, involved in the development and invasion of many tumors, including PTC. The serum level of NDRG3 was lower in PTC patients, especially in patients with lymph node metastases and/or extrathyroidal extension. To evaluate the clinical relevance of these findings needs further investigations.

The 10 articles in this Research Topic contributed to our knowledge regarding prognostic factors in PTC. The more general use of artificial intelligence and machine learning provides a new option to proceed in patient management and implement personalized medicine.

Author contributions

EM: Writing – original draft, Writing – review & editing.

Conflict of interest

The author declares that the research was conducted in the absence of any commercial or financial relationships that could be construed as a potential conflict of interest.

The author(s) declared that they were an editorial board member of Frontiers, at the time of submission. This had no impact on the peer review process and the final decision

Publisher's note

Reference

1. Haugen BR, Alexander EK, Bible KC, Doherty GM, Mandel SJ, Nikiforov YE, et al. 2015 American thyroid association management guidelines for adult patients with thyroid nodules and differentiated thyroid cancer: the american thyroid association guidelines task force on thyroid nodules and differentiated thyroid cancer. *Thyroid* (2016) 26(1):1–133. doi: 10.1089/thy.2015.0020

frontiers | Frontiers in Endocrinology

TYPE Original Research
PUBLISHED 23 November 2022
DOI 10.3389/fendo.2022.1030045

OPEN ACCESS

EDITED BY
Eleonora Lori,
Sapienza University of Rome, Italy

REVIEWED BY
Jian-jun Tang,
Changzhou Wujin People's Hospital, China
Junyi Wu,
Fujian Medical University, China
Rao Sun,
Huazhong University of Science and Technology, China

*CORRESPONDENCE
Yong Jiang
2021569490@qq.com

†These authors have contributed equally to this work

SPECIALTY SECTION
This article was submitted to Cancer Endocrinology, a section of the journal Frontiers in Endocrinology

RECEIVED 28 August 2022
ACCEPTED 07 November 2022
PUBLISHED 23 November 2022

CITATION
Feng J-W, Ye J, Qi G-F, Hong L-Z, Wang F, Liu S-Y and Jiang Y (2022) LASSO-based machine learning models for the prediction of central lymph node metastasis in clinically negative patients with papillary thyroid carcinoma.
Front. Endocrinol. 13:1030045.
doi: 10.3389/fendo.2022.1030045

LASSO-based machine learning models for the prediction of central lymph node metastasis in clinically negative patients with papillary thyroid carcinoma

Jia-Wei Feng†, Jing Ye†, Gao-Feng Qi, Li-Zhao Hong, Fei Wang, Sheng-Yong Liu and Yong Jiang*

The Third Affiliated Hospital of Soochow University, Changzhou First People's Hospital, Changzhou, Jiangsu, China

Background: The presence of central lymph node metastasis (CLNM) is crucial for surgical decision-making in clinical N0 (cN0) papillary thyroid carcinoma (PTC) patients. We aimed to develop and validate machine learning (ML) algorithms-based models for predicting the risk of CLNM in cN0 patients.

Methods: A total of 1099 PTC patients with cN0 central neck from July 2019 to March 2022 at our institution were retrospectively analyzed. All patients were randomly split into the training dataset (70%) and the validation dataset (30%). Eight ML algorithms, including the Logistic Regression, Gradient Boosting Machine, Extreme Gradient Boosting (XGB), Random Forest (RF), Decision Tree, Neural Network, Support Vector Machine and Bayesian Network were used to evaluate the risk of CLNM. The performance of ML models was evaluated by the area under curve (AUC), sensitivity, specificity, and decision curve analysis (DCA).

Results: We firstly used the LASSO Logistic regression method to select the most relevant factors for predicting CLNM. The AUC of XGB was slightly higher than RF (0.907 and 0.902, respectively). According to DCA, RF model significantly outperformed XGB model at most threshold points and was therefore used to develop the predictive model. The diagnostic performance of RF algorithm was dependent on the following nine top-rank variables: size, margin, extrathyroidal extension, sex, echogenic foci, shape, number, lateral lymph node metastasis and chronic lymphocytic thyroiditis.

Conclusion: By incorporating clinicopathological and sonographic characteristics, we developed ML-based models, suggesting that this non-invasive method can be applied to facilitate individualized prediction of occult CLNM in cN0 central neck PTC patients.

KEYWORDS

papillary thyroid carcinoma, central lymph node metastasis, machine learning, prediction model, random forest

Introduction

Thyroid papillary carcinoma (PTC), the most common histological type of thyroid cancer, has been increasing rapidly (1). The incidence of lymph node metastasis (LNM) is high, ranging from 49% to 90% (2, 3). Central compartment is the first area for the metastasis of PTC. This area extends from the inferior border of the hyoid bone to the superior border of the sternum and is bilaterally bounded by the bilateral common carotid arteries. According to previous studies, PTC patients with central lymph node metastasis (CLNM) have an increased risk of regional recurrence (4, 5).

It is still controversial whether clinically negative (cN0) central neck patients should routinely perform preventive central node dissection (CND). Guidelines from China and Japan are more aggressive, and they suggest that prophylactic CND should be routinely performed with appropriate protection of the parathyroid glands and recurrent laryngeal nerve (6, 7). Conversely, for T1 or T2, non-invasive and cN0 PTC patients, the American Thyroid Association (ATA) guidelines do not recommend prophylactic CND (8). Therefore, the status of the central lymph nodes is crucial for the management of PTC patients, especially the decision-making of surgical methods.

Currently, high-resolution ultrasound is still the first choice for preoperative evaluation of cervical lymph nodes in patients with PTC. However, its sensitivity is low, resulting in some false-negative rates. As reported, the diagnostic sensitivity of ultrasound to cervical LNM is only about 20% to 40% (9, 10). Hence, occult LNM has been reported to occur in about 27% to 55% of PTC patients with cN0 neck (11, 12).

Although the risk factors of CLNM have been reported and several prediction models have been established, these results are inconsistent. This is mainly due t
o the complexity of medical data, and there are significant differences in the calculation methods of the model. Therefore, we intend to use a new type of artificial intelligence, namely machine learning (ML), to analyze the connections between important data and make accurate decisions (13–17).

By using clinical and sonographical characteristics associated with CLNM, we aimed to develop models based on eight ML algorithms to predict CLNM in patients with cN0 central neck. And then, by selecting one model that performs best in predicting the risk of CLNM, personal strategies could be proposed to help clinicians to make therapeutic decisions.

Materials and methods

Study population

This retrospective study was approved by the Ethics Committee of Changzhou First People's Hospital, and written informed consent was obtained from all patients. Consecutive patients who underwent initial thyroid surgery at our institution between July 2019 and March 2022 were retrospectively reviewed. Exclusion criteria were as follows: (1) non-PTCs or other subtypes than classic PTC; (2) preoperative ultrasound suspected CLNM; (3) history of prior treatment for head and neck cancer; (4) history of cervical radiation exposure in childhood; (5) family history of thyroid cancer; (6) history with other malignancy; (7) incomplete clinical data; (8) loss to follow-up; (9) patients who underwent non-curative surgery (residual tumor or lymph node detected within 6 months of initial surgery). A total of 1099 patients were enrolled in this study.

Surgical strategy

All patients were treated for thyroid nodules and confirmed as Bethesda Categories V or VI based on ultrasound-guided fine needle aspiration cytology (FNAC). Cervical lymph nodes with the following characteristics were suspected of metastases: hyperechoic changes, roundness or necrosis, loss of the fatty hilum, microcalcification or peripheral vascularity (18). FNAC was performed preoperatively to confirm the histopathological diagnosis of suspicious lateral lymph nodes.

All patients underwent total thyroidectomy or thyroid lobectomy. According to the Chinese guidelines for diagnosis and treatment of differentiated thyroid carcinoma, on the premise of effectively protecting the parathyroid gland and recurrent laryngeal nerve, CND is routinely performed for PTC patients, even in patients with cN0 central neck. Ipsilateral CND is performed for ipsilateral lesion; bilateral CND is performed for isthmus lesion and bilateral lesions. According to the ATA guidelines (8) and Chinese guidelines, lateral neck dissection (LND) is not recommended for patients with cN0 lateral neck. In our institution, LND was performed only in patients with high suspicion of lateral lymph node metastasis (LLNM) based on preoperative imaging data and FNAC.

Clinical characteristics and sonographical features

A total of 17 variables were analyzed in this study. Clinicopathological characteristics included sex, age, body mass index (BMI), diabetes, BRAF V600E mutation, chronic lymphocytic thyroiditis (CLT), maximum tumor size, the number of foci, bilaterality, location, extrathyroidal extension (ETE) detected during surgery, and LLNM. BMI (kg/m^2) was defined as weight (kg) divided by height (m) squared. According to the World Health Organization-BMI standard, enrolled PTC

patients were divided into normal (BMI < 25 kg/m^2), overweight (25 ≤ BMI < 30 kg/m^2), and obese (BMI ≥ 30 kg/m^2) group. The diagnosis of CLT included any of the following: (i) elevated antibodies to thyroid peroxidase level (>50 IU/mL), and/or (ii) findings of diffuse heterogeneity on ultrasound, and/or (iii) diffuse lymphocytic thyroiditis on histopathology (19). ETE detected during surgery was defined as the primary tumor extending through the thyroid capsule to perithyroidal soft tissue such as perithyroidal fat, or involving strap muscles, or extending to surrounding structures such as larynx, trachea, esophagus, recurrent laryngeal nerve, subcutaneous soft tissue, skin, internal jugular vein, or carotid artery (20).

Preoperative sonographical characteristics of each nodule included the following features: nodular composition, echogenicity, echogenic foci (calcification), shape (aspect ratio) and margin (including irregular shape and ETE). ETE detected by ultrasound was defined as a tumor with capsular abutment of more than 25% of its perimeter on ultrasound (21). More than two radiologists with 10 years of experience in thyroid cancer ultrasound diagnosis evaluated the ultrasound images.

Feature selection

The datasets were randomly assigned 70% of datasets to the training set (769 patients) and 30% of datasets to the validation set (330 patients). Feature selection plays an important role in reducing computational complexity and improving classification accuracy. We used the LASSO Logistic regression method to select the best predictive features from the 17 features mentioned above, and finally got the 13 features that were most relevant for predicting CLNM (Figure 1).

Construction, validation, and performance of ML-based models

Eight ML algorithms, including Logistic Regression (LR), Gradient Boosting Machine (GBM), Extreme Gradient Boosting (XGB), Random Forest (RF), Decision Tree (DT), Neural Network (NNET), Support Vector Machine (SVM) and Bayesian Network (BN) were applied in this study (16, 17, 22–24).

By using the same thresholds determined in the training set, we further tested the predictive performance of eight models in the independent validation set. We adopted 10-fold cross-validation method to minimize the adverse effect of overfitting and verify the accuracy of the models. The predictive performance of the above models was assessed by the receiver operating characteristic (ROC) curve and area under the curve (AUC). The closer the AUC was to 1, the better performance of the model. The sensitivity and specificity of the above models were also calculated. Additionally, we employed decision curve analysis (DCA) to assess the clinical utility of the above models s (25).

Statistical analysis

All statistical analysis was performed by using SPSS Version 25.0 software (Chicago, IL, USA), and R software Version 3.5.3 (The R Foundation for Statistical Computing). Pearson Chi-square test or Fisher's exact test was used for categorical data. Normally distributed quantitative parameters were compared by Student's t-test, while non- normally distributed parameters were compared by the Mann-Whitney U test. A P value < 0.05

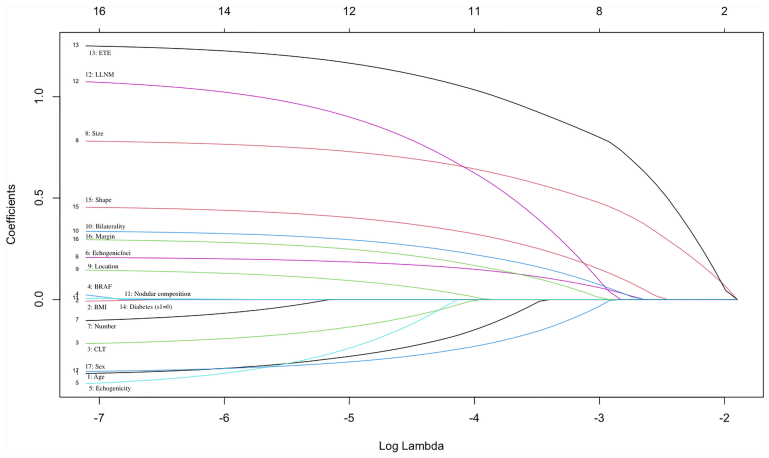

FIGURE 1
Selection of significant parameters in clinicopathologic variables in the training set. The values of the coefficients and the corresponding lambda values, each curve represents each feature in the model.

was considered statistically significant. R software (Version 3.5.3) was used to develop ML-based models and DCA.

Results

Demographics and sonographic features of PTC patients

Table 1 shows the clinical and sonographic characteristics of the PTC patients in the training set, validation set, CLNM-positive and CLNM-negative group in the training set. The 1099 patients were divided into two groups randomly: approximately 769 (70%) cases were conducted as the training set, and the remaining around 330 (30%) cases were used as the validation set. There were no significant differences in clinicopathological and sonographic features between the training set and the validation set (P >0.05 for all comparisons), justifying their use as training and validation cohorts.

In the training set, CLNM were observed in 389 (50.6%) cases. A significant difference was found in gender between CLNM-positive and CLNM-negative patients; 38.8% of males and 61.2% of females were CLNM-positive patients (P<0.001). Sonographic features, such as shape, margin and echogenic foci were all associated with CLNM. Moreover, CLNM presented the significant association with tumor size, the number of foci, bilaterality, location, ETE detected during surgery and LLNM (all P<0.05).

Feature selection

We used the LASSO Logistic regression method to further select the optimal predictive features from the above characteristics. The optimal set of features that were most relevant to the prediction of CLNM included the following 13 features: sex, age, CLT, echogenicity, echogenic foci, shape, margin, size, location, bilaterality, number, ETE detected during surgery, LLNM (Figure 1).

Predictive performance of ML-based models

Figure 2 and Table 2 show the predictive performance of ML-based models. In the training set, the AUCs of LR, GBM, XGB, RF, DT, NNET, SVM and BN were 0.744, 0.878, 0.907, 0.902, 0.692, 0.889, 0.771 and 0.781, respectively (Figure 2A). In the validation set, the AUCs of LR, GBM, XGB, RF, DT, NNET, SVM and BN were 0.693, 0.858, 0.849, 0.843, 0.652, 0.811, 0.750 and 0.777, respectively (Figure 2B). In the training cohort, the XGB model performed the best, followed by RF, NNET, and GBM. However, the sensitivity and specificity of RF were higher than that of XGB. All ML-based models except DT (AUC=0.777) and SVM (AUC=0.824) were better than the conventional method, LR (AUC=0.837). Apart from the DT, All ML-based models were better than the conventional method (LR).

Moreover, the mixed Lift curves of the eight ML models were applied in the training and validation set (Figure 3). Different from the ROC curve, the Lift curve takes into account the accuracy of the classifier: the ratio of the number of positive classes obtained with the classifier to the number of positive classes obtained randomly without the classifier. XGB achieves the best diagnostic performance among the current mix Lift curves, followed by RF, NNET and GBM.

Clinical usefulness of ML-based models

DCA was further used to evaluate the clinical values of these models (Figures 4). The solid black line (None line) represents the net benefit is zero when none of patients receive CND, assuming that all patients have no positive nodes in the central compartment. On the contrary, the solid grey line (All line) represents the net benefits at the time when all patients have CLNM and receive CND. Most of these models presented better net benefits than two control models that were represented by solid black and solid grey lines. Four models (RF, XGB, NNET, and GBM) performed significantly better than the others at most of threshold points. In the training cohort, RF performed significantly better than the others at most of threshold points, followed by XGB (Figures 4A). In the validation cohort, GBM performed the best at the threshold range of 0.2 to 0.4, but sharply decreased at the threshold range of 0.4 to 0.7. RF performed the best at the threshold range of 0.4 to 0.7, but sharply decreased at the threshold range of 0.8 to 0.9 (Figures 4B).

Relative importance of variables in ML-based models

Considering favorable AUCs and clinical benefits based on the DCA, we selected XGB, RF, NNET, and GBM as the models with the most potential for predicting CLNM in cN0 PTC patients. By the feature selection approach, we ranked 13 variables based on their predictive importance in each potential model. The ranks of each variable in different models were described in Figure 5. Size, margin and sex were considered as the relatively important variables for predicting CLNM in the vast majority of models.

The AUCs of RF and XGB reached the highest when 9 variables were introduced (Figure 6). As for GBM and NNET reached the highest when 11 and 10 variables were introduced (Figure 6).

10.3389/fendo.2022.1030045

TABLE 1 Clinical and ultrasonic characteristics of the PTC patients.

Characteristics	Training set				Validation set (n = 330)	*P* value*
	Total (n = 769)	CLNM+(n = 389)	CLNM−(n = 380)	*P* value		
Sex						
Male	246 (32.0%)	151 (38.8%)	95 (25.0%)		100 (30.3%)	
Female	523 (68.0%)	238 (61.2%)	285 (75.0%)	<0.001	230 (69.7%)	0.581
Age (Y)						
≥55	142 (18.5%)	62 (15.9%)	80 (21.1%)		64 (19.4%)	
<55	627 (81.5%)	327 (84.1%)	300 (78.9%)	0.068	266 (80.6%)	0.718
BMI (kg/m^2)						
Normal	32 (4.2%)	21 (5.4%)	11 (2.9%)		12 (3.6%)	
Overweight	467 (60.7%)	225 (57.8%)	242 (63.7%)		207 (62.7%)	
Obesity	270 (35.1%)	143 (36.8%)	127 (33.4%)	0.101	111 (33.6%)	0.797
Diabetes						
Absence	677 (88.0%)	349 (89.7%)	328 (86.3%)		288 (87.3%)	
Presence	92 (12.0%)	40 (10.3%)	52 (13.7%)	0.146	42 (12.7%)	0.723
BRAF V600E mutation						
Negative	85 (11.1%)	43 (11.1%)	42 (11.1%)		41 (12.4%)	
Positive	684 (88.9%)	346 (88.9%)	338 (88.9%)	1.000	289 (87.6%)	0.513
CLT						
Presence	234 (30.4%)	112 (28.8%)	122 (32.1%)		118 (35.8%)	
Absence	535 (69.6%)	277 (71.2%)	258 (67.9%)	0.318	212 (64.2%)	0.083
Maximum tumor size (cm)						
≤1	470 (61.1%)	176 (45.2%)	294 (77.4%)		208 (63.0%)	
>1 to ≤2	201 (26.1%)	141 (36.2%)	60 (15.8%)		87 (26.4%)	
>2 to ≤4	80 (10.4%)	58 (14.9%)	22 (5.8%)		28 (8.5%)	
>4	18 (2.3%)	14 (3.6%)	4 (1.1%)	<0.001	7 (2.1%)	0.788
The number of foci						
1	513 (66.7%)	226 (58.1%)	287 (75.5%)		230 (69.7%)	
2	188 (24.4%)	123 (31.6%)	65 (17.1%)		72 (21.8%)	
3 or more	68 (8.8%)	40 (10.3%)	28 (7.4%)	<0.001	28 (8.5%)	0.603
Bilaterality						
Absence	607 (78.9%)	282 (72.5%)	325 (85.5%)		270 (81.8%)	
Presence	162 (21.1%)	107 (27.5%)	55 (14.5%)	<0.001	60 (18.2%)	0.275
Location						
Middle/Lower	516 (67.1%)	311 (79.9%)	205 (53.9%)		235 (71.2%)	
Upper	253 (32.9%)	78 (20.1%)	175 (46.1%)	<0.001	95 (28.8%)	0.179
Nodular composition						
Mixed cystic and solid	7 (0.9%)	4 (1.0%)	3 (0.8%)		5 (1.5%)	
Solid	762 (99.1%)	385 (99.0%)	377 (99.2%)	0.727	325 (98.5%)	0.376
Echogenicity						
Hyperechoic or isoechoic	25 (3.3%)	16 (4.1%)	9 (2.4%)		12 (3.6%)	
Hyperechoic	731 (95.1%)	365 (93.8%)	366 (96.3%)		317 (96.1%)	
Very hypoechoic	13 (1.7%)	8 (2.1%)	5 (1.3%)	0.280	1 (0.3%)	0.164
Shape						
A/T ≤1	273 (35.5%)	108 (27.8%)	165 (43.4%)		128 (38.8%)	
A/T >1	496 (64.5%)	281 (72.2%)	215 (56.6%)	<0.001	202 (61.2%)	0.299
Margin						
Smooth	487 (63.3%)	222 (57.1%)	265 (69.7%)		210 (63.6%)	
Lobulated or irregular	178 (23.1%)	97 (24.9%)	81 (21.3%)		80 (24.2%)	

(Continued)

TABLE 1 Continued

Characteristics	Training set				Validation set (n = 330)	*P* value*
	Total (n = 769)	CLNM+(n = 389)	CLNM−(n = 380)	*P* value		
ETE	104 (13.5%)	70 (18.0%)	34 (8.9%)	<0.001	40 (12.1%)	0.791
Echogenic foci						
None/large comet-tail artifacts	234 (30.4%)	87 (22.4%)	147 (38.7%)		104 (31.5%)	
Macrocalcifications	43 (5.6%)	24 (6.2%)	19 (5.0%)		19 (5.8%)	
Peripheral calcifications	7 (0.9%)	5 (1.3%)	2 (0.5%)		2 (0.6%)	
Punctate echogenic foci	485 (63.1%)	273 (70.2%)	212 (55.8%)	<0.001	205 (62.1%)	0.938
ETE detected during surgery						
Absence	628 (81.7%)	275 (70.7%)	353 (92.9%)		284 (86.1%)	
Presence	141 (18.3%)	114 (29.3%)	27 (7.1%)	<0.001	46 (13.9%)	0.075
LLNM						
Absence	703 (91.4%)	337 (86.6%)	366 (96.3%)		306 (92.7%)	
Presence	66 (8.6%)	52 (13.4%)	14 (3.7%)	<0.001	24 (7.3%)	0.468

PTC, papillary thyroid carcinoma; Y, year; BMI, body mass index; CLT, chronic lymphocytic thyroiditis; A/T, aspect ratio (height divided by width on transverse views); ETE, extrathyroidal extension; CLNM, central lymph node metastasis; LLNM, lateral lymph node metastasis.
P value < 0.05 indicates a significant difference between CLNM+ and CLNM− group in the training set.
P value* < 0.05 indicates a significant difference between training and validation sets.

Taking into account the sensitivity, specificity, AUC, Lift curve and DCA of the model, we chose RF as the best predictive model in this study. The nine top-rank variables were identified to construct the best predictive model, including size, margin, ETE, sex, echogenic foci, shape, number, LLNM and CLT.

Discussion

At present, some risk factors related to CLNM have been identified, such as tumor differentiation, gene types, etc (26). However, these risk factors are only available after surgery, and they can not provide important information for the preoperative therapeutic decisions. In addition, due to the air in the trachea and the complex structure of the sternum and clavicle, ultrasound is difficult to detect CLNM accurately (9, 10). Combined with the above considerations, we incorporated some variables that can be obtained before and during the operation to build non-invasive and valuable ML models to predict CLNM.

The advantage of ML algorithms is their ability to automatically learn from input data and identify patterns and trends in these data. At present, several studies have used ML for the differential diagnosis of benign and malignant thyroid nodules (27, 28). In addition, ML has also been used to predict

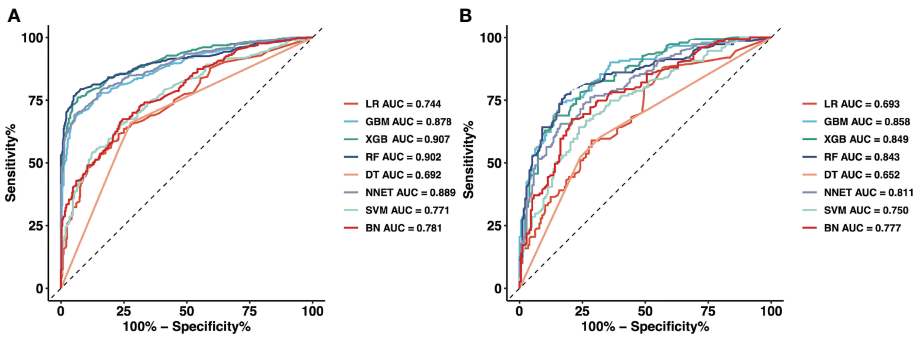

FIGURE 2
The mixed ROC curves of the eight machine learning models for prediction of CLNM. **(A)** The mixed ROC curves in the training cohort; **(B)** The mixed ROC curves in the validation cohort. *ROC*, receiver operating characteristic; *CLNM*, Central lymph node metastasis; *LR*, Logistic Regression; *GBM*, Gradient Boosting Machine; *XGB*, Extreme Gradient Boosting; *RF*, Random Forest; *DT*, Decision Tree; *NNET*, Neural Network; *SVM*, Support Vector Machine; *BN*, Bayesian Network.

TABLE 2 Predictive performance comparison of the eight types of machine learning algorithms in the training and validation dataset.

Methods	Training dataset			Validation dataset		
	AUC	Sensitivity	Specificity	AUC	Sensitivity	Specificity
LR	0.744	0.615	0.771	0.693	0.881	0.433
GBM	0.878	0.692	0.937	0.858	0.742	0.837
XGB	0.907	0.762	0.934	0.849	0.682	0.865
RF	0.902	0.767	0.950	0.843	0.795	0.798
DT	0.692	0.659	0.724	0.652	0.603	0.680
NNET	0.889	0.692	0.945	0.811	0.656	0.837
SVM	0.771	0.541	0.876	0.750	0.642	0.764
BN	0.781	0.674	0.755	0.777	0.675	0.792

AUC, the area under the curve; LR, logistic regression; GBM, gradient boosting machine; XGB, extreme gradient boosting; RF, random forest; DT, decision tree; NNET, neural network; SVM, support vector machine; BN, Bayesian network.

LNM in some other malignant tumors, such as breast cancer and osteosarcoma, etc (29, 30). However, there is little research on the application of ML model predicting LNM in PTC patients. Lee et al. (31) applied clinical records for 804 consecutive patients to develop a computer-aided diagnosis system to identify and differentiate metastatic lymph nodes in thyroid cancer. However, the specificity of the model is relatively low, and the screening results should also be verified by experienced physicians. In addition, they used only one ML model and did not compare the performance of multiple ML models in distinguishing metastatic lymph nodes in patients with thyroid cancer. The predictive performance of different machine learning algorithms is different. We adopted the eight most important ML algorithms to construct the CLNM prediction model, and selected an optimal prediction model from these to ensure the effectiveness.

We first used the LASSO Logistic regression method to exclude four variables (BMI, nodular composition, BRAF V600E mutation and diabetes) that would affect the fitting. And then, modeling the training set of 769 cases of data showed that four excellent models (XGB, RF, NNET, and GBM) performed better in both the ROC analysis and mix Lift curves. The AUC of XGB was slightly higher than RF. However, the RF model performed significantly better than the XGB model at most of threshold points according to DCA. Therefore, we choose RF as the best predictive model in this study to distinguish CLNM from non-CLNM. The structure of RF is simple. It is operated by constructing a large number of decision trees and outputting classes as a single tree (classification) or average prediction (regression) model. Compared with similar methods, RF is more efficient. From a computational point of view, RF has the advantage of handling both regression and

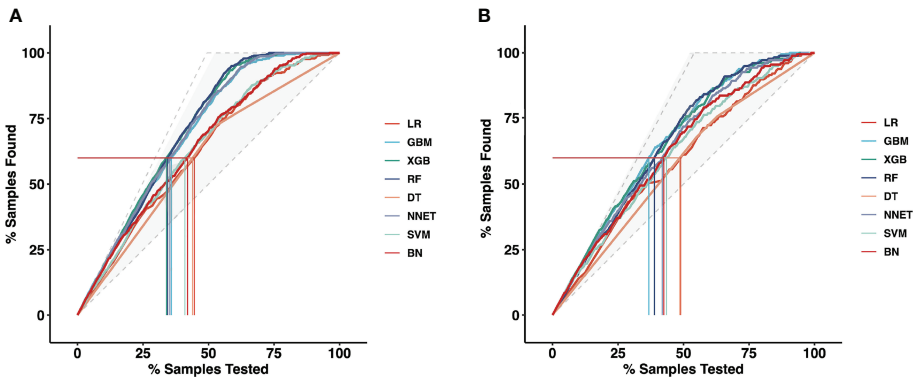

FIGURE 3
The mixed Lift curves of the eight machine learning models for prediction of CLNM. The drawing process of the Lift curve is similar to the ROC curve, the difference is that the Lift value and the robust plane pose change in opposite directions, forming the opposite form of the Lift curve and the ROC curve. **(A)** The mixed Lift curves in the training cohort; **(B)** The mixed Lift curves in the validation cohort. *CLNM*, Central lymph node metastasis; *ROC*, receiver operating characteristic; *LR*, Logistic Regression; *GBM*, Gradient Boosting Machine; *XGB*, Extreme Gradient Boosting; *RF*, Random Forest; *DT*, Decision Tree; *NNET*, Neural Network; *SVM*, Support Vector Machine; *BN*, Bayesian Network.

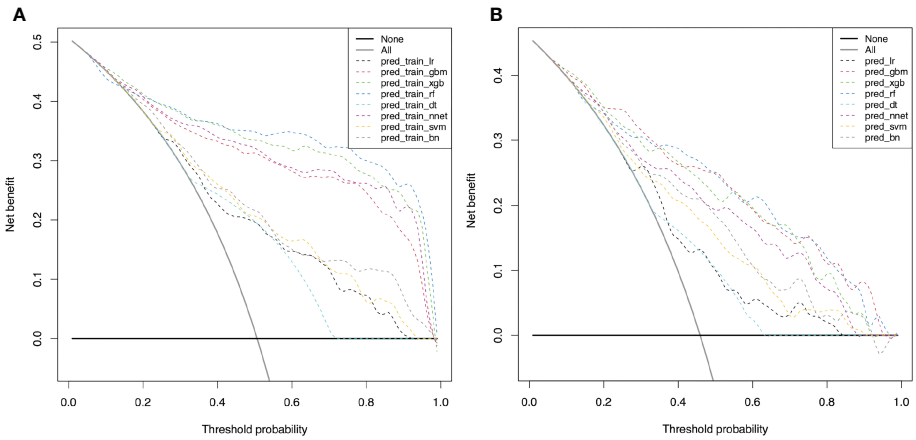

FIGURE 4
Decision curve for predictive models based on machine learning models for prediction of CLNM. **(A)** The decision curve in the training cohort; **(B)** The decision curve in the validation cohort. *CLNM*, Central lymph node metastasis; *LR*, Logistic Regression; *GBM*, Gradient Boosting Machine; *XGB*, Extreme Gradient Boosting; *RF*, Random Forest; *DT*, Decision Tree; *NNET*, Neural Network; *SVM*, Support Vector Machine; *BN*, Bayesian Network.

classification problems. High dimensional problems can also be directly handled through RF (32). From a statistical point of view, RF has the following characteristics, that is, the priority of characteristics, different weight coefficients fall into different categories, and illustration and unsupervised learning ability (33). According to previous meta-analysis of metastatic lymph node studies, computed tomography (CT) demonstrated a pooled sensitivity of 57% and a specificity of 85% in detecting

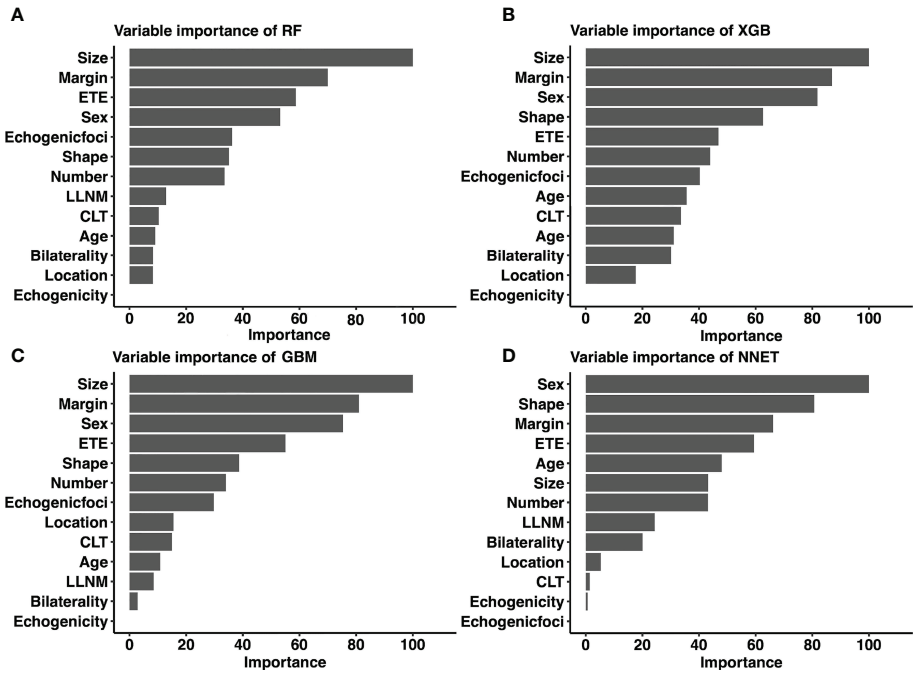

FIGURE 5
Relative importance ranking of each input variable for prediction of CLNM in the machine learning models. **(A)** RF model; **(B)** XGB model; **(C)** GBM model; **(D)** NNET model. *CLNM*, Central lymph node metastasis; *ETE*, extrathyroidal extension; *LLNM*, lateral lymph node metastasis; *CLT*, chronic lymphocytic thyroiditis; *RF*, Random Forest; *XGB*, Extreme Gradient Boosting; *GBM*, Gradient Boosting Machine; *NNET*, Neural Network.

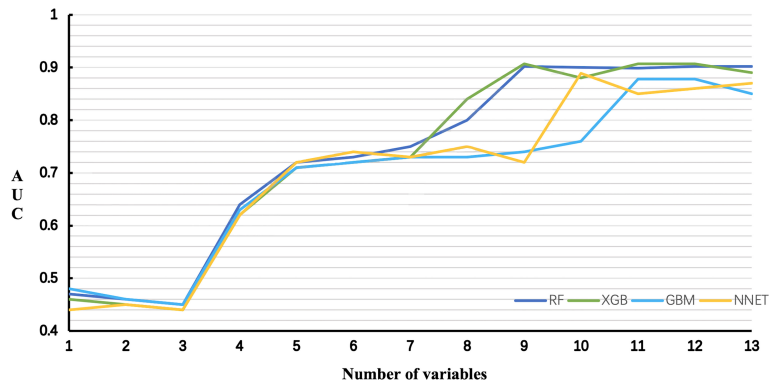

FIGURE 6
Predictive performance of the RF, XGB, GBM, NNET models with different numbers of variables. *RF*, Random Forest; *XGB*, Extreme Gradient Boosting; *GBM*, Gradient Boosting Machine; *NNET*, Neural Network.

CLNM, and ultrasound demonstrated a pooled sensitivity of 38% and a specificity of 91%. Combined CT/ultrasound demonstrated a pooled sensitivity of 69% and a specificity of 81% (34). When we compared the diagnostic performance of the RF model with that in the meta-analysis, our RF model achieved better sensitivity (0.767) and specificity (0.950).

The connection between variables and results in most ML-based models is invisible. By using classifier-specific estimators, we got the predictive importance of variables in each model (Figure 5). Therefore, the nine top-rank variables were identified to be the most important risk factors for CLNM in the RF model: size, margin, ETE, sex, echogenic foci, shape, number, LLNM and CLT. It is important to note that size was the largest contributor to scores in most models (including RF, XGB and GBM), which was consistent with other reports (35). Tumor size is widely used in several staging systems, including the American Joint Committee on Cancer staging system. And larger tumor size was associated with more aggressive features in PTC (35). Based on the combined RF model incorporating clinicopathological and sonographic features, for patients with several risk factors of CLNM, prophylactic CND is strongly recommended to reduce recurrence rates. In addition, it is recommended that experienced surgeons perform detailed operations on these high-risk patients, during which carbon nanoparticles suspension injection can be used to prevent miss of small metastatic lymph nodes. Otherwise, prophylactic CND should be avoided to reduce complications of parathyroid glands and recurrent laryngeal nerve. In addition, for high-risk patients who did not undergo CND, these patients should be followed up more closely after surgery to increase vigilance against occult CLNM.

The strength of this research lies in the innovation of technology and method. Although CLNM is predicted by filtering the best model from eight ML methods, there are also limitations. The first is to retrospectively study the inherent limitations in the design. This study is a single-center retrospective study, our results may be biased and lack generalizability and robustness assessments. Second, the patients who participated in our study were the local population of China, most of whom were women. Residual confounding variables of unmeasurable factors such as race and region cannot be ruled out. Prospective multi-center clinical trials need to be carried out in subsequent studies to obtain more objective conclusions. Third, the criteria used to evaluate ultrasound characteristics were subjective. Nevertheless, the consistency between the observers of each feature in this study was very good. Last, most of algorithms are invisible to users. In the future study, by using the web-based calculator which established based on our prediction model, we can apply our findings to other population.

In conclusion, by incorporating clinicopathological and sonographic characteristics, we developed ML-based models, suggesting that this non-invasive method can be applied to facilitate individualized prediction of occult CLNM in cN0 central neck PTC patients. The status of lymph nodes is evaluated through the RF model, and it is recommended to perform prophylactic CND for high-risk patients.

Data availability statement

The raw data supporting the conclusions of this article will be made available by the authors, without undue reservation.

Ethics statement

Informed consent was obtained from all individual participants included in the study. Written informed consent was obtained from the individual(s) for the publication of any potentially identifiable images or data included in this article.

Author contributions

J-WF and L-ZH: Writing - Original Draft, Software, Data Curation. S-YL: Validation, Formal analysis, Data Curation. FW: Conceptualization. JY and G-FQ: Validation, Investigation. YJ: Writing - Review and Editing, Visualization, Supervision. All authors contributed to the article and approved the submitted version.

Acknowledgments

Lei Qin, the English language editor, was responsible for correcting language and grammar issues.

Conflict of interest

The authors declare that the research was conducted in the absence of any commercial or financial relationships that could be construed as a potential conflict of interest.

Publisher's note

All claims expressed in this article are solely those of the authors and do not necessarily represent those of their affiliated organizations, or those of the publisher, the editors and the reviewers. Any product that may be evaluated in this article, or claim that may be made by its manufacturer, is not guaranteed or endorsed by the publisher.

References

1. Scheffel RS, Dora JM, Maia AL. BRAF mutations in thyroid cancer. *Curr Opin Oncol* (2022) 34(1):9–18. doi: 10.1097/CCO.0000000000000797

2. Huang Y, Yin Y, Zhou W. Risk factors for central and lateral lymph node metastases in patients with papillary thyroid micro-carcinoma: Retrospective analysis on 484 cases. *Front Endocrinol (Lausanne)* (2021) 12:640565. doi: 10.3389/fendo.2021.640565

3. Feng JW, Qu Z, Qin AC, Pan H, Ye J, Jiang Y. Significance of multifocality in papillary thyroid carcinoma. *Eur J Surg Oncol* (2020) 46(10 Pt A):1820–8. doi: 10.1016/j.ejso.2020.06.015

4. Jiang LH, Yin KX, Wen QL, Chen C, Ge MH, Tan Z. Predictive risk-scoring model for central lymph node metastasis and predictors of recurrence in papillary thyroid carcinoma. *Sci Rep* (2020) 10(1):710. doi: 10.1038/s41598-019-55991-1

5. Feng JW, Ye J, Wu WX, Qu Z, Qin AC, Jiang Y. Management of cN0 papillary thyroid microcarcinoma patients according to risk-scoring model for central lymph node metastasis and predictors of recurrence. *J Endocrinol Invest* (2020) 43(12):1807–17. doi: 10.1007/s40618-020-01326-1

6. Ling Y, Zhang L, Li K, Zhao Y, Zhao J, Jia L, et al. Carbon nanoparticle-guided intraoperative lymph node biopsy predicts the status of lymph nodes posterior to right recurrent laryngeal nerve in cN0 papillary thyroid carcinoma. *Gland Surg* (2021) 10(5):1554–63. doi: 10.21037/gs-20-920

7. Takami H, Ito Y, Okamoto T, Yoshida A. Therapeutic strategy for differentiated thyroid carcinoma in Japan based on a newly established guideline managed by Japanese society of thyroid surgeons and Japanese association of endocrine surgeons. *World J Surg* (2011) 35(1):111–21. doi: 10.1007/s00268-010-0832-6

8. Haugen BR, Alexander EK, Bible KC, Doherty GM, Mandel SJ, Nikiforov YE, et al. 2015 American Thyroid association management guidelines for adult patients with thyroid nodules and differentiated thyroid cancer: The American thyroid association guidelines task force on thyroid nodules and differentiated thyroid cancer. *Thyroid* (2016) 26(1):1–133. doi: 10.1089/thy.2015.0020

9. Alabousi M, Alabousi A, Adham S, Pozdnyakov A, Ramadan S, Chaudhari H, et al. Diagnostic test accuracy of ultrasonography vs computed tomography for papillary thyroid cancer cervical lymph node metastasis: A systematic review and meta-analysis. *JAMA Otolaryngol Head Neck Surg* (2022) 148(2):107–18. doi: 10.1001/jamaoto.2021.3387

10. Xu SY, Yao JJ, Zhou W, Chen L, Zhan WW. Clinical characteristics and ultrasonographic features for predicting central lymph node metastasis in clinically node-negative papillary thyroid carcinoma without capsule invasion. *Head Neck* (2019) 41(11):3984–91. doi: 10.1002/hed.25941

11. Lim YS, Lee JC, Lee YS, Lee BJ, Wang SG, Son SM, et al. Lateral cervical lymph node metastases from papillary thyroid carcinoma: Predictive factors of nodal metastasis. *Surgery* (2011) 150(1):116–21. doi: 10.1016/j.surg.2011.02.003

12. Chen Q, Liu Y, Lu W, Zhang L, Su A, Liu F, et al. Pretracheal lymph node subdivision in predicting contralateral central lymph node metastasis for unilateral papillary thyroid carcinoma: Preliminary results. *Front Endocrinol (Lausanne)* (2022) 13:921845. doi: 10.3389/fendo.2022.921845

13. West E, Mutasa S, Zhu Z, Ha R. Global trend in artificial intelligence-based publications in radiology from 2000 to 2018. *AJR Am J Roentgenol* (2019) 213 (6):1204–6. doi: 10.2214/AJR.19.21346

14. Wu Y, Rao K, Liu J, Han C, Gong L, Chong Y, et al. Machine learning algorithms for the prediction of central lymph node metastasis in patients with papillary thyroid cancer. *Front Endocrinol (Lausanne)* (2020) 11:577537. doi: 10.3389/fendo.2020.577537

15. Enrico C. Precision oncology: The promise of big data and the legacy of small data. *Front ICT* (2017) 4:22. doi: 10.3389/fict.2017.00022

16. Dominietto MD, Capobianco E. Expected impacts of connected multimodal imaging in precision oncology. *Front Pharmacol* (2016) 7:451. doi: 10.3389/fphar.2016.00451

17. Capobianco E. Systems and precision medicine approaches to diabetes heterogeneity: a big data perspective. *Clin Transl Med* (2017) 6(1):23. doi: 10.1186/s40169-017-0155-4

18. Lesnik D, Cunnane ME, Zurakowski D, Acar GO, Ecevit C, Mace A, et al. Papillary thyroid carcinoma nodal surgery directed by a preoperative radiographic map utilizing CT scan and ultrasound in all primary and reoperative patients. *Head Neck* (2014) 36(2):191–202. doi: 10.1002/hed.23277

19. Grani G, Carbotta G, Nesca A, D'Alessandri M, Vitale M, Del Sordo M, et al. A comprehensive score to diagnose hashimoto's thyroiditis: a proposal. *Endocrine* (2015) 49(2):361–5. doi: 10.1007/s12020-014-0441-5

20. Tuttle RM, Haugen B, Perrier ND. Updated American joint committee on Cancer/Tumor-Node-Metastasis staging system for differentiated and anaplastic thyroid cancer (Eighth edition): What changed and why? *Thyroid* (2017) 27 (6):751–6. doi: 10.1089/thy.2017.0102

21. Jainulabdeen T, Ramaswamy B, Devaraja K, Paruthikunnan SM, Bhandarkar AM. Preoperative staging of differentiated thyroid carcinomas: Comparison of USG and CT with intraoperative findings and histopathology. *Indian J Otolaryngol Head Neck Surg* (2019) 71(3):327–33. doi: 10.1007/s12070-019-01663-5

22. Gonzalez GH, Tahsin T, Goodale BC, Greene AC, Greene CS. Recent advances and emerging applications in text and data mining for biomedical discovery. *Brief Bioinform* (2016) 17(1):33–42. doi: 10.1093/bib/bbv087

23. Ngiam KY, Khor IW. Big data and machine learning algorithms for health-care delivery. *Lancet Oncol* (2019) 20(5):e262–73. doi: 10.1016/S1470-2045(19) 30149-4

24. Zhu J, Zheng J, Li L, Huang R, Ren H, Wang D, et al. Application of machine learning algorithms to predict central lymph node metastasis in T1-T2, non-invasive, and clinically node negative papillary thyroid carcinoma. *Front Med (Lausanne)* (2021) 8:635771. doi: 10.3389/fmed.2021.635771

25. Van Calster B, Wynants L, Verbeek JFM, Verbakel JY, Christodoulou E, Vickers AJ, et al. Reporting and interpreting decision curve analysis: A guide for investigators. *Eur Urol* (2018) 74(6):796–804. doi: 10.1016/j.eururo.2018.08.038

26. Wang Y, Guan Q, Xiang J. Nomogram for predicting central lymph node metastasis in papillary thyroid microcarcinoma: A retrospective cohort study of 8668 patients. *Int J Surg* (2018) 55:98–102. doi: 10.1016/j.ijsu.2018.05.023

27. Daniels K, Gummadi S, Zhu Z, Wang S, Patel J, Swendseid B, et al. Machine learning by ultrasonography for genetic risk stratification of thyroid nodules. *JAMA Otolaryngol Head Neck Surg* (2020) 146(1):36–41. doi: 10.1001/jamaoto.2019.3073

28. Zhao CK, Ren TT, Yin YF, Shi H, Wang HX, Zhou BY, et al. A comparative analysis of two machine learning-based diagnostic patterns with thyroid imaging reporting and data system for thyroid nodules: Diagnostic performance and unnecessary biopsy rate. *Thyroid* (2021) 31(3):470–81. doi: 10.1089/thy.2020.0305

29. Wu Q, Deng L, Jiang Y, Zhang H. Application of the machine-learning model to improve prediction of non-sentinel lymph node metastasis status among breast cancer patients. *Front Surg* (2022) 9:797377. doi: 10.3389/fsurg.2022.797377

30. Li W, Liu Y, Liu W, Tang ZR, Dong S, Li W, et al. Machine learning-based prediction of lymph node metastasis among osteosarcoma patients. *Front Oncol* (2022) 12:797103. doi: 10.3389/fonc.2022.797103

31. Lee JH, Baek JH, Kim JH, Shim WH, Chung SR, Choi YJ, et al. Deep learning-based computer-aided diagnosis system for localization and diagnosis of metastatic lymph nodes on ultrasound: A pilot study. *Thyroid* (2018) 28(10):1332–8. doi: 10.1089/thy.2018.0082

32. Galicia A, Talavera-Llames R, Troncoso A, Koprinska I, Martínez-lvarez F. Multi-step forecasting for big data time series based on ensemble learning. *Knowledge-Based Syst* (2018) 163:830–41. doi: 10.1016/j.knosys.2018.10.009

33. Savargiv M, Masoumi B, Keyvanpour MR. A new random forest algorithm based on learning automata. *Comput Intell Neurosci* (2021) 2021:5572781. doi: 10.1155/2021/5572781

34. Suh CH, Baek JH, Choi YJ, Lee JH. Performance of CT in the preoperative diagnosis of cervical lymph node metastasis in patients with papillary thyroid cancer: A systematic review and meta-analysis. *AJNR Am J Neuroradiol* (2017) 38 (1):154–61. doi: 10.3174/ajnr.A4967

35. Feng JW, Hong LZ, Wang F, Wu WX, Hu J, Liu SY, et al. A nomogram based on clinical and ultrasound characteristics to predict central lymph node metastasis of papillary thyroid carcinoma. *Front Endocrinol (Lausanne)* (2021) 12:666315. doi: 10.3389/fendo.2021.666315

frontiers | Frontiers in Endocrinology

TYPE Original Research
PUBLISHED 20 December 2022
DOI 10.3389/fendo.2022.1091462

OPEN ACCESS

EDITED BY
An-Chen Qin,
Affiliated Suzhou Hospital of Nanjing Medical University, China

REVIEWED BY
Yasemin Giles Senyürek,
Istanbul University, Turkey
Mehmet Taner Ünlü,
Şişli Hamidiye Etfal Education and Research Hospital, Turkey

*CORRESPONDENCE
Jinxing Quan
quanxt@sina.com

†These authors have contributed equally to this work and share first authorship

SPECIALTY SECTION
This article was submitted to Cancer Endocrinology, a section of the journal Frontiers in Endocrinology

RECEIVED 07 November 2022
ACCEPTED 29 November 2022
PUBLISHED 20 December 2022

CITATION
Wang J, Wang J, Quan J, Liu J, Tian L and Dong C (2022) Relationship between serum NDRG3 and papillary thyroid carcinoma.
Front. Endocrinol. 13:1091462.
doi: 10.3389/fendo.2022.1091462

Relationship between serum NDRG3 and papillary thyroid carcinoma

Jiahao Wang[1†], Jun Wang[2†], Jinxing Quan[3*], Juxiang Liu[3], Limin Tian[3] and Changhong Dong[4]

[1]The First Clinical College of Gansu University of Chinese Medicine, Lanzhou, Gansu, China, [2]Department of Thyroid and Breast Surgery, Gansu Cancer Hospital, Lanzhou, Gansu, China, [3]Department of Endocrinology in Gansu Provincial People's Hospital and The First Clinical College of Gansu University of Chinese Medicine, Lanzhou, Gansu, China, [4]Radiotherapy Department of Gansu Maternal and Child Health Hospital, Lanzhou, Gansu, China

Background: In recent years, papillary thyroid carcinoma is considered to be one of the fastest increaseing cancer. NDRG family member 3 (NDRG3) has been proposed as a molecular marker of tumor, and is expected to be used in clinic.

Methods: Enzyme-linked immunosorbent assay was used to detect the serum NDRG3 expression in 81 papillary thyroid carcinoma cases, 75 benign thyroid nodules cases and 77 healthy control cases, respectively. Electrochemiluminescence method was applied to measure the levels of triiodothyronine, tetraiodothyronine, thyrotropin, thyroglobulin antibody and thyroid peroxidase antibody. Immunohistochemical staining was used to detect the expression of NDRG3 in papillary thyroid carcinoma, benign thyroid nodules and normal tissues adjacent to cancer.

Results: The expression of serum triiodothyronine, tetraiodothyronine, thyrotropin, thyroglobulin antibody and thyroid peroxidase antibody and NDRG3 were significantly different among benign thyroid nodules, papillary thyroid carcinoma cases and healthy control groups (P <0.001). Only the expression of serum NDRG3 was significantly different between benign thyroid nodules and papillary thyroid carcinoma groups (P <0.001). Immunohistochemistry showed that NDRG3 was expressed in all three groups, the lowest in papillary thyroid carcinoma, the second in benign thyroid nodules, and the highest in normal tissues adjacent to cancer. Logistic regression analysis showed that serum NDRG3 was an independent protective factor for papillary thyroid carcinoma (OR =0.964, 95%CI =0.953 to 0.974, P <0.001). The ROC curve of non-papillary thyroid carcinoma diagnosed by serum NDRG3 showed the optimal cut-off value of 481.38 pg/ml, sensitivity of 72.4%, specificity of 90.1%, and the maximum area under the curve (AUC =0.902, 95%CI =0.863 to 0.940, P <0.001). The ROC curve of benign

thyroid nodules diagnosed by serum NDRG3 showed the optimal critical value of 459.28 pg/ml, sensitivity of 81.3%, and specificity of 74.1% (AUC =0.863, 95% CI =0.808 to 0.919, P <0.001). The expression level of serum NDRG3 was significantly correlated with extrathyroid extensionand (P =0.007) and lymphatic metastasis of papillary thyroid carcinoma (P =0.019).

Conclusions: The decrease of NDRG3 expression can not only differential diagnosis benign thyroid nodules and papillary thyroid carcinoma, but also serve as a molecular marker for the diagnosis of papillary thyroid carcinoma.

KEYWORDS

benign thyroid nodules, papillary thyroid carcinoma, NDRG3, differential diagnosis value, molecular marker

Introduction

Thyroid nodule is the most common thyroid disease, with an increasing global morbidity in recent years, which is rising with the progress of detection methods (1, 2). Ultrasound is the optimal imaging method for thyroid examination (3). The prevalence of ultrasound has increased the morbidity of thyroid nodules at home and abroad, but may lead to overdiagnosis and unnecessary intervention (4, 5). Since more than 90% of thyroid nodules are asymptomatic benign lesions, only 10% of thyroid nodules are susceptible to thyroid cancer (4, 6). Despite the accuracy and economic applicability, there still exists 2-16% interpreted uncertainty of fine needle aspiration cytology to distinguish benign from malignant thyroid nodules (7). In the past 20 years, the incidental thyroid nodules detected by ultrasound have led to a rapid increase in the morbidity of low-risk papillary thyroid cancer (8). It is estimated that, thyroid cancer will become the four most common malignancies by 2030 (9). Although the morbidity of thyroid cancer has tripled in the past three decades (10, 11), the mortality rate remains relatively stable (12, 13). Papillary thyroid carcinoma (PTC), accounting for 84% of thyroid cancers, is the most common histopathological type of thyroid cancer. Although PTC patients can achieve a favourable prognosis, the 5-year survival rate generally exceeds 97%, and the 10-year survival rate exceeds 90% (14). In addition, there are still a significant number of patients with invasive metastasis, recurrence and iodine-131 resistance, resulting in adverse outcomes. For instance, studies have found that approximately 10-15% of patients may progress to potentially fatal recurrent diseases (15, 16). Accurate preoperative clinical diagnosis has proved difficult due to the lack of specific diagnostic tests for PTC. Therefore, there is an urgent need for a convenient, non-invasive and specific diagnostic method to distinguish PTC from benign thyroid nodules (BTN).

Molecular markers are expected to be used for early detection or screening of thyroid cancer, differentiation of benign and malignant diseases, histological identification, staging and treatment response, diagnosis and prognosis of recurrence (17). The American thyroid Association and the European thyroid Association have published guidelines recommending the detection of molecular markers for uncertain nodules (18). MYC is a human proto-oncogene, including C-MYC, N-MYC and L-MYC, involved in the occurrence, development, invasion and metastasis of tumors. Abnormal expression of MYC in PTC has been reported in a slew of literatures (19). The NDRG family is a downstream regulator of MYC. The AceView database of NCBI showed that, NDRG family members have a NDR-α/β hydrolase folding region and several functional sites, such as phosphorylation sites, acetylation sites, ubiquitin sites, etc. The members of the NDRG family are intracellular proteins, which are composed of 340-394 amino acid residues with amino acid homology of 53-65%. The NDRG family is generally divided into two subfamilies, one composed of NDRG1 and NDRG3 with a homology of 67%, and the other composed of NDRG2 and NDRG4 with a homology of 58% (20). NDRG3 is a downstream regulatory factor of MYC, with a total length of 2588 base pairs. It is mainly expressed in ovary, prostate, testis, brain, spinal cord, thymus, heart and kidney (21). NDRG3 is located on chromosome 20q11.21-11.23 and encodes at least two subtypes, 375 and 363 amino acids, respectively, with an apparent molecular weight of 41 and 40 kDa, respectively (22). However, the relationship between NDRG3 and PTC has not been reported.

Abbreviations: NDRG3, NDRG family member 3; PTC, Papillary thyroid carcinoma; BTN, Benign thyroid nodules; HC, Healthy controls; T3, Triiodothyronine; T4, tetraiodothyronine; TSH, thyrotropin; TGAb, thyroglobulin antibody; TPOAb, thyroidperoxidase antibody.

Therefore, this study aimed to investigate the differential diagnostic value of NDRG3 in patients with BTN and PTC by detecting the serum and tissues expression level of NDRG3 in normal individuals, BTN and PTC patients, and analyze the relationship between the serum expression level of NDRG3 and clinicopathology of PTC.

Materials and methods

Study subjects

From June 2019 to June 2022, patients with thyroid nodules underwent an operation in the Department of Head and Neck Surgery, Gansu Cancer Hospital and Gansu people's Hospital were divided into BTN group (n =75, 17 males and 58 females), and PTC group (n =81, 20 males and 61 females) according to pathological results. These patients did not have any other diseases before diagnosis and had not received any other treatment before the operation. In the same period, 77 healthy volunteers who underwent physical examination in the Physical Examination Center of Gansu Provincial People's Hospital were selected as the healthy control group (HC). The HC group received thyroid function, ultrasound and other examinations to exclude any disease, including 21 men and 56 women. All specimens were obtained with written informed consent. The study was designed to comply with the ethical standards set out in the 1975 Helsinki Declaration and was approved by the Institution Review Board of the Hospital (IRB No. 2022-224).

Data collection

Medical data of gender and age were recorded in detail for all subjects. Fasting blood was collected from all subjects, and thyroid function triiodothyronine (T3), tetraiodothyronine (T4), thyrotropin (TSH), thyroglobulin antibody (TGAB) and thyroid peroxidase antibody (TPOAb) was detected by chemiluminescence. 5 ml of total blood from the cubital vein was collected 2-3 days before operation. The specimens were placed in a vacuum blood collection jar without anticoagulant, refrigeratea at 4°C and centrifuged at 3000 r/min for 72 hours. After 10-15min, the supernatant was taken, placed in a centrifuge tube and stored in a refrigerator at -80°C. The postoperative pathological tissue was collected, fixed with 4% formaldehyde, washed, dehydrated, transparent, impregnated and embedded, and paraffin sections were prepared.

Main reagents and sources

Serum NDRG3 concentration was detected by Enzyme-linked immunosorbent assay (ELISA) kit, purchased from Shanghai FANKEL Industrial Co., Ltd. The antibody of NDRG3 was purchased from Affinity Biosciences company.

Experimental method

The main steps were as follows: the prepared standards and specimens were added to the microwell plate and shaken at 37°C for 30 min. After washing the microplate, 50 μL of secondary antibody was added and placed at room temperature for 30 min. After washing, the substrate was added, the color was shaded at 37°C for 10 minutes, and then the termination solution was added. Absorbance (OD) was measured with a microplate reader at a wavelength of 450 nm, and the concentration of human NDRG3 in the specimens was calculated with a standard curve. Sections of 6 cases of PTC, paracancerous normal tissues and BTN were randomly selected and the immunohistochemical experiment was carried out by Shaanxi Yike Biotechnology Co., Ltd. The results showed that the nucleus stained with hematoxylin was blue and the positive expression of diaminodiamine(DAB) was brown.

Statistical methods

SPSS25.0 (IBM, Armonk, NY, USA) was used for data analysis. Non-normal distribution data were described by the median (interquartile range [IQR]: 25–75 percentiles), difference analysis was carried out by Kruskal-Wallis test, and pairwise comparison was tested by Mann-WhitneyU test. Counting data were described in the form of frequency (percentage), and chi-square analysis was used for difference analysis. The immunohistochemical images were analyzed by Image-pro plus, and the data obtained were processed by one-way ANOVA. P <0.05 was considered statistically significant.

Results

Comparison of baseline characteristics and experimental indexes

As shown in Table 1, the index levels of 81 PTC patients, 75 BTN patients, and 77 healthy individuals were compared. The difference analysis of age and gender showed that no significant difference in this variable among BTN, PTC and HC groups (P >0.05). The difference analysis of T3, T4, TSH, TGAb and TPOAb showed that there were significant differences in this variable among BTN, PTC and HC (all P <0.001), between HC and PTC (all P <0.001), and between HC and BTN (all P <0.05). However, there was no significant difference between BTN and PTC (all P >0.05). The difference analysis of NDRG3 showed

significant difference in this variable among BTN, PTC and HC, HC and PTC, BTN and PTC, and HC and BTN (all P <0.001).

Immunohistochemistry

Thyroid follicular epithelial cells and cancer cells showed positive expression of NDRG3, and the nucleus and cytoplasm were stained brown (Figure 1). There was significant difference in NDRG3 between benign nodule group and adjacent normal tissue (P <0.001), between PTC group and adjacent normal tissue (P < 0.001), and between nodule group and PTC group (P <0.01).

Relationship between each experimental index and PTC

Spearman correlation analysis of PTC and other factors showed that serum levels of T3, T4, TSH, TGAb, and TPOAb were positively correlated with PTC (r =0.562, P =0.002; r =0.360, P <0.001; r =0.254, P <0.001; r =0.711, P <0.001; r =0.605, P <0.001; r =0.489, P <0.001). However, NDRG3 was significantly negative correlated with PTC (r =-0.700, P <0.001). After adjusting for T3, T4, TSH, TGAb, TPOAb and other factors, logical regression analysis showed that elevated serum NDRG3 expression was an independent protective factor for PTC (OR =0.964, 95%CI =0.953 to 0.974, P <0.001) (Table 2).

Diagnostic efficacy of serum NDRG3 between benign and malignant nodules

All the subjects were divided into PTC group and non-PTC group. The serum NDRG3 was used as a test variable, and the group non-PTC as the state variable to plot the ROC curve (Figure 2A). The optimal cut-off value of NDRG3 for the diagnosis of non-PTC group was 481.38 pg/ml, the sensitivity was 72.4%, the specificity was 90.1%, and the maximum area under the curve (AUC =0.902, 95%CI =0.863 to 0.940, P <0.001).

In the PTC and BTN groups, serum NDRG3 was used as the test variable and BTN as the state variable, so as to plot the ROC curve (Figure 2B). The optimal cut-off value of NDRG3 for BTN diagnosis was 459.28pg/ml, with a sensitivity of 81.3%, a specificity of 74.1%, and a maximum area under the curve (AUC =0.863, 95%CI =0.808 to 0.919, P <0.001).

Clinicopathological relationship between NDRG3 and PTC

As shown in Table 3, among the 81 PTC patients, the serum NDRG3 levels of PTC patients with different clinicopathological features were compared: ①Gender: 20 males and 61 females; ②Age: 63 patients aged <55 years and 18 patients aged ≥55 years; ③Degree of tumor invasion: 64 cases of PTC had unilateral invasion and 17 cases had bilateral invasion; ④Tumor length: 60 patients ≤10mm and 21 patients >10mm; ⑤Extrathyroidal extension: present in 28 patients and absent in 53 patients; ⑥Lymphatic metastasis: present in 15 patients and absent in 66 patients. In terms of TNM staging, there were 62 cases with stage I to II and 19 cases with stage III to IV, with the basis of the AJCC 8th edition criteria for diagnosis and staging of thyroid cancer. The level of serum NDRG3 in patients with lymph node metastasis and extrathyroidal extension PTC was significantly lower than that in patients without lymph node metastasis (P =0.019) and extrathyroidal extension (P =0.007). There was no significant difference in serum NDRG3 level in PTC patients with different gender, age, length, TNM stage and tumor invasion site.

TABLE 1 Baseline Characteristics and comparison of experimental indexes.

Characteristics	PTC (n=81)	BTN (n=75)	HC (n=77)	*P*-Value
Gender				
Female(%)	61 (75.3%))	58 (77.3%)	56 (72.7%)	0.805
male(%)	20 (24.7%)	17 (22.7%)	21 (27.3%)	
Age(years)	45 (37, 54)	47 (38, 55)	44 (35, 48)	0.073
T3(nmol/L)	2.04 (1.92, 2.25)*	2.03 (1.83, 2.31)*	1.51 (1.37, 1.69)	<0.001
T4(nmol/L)	117.20 (101.80, 131.35)*	113.30 (98.83, 122.80)*	99.35 (88.76, 110.37)	<0.001
TSH(uIU/L)	2.95 (1.77, 4.33)*	2.52 (1.59, 3.90)*	1.99 (1.28, 2.83)	<0.001
TGAb(IU/ml)	22.00 (18.18, 38.84)*	19.55 (14.84, 29.77)*	1.47 (0.84, 2.37)	<0.001
TPOAb(IU/ml)	3.21 (2.24, 13.22)*	3.57 (1.99, 5.18)*	0.50 (0.30, 1.15)	<0.001
NDRG3(pg/ml)	420.89 (375.57, 460.00)*#	490.45 (461.28, 517.60)*	532.05 (499.86, 583.42)	<0.001

PTC, Papillary thyroid carcinoma; BTN, Benign thyroid nodules; HC, Healthy controls; T3, Triiodothyronine; T4, tetraiodothyronine; TSH, thyrotropin; TGAb, thyroglobulin antibody; TPOAb, thyroidperoxidase antibody; *represents a statistically significant difference compared with the HC, and #represents a statistically significant difference compared with the BTN.

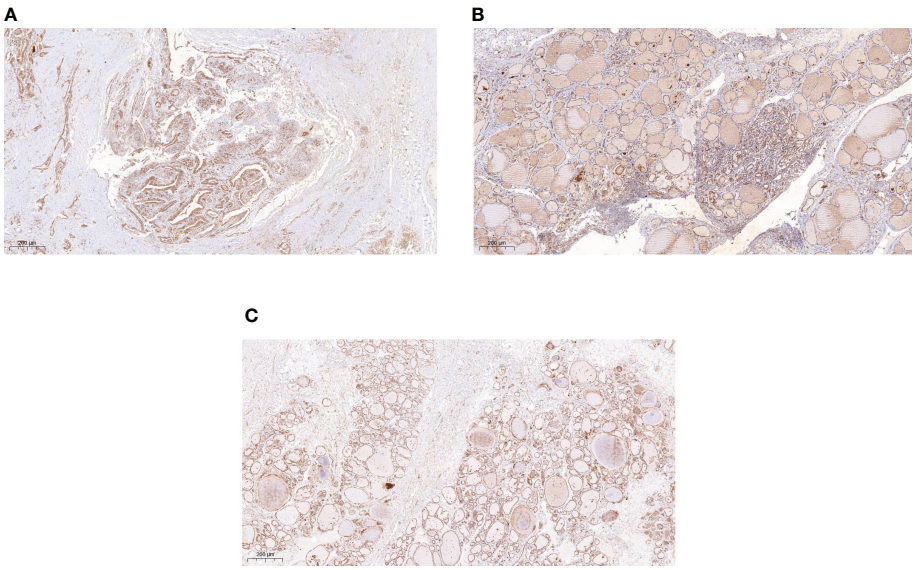

FIGURE 1
The expression of NDRG3 in PTC, paracancerous normal tissues and BTN (200X) **(A)** Positive expression of NDRG3 in PTC tissues; **(B)** Positive expression of NDRG3 in normal tissues adjacent to cancer; **(C)** Positive expression of NDRG3 in BTN tissues. The nucleus and cytoplasm are stained.

Discussion

There is an ever-growing global morbidity of thyroid nodules with each passing year. Surgery remains the foremost choice of treatment. The high diagnostic rate of uncertain nodules imposes an unbearable economic burden on individuals and society, and significantly reduces the quality of life. Therefore, it is a clinical challenge to perform a surgery on patients with a risk of cancer, and unnecessary surgery should be avoided. It has been pointed out that, for patients with uncertain nodules, the detection of molecular markers can be selected as a supplement. Our current results showed that it can be used as a diagnostic molecular marker for PTC.

We analyzed the preoperative general data and experimental data of serum T3, T4, TSH, TGAb, TPOAb and NDRG3 in 81 PTC patients, 75 BTN patients, 77 healthy volunteers during the same period. The results showed that the median of serum NDRG3 was the lowest in PTC group, followed by BTN group, and the highest in HC group. The median value of serum NDRG3 in PTC group was significantly lower than that in the other two groups. Then we did an immunohistochemical experiment and found that the expression of NDRG3 in the tissues of the three groups was consistent with that in blood, which indicated that the production of NDRG3 was reduced or consumed in thyroid papillary carcinoma and thyroid nodules, so a decrease was detected. We speculate that NDRG3 may be involved in the development of this cellular proliferative disease. It has been found that oxygen and lactic acid regulate NDRG3-mediated lactic acid-dependent signaling pathway. Oxygen negatively regulates NDRG3 expression at the protein level through (proline hydroxylase2) PHD2/(von Hippel Lindau disease) VHL system (23). As

TABLE 2 Binary logistic regression Analysis of PTC and various factors.

Variables	B	S.E.	Wald	Sig.	Exp (B)	95% C.I. for EXP (B)	
						Lower	Upper
T3	0.990	0.061	2.663	0.103	1.104	0.980	1.243
T4	0.006	0.010	0.336	0.562	1.006	0.986	1.027
TSH	0.135	0.107	1.588	0.208	1.145	0.928	1.413
TGAb	0.003	0.003	0.939	0.333	1.003	0.997	1.008
TPOAb	0.028	0.015	3.417	0.065	1.029	0.998	1.060
NDRG3	-0.037	0.006	45.024	0.000	0.964	0.953	0.974

T3, Triiodothyronine; T4, tetraiodothyronine; TSH, thyrotropin; TGAb, thyroglobulin antibody; TPOAb, thyroidperoxidase antibody.

TABLE 3 Relationship between NDRG3 and clinical parameters of patients with PTC.

Characteristics	Case	NDRG3	Z-value	*P*-value
Gender				0.706
Male	20	436.943 (365.832, 469.554)	-0.378	
Female	61	417.366 (379.069, 458.137)		
Age(year)				0.478
<55	63	414.179 (376.072, 458.993)	-0.710	
≥55	18	431.234 (361.265, 472.580)		
Location of involvement				0.339
Unilateral	64	421.599 (380.211, 460.498)	-0.957	
Bilateral	17	417.366 (355.592, 450.501)		
Tumor size(mm)				0.242
≤10mm	60	427.808 (376.286, 461.847)	-1.169	
>10mm	21	397.052 (368.294, 440.154)		
Extrathyroidal extension				0.007
yes	28	393.413 (346.029, 433.696)	-2.711	
no	53	433.731 (394.554, 462.701)		
Lymph node metastasis				0.019
yes	15	379.926 (347.099, 432.304)	-2.347	
no	66	427.808 (392.307, 462.346)		
TNM stages				0.061
I-II	62	429.164 (380.354, 462.346)	-1.873	
III-IV	19	397.052 (347.099, 434.159)		

Values are presented as median (interquartile range).

members of the NDRG family of oxygen sensors, they exhibit tumor suppressive behavior in various cancers, and their expression is considered to be a good prognostic marker (24). In addition, some studies have found that NDRG3 may be a target for controlling the invasive behavior of hypoxic cancer cells (25). But we do not know its performance in oxygen-rich tissues, we know that cellular hypoxia usually occurs in organs with insufficient blood supply or cells with strong metabolism, while the blood supply of thyroid is abundant, so there is little hypoxia. According to the above point of view, under pathological conditions, NDRG3 may increase in anoxic tissues and decrease in oxygen-enriched tissues. However, studies have found that NDRG3 is highly expressed in gastric and prostate cancer (24, 26), while low expression in breast cancer and oral squamous cell carcinoma (21, 27). From the above studies, it seems that the high expression of NDRG3 in anoxic cancer tissues and the low expression in oxygen-rich cancer tissues seems to be unreasonable.

Recent studies have found that the same member of the NDRG family can have both tumor promotion and inhibition at the same time, which may be determined by the tissue specificity of each member. It has been found that NDRG3 is capable of activating RAF-ERK pathway under hypoxia and accelerating tumor occurrence and development through the accumulation of lactic acid (28). NDRG3 regulates meiotic double-strand DNA break repair by regulating ERK signal pathway in male germ cells (29). In addition, NDRG3 also up-regulate the expression of angiogenic chemokine 43 (CXCL1, CXCL3 and CXCL5), enhance the expression of Angiogen-44, thereby ultimately promoting tumor progression (30). However, in our study, the expression of NDRG3 decreased in two diseases with active proliferation of benign and malignant cells. NDRG3 may be involved in the pathogenesis of PTC as a tumor suppressor gene, the reason of which may be related to the metabolic transformation of cancer cells. It has been found that, NDRG3 is degraded under normoxic conditions, but becomes very stable under hypoxic conditions by binding to lactic acid, even in the case of cell reoxygenation (31). Raquel Guimarães Coelho et al. found the Warburg effect in PTC cell line, indicating enhanced glycolysis and lactic acid fermentation in PTC (32). This may prove that the binding of lactic acid and NDRG3 exists in PTC, so NDRG3 is induced to increase, but combined with more, and eventually detected decrease. In addition, the study found that some BTN may have genetic changes, leading to metabolic changes, similar to thyroid cancer (33), so the NDRG3 detectable in BTN is reduced, but there is no more evidence to support this view. Another study found that NDRG3 increase at the early stage of hypoxia and then decrease during persistent hypoxia (34). Therefore, the same type of cancer may have different manifestations in different stages. Our results showed that the expression of NDRG3 was closely related to extrathyroid extension and lymph node metastasis of PTC. The median value

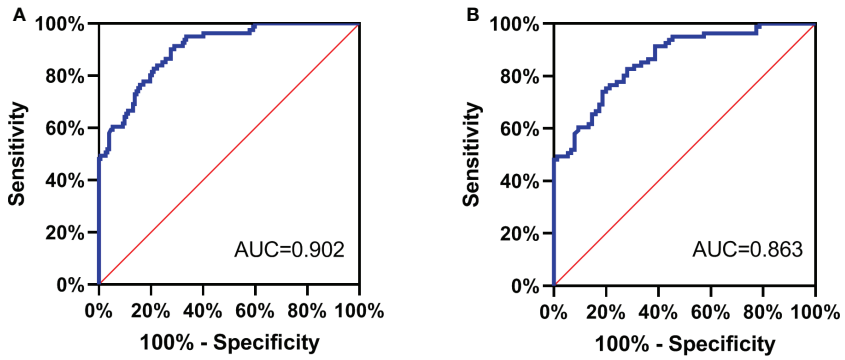

FIGURE 2
(A) All the subjects were divided into PTC group and non-PTC group. The serum NDRG3 was used as a test variable, and the group non-PTC as the state variable to plot the ROC curve; **(B)** In the PTC and BTN groups, serum NDRG3 was used as the test variable and BTN as the state variable, so as to plot the ROC curve.

of serum NDRG3 in PTC patients with extrathyroid extension and lymph node metastasis was significantly lower than that in PTC patients without both. Our experiments may suggest that the low expression of NDRG3 is related to the malignant degree of PTC. For example, the description of NDRG3 is inconsistent in the study of breast cancer and liver cancer. The expression of NDRG3 is down-regulated in breast cancer patients, especially in the late stage of the disease (21). In another breast cancer study, the expression of NDRG3 protein is increased, which is related to the invasive biological phenotype and poor prognosis of patients with invasive breast cancer (35). The results of Wang showed that the expression of NDRG3 is up-regulated in hepatocellular carcinoma cells, which reversing the malignant phenotype of hepatocellular carcinoma cells (36). The expression of NDRG3 change the sensitivity of cancer cells to chemotherapeutic drugs, which may be a potential therapeutic strategy for the treatment of liver cancer in the future (37). In conclusion, our study found that the low expression of NDRG3 in PTC is associated with poor prognosis.

Therefore, we speculate that the increased expression of NDRG3 in the general population may indicate the occurrence of hypoxic disease or in the early stage of hypoxia. The decrease or increase of NDRG3 in cancer may be related to the state at that time. If the cell hypoxia persists, lactic acid accumulates, NDRG3 is induced, and the binding with lactic acid increases, the detectable amount decreases. On the contrary, if there is no hypoxia in the cells, NDRG3 will not be pathologically induced and can be expressed normally, and relatively more can be detected in the end. In addition, we speculate that the increase of serum NDRG3 in the general population may play a role as tumor suppressor gene, while a role as carcinogenic gene under the combination of NDRG3 and accumulated lactic acid. These contradictory data may be attributed to differences in tumor micro-environment, tumor type or experimental methods. More specimens are essential to be included in the further study, so as to validate our current findings. There remains several limitations in this study. For example, there is a lack of detailed differentiation of PTC variants and studies of NDRG3 in benign counterparts. We only analyzed a small number of cases, which can be call a limited tissue population study, may be biased, and the experimental design needs further research and improvement.

In Conclusion, the low expression of NDRG3 has a certain differential diagnostic value in patients with BTN and PTC. It is related to the occurrence and development of PTC, and may be a potential marker for diagnosing PTC.

Data availability statement

The original contributions presented in the study are included in the article/supplementary material. Further inquiries can be directed to the corresponding author.

Ethics statement

The studies involving human participants were reviewed and approved by The Medical Ethics Committee of Gansu Provincial people's Hospital approved the protocol. The patients/participants provided their written informed consent to participate in this study.

Author contributions

JHW contributed to the conception and design of the experiment and data analysis. JW, CD and LT un contributed to the acquisition of data. JHW drafted the study, which was revised by JL and JQ. All authors contributed to the article and approved the submitted version.

Funding

This study was funded by Gansu Provincial Health Commission (GSWSKY2017-03), and Gansu Provincial people's Hospital (2019-155).

Acknowledgments

The authors would like to thank Xingwang Zhang, director of the Laboratory Department of Gansu Provincial people's Hospital, for providing us with professional guidance on technology of ELISA testing.

Conflict of interest

The authors declare that the research was conducted in the absence of any commercial or financial relationships that could be construed as a potential conflict of interest.

Publisher's note

All claims expressed in this article are solely those of the authors and do not necessarily represent those of their affiliated organizations, or those of the publisher, the editors and the reviewers. Any product that may be evaluated in this article, or claim that may be made by its manufacturer, is not guaranteed or endorsed by the publisher.

References

1. Zhang Z, Reiding KR, Wu J, Li Z, Xu X. NDistinguishing benign and malignant thyroid nodules and identifying lymph node metastasis in papillary thyroid cancer by plasma-glycomics. *Front Endocrinol* (2021) 12:692910. doi: 10.3389/fendo.2021.692910

2. Saraph S, Cohen H, Ronen O. Effect of needle gauge on thyroid FNA diagnostic rate. *Endocrine* (2021) 74(3):625–31. doi: 10.1007/s12020-021-02797-9

3. Zhou JQ, Yin LX, Wei X, Zhang S, Song YY, Luo BM. 2020 Chinese guidelines for ultrasound malignancy risk stratification of thyroid nodules: The c-TIRADS. *Endocrine* (2020) 70(2):256–79. doi: 10.1007/s12020-020-02441-y

4. Song Y, Xu G, Ma T, Zhu Y, Yu H, Yu W, et al. Utility of a multigene testing for preoperative evaluation of indeterminate thyroid nodules: A prospective blinded single center study in China. *Cancer Med* (2020) 9(22):8397–405. doi: 10.1002/cam4.3450

5. Staibano P, Forner D, Noel CW, Zhang H, Gupta M, Monteiro E, et al. Ultrasonography and fine-needle aspiration in indeterminate thyroid nodules: A systematic review of diagnostic test accuracy. *Laryngoscope* (2022) 132(1):242–51. doi: 10.1002/lary.29778

6. Li Y, Jin C, Li J, Tong M, Wang M, Huang J, et al. Prevalence of thyroid nodules in China: A health examination cohort-based study. *Front Endocrinol* (2021) 12:676144. doi: 10.3389/fendo.2021.676144

7. Qiu Y, Xing Z, Liu J, Peng Y, Zhu J, Su A. Diagnostic reliability of elastography in thyroid nodules reported as indeterminate at prior fine-needle aspiration cytology (FNAC): A systematic review and Bayesian meta-analysis. *Eur Radiol* (2020) 30(12):6624–34. doi: 10.1007/s00330-020-07023-0

8. Ha EJ, Chung SR, Na DG, Ahn HS, Chung J, Lee JY. 2021 Korean thyroid imaging reporting and data system and imaging-based management of thyroid nodules: Korean society of thyroid radiology consensus statement and recommendations. *Korean J Radiol* (2021) 22(12):2094–123. doi: 10.3348/kjr.2021.0713

9. Krajewska J, Kukulska A, Oczko-Wojciechowska M, Kotecka-Blicharz A, Drosik-Rutowicz K, Haras-Gil M, et al. Early diagnosis of low-risk papillary thyroid cancer results rather in overtreatment than a better survival. *Front Endocrinol (Lausanne)* (2020) 11:571421. doi: 10.3389/fendo.2020.571421

10. Shi R, Qu N, Luo T, Xiang J, Liao T, Sun G, et al. Programmed death-ligand 1 expression in papillary thyroid cancer and its correlation with clinicopathologic factors and recurrence. *Thyroid* (2017) 27(4):537–45. doi: 10.1089/thy.2016.0228

11. Kowalik A, Kowalska A, Walczyk A, Chodurska R, Kopczyński J, Chrapek M, et al. Evaluation of molecular diagnostic approaches for the detection of BRAF p.V600E mutations in papillary thyroid cancer: Clinical implications. *PloS One* (2017) 12(6):e0179691. doi: 10.1371/journal.pone.0179691

12. Lin JK, Sakoda LC, Darbinian J, Socarras M, Chiao W, Calixto N, et al. Risk of mortality between untreated and treated papillary thyroid cancer: A matched cohort analysis. *Ann Otol Rhinol Laryngol* (2020) 129(3):265–72. doi: 10.1177/0003489419885403

13. Lin JK, Sakoda LC, Darbinian J, Chiao W, Calixto N, Gurushanthaiah D, et al. Understanding the natural history of papillary thyroid cancer: Case series. *Head Neck* (2019) 41(12):4164–70. doi: 10.1002/hed.25967

14. Huang F, Wang L, Jia H. Research trends for papillary thyroid carcinoma from 2010 to 2019: A systematic review and bibliometrics analysis. *Medicine* (2021) 100(21):e26100. doi: 10.1097/MD.0000000000026100

15. Kaliszewski K, Diakowska D, Nowak Ł., Wojtczak B, Rudnicki J. The age threshold of the 8th edition AJCC classification is useful for indicating patients with aggressive papillary thyroid cancer in clinical practice. *BMC Cancer* (2020) 20 (1):1166. doi: 10.1186/s12885-020-07636-0

16. Ullmann TM, Gray KD, Moore MD, Zarnegar R, Fahey TJ. Current controversies and future directions in the diagnosis and management of differentiated thyroid cancers. *Gland Surg* (2018) 7(5):473–86. doi: 10.21037/gs.2017.09.08

17. Nambron R, Rosenthal R, Bahl D. Diagnosis and evaluation of thyroid nodules-the clinician's perspective. *Radiol Clin North Am* (2020) 58(6):1009–18. doi: 10.1016/j.rcl.2020.07.007

18. Ngo HTT, Nguyen TPX, Vu TH, Jung CK, Hassell L, Kakudo K, et al. Impact of molecular testing on the management of indeterminate thyroid nodules among Western and Asian countries: A systematic review and meta-analysis. *Endocr Pathol* (2021) 32(2):269–79. doi: 10.1007/s12022-020-09643-0

19. Ying X, Chen L, Xie J, Hu Y, Wu Q, Cao L, et al. ANXA1 (Annexin A1) regulated by MYC (MYC proto-oncogene) promotes the growth of papillary thyroid carcinoma. *Bioengineered* (2021) 12(2):9251–65. doi: 10.1080/21655979.2021.1996511

20. Yang X, An L, Li X. NDRG3 and NDRG4 two novel tumor-related genes. *BioMed Pharmacother* (2013) 67(7):681–4. doi: 10.1016/j.biopha.2013.04.009

21. Estiar MA, Zare A, Esmaeili R, Farahmand L, Fazilaty H, Jafari D, et al. Clinical significance of NDRG3 in patients with breast cancer. *Future Oncol* (2017) 13(11):961–9. doi: 10.2217/fon-2016-0457

22. Yang Q, Zhang X, Shi Y, He Y, Sun Z, Shi H, et al. Increased expression of NDRG3 in mouse uterus during embryo implantation and in mouse endometrial stromal cells during *In vitro* decidualization. *Reprod Sci* (2018) 25(8):1197–207. doi: 10.1177/1933719117737843

23. Park KC, Lee DC, Yeom YI. NDRG3-mediated lactate signaling in hypoxia. *BMB Rep* (2015) 48(6):301–2. doi: 10.5483/bmbrep.2015.48.6.080

24. Lee GY, Shin S, Shin H, Chun Y, Park J. NDRG3 lowers the metastatic potential in prostate cancer as a feedback controller of hypoxia-inducible factors. *Exp Mol Med* (2018) 50(5):1–13. doi: 10.1038/s12276-018-0089-y

25. Lee GY, Chun YA, Shin H, Park J. Potential role of the n-MYC downstream-regulated gene family in reprogramming cancer metabolism under hypoxia. *Oncotarget* (2016) 7(35):57442–51. doi: 10.18632/oncotarget.10684

26. Liu Y, Xia J, Zhou Y, Shao S. High expression of NDRG3 correlates with poor prognosis in gastric cancer patients. *Rev Esp Enferm Dig* (2021) 113(7):524–8. doi: 10.17235/reed.2021.7723/2020

27. Lee J, Chiang K, Feng T, Chen Y, Chuang S, Tsui K, et al. The iron chelator Dp44mT effectively inhibits human oral squamous cell carcinoma cell growth *in vitro* and *in vivo*. *Int J Mol Sci* (2016) 17(9):1435. doi: 10.3390/ijms17091435

28. Cui C, Lin H, Shi Y, Pan R. Hypoxic postconditioning attenuates apoptosis *via* inactivation of adenosine a receptor through NDRG3-Raf-ERK pathway. *Biochem Biophys Res Commun* (2017) 491(2):277–84. doi: 10.1016/j.bbrc.2017.07.112

29. Pan H, Zhang X, Jiang H, Jiang X, Wang L, Qi Q, et al. Ndrg3 gene regulates DSB repair during meiosis through modulation the ERK signal pathway in the male germ cells. *Sci Rep* (2017) 7:44440. doi: 10.1038/srep44440

30. Luo X, Hou N, Chen X, Xu Z, Xu J, Wang L, et al. High expression of NDRG3 associates with unfavorable overall survival in non-small cell lung cancer. *Cancer Biomark* (2018) 21(2):461–9. doi: 10.3233/CBM-170711

31. Zhang J, Zhang Q. VHL and hypoxia signaling: Beyond HIF in cancer. *Biomedicines* (2018) 6(1):35. doi: 10.3390/biomedicines6010035

32. Coelho RG, Cazarin JDM, de Albuquerque JPAC, de Andrade BM, Carvalho DP. Differential glycolytic profile and warburg effect in papillary thyroid carcinoma cell lines. *Oncol Rep* (2016) 36(6):3673–81. doi: 10.3892/or.2016.5142

33. de KEJ, van E.G.A.C.H., Bussink J, Frielink C, de GL, Kusters B, et al. FDG uptake and expression of immunohistochemical markers related to glycolysis hypoxia and proliferation in indeterminate thyroid nodules. *Mol Imaging Biol* (2022). doi: 10.1007/s11307-022-01776-4

34. Yao Y, Wang W, Jing L, Wang Y, Li M, Hou X, et al. Let-7f regulates the hypoxic response in cerebral ischemia by targeting NDRG3. *Neurochem Res* (2017) 42(2):446–54. doi: 10.1007/s11064-016-2091-x

35. Kim MC, Park MH, Kang SH, Bae YK. NDRG3 protein expression is associated with aggressive biologic phenotype and unfavorable outcome in patients with invasive breast cancer. *Int J Clin Exp Pathol* (2019) 12 (10):3886–93.

36. Ma J, Liu S, Zhang W, Zhang F, Wang S, Wu L, et al. High expression of NDRG3 associates with positive lymph node metastasis and unfavourable overall survival in laryngeal squamous cell carcinoma. *Pathology* (2016) 48(7):691–6. doi: 10.1016/j.pathol.2016.08.005

37. Du Z, Niu S, Xu X, Xu Q. MicroRNA31-NDRG3 regulation axes are essential for hepatocellular carcinoma survival and drug resistance. *Cancer Biomark* (2017) 19(2):221–30. doi: 10.3233/CBM-170568

frontiers | Frontiers in Endocrinology

TYPE Original Research
PUBLISHED 09 March 2023
DOI 10.3389/fendo.2023.1138085

OPEN ACCESS

EDITED BY
Emese Mezosi,
University of Pécs, Hungary

REVIEWED BY
Claudio Casella,
University of Brescia, Italy
Hanqing Lin,
First Affiliated Hospital of Fujian Medical University, China
Lv Tian,
Zhejiang Provincial People's Hospital, China

*CORRESPONDENCE
Jian Zhou
zhoujian1987817@163.com
Lei Tao
doctortaolei@163.com
Wei Cai
caiwei@shsmu.edu.cn

†These authors share first authorship

SPECIALTY SECTION
This article was submitted to Thyroid Endocrinology, a section of the journal Frontiers in Endocrinology

RECEIVED 05 January 2023
ACCEPTED 20 February 2023
PUBLISHED 09 March 2023

CITATION
Yang Z, Heng Y, Zhou J, Tao L and Cai W (2023) Central and lateral neck involvement in papillary thyroid carcinoma patients with or without thyroid capsular invasion: A multi-center analysis. *Front. Endocrinol.* 14:1138085. doi: 10.3389/fendo.2023.1138085

Central and lateral neck involvement in papillary thyroid carcinoma patients with or without thyroid capsular invasion: A multi-center analysis

Zheyu Yang[1†], Yu Heng[2†], Jian Zhou[2*], Lei Tao[2*] and Wei Cai[1*]

[1]Department of General Surgery, Ruijin Hospital, Shanghai Jiaotong University School of Medicine, Shanghai, China, [2]Department of Otorhinolaryngology, ENT Institute, Eye & ENT Hospital, Fudan University, Shanghai, China

Purposes: To quantitatively predict the probability of cervical lymph node metastasis for papillary thyroid carcinomas (PTC) patients with or without thyroid capsular invasion (TCI), to guide the decision-making of management strategies for neck regions.

Methods: A total of 998 PTC patients from three medical centers were retrospectively analyzed.

Results: Patients with positive TCI (TCI group) exhibited higher risks for both CLNM and LLNM than those with negative TCI (no-TCI group). Patients receiving lateral lymph node dissection showed significantly higher incidence of relatively severe postoperative complications. For no-TCI group, factors including age less than 55 years old, male, the presence of bilateral disease and multifocality, and maximum tumor diameter (MTD)>=0.5cm were confirmed to be independent risk factors for CLNM, while the presence of bilateral disease and ipsilateral nodular goiter (iNG), and maximum positive CLN diameter (MCLND)>1.0cm independent factors for LLNM. Independent risk factors of LLNM for patients within the TCI group included MCLND>1.0cm, positive CLN number>=3, and the presence of iNG. Predictive models of CLNM and LLNM were established based on the aforementioned risk factors for patients within no-TCI and TCI groups. A meticulous and comprehensive risk stratification flow chart was established for a more accurate evaluation of central neck involvement including both CLNM and LLNM risk in PTC patients.

Conclusions: A meticulous and comprehensive stratification flow chart for PTC patients for quantitatively evaluating both CLNM and LLNM was constructed.

KEYWORDS

papillary thyroid carcinoma, central lymph node metastasis, lateral lymph node metastasis, thyroid capsular invasion, risk stratification

1 Introduction

The incidence of Papillary thyroid carcinoma (PTC) continues to increase in recent years, ranking first among all kinds of malignancy of the endocrine system (1, 2). Although PTC patients generally exhibit satisfactory long-term overall and recurrence-free survival, approximately 20%-80% of patients were found to have neck metastasis when diagnosed (3–5). Ultrasonography (US) is the most common detection technique for the diagnosis of PTC. Although the application of high-resolution ultrasonography (US) and US-guided fine-needle aspiration (FNA) biopsy have increased the detection rate of PTC and corresponding neck involvement, it has been reported that the primary imaging modality ultrasound showed low sensitivity for detecting neck involvement, especially for the central compartment, which may be shadowed by nearby tissues including thyroid, collarbone, and trachea (6, 7).

Previous studies have shown that the rate of undetected central lymph node metastasis (CLNM) before surgery was higher than 30% (8, 9), thus prophylactic central lymph node dissection (CLND) is strongly recommended for all patients with clinical N0 PTC in many clinical centers. However, prophylactic surgical intervention involving the central neck compartment is considered over-treatment in some regions. Therefore, the management of the central neck is still controversial for PTC patients (10). On the other hand, although the detection rate of preoperative US for lateral lymph node metastasis (LLNM) was relatively high, ranging from 60.5% to 80.3% (11, 12), the occult LLNM rates are still reported to hover at 20% to 40% (13, 14). Furthermore, given the relatively high risk of postoperative complications resulting from lateral lymph node dissection (LLND), prophylactic LLND is generally not accepted as a standard strategy for PTC patients. Thus, there is great value in developing a more refined stratification system for assessing LLNM risk in PTC patients.

Thyroid capsular invasion (TCI), which is defined as a tumor clinging close to the junction of the thyroid and adjacent soft tissue and has invaded beyond the thyroid and surrounding fibrous, fat, and even skeletal muscle tissues (13), has been proven to be significantly associated with both CLNM and LLNM (8, 13, 14). Patients with TCI exhibit significantly higher neck involvement rates compared to those with no TCI, indicating distinct local metastasis risks between patients with or without TCI. However, these two groups of patients are often analyzed together, and no existing literature has discussed those patients respectively.

Here in our study, a comprehensive and meticulous evaluating system that can efficaciously quantify risks of CLNM and LLNM for PTC patients with TCI or not was established.

2 Materials and methods

2.1 Patient cohort

The study has been submitted to the Chinese Clinical Trial Registry chictr.org.cn. The assigned Unique Identifying Number is ChiCTR2100043353.

Initial surgery was conducted for 1112 patients with thyroid cancer at the following three hospitals between 2018 and 2020: Department of Otorhinolaryngology, Head and Neck Surgery at the Eye, Ear, Nose and Throat Hospital of Fudan University, Department of General Surgery at Ruijin Hospital of Shanghai Jiao Tong University School of Medicine, and Department of General Surgery, Civil Aviation Shanghai Hospital. Patients with any of the following criteria were excluded from this research: 1) Pathological type other than PTC (N=73); 2) Having received thyroid-related surgery previously (N=27); 3) History or coexistence of other primary tumors (N=14). At last, a total of 998 patients were enrolled in this research. This study was approved by the Institutional Ethics Committee of the Eye & ENT Hospital of Fudan University, the Ruijin Hospital of Shanghai Jiao Tong University School of Medicine, and the Department of General Surgery, Civil Aviation Shanghai Hospital. All participants gave informed consent to take part in the study.

2.2 Surgical management and cervical lymph node metastases

Aside from a total thyroidectomy or thyroid lobectomy, CLND was prophylactically conducted for every patient. LLND was performed for patients with preoperative detected LLNM by US or US-guided FNA. Those highly suspected to have lateral neck metastases were assessed by surgeons before or during operation. Clinicopathological information including TCI, maximum tumor diameter (MTD), multifocality, CLNM, LLNM, positive CLN number (CLNN), maximum positive CLN diameter (MCLND), ipsilateral nodular goiter (iNG) and ipsilateral Hashimoto thyroiditis, were obtained from histopathological results of surgical specimens. The thyroid glands were categorized into three equal volumes (upper portion, middle portion, and lower portion) according to the generally accepted consensus. Tumors with a maximum diameter of more than 2.0cm, primarily located in the upper 1/3 portion, and do not exceed the lower 1/3 thyroid gland were also defined as upper portion tumors.

2.3 Statistical analysis

Statistical analysis was performed using SPSS Statistics version 24.0 (SPSS Inc., Chicago, IL, USA). Chi-square and independent t-tests were conducted respectively for the comparison of categorical and continuous variables between different groups. Logistic univariate and multivariate regression analyses were performed for screening out independent predictors for CLNM and LLNM for PTC patients, which were further used for constructing a nomogram. The construction of the nomogram was performed by R software (version 3.5.1; R Development Core Team). Then the concordance index (C-index), receiver operating characteristic (ROC) curve, and the calibration curve were used for examination of our newly created nomograms. Patients were divided into different subgroups with extremely different CLNM and LLNM neck involvement rates According to the distribution of

total scores based on newly-created nomograms respectively. A P value of <0.05 was considered statistically significant.

3 Results

3.1 Patients' basic demographics and clinicopathological characteristics

A total of 998 patients who were diagnosed as PTC by postoperative pathology were analyzed in this research. The mean age of all patients was 42.68 years, with an SD of 12.52 years. The baseline demographics and clinicopathological characteristics of the patients enrolled are shown in Table 1. Patients with negative TCI (No-TCI group) were significantly older than those with positive TCI (TCI group, 43.80± 12.38 vs. 40.83 ± 12.56, p-value= 0.000). Patients within the TCI group showed significantly larger tumor sizes than those within the no-TCI group, and the presence of bilateral disease, multifocality, and iNG were significantly more common in the TCI group than in the no-TCI group (p-value<0.05). However, ipsilateral Hashimoto thyroiditis was more common in the no-TCI group than in the TCI group (p-value=0.008).

As CLND was prophylactically performed for all patients regardless of whether central neck involvement was detected before surgery, CLNM was easy to confirm by postoperative pathology. 503 (50.4%) patients exhibited CLNM in our cohort, with 290 (77.1%) in the TCI group and 213 (34.2%) in the no-TCI group. Patients with positive TCI were significantly more likely to develop central neck involvement than those with negative TCI (p-value=0.000).

However, LLND was conducted only for those with preoperatively detected positive or highly suspicious LLNM by surgeons before or during intraoperative phases. In the TCI group, 83 of the 290 patients with positive CLNM received CLND +LLND and 73 patients were diagnosed as having lateral neck involvement by postoperative pathology. 12 of the other 207 patients with positive CLNM receiving CLND alone in the TCI group were detected to have LLNM within six months after the initial surgery. In total, 85 (29.3%) of 290 patients with positive CLNM in the TCI group were considered as having lateral lymph node involvement before surgery (Diagram shown in Figure 1). For the 213 patients with positive CLNM within the no-TCI group, 39 patients received LLND and 30 of them were proven to have pathological-detected CLNM. Among the other 174 patients receiving CLND only, 5 were detected to have lateral lymph node metastases within six months after the initial surgery. In total, 35 (16.4%) of 213 patients with CLNM in the no-TCI group were considered as having preoperative LLNM. For patients with positive CLNM, those within the TCI group showed a significantly higher LLNM rate than those within the no-TCI group (p-value=0.001). Moreover, 35 (3.5%) of all the 998 patients enrolled experienced tumor recurrence in our study, with 16 (2.6%) in the no-TCI group and 19 (5.1%) in the TCI group. Patients within the TCI group exhibited a significantly higher rate of tumor recurrence than those within the no-TCI group (p-value=0.039, Table 1).

3.2 Comparisons between patients with CLNM and LLNM or not for patients within no-TCI and TCI groups

First, we compared patients with CLNM or not within no-TCI and TCI groups. For patients within the no-TCI group, the presences of bilateral disease and multifocality were significantly more frequently detected in patients with positive CLNM than in those with negative CLNM (p-value=0.000 and 0.000, respectively, shown in Supplementary Table S1). 47.4% of patients are men within the positive CLNM group, the rate of which was significantly higher than that of patients with negative CLNM (28.4%, p-value=0.000). Moreover, patients with positive CLNM also showed younger ages and significantly larger tumor sizes than those with negative CLNM among the no-TCI group (p-value=0.000 and 0.000, respectively). For patients within the TCI group, patients with positive CLNM also showed younger ages, significantly larger tumor sizes, increased percentage of males, and more frequent detection of multifocality than those with negative CLNM (p-value<0.05). However, no significant difference was found in terms of the presence of bilateral disease between patients with CLNM or not among patients within the TCI group.

In terms of LLNM, 35 in 213 and 85 in 290 patients with positive CLNM showed LLNM in no-TCI and TCI groups respectively. For patients within no-TCI and TCI groups, patients with positive LLNM both showed significantly larger tumor sizes, large maximum positive CLN diameter (MCLND), more positive CLN numbers (CLNN), and more frequent detection of iNG than those with negative LLNM (p-value<0.05, Supplementary Table S1). For patients within the no-TCI group, the presence of bilateral disease was significantly more frequent in patients with positive LLNM than that in patients with negative LLNM (45.7% vs. 23.0%, p-value=0.006). For patients within the TCI group, no significant difference was found in terms of the presence of bilateral disease between patients with LLNM or not. However, an significantly increased percentage of males was found in patients exhibiting positive LLNM than in those without (51.8% vs. 40.0%, p-value=0.008).

3.3 Surgery-related complications after CLND alone and CLND+LLND

Among the 998 patients enrolled, 874 received CLND only and the other 124 received both CLND and LLND. Patients receiving CLND alone showed a comparable incidence rate of temporary postoperative hypoparathyroid hormone and hoarseness with those receiving LLND (20.8% vs. 23.4% and 10.1% vs. 12.9%, p-value=0.513 and 0.334, respectively, Supplementary Table S2). However, those receiving CLND+LLND showed significantly higher incidence rates of relatively severe postoperative complications including permanent postoperative hypoparathyroid hormone (4.8% vs. 1.6%, p-value=0.016) and hoarseness (4.0% vs. 1.5%, p-value=0.046), and chyle leakage (3.2% vs. 0.2%, p-value=0.000) than those receiving CLND alone.

10.3389/fendo.2023.1138085

TABLE 1 The clinicopathological characteristics of all patients.

	All Patients		No-TCI		TCI		
	n=998	%	n=622	%	n=376	%	P value
Age (mean ± SD)	42.68 ± 12.52		43.80 ± 12.38		40.83 ± 12.56		0.000
BMI (mean ± SD)	23.73 ± 3.76		23.66 ± 3.78		23.85 ± 3.74		0.458
Maximum tumor diameter (mean ± SD)	0.88 ± 0.72		0.74 ± 0.59		1.12 ± 0.83		0.000
Gender							0.022
Male	199	19.9	138	22.2	61	16.2	
Female	799	80.1	484	77.8	315	83.8	
History of smoking							0.354
No	928	93.0	582	93.6	346	92.0	
Yes	70	7.0	40	6.4	30	8.0	
History of alcoholism							0.381
No	930	**93.2**	583	93.7	347	92.3	
Yes	68	6.8	39	6.3	29	7.7	
History of hypertension							0.759
No	817	81.9	511	82.2	306	81.4	
Yes	181	18.1	111	17.8	70	18.6	
History of diabetes							0.086
No	927	92.9	571	91.8	356	94.7	
Yes	71	7.1	51	8.2	20	5.3	
Bilateral disease							0.005
Absent	792	79.4	511	82.2	281	74.7	
Present	206	20.6	111	17.8	95	25.3	
Multifocality							0.000
Absent	700	70.1	465	74.8	235	62.5	
Present	298	29.9	157	25.2	141	37.5	
Tumor location							0.097
Upper portion	270	27.1	157	25.2	113	30.1	
Middle/Lower portion	728	72.9	465	74.8	263	69.9	
Number of positive CLN (for positive CLNM only, n =503)							0.084
1-2	256	50.9	120	56.3	136	46.9	
3-4	117	23.3	47	22.1	70	24.1	
>= 5	130	25.8	46	21.6	84	29.0	
Maximum diameter of positive CLN (for positive CLNM only, n =503)							0.256
< 1.0cm	389	77.3	170	79.8	219	75.5	
>= 1.0cm	114	22.7	43	20.2	71	24.5	
PTC with ipsilateral Hashimoto thyroiditis							0.008
No	798	80.0	481	77.3	317	84.3	

(Continued)

10.3389/fendo.2023.1138085

TABLE 1 Continued

	All Patients		No-TCI		TCI		
	n=998	%	n=622	%	n=376	%	P value
Yes	200	20.0	141	22.7	59	15.7	
PTC with ipsilateral nodular goiter							0.001
No	712	71.3	467	75.1	245	65.2	
Yes	286	28.7	155	24.9	131	34.8	
CLNM							0.000
No	495	49.6	409	65.8	86	22.9	
Yes	503	50.4	213	34.2	290	77.1	
LLNM (for positive CLNM only, n =503)							0.001
No	383	76.1	178	83.6	205	70.7	
Yes	120	23.9	35	16.4	85	29.3	
Recurrence							0.039
No	963	96.5	606	97.4	357	94.9	
Yes	35	3.5	16	2.6	19	5.1	

TCI, thyroid capsular invasion; BMI, body mass index; CLN, central lymph node; PTC, papillary thyroid carcinoma; CLNM, central lymph node metastasis; LLNM, lateral lymph node metastasis.

3.4 Risk stratification for CLNM in patients within no-TCI and TCI groups

The central lymph node involvement rates for no-TCI and TCI groups were 34.2% (213 in 622) and 77.1% (290 in 376), respectively. Univariate and multivariate logistic regression analyses were then performed to screen out independent risk factors of CLNM for patients with negative and positive TCI. The results showed that factors including age less than 55 years old, male, the presence of bilateral disease and multifocality, and maximum tumor diameter (MTD)>=0.5cm were proven to be associated with CLNM for patients in the no-TCI group by univariate analysis, and were enrolled in the following multivariate analysis. The results showed that the aforementioned five factors were all confirmed to be independent risk factors of CLNM for patients with negative TCI (shown in Table 2).

For patients within the TCI group, factors including age less than 55 years old, male, history of diabetes, MTD>=1.0cm, and the presence of multifocality were proven to be associated with CLNM by univariate analysis and were then enrolled in multivariate analysis. As a result, all factors were confirmed to be independent risk factors of CLNM except the history of diabetes for patients with positive TCI (shown in Table 3).

Then the five selected independent risk factors were used to create the prediction nomogram model of CLNM for patients with negative TCI (shown in Figure 2A). For evaluation and validation of the nomogram, we conducted an internal validation by 1000 bootstrap resamples to assess the prediction accuracy of CLNM for patients with negative TCI in terms of C-index. C-index turned out to be 0.747 (95% CI, 0.705-0.788), and 0.739 (95% CI, 0.724-0.754) after bootstrapping, which demonstrated good accuracy of our prediction model. The ROC curve and the calibration plot were shown in Figures 2B, C, both showing the fair agreement between the actual and assessed probability of CLNM in patients with negative TCI.

Each factor that made up the nomogram has its own risk points for CLNM. Then each patient within the no-TCI group would gain a total risk score by summing up the risk scores of the five selected factors in our nomogram. Based on the distribution of the total risk score, patients within the no-TCI group were classified into three subgroups by two cutoff values:

(1) a low CLNM risk subgroup (with CLNM risk score of <30, n=112),

(2) a moderate CLNM risk subgroup (30<= CLNM risk score of <80, n=194),

(3) a high CLNM risk subgroup (with CLNM risk score ≥80, n=316).

The CLNM rates of the low-risk subgroup were proven to be only 10.7% (12 in 112), while it went as high as 51.3% (162 in 316) for the high-risk subgroup, showing markedly different risks of CLNM among the three subgroups of patients in the no-TCI group (20.1% (39 in 194) for moderate-risk group, shown in Supplementary Table S3).

The CLNM rate of patients within the TCI group was up to 77.1% (290 in 376). Considering the extremely high central neck involvement rate, patients with positive TCI were all identified as having a high-risk of CLNM in our research.

10.3389/fendo.2023.1138085

TABLE 2 Univariate and multivariate analyses for PTC patients with negative TCI.

	Univariate analysis		Multivariate analysis			Univariate analysis		Multivariate analysis	
	Hazard ratio (95% CI)	P value	Hazard ratio (95% CI)	P value		Hazard ratio (95% CI)	P value	Hazard ratio (95% CI)	P value
Analyzing all No-TCI patients to screen out independent factors for CLNM					*Analyzing No-TCI patients with positive CLNM to screen out independent factors for LLNM*				
Factors selected					***Factors selected***				
Age		***0.002***		**0.001**	**Age**		0.517		
>= 55 vs. < 55	***0.505 (0.327-0.782)***		***0.428 (0.263-0.697)***		>= 55 vs. < 55	0.691 (0.226-2.112)			
BMI		0.780			**BMI**		0.436		
> 23 vs. <= 23	1.049 (0.752-1.462)				> 23 vs. <= 23	1.340 (0.641-2.802)			
Gender		***0.000***		***0.000***	**Gender**		0.881		
Male vs. Female	***2.278 (1.614-3.214)***		***2.267 (1.552-3.312)***		Male vs. Female	1.057 (0.512-2.183)			
History of smoking		0.071			**History of smoking**		0.230		
Yes vs. No	1.810 (0.950-3.446)				Yes vs. No	1.952 (0.655-5.823)			
History of alcoholism		0.207			**History of alcoholism**		0.414		
Yes vs. No	1.526 (0.792-2.940)				Yes vs. No	1.638 (0.501-5.354)			
History of hypertension		0.657			**History of hypertension**		0.162		
Yes vs. No	0.906 (0.585-1.402)				Yes vs. No	0.412 (0.119-1.427)			
History of diabetes		0.096			**History of diabetes**		0.447		
Yes vs. No	0.566 (0.290-1.106)				Yes vs. No	0.447 (0.056-3.574)			
Bilateral disease		***0.000***		***0.023***	**Bilateral disease**		***0.007***		***0.047***
Yes vs. No	***2.402 (1.583-3.645)***		***1.741 (1.081-2.803)***		Yes vs. No	***2.814 (1.328-5.963)***		***2.960 (1.016-8.620)***	
Maximum tumor diameter		***0.000***		***0.000***	**Maximum tumor diameter**		***0.030***		0.461
>= 0.5cm vs. < 0.5cm	***2.232 (1.584-3.147)***		***2.136 (1.463-3.117)***		>= 1.0cm vs. < 1.0cm	***2.281 (1.085-4.794)***		1.527 (0.496-4.699)	
Tumor location		0.464			**Tumor location**		0.438		
Upper vs. Middle/Lower	0.866 (0.589-1.274)				Upper vs. Middle/Lower	1.380 (0.612-3.113)			

(Continued)

TABLE 2 Continued

	Univariate analysis		Multivariate analysis			Univariate analysis		Multivariate analysis	
	Hazard ratio (95% CI)	P value	Hazard ratio (95% CI)	P value		Hazard ratio (95% CI)	P value	Hazard ratio (95% CI)	P value
Analyzing all No-TCI patients to screen out independent factors for CLNM					*Analyzing No-TCI patients with positive CLNM to screen out independent factors for LLNM*				
Multifocality		***0.000***		***0.000***	**Multifocality**		***0.031***		0.956
Yes vs. No	***5.055 (3.438-7.434)***		***4.684 (3.095-7.089)***		Yes vs. No	***2.271 (1.076-4.795)***		1.032 (0.334-3.189)	
PTC with ipsilateral nodular goiter		0.857			**PTC with ipsilateral nodular goiter**		***0.011***		***0.045***
Yes vs. No	1.036 (0.707-1.517)				Yes vs. No	***2.673 (1.253-5.703)***		***3.066 (1.025-9.172)***	
PTC with ipsilateral Hashimoto thyroiditis		0.584			**PTC with ipsilateral Hashimoto thyroiditis**		0.788		
Yes vs. No	1.116 (0.754-1.652)				Yes vs. No	1.121 (0.487-2.579)			
					Maximum diameter of positive CLN		***0.000***		***0.000***
					> 1.0cm vs. <= 1.0cm	***34.172 (13.330-87.603)***		***27.588 (9.116-83.492)***	
					Number of positive CLN		***0.000***		0.199
					>=3 vs. <3	***2.827 (1.797-4.449)***		1.502 (0.807-2.794)	

PTC, papillary thyroid carcinoma; TCI, thyroid capsular invasion; CLNM, central lymph node metastasis; LLNM, lateral lymph node metastasis; BMI, body mass index; CLN, central lymph node. The bold values represent statistically significant.

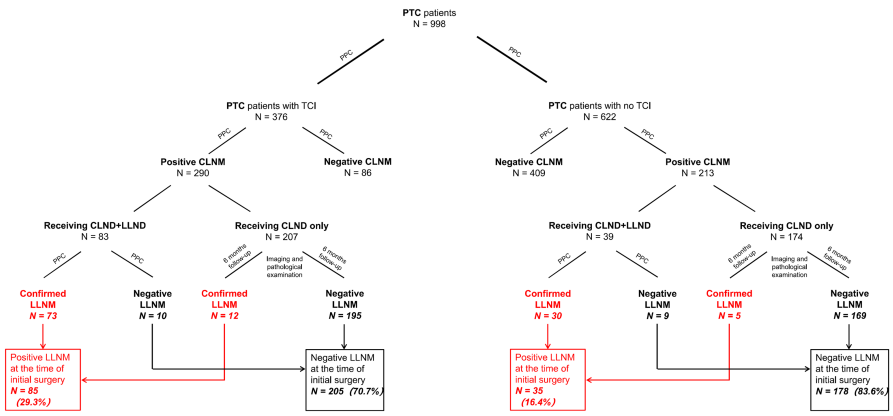

FIGURE 1
Flow diagram of case selection steps and follow-up information for patients enrolled. PTC, papillary thyroid carcinoma; PPC, postoperative pathology confirmed metastasis; CLNM, central lymph node metastasis; LLNM, lateral lymph node metastasis; CLND, central lymph node dissection; LLND, lateral lymph node dissection.

10.3389/fendo.2023.1138085

TABLE 3 Univariate and multivariate analyses for PTC patients with positive TCI.

	Univariate analysis		Multivariate analysis			Univariate analysis		Multivariate analysis	
	Hazard ratio (95% CI)	P value	Hazard ratio (95% CI)	P value		Hazard ratio (95% CI)	P value	Hazard ratio (95% CI)	P value
Analyzing all PTC patients with positive TCI to screen out independent factors for CLNM					*Analyzing positive TCI patients with CLNM to screen out independent factors for LLNM*				
Factors selected					***Factors selected***				
Age		***0.000***		***0.000***	**Age**		0.785		
>= 55 vs. < 55	***0.266 (0.149-0.474)***		***0.286 (0.148-0.551)***		>= 55 vs. < 55	0.893 (0.397-2.011)			
BMI		0.380			**BMI**		0.578		
> 23 vs. <= 23	0.804 (0.494-1.308)				> 23 vs. <= 23	1.155 (0.695-1.919)			
Gender		***0.000***		***0.002***	**Gender**		***0.009***		0.507
Male vs. Female	***2.917 (1.614-5.271)***		***2.704 (1.432-5.107)***		Male vs. Female	***1.982 (1.187-3.311)***		1.283 (0.614-2.679)	
History of smoking		0.203			**History of smoking**		0.286		
Yes vs. No	2.019 (0.685-5.954)				Yes vs. No	1.575 (0.684-3.627)			
History of alcoholism		0.866			**History of alcoholism**		0.788		
Yes vs. No	0.926 (0.382-2.249)				Yes vs. No	1.137 (0.446-2.896)			
History of hypertension		0.118			**History of hypertension**		0.137		
Yes vs. No	0.629 (0.352-1.124)				Yes vs. No	0.568 (0.269-1.197)			
History of diabetes		***0.020***		0.105	**History of diabetes**		0.602		
Yes vs. No	***0.337 (0.135-0.843)***		0.397 (0.130-1.213)		Yes vs. No	1.397 (0.398-4.902)			
Bilateral disease		0.625			**Bilateral disease**		0.238		
Yes vs. No	1.151 (0.654-2.026)				Yes vs. No	1.403 (0.800-2.461)			
Maximum tumor diameter		***0.000***		***0.004***	**Maximum tumor diameter**		***0.000***		0.063
>= 1.0cm vs. < 1.0cm	***2.543 (1.513-4.274)***		***2.303 (1.315-4.032)***		>= 1.0cm vs. < 1.0cm	***2.958 (1.728-5.064)***		1.984 (0.964-4.081)	
Tumor location		0.564			**Tumor location**		0.086		
Upper vs. Middle/Lower	0.859 (0.512-1.440)				Upper vs. Middle/Lower	1.605 (0.935-2.755)			

(Continued)

10.3389/fendo.2023.1138085

TABLE 3 Continued

	Univariate analysis		Multivariate analysis			Univariate analysis		Multivariate analysis	
	Hazard ratio (95% CI)	P value	Hazard ratio (95% CI)	P value		Hazard ratio (95% CI)	P value	Hazard ratio (95% CI)	P value
Analyzing all PTC patients with positive TCI to screen out independent factors for CLNM					*Analyzing positive TCI patients with CLNM to screen out independent factors for LLNM*				
Multifocality		***0.000***		***0.000***	**Multifocality**		0.134		
Yes vs. No	***4.007 (2.161-7.432)***		***4.159 (2.158-8.015)***		Yes vs. No	1.475 (0.887-2.452)			
PTC with ipsilateral nodular goiter		0.121			**PTC with ipsilateral nodular goiter**		***0.000***		***0.000***
Yes vs. No	0.677 (0.413-1.109)				Yes vs. No	***3.241 (1.907-5.507)***		***4.832 (2.303-10.137)***	
PTC with ipsilateral Hashimoto thyroiditis		0.612			**PTC with ipsilateral Hashimoto thyroiditis**		0.300		
Yes vs. No	0.847 (0.445-1.610)				Yes vs. No	0.671 (0.315-1.427)			
					Maximum diameter of positive CLN		***0.000***		***0.000***
					> 1.0cm vs. <= 1.0cm	***27.773 (13.703-56.291)***		***22.980 (10.473-50.420)***	
					Number of positive CLN		***0.000***		***0.033***
					>=3 vs. <3	***1.962 (1.445-2.663)***		***1.560 (1.036-2.350)***	

PTC, papillary thyroid carcinoma; TCI, thyroid capsular invasion; CLNM, central lymph node metastasis; LLNM, lateral lymph node metastasis; BMI, body mass index; CLN, central lymph node. The bold values represent statistically significant.

3.5 Risk stratification for LLNM in patients within no-TCI group

For the 213 patients with positive CLNM in the no-TCI group, univariate and multivariate analyses were conducted for screening out high-risk factors for LLNM and the results were shown in Table 2. Factors including the presence of bilateral disease and iNG, and MCLND>1.0cm were confirmed as independent factors for LLNM and were used for constructing a prediction model for patients with positive CLNM within the no-TCI group (Figure 3A). The C-index for predicting LLNM turned out to be 0.897 (95% CI, 0.833-0.961), and 0.881 (95% CI, 0.855-0.907) after bootstrapping, indicating satisfactory accuracy of our newly-established nomogram. The corresponding ROC curve and calibration plot were shown in Figures 3C, E, both showing great agreement between the actual and estimated possibility of LLNM in patients with positive CLNM in the no-TCI group.

According to the distribution of total scores based on the newly-created nomogram, patients with CLNM in the no-TCI group were also divided into three subgroups with extremely different lateral neck involvement rates: 1.0% (1 in 98), 9.7% (7 in 72), and 62.8% (27 in 43) for low-, moderate-, and high-risk subgroups (p-value=0.000, shown in Supplementary Table S3).

3.6 Risk stratification for LLNM in patients within TCI group

For the 290 patients with positive CLNM in TCI group, factors including MCLND>1.0cm, positive CLN number (CLNN)>=3, and the presence of iNG were confirmed as independent risk factors for LLNM (Table 3) and were used for constructing prediction model for patients with positive CLNM within no-TCI group (Figure 3B). The C-index was 0.770 (95% CI, 0.714-0.826), and 0.759 (95% CI,

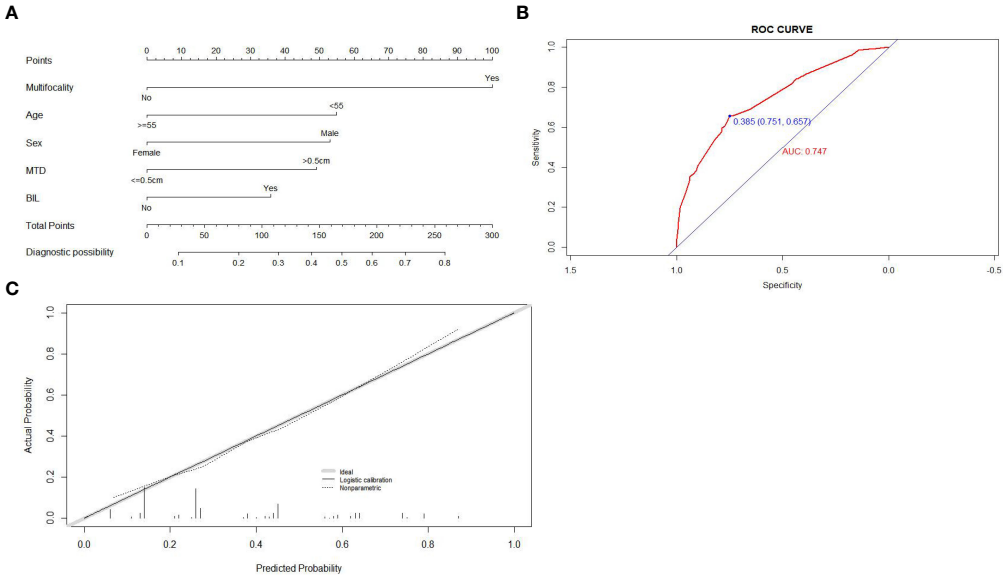

FIGURE 2
Construction, assessment, and validation of the predictive model of CLNM for patients within no-TCI group. **(A)** The nomograms for predicting CLNM risk in patients within no-TCI group; **(B)** The ROC curve and AUC of the nomogram for predicting CLNM risk in patients within no-TCI group; **(C)** The calibration curve of the nomogram for predicting CLNM risk in patients within no-TCI group. Actual probability is plotted on the y-axis, and nomogram predicted probability on the x-axis. CLNM, central lymph node metastasis; TCI, thyroid capsular invasion; ROC, receiver operating characteristics.

0.739-0.779) after bootstrapping, exhibiting satisfactory accuracy. The corresponding ROC curve and calibration plot were exhibited in Figures 3D, F.

Paitents with positive CLNM in TCI group were also classified into three subgroups according to newly-created nomogram targeting them by two cutoff values:

(1) a low LLNM risk subgroup (with LLNM risk score of <50, n=75),

(2) a moderate LLNM risk subgroup (50<= LLNM risk score of <100, n=83),

(3) a high LLNM risk subgroup (with LLNM risk score ≥100, n=132).

The LLNM rates of low-, moderate-, and high-risk subgroups were proven to be 1.3% (1 in 75), 20.5% (17 in 83), and 50.8% (67 in 132) for low-, moderate-, and high-risk subgroups, indicating a significant different lateral neck involvement rates (p-value=0.000, shown in Supplementary Table S3).

3.7 Comprehensive cervical lymph node metastasis assessment flow chart for patients with PTC

The aforementioned prediction models were integrated and were presented as a comprehensive cervical lymph node metastasis evaluation flow chart including both CLNM and LLNM for all patients with PTC in Figure 4.

4 Discussion

Debates on the optimal management strategy of neck regions for patients with PTC have existed for a long time. Many previous studies have screened out several risk factors for cervical lymph node metastasis including central and lateral neck involvement (8, 13, 15), for example, thyroid capsular invasion (TCI), larger tumor sizes, and younger ages for central lymph node metastasis (CLNM), and TCI, number of involved lymph nodes in central neck regions, and tumors located on upper portion for lateral lymph node metastasis (LLNM). Of these, capsular involvement is one of the most common and recognized risk factors for both CLNM and LLNM. Here in our research, based on whether TCI exists, patients with papillary thyroid carcinoma (PTC) were divided into two subgroups: TCI and no-TCI groups. The risk of CLNM and LLNM in each group was discussed and the risk prediction models of these two neck regions for the two groups were also constructed. Furthermore, we summarized and integrated the aforementioned prediction models, to establish a comprehensive evaluation process of cervical lymph node involvement risk for each patient with PTC, which provides certain guidance and basis for the standard clinical decision selection of cervical management for those patients.

TCI in our study was defined as a tumor clinging closely to the junction of thyroid and adjacent soft tissue, that can invade beyond the thyroid and surrounding tissues. Some previous studies take extrathyroidal extension (ETE) as the research index for predicting neck involvement for patients with PTC (16, 17), and those with microscopic and macroscopic ETE both showed significantly higher neck involvement rates and poor prognosis outcomes than those

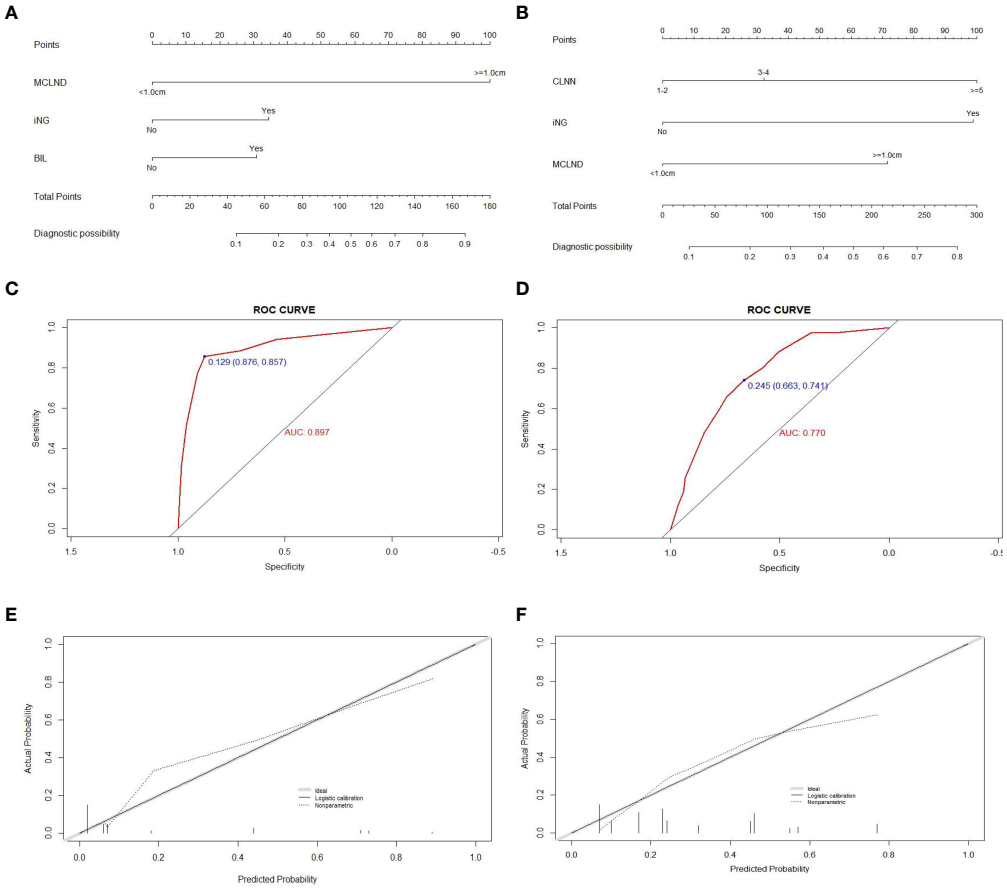

FIGURE 3
Construction, assessment, and validation of the predictive model of LLNM. **(A, B)** The nomograms for predicting LLNM risk in patients within no-TCI and TCI groups, respectively; **(C, D)** The ROC curve and AUC of the nomograms for predicting LLNM risk in patients within no-TCI and TCI groups, respectively; **(E, F)** The calibration curves of the nomogram for predicting LLNM risk in patients within no-TCI and TCI groups, respectively. Actual probability is plotted on the y-axis, and nomogram predicted probability on the x-axis. LLNM, lateral lymph node metastases; TCI, thyroid capsular invasion; ROC, receiver operating characteristics.

with negative ETE (18), indicating the pivotal role of capsular invasion status in the decision-making of management strategies for PTC patients. The reason why we chose TCI rather than ETE for patient stratification is because TCI is an extension of the concept of ETE, which includes both microscopic and macroscopic ETE, and also those where the tumor do not invade beyond the capsular and is merely in contact. Studies have shown that the probability of cervical lymph node metastasis in patients with positive TCI was significantly higher than in those with encapsulated tumors (8, 13, 19). Our results also confirmed the significantly high risk of both CLNM and LLNM for patients within the TCI group than the no-TCI group.

In terms of CLNM, younger age, male, the presence of multifocality, and large tumor size were confirmed to be independent factors for patients within both no-TCI and TCI groups, while the presence of bilateral disease was identified to be closely associated with CLNM only for patients within the no-TCI group. The CLNM rate was 34.2% (213 in 622) for all patients within the no-TCI group, and 10.7% (12 in 112) and 51.3% (162 in 316) for low- and high- CLNM risk subgroups after stratification using our newly-created nomogram, demonstrating excellent results for screening out patients with high risks of CLNM within this population that was traditionally considered to be low-risk (20). However, for patients with positive TCI, the CLNM rate was up to nearly 80%, indicating the extremely high risk of CLNM in those patients.

As for lateral neck metastasis, considering that skip metastasis (positive LLNM with no CLNM involvement) is rare in PTC patients, the risk of LLNM was analyzed for those with positive CLNM in no-TCI and TCI groups respectively. Features including both primary tumor and metastatic lymph nodes of the central compartment were enrolled to select out risk factors of LLNM for patients within different groups. Although factors including the presence of iNG and larger positive CLN size were proven to be independent risk factors of lateral neck involvement for both patients within no-TCI and TCI groups, the difference still exists between these two groups: the presence of bilateral disease was significantly associated with LLNM in patients of the no-TCI group rather than TCI group, while higher count of positive CLN was identified as high-risk factors for patients within TCI group, which further indicates the significant implications of our study to separate patients by the presence of TCI. Predictive nomograms

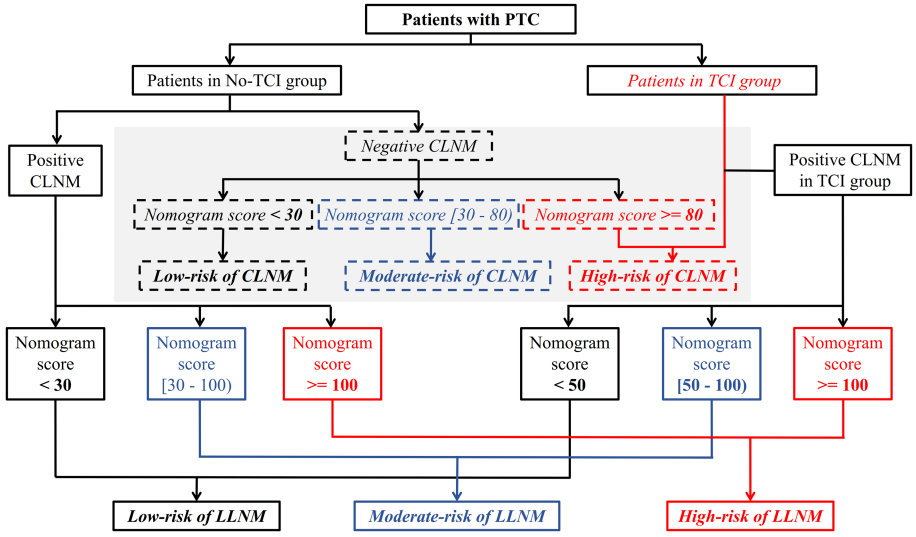

FIGURE 4
A meticulous and comprehensive stratification flow chart of cervical lymph node metastasis risk including both CLNM and LLNM for patients with PTC. CLNM, central lymph node metastasis; LLNM, lateral lymph node metastases; PTC, papillary thyroid carcinoma.

were established for patients within these two groups based on their respective risk factors. As a result, although the presence of positive CLNM was repeatedly proven by previous studies as a high-risk factor of LLNM (13, 15, 21, 22) for patients with PTC, here in our study, a small portion of patients with total LLNM risk scores <30 and <50 according to their own predictive nomograms were screened out and were considered as low-risk subgroup of LLNM within these patients, with LLNM rate of 1.0% (1 in 98) and 1.3% (1 in 75) for patients within no-TCI and TCI groups, respectively.

Finally, all the aforementioned results were integrated as a detailed cervical metastasis risk stratification flow chart for patients with PTC. Even though no clinically positive CLNM was found, patients with positive TCI, and patients who show negative TCI and with a total score no less than 80 based on the corresponding nomogram, are regarded as having a high risk of CLNM, and a closer follow-up scheme should be conducted for them. Considering that the incidence rates of postoperative complications including permanent postoperative hypoparathyroid hormone and hoarseness, and chyle leakage were proven to be significantly higher in those receiving lymph node dissection involving lateral neck regions in our study, the administration of prophylactic LLND should be minimized for PTC patients. Using the newly-created risk stratification flow chart for LLNM in our study, for patients with clinically positive CLNM, those with positive and negative TCI and with a total score no less than 100 according to their respective prediction models, are identified as having a high risk of LLNM, and a closer examination of lateral neck regions as well as a follow-up with shorter intervals should be conducted for these patients. Even LLND with a prophylactic purpose could be considered based on patients' preferences. However, no intervention of the lateral neck region is needed for patients classified as low-risk of LLNM (patients within no-TCI and TCI groups who received a total score of less than 30 and 50 based on their respective prediction models) considering the extremely low lateral neck involvement rates.

5 Conclusions

A meticulous and comprehensive stratification flow chart for PTC patients for quantitatively evaluating cervical lymph node metastasis risk including both CLNM and LLNM was constructed, which may aid in clinical decision-making for the management of neck regions.

Data availability statement

The raw data supporting the conclusions of this article will be made available by the authors, without undue reservation.

Ethics statement

The studies involving human participants were reviewed and approved by the Institutional Ethics Committee of the Eye & ENT Hospital of Fudan University, the Ruijin Hospital of Shanghai Jiao Tong University School of Medicine, and the Department of General Surgery, Civil Aviation Shanghai Hospital. The patients/participants provided their written informed consent to participate in this study.

Author contributions

(1) Conception and design or analysis and interpretation of data: all authors. (2) Drafting of the manuscript or revising it for

important intellectual content: ZY, YH, LT. (3) All authors contributed to the article and approved the submitted version.

Funding

This study was supported by of the Major Clinical Research Project of Shanghai Shen-kang Hospital Clinical Development Center under Grant (Grant numbers: SHDC2020CR6011); the Science and Technology Innovation Project of Shanghai Shen-kang Hospital Clinical Development Center under Grant (Grant numbers: SHDC12015114); the National Natural Science Foundation of China under Grant (Grant numbers: 81772878, 82003178); the Shanghai Municipal Key Clinical Specialty under Grant (Grant numbers: shslczdzk00801); the Science and Technology Committee of Shanghai under Grant (Grant numbers: 20MC1920200); the Science and Technology Commission of Shanghai Municipality under Grant (Grant numbers: 20Y11902200); the Shanghai Anti-Cancer Development Foundation under Grant (Grant numbers: H6001-008); and the Training Program of the Excellent Doctors of Fudan University under Grant (Grant numbers: QT00140).

Conflict of interest

The authors declare that the research was conducted in the absence of any commercial or financial relationships that could be construed as a potential conflict of interest.

Publisher's note

Supplementary material

The Supplementary Material for this article can be found online at: https://www.frontiersin.org/articles/10.3389/fendo.2023.1138085/full#supplementary-material

References

1. Siegel RL, Miller KD, Jemal A. Cancer statistics, 2020. *CA Cancer J Clin* (2020) 70 (1):7–30. doi: 10.3322/caac.21590

2. James BC, Mitchell JM, Jeon HD, Vasilottos N, Grogan RH, Aschebrook-Kilfoy B. An update in international trends in incidence rates of thyroid cancer, 1973-2007. *Cancer Causes Control* (2018) 29(4-5):465–73. doi: 10.1007/s10552-018-1023-2

3. Haugen BR, Alexander EK, Bible KC, Doherty GM, Mandel SJ, Nikiforov YE, et al. 2015 American thyroid association management guidelines for adult patients with thyroid nodules and differentiated thyroid cancer: The American thyroid association guidelines task force on thyroid nodules and differentiated thyroid cancer. *Thyroid* (2016) 26(1):1–133. doi: 10.1089/thy.2015.0020

4. Lim H, Devesa SS, Sosa JA, Check D, Kitahara CM. Trends in thyroid cancer incidence and mortality in the united states, 1974-2013. *JAMA* (2017) 317(13):1338–48. doi: 10.1001/jama.2017.2719

5. Luo DC, Xu XC, Ding JW, Zhang Y, Peng Y, Pan G, et al. Clinical value and indication for the dissection of lymph nodes posterior to the right recurrent laryngeal nerve in papillary thyroid carcinoma. *Oncotarget* (2017) 8(45):79897–905. doi: 10.18632/oncotarget.20275

6. Lesnik D, Cunnane ME, Zurakowski D, Acar GO, Ecevit C, Mace A. Papillary thyroid carcinoma nodal surgery directed by a preoperative radiographic map utilizing CT scan and ultrasound in all primary and reoperative patients. *Head Neck* (2014) 36:191e202. doi: 10.1002/hed.23277

7. Stulak JM, Grant CS, Farley DR, Thompson GB, van Heerden JA, Hay ID, et al. Value of preoperative ultrasonography in the surgical management of initial and reoperative papillary thyroid cancer. *Arch Surg* (2006) 141(5):489–94; discussion 494-6. doi: 10.1001/archsurg.141.5.489

8. Yang Z, Heng Y, Lin J, Lu C, Yu D, Tao L, et al. Nomogram for predicting central lymph node metastasis in papillary thyroid cancer: A retrospective cohort study of two clinical centers. *Cancer Res Treat* (2020) 52(4):1010–8. doi: 10.4143/crt.2020.254

9. Mulla M, Schulte KM. Central cervical lymph node metastases in papillary thyroid cancer: a systematic review of imaging-guided and prophylactic removal of the central compartment. *Clin Endocrinol (Oxf)* (2012) 76(1):131–6. doi: 10.1111/j.1365-2265.2011.04162.x

10. Sturgeon C, Yang A, Elaraj D. Surgical management of lymph node compartments in papillary thyroid cancer. *Surg Oncol Clin N Am* (2016) 25(1):17–40. doi: 10.1016/j.soc.2015.08.013

11. Ahn JE, Lee JH, Yi JS, Shong YK, Hong SJ, Lee DH, et al. Diagnostic accuracy of CT and ultrasonography for evaluating metastatic cervical lymph nodes in patients with thyroid cancer. *World J Surg* (2008) 32(7):1552–8. doi: 10.1007/s00268-008-9588-7

12. Hwang HS, Orloff LA. Efficacy of preoperative neck ultrasound in the detection of cervical lymph node metastasis from thyroid cancer. *Laryngoscope* (2011) 121 (3):487–91. doi: 10.1002/lary.21227

13. Heng Y, Yang Z, Zhou L, Lin J, Cai W, Tao L. Risk stratification for lateral involvement in papillary thyroid carcinoma patients with central lymph node metastasis. *Endocrine* (2020) 68(2):320–8. doi: 10.1007/s12020-020-02194-8

14. Luo H, Yan F, Lan L, Ma B, Zhao H, He Y, et al. Ultrasonographic features, nodule size, capsular invasion, and lymph node metastasis of solitary papillary carcinoma of thyroid isthmus. *Front Oncol* (2020) 10:558363. doi: 10.3389/fonc.2020.558363

15. Feng JW, Yang XH, Wu BQ, Sun DL, Jiang Y, Qu Z. Predictive factors for central lymph node and lateral cervical lymph node metastases in papillary thyroid carcinoma. *Clin Transl Oncol* (2019) 21(11):1482–91. doi: 10.1007/s12094-019-02076-0

16. Shaha AR. Extrathyroidal extension-what does it mean. *Oral Oncol* (2017) 68:50–2. doi: 10.1016/j.oraloncology.2017.03.008

17. Kim JW, Roh JL, Gong G, Cho KJ, Choi SH, Nam SY, et al. Extent of extrathyroidal extension as a significant predictor of nodal metastasis and extranodal extension in patients with papillary thyroid carcinoma. *Ann Surg Oncol* (2017) 24 (2):460–8. doi: 10.1245/s10434-016-5594-4

18. Park JS, Chang JW, Liu L, Jung SN, Koo BS. Clinical implications of microscopic extrathyroidal extension in patients with papillary thyroid carcinoma. *Oral Oncol* (2017) 72:183–7. doi: 10.1016/j.oraloncology.2017.02.008

19. Akbulut D, Kuz ED, Kursun N, Dizbay Sak S. Capsular invasion matters also in "Papillary patterned" tumors: A study on 121 cases of encapsulated conventional variant of papillary thyroid carcinoma. *Endocr Pathol* (2021) 32(3):357–67. doi: 10.1007/s12022-020-09650-1

20. Liu W, Wang S, Xia X. Risk factor analysis for central lymph node metastasis in papillary thyroid microcarcinoma. *Int J Gen Med* (2021) 14:9923–9. doi: 10.2147/IJGM.S346143

21. Kim K, Zheng X, Kim JK, Lee CR, Kang SW, Lee J, et al. The contributing factors for lateral neck lymph node metastasis in papillary thyroid microcarcinoma (PTMC). *Endocrine* (2020) 69(1):149–56. doi: 10.1007/s12020-020-02251-2

22. Zhan S, Luo D, Ge W, Zhang B, Wang T. Clinicopathological predictors of occult lateral neck lymph node metastasis in papillary thyroid cancer: A meta-analysis. *Head Neck* (2019) 41(7):2441–9. doi: 10.1002/hed.25762

frontiers | Frontiers in Endocrinology

TYPE Original Research
PUBLISHED 14 April 2023
DOI 10.3389/fendo.2023.1156664

OPEN ACCESS

EDITED BY
Emese Mezosi,
University of Pécs, Hungary

REVIEWED BY
Pietro Locantore,
Catholic University of the Sacred Heart, Rome, Italy
Zhichao Xing,
Sichuan University, China

*CORRESPONDENCE
Jian Wu
wo_doctor@163.com

SPECIALTY SECTION
This article was submitted to Thyroid Endocrinology, a section of the journal Frontiers in Endocrinology

RECEIVED 01 February 2023
ACCEPTED 30 March 2023
PUBLISHED 14 April 2023

CITATION
Wang B, Zhu C-R, Fei Y, Liu H, Yao X-M and Wu J (2023) Prelaryngeal and/or pretracheal lymph node metastasis could help to identify papillary thyroid carcinoma with intermediate risk from unilateral lobe cT1-2N0 papillary thyroid carcinoma. *Front. Endocrinol.* 14:1156664. doi: 10.3389/fendo.2023.1156664

Prelaryngeal and/or pretracheal lymph node metastasis could help to identify papillary thyroid carcinoma with intermediate risk from unilateral lobe cT1-2N0 papillary thyroid carcinoma

Bin Wang[1], Chun-Rong Zhu[2], Yuan Fei[1], Hong Liu[1], Xin-Min Yao[1] and Jian Wu[1]*

[1]Center of Breast and Thyroid Surgery, Department of General Surgery, The Third People's Hospital of Chengdu, Chengdu, Sichuan, China, [2]Department of Oncology Ward 2, The Third People's Hospital of Chengdu, Chengdu, Sichuan, China

Objective: The study aims to explore the possibility of prelaryngeal and/or pretracheal lymph node metastasis in identifying papillary thyroid carcinoma with more than 5 metastatic central lymph nodes from unilateral lobe cT1-2N0 papillary thyroid carcinoma.

Methods: A retrospective analysis was conducted on patients who underwent the initial thyroid surgery for unilateral lobe cT1-2N0 PTC in a single tertiary center between July 2018 to December 2022. Multivariable binary logistic regression analysis was used to identify risk factors for unilateral lobe cT1-2N0 papillary thyroid carcinoma with more than 5 metastatic central lymph nodes.

Results: A total of 737 patients were included in the study and 399 patients were confirmed to suffer from occult central lymph node metastasis. The larger size of the largest diameter of tumor (> 1cm; OR = 3.3, 95%CI 1.6 – 6.83; p = 0.001), pretracheal lymph node metastasis (OR = 5.91, 95%CI 2.73 – 12.77; p < 0.001), prelaryngeal lymph node metastasis (OR = 3.74, 95%CI 1.73 – 8.1; p = 0.001), ipsilateral paratracheal lymph node metastasis (OR = 12.22, 95%CI 3.43 – 43.48; p < 0.001), and contralateral paratracheal lymph node metastasis (OR = 7.68, 95% CI 3.86 – 15.3; p < 0.001) were confirmed to be risk factors for unilateral lobe cT1-2N0 PTC with more than 5 metastatic central lymph nodes. When more than two metastatic prelaryngeal and/or pretracheal lymph nodes occurred, the incidence of more than 5 metastatic central lymph nodes was 71.2%.

Conclusion: Prelaryngeal and/or pretracheal lymph node metastasis could help to identify papillary thyroid carcinoma with more than 5 metastatic central lymph nodes

from unilateral lobe cT1-2N0 papillary thyroid carcinoma. When more than two metastatic pretracheal and/or prelaryngeal lymph nodes occurred, total thyroidectomy and ipsilateral central lymph node dissection should be performed and contralateral paratracheal lymph node dissection might be also necessary.

KEYWORDS

pretracheal lymph node, prelaryngeal lymph node, paratracheal lymph node, papillary thyroid carcinoma, intermediate risk

Introduction

Although central lymph node metastasis occurred in 36.4% ~64.7% of clinically node-negative papillary thyroid carcinoma (cN0 PTC) (1–3), the idea that prophylactic central neck dissection should not be routinely performed for small (T1 or T2), noninvasive, cN0 PTC is strongly recommended by the 2015 American Thyroid Association Management Guidelines for Adult Patients with Thyroid Nodules and Differentiated Thyroid Cancer (2015 ATA Guidelines) with moderate-quality evidence (4). The reason for the recommendation was that the 2015 ATA Guidelines concluded that prophylactic dissection does not have an improvement in long-term patient outcome with increasing the likelihood of temporary morbidity and that the effect of the upgrade stage from cN0 to pN1 on overall survival is small (4). While, according to the 2015 ATA Initial Risk Stratification System, it was regarded as the intermediate risk that more than 5 metastatic central lymph nodes with all involved lymph nodes <3 cm in largest dimension (4). And patients with intermediate-risk level PTC should be considered to accept radioactive iodine adjuvant therapy, which means total thyroidectomy is necessary (4). At present, there are no guidelines, consensus, or indicators for total thyroidectomy and central neck dissection for cT1-2N0 PTC with potential intermediate risk.

The central lymph node consists of the prelaryngeal lymph node, pretracheal lymph node, and paratracheal (or trachea-esophageal groove) lymph node (5, 6). In recent years, several studies explored the significance of prelaryngeal lymph node metastasis in PTC and found that prelaryngeal lymph node metastasis was positively associated with paratracheal and lateral lymph node metastasis (3, 7–10). A similar result was obtained between pretracheal lymph node metastasis and paratracheal lymph node metastasis (6, 11, 12). However, some aforementioned studies included isthmic PTC and/or bilateral lobe PTC, which might increase the risk of lymph node metastasis and then the relationship between prelaryngeal/pretracheal lymph node metastasis and paratracheal lymph node metastasis might be affected.

Here, we conducted the retrospective study to explore the possibility of prelaryngeal and/or pretracheal lymph node metastasis in identifying PTC with more than 5 metastatic central lymph nodes from unilateral lobe cT1-2N0 PTC, and assess the association of prelaryngeal and/or pretracheal lymph node metastasis with paratracheal lymph node metastasis, and identify risk factors for unilateral lobe cT1-2N0 PTC with more than 5 metastatic central lymph nodes.

Patients and methods

Patients

The study began with a review of patients who underwent thyroid surgery for PTC at our institution from July 2018 to December 2022. Patients who underwent the initial thyroid surgery for unilateral lobe cT1-2N0 PTC were considered for inclusion. Patients with bilateral lobe PTC or isthmic PTC confirmed by postoperative pathological reports were excluded. The study was approved by the Medical Ethics Committee of The Third People's Hospital of Chengdu. And informed consent about the application of clinical data to medical research was routinely obtained from all the subjects before they were discharged.

Indications for surgery and surgical procedure

Total thyroidectomy was performed for the following indications: 1) the largest diameter of the tumor was more than 1cm; 2) the preoperative image discovered thyroid nodule in the contralateral lobe; 3) capsular invasion was confirmed by intraoperative frozen pathology; 4) prelaryngeal and/or pretracheal lymph node metastasis was confirmed by intraoperative frozen pathology. Otherwise, lobe thyroidectomy was performed. Ipsilateral central lymph node (including prelaryngeal lymph node, pretracheal lymph node, and ipsilateral paratracheal lymph node) dissection was routinely performed. Contralateral paratracheal lymph node dissection was performed when capsular invasion and/or prelaryngeal and/or pretracheal lymph node metastasis was confirmed by intraoperative frozen pathology.

Two professional thyroid surgeons (Wu J and Yao X) performed all surgeries. The surgical procedures are conducted as follows. After anesthesia, the patient was adjusted to hyperextension

of the head. A transverse incision located at 1cm beyond the suprasternal fossa was the surgical entrance. The flap with platysma muscle was then dissociated and it bordered superiorly by the thyroid cartilage, inferiorly by the sternum, and laterally on each side by the sternocleidomastoid muscle. After the strap muscles were separated *via* linea alba cervicalis, the space between the thyroid with central tissue and strap muscles was opened. Following that, the prelaryngeal and pretracheal tissues were routinely resected and examined by intraoperative frozen pathology. After that, thyroidectomy and paratracheal lymph node dissection were performed in sequence. The resected thyroid was also routinely examined by intraoperative frozen pathology.

Data collection

The following data were collected: demographic characteristics, comorbidities, tumor characteristics, details of surgical extent, and the number of lymph nodes and metastatic lymph nodes in each subgroup of the central zone.

Statistical analysis

All the statistical analyses were performed using SPSS version 23.0 software (SPSS Inc, Chicago, IL). Continuous data were expressed as mean ± standard deviation (SD) and analyzed using Student's t-test or Mann–Whitney test. Categorical data were shown as absolute numbers and analyzed using Pearson's Chi-square test or Fisher's exact test. These variables with potentially statistically significant in univariate analysis ($p < 0.1$) were included in the multivariable binary logistic regression analysis. Statistical significance was set at $P < 0.05$.

Result

A total of 737 patients were included in the study and 399 patients were confirmed to suffer from occult central lymph node metastasis. Among them, 198, 58, 350, and 81 patients suffered from pretracheal lymph node metastasis, prelaryngeal lymph node metastasis, ipsilateral paratracheal lymph node metastasis, and contralateral paratracheal lymph node metastasis, respectively. Prelaryngeal lymph node metastasis and pretracheal lymph node metastasis simultaneously occurred in forty-one patients. Among these patients without prelaryngeal lymph node metastasis, 436 had no lymph node in the prelaryngeal tissue. It happened to 47 patients that there was no lymph node in the pretracheal tissue. Three hundred and thirty-three cases suffered from left-lobe PTC. Among them, 43, 139, and 151 underwent left lobe thyroidectomy plus left central lymph node dissection, total thyroidectomy plus left central lymph node dissection, and total thyroidectomy plus bilateral central lymph node dissection, respectively.

According to the univariate analysis, there were no significant differences in gender, hyperthyroidism, hypothyroidism, and Hashimoto's Thyroiditis between patients with pretracheal lymph node metastasis and patients without pretracheal lymph node metastasis (Table 1). The age, hypertension, diabetes, nodular goiter, multifocal tumors, capsular invasion, the largest diameter of tumor, and tumor location were associated with pretracheal lymph node metastasis ($P = 0.001$, $P = 0.049$, $P = 0.031$, $P = 0.023$, $P = 0.008$, $P < 0.001$, $P < 0.001$, and $P = 0.014$, respectively; Table 1). It was significantly different in the incidences of prelaryngeal lymph node metastasis ($P < 0.001$, Table 1), ipsilateral paratracheal lymph node metastasis ($P < 0.001$, Table 1), contralateral paratracheal lymph node metastasis ($P < 0.001$, Table 1), and more than 5 metastatic central lymph nodes ($P < 0.001$, Table 1) between patients with and without pretracheal lymph node metastasis. The multivariate analysis indicated that young (< 55y; OR = 0.38, 95%CI 0.23 – 0.64; $p < 0.001$; Table 1), unifocal tumors (OR = 0.51, 95%CI 0.21 – 0.98; $p = 0.044$; Table 1), capsular invasion (OR = 2.7, 95%CI 1.88 – 3.87; $p < 0.001$; Table 1), the larger size of the largest diameter of tumor (> 1cm; OR = 2.45, 95%CI 1.71 – 3.52; $p < 0.001$; Table 1), and non-upper lesion (OR = 0.59, 95%CI 0.39 – 0.89; $p = 0.013$; Table 1) were independent risk factors for pretracheal lymph node metastasis.

The univariate analysis suggested that gender, capsular invasion, and the largest diameter of the tumor might be related to prelaryngeal lymph node metastasis (Table 2). The multivariate analysis further confirmed that male (OR = 0.4, 95%CI 0.23 – 0.7; $p = 0.001$; Table 2), capsular invasion (OR = 2.81, 95%CI 1.57 – 5.03; $p = 0.001$; Table 2), and larger size of the largest diameter of tumor (> 1cm; OR = 2.11, 95%CI 1.15 – 3.88; $p = 0.016$; Table 2) were independent risk factors for prelaryngeal lymph node metastasis. There were also significant differences in the incidences of pretracheal lymph node metastasis ($P < 0.001$, Table 2), ipsilateral paratracheal lymph node metastasis ($P < 0.001$, Table 2), contralateral paratracheal lymph node metastasis ($P < 0.001$, Table 2), and more than 5 metastatic central lymph nodes ($P < 0.001$, Table 2) between patients with and without prelaryngeal lymph node metastasis.

As shown in Table 3, gender, age, diabetes, capsular invasion, the largest diameter of tumor, pretracheal lymph node metastasis, and prelaryngeal lymph node metastasis might be associated with ipsilateral paratracheal lymph node metastasis. It was confirmed that male (OR = 0.57, 95%CI 0.4 – 0.82; $p = 0.002$; Table 3), the larger size of the largest diameter of tumor (> 1cm; OR = 1.8, 95%CI 1.3 – 2.5; $p < 0.001$; Table 3), pretracheal lymph node metastasis (OR = 6.23, 95%CI 4.13 – 9.4; $p < 0.001$; Table 3), and prelaryngeal lymph node metastasis (OR = 2.22, 95%CI 1.05 – 4.66; $p = 0.036$; Table 3) were independent risk factors for ipsilateral paratracheal lymph node metastasis by the multivariate analysis. The incidences of contralateral paratracheal lymph node metastasis (20.3% vs 2.6%, $p < 0.001$; Table 3) and more than 5 metastatic central lymph nodes (23.1% vs 0.8%, $p < 0.001$; Table 3) were higher in patients with ipsilateral paratracheal lymph node metastasis than that in patients without ipsilateral paratracheal lymph node metastasis.

Table 4 showed the risk factors for contralateral paratracheal lymph node metastasis. Although age, capsular invasion, the largest diameter of the tumor, tumor location, pretracheal lymph node metastasis, prelaryngeal lymph node metastasis, and ipsilateral paratracheal lymph node metastasis were discovered association

10.3389/fendo.2023.1156664

TABLE 1 The risk factors for pretracheal lymph node metastasis.

Variables	Univariate Analysis			Multivariate Analysis (G=761.335, P<0.001)		
	PT-LN(+) n=198	PT-LN(-) n=539	P	OR	95%CI	P
Gender(F/M)	134/64	397/142	0.109			
Age (years)	38.6 ± 11.8	45.6 ± 12.2	<0.001			
≥55	22	117	0.001	0.38	0.23 — 0.64	<0.001
<55	176	422				
Hypertension	13	62	0.049			
Diabetes	1	18	0.031			
Hyperthyroidism	5	18	0.573			
Hypothyroidism	2	9	0.755			
Hashimoto's Thyroiditis	64	147	0.179			
Nodular goiter	90	296	0.023			
Multifocal tumors	12	70	0.008	0.51	0.26 — 0.98	0.044
Capsular invasion	109	144	<0.001	2.7	1.88 — 3.87	<0.001
Largest tumor size (mm)	14.6 ± 7.4	10.9 ± 6.8	<0.001			
>10(%)	126 (38.3)	203 (61.7)	<0.001	2.45	1.71 — 3.52	<0.001
≤10(%)	72 (17.6)	336 (82.4)				
Tumor location (upper/middle/lower)	42/87/69	155/238/146	0.014	0.59	0.39 — 0.89	0.013
Surgical extent			<0.001			
LT+UCND	0	91				
TT+UCND	0	301				
TT+BCND	198	147				
PL-LNM(%)	41 (70.7)	17 (29.3)	<0.001			
Ipa-LNM(%)	160 (45.7)	190 (54.3)	<0.001			
Cpa-LNM(%)	69 (85.2)	12 (14.8)	<0.001			
Total number of metastatic lymph nodes	5.3 ± 3.9	0.9 ± 1.6	<0.001			
>5(%)	73 (86.9)	11 (13.1)	<0.001			
≤5(%)	125 (19.1)	528 (80.9)				

PT-LN, pretracheal lymph node; F, female; M, male; LT, lobe thyroidectomy; TT, total thyroidectomy; UCND, unilateral central lymph node dissection; BCND, bilateral central lymph node dissection; PL-LNM, prelaryngeal lymph node metastasis; Ipa-LNM, ipsilateral paratracheal lymph node metastasis; Cpa-LNM, contralateral paratracheal lymph node metastasis.

with contralateral paratracheal lymph node metastasis by the univariate analysis, the multivariate analysis demonstrated that larger size of the largest diameter of tumor (> 1cm; OR = 2.64, 95%CI 1.43 – 4.87; p = 0.002; Table 4), pretracheal lymph node metastasis (OR = 11.2, 95%CI 5.62 – 22.32; p < 0.001; Table 4), prelaryngeal lymph node metastasis (OR = 4.3, 95%CI 2.16 – 8.55; p < 0.001; Table 4), and ipsilateral paratracheal lymph node metastasis (OR = 2.84, 95%CI 1.32 – 6.07; p = 0.007; Table 4) were independent risk factors for contralateral paratracheal lymph node metastasis. There were more metastatic lymph nodes in patients with contralateral paratracheal lymph node metastasis (Table 4).

The analyses of potential risk factors for more than 5 metastatic central lymph nodes were shown in Table 5. Gender, age, capsular invasion, the largest diameter of tumor, tumor location, pretracheal lymph node metastasis, prelaryngeal lymph node metastasis, ipsilateral paratracheal lymph node metastasis, and contralateral paratracheal lymph node metastasis were included in the multivariate analysis. The larger size of the largest diameter of tumor (> 1cm; OR = 3.3, 95%CI 1.6 – 6.83; p = 0.001; Table 5), pretracheal lymph node metastasis (OR = 5.91, 95%CI 2.73 – 12.77; p < 0.001; Table 5), prelaryngeal lymph node metastasis (OR = 3.74, 95%CI 1.73 – 8.1; p = 0.001; Table 5), ipsilateral paratracheal lymph node metastasis (OR = 12.22, 95%CI 3.43 – 43.48; p < 0.001; Table 5), and contralateral paratracheal lymph node metastasis (OR = 7.68, 95%CI 3.86 – 15.3; p < 0.001; Table 5) were confirmed to be risk factors.

It was detailed in Table 6 that the correlations of different combinations of different statuses of prelaryngeal and pretracheal

10.3389/fendo.2023.1156664

TABLE 2 The risk factors for prelaryngeal lymph node metastasis.

Variables	Univariate Analysis			Multivariate Analysis (G=370.567, P<0.001)		
	PL-LN(+) n=58	PL-LN (-) n=679	P	OR	95%CI	P
Gender (F/M)	31/27	500/179	0.001	0.4	0.23 — 0.7	0.001
Age (years)	39.9 ± 13.1	44.1 ± 12.4	0.13			
≥55	9	130	0.498			
<55	49	549				
Hypertension	5	70	0.683			
Diabetes	0	19	0.39			
Hyperthyroidism	2	21	0.701			
Hypothyroidism	0	11	0.68			
Hashimoto's Thyroiditis	19	192	0.469			
Nodular goiter	32	354	0.657			
Multifocal tumors	6	76	0.844			
Capsular invasion	35	218	<0.001	2.81	1.57 — 5.03	0.001
Largest tumor size (mm)	16.2 ± 8.8	11.6 ± 6.9	<0.001			
>10 (%)	40 (12.2)	289 (87.8)	<0.001	2.11	1.15 — 3.88	0.016
≤10 (%)	18 (4.4)	390 (95.6)				
Tumor location (upper/middle/lower)	14/29/15	183/296/200	0.931			
Surgical extent			<0.001			
LT+UCND	0	91				
TT+UCND	0	301				
TT+BCND	58	287				
PT-LNM (%)	41 (20.7)	157 (79.3)	<0.001			
Ipa-LNM (%)	47 (13.4)	303 (86.6)	<0.001			
Cpa-LNM (%)	28 (34.6)	53 (65.4)	<0.001			
Total number of metastatic lymph nodes	7.3 ± 5.2	1.6 ± 2.4	<0.001			
>5 (%)	30 (35.7)	54 (65.3)	<0.001			
≤5 (%)	28 (4.3)	625 (95.7)				

PL-LN, prelaryngeal lymph node; F, female; M, male; LT, lobe thyroidectomy; TT, total thyroidectomy; UCND, unilateral central lymph node dissection; BCND, bilateral central lymph node dissection; PT-LNM, pretracheal lymph node metastasis; Ipa-LNM, ipsilateral paratracheal lymph node metastasis; Cpa-LNM, contralateral paratracheal lymph node metastasis.

lymph nodes with ipsilateral paratracheal lymph node metastasis, contralateral paratracheal lymph node metastasis, and more than 5 metastatic central lymph nodes. The more the metastatic prelaryngeal and/or pretracheal lymph nodes was, the higher the incidences of ipsilateral paratracheal lymph node metastasis, contralateral paratracheal lymph node metastasis, and more than 5 metastatic central lymph nodes were. The incidences of ipsilateral and contralateral paratracheal lymph node metastasis were more than 58% and 35% in patients with prelaryngeal lymph node metastasis, respectively (Table 6). During patients with pretracheal lymph node metastasis, the incidences of ipsilateral and contralateral paratracheal lymph node metastasis were 74% and 25%, respectively (Table 6). When the number of pretracheal metastatic lymph nodes was more than one, the incidences of ipsilateral paratracheal lymph node metastasis, contralateral paratracheal lymph node metastasis, and more than 5 metastatic central lymph nodes were more than 85%, 37%, and 49%, respectively (Table 6). When there was no prelaryngeal and pretracheal lymph node metastasis, the incidence of ipsilateral paratracheal lymph node metastasis still reached up to 34.5%, but the incidence of contralateral paratracheal lymph node metastasis and more than 5 metastatic central lymph nodes were only 1.1% and 1.7% (Table 6). However, when patients simultaneously suffered from prelaryngeal and pretracheal lymph node metastasis, the incidences of ipsilateral paratracheal lymph node metastasis, contralateral paratracheal lymph node metastasis, and more than 5 metastatic central lymph nodes were 85.7%, 50%, and 35.7%, respectively (Table 6).

10.3389/fendo.2023.1156664

TABLE 3 The risk factors for ipsilateral paratracheal lymph node metastasis.

Variables	Univariate Analysis			Multivariate Analysis (G=862.978, P<0.001)		
	Ipa-LN(+) n=350	Ipa-LN (-) n=387	P	OR	95%CI	P
Gender (F/M)	229/121	302/85	<0.001	0.57	0.4 — 0.82	0.002
Age (years)	41.5 ± 12.0	45.8 ± 12.5	<0.001			
≥55	53	86	0.014			
<55	297	301				
Hypertension	32	43	0.377			
Diabetes	4	15	0.019			
Hyperthyroidism	9	14	0.415			
Hypothyroidism	6	5	0.637			
Hashimoto's Thyroiditis	95	116	0.396			
Nodular goiter	179	207	0.524			
Multifocal tumors	37	45	0.649			
Capsular invasion	143	110	<0.001			
Largest tumor size (mm)	13.7 ± 7.7	10.3 ± 6.3	<0.001			
>10 (%)	197 (59.9)	132 (40.1)	<0.001	1.8	1.3 — 2.5	<0.001
≤10 (%)	153 (37.5)	255 (62.5)				
Tumor location (upper/middle/lower)	87/150/113	110/175/102	0.084			
Surgical extent			<0.001			
LT+UCND	22	69				
TT+UCND	105	196				
TT+BCND	223	122				
PT-LNM (%)	160 (80.8)	38 (19.2)	<0.001	6.23	4.13 — 9.4	<0.001
PL-LNM (%)	47 (81.0)	11 (19.0)	<0.001	2.22	1.05 — 4.66	0.036
Cpa-LNM (%)	71 (87.7)	10 (12.3)	<0.001			
Total number of metastatic lymph nodes	4.0 ± 3.5	0.3 ± 0.9	<0.001			
>5 (%)	81 (96.4)	3 (3.6)	<0.001			
≤5 (%)	269 (41.2)	384 (58.8)				

Ipa-LN, ipsilateral paratracheal lymph node; F, female; M, male; LT, lobe thyroidectomy; TT, total thyroidectomy; UCND, unilateral central lymph node dissection; BCND, bilateral central lymph node dissection; PT-LNM, pretracheal lymph node metastasis; PL-LNM, prelaryngeal lymph node metastasis; Cpa-LNM, contralateral paratracheal lymph node metastasis.

Discussion

The present study indicated that the larger size of the largest diameter of tumor (> 1cm) was a risk factor for pretracheal lymph node metastasis, prelaryngeal lymph node metastasis, paratracheal lymph node metastasis, and more than 5 metastatic central lymph nodes, and that both prelaryngeal lymph node metastasis and pretracheal lymph node metastasis were risk factors for paratracheal lymph node metastasis and more than 5 metastatic central lymph nodes, that capsular invasion was a risk factor for prelaryngeal lymph node metastasis and pretracheal lymph node metastasis.

In the present study, the incidence of occult central lymph node metastasis was 54.1% in unilateral lobe cT1-2N0 PTC, which was consistent with previous studies (1–3, 6). The incidence of ipsilateral paratracheal lymph node metastasis was 47.5%, while the incidence of more than 5 metastatic central lymph nodes was 11.4%. In consideration of the non-negligible incidence of more than 5 metastatic central lymph nodes, the great gap between this incidence and the incidence of occult central lymph node metastasis, and the increasing likelihood of temporary morbidity for prophylactic central lymph node dissection (4, 13), a feasible and reliable method without increasing the likelihood of temporary morbidity to identify PTC with more than 5 metastatic central lymph nodes from unilateral lobe cT1-2N0 PTC was necessary.

During patients with PTC of which the largest diameter was more than 1 cm in this study, the incidences of central lymph node metastasis, pretracheal lymph node metastasis, prelaryngeal lymph

TABLE 4 The risk factors for contralateral paratracheal lymph node metastasis.

Variables	Univariate Analysis			Multivariate Analysis (G=329.058, P<0.001)		
	Cpa-LN(+) n=81	Cpa-LN(-) n=656	P	OR	95%CI	P
Gender (F/M)	51/30	480/176	0.053			
Age (years)	38.5 ± 13.1	44.4 ± 12.2	<0.001			
≥55	9	130	0.059			
<55	72	526				
Hypertension	9	66	0.768			
Diabetes	1	18	0.711			
Hyperthyroidism	4	19	0.306			
Hypothyroidism	1	10	>0.99			
Hashimoto's Thyroiditis	22	189	0.757			
Nodular goiter	42	344	0.92			
Multifocal tumors	11	71	0.457			
Capsular invasion	48	205	<0.001			
Largest tumor size (mm)	16.6 ± 8.6	11.3 ± 6.8	<0.001			
>10 (%)	62 (18.9)	267 (81.1)	<0.001	2.64	1.43 — 4.87	0.002
≤10 (%)	19 (4.7)	389 (95.3)				
Tumor location (upper/middle/lower)	17/31/33	180/294/182	0.026			
Surgical extent			<0.001			
LT+UCND	0	91				
TT+UCND	0	301				
TT+BCND	81	264				
PT-LNM (%)	69 (34.8)	129 (65.2)	<0.001	11.2	5.62 — 22.32	<0.001
PL-LNM (%)	28 (48.3)	30 (51.7)	<0.001	4.3	2.16 — 8.55	<0.001
Ipa-LNM (%)	71 (20.1)	279 (79.9)	<0.001	2.84	1.32 — 6.09	0.007
Total number of metastatic lymph nodes	8.0 ± 4.5	1.3 ± 1.9	<0.001			
>5 (%)	52 (61.9)	32 (38.1)	<0.001			
≤5 (%)	29 (4.4)	624 (95.6)				

Cpa-LN, contralateral paratracheal lymph node; F, female; M, male; LT, lobe thyroidectomy; TT, total thyroidectomy; UCND, unilateral central lymph node dissection; BCND, bilateral central lymph node dissection; PT-LNM, pretracheal lymph node metastasis; PL-LNM, prelaryngeal lymph node metastasis; Ipa-LNM, ipsilateral paratracheal lymph node metastasis.

node metastasis, ipsilateral paratracheal lymph node metastasis, contralateral paratracheal lymph node metastasis, and more than 5 metastatic central lymph nodes were 67.8%, 38.3%, 12.2%, 59.9%, 18.9%, and 20.7%, respectively. The larger diameter increased the risk of central lymph node metastasis, which was also revealed by previous studies (8, 14, 15). The larger diameter means stronger invasiveness and/or a longer developmental time, which might increase the risk of lymph node metastasis (3, 14, 16).

Previous studies have suggested the predictive value of prelaryngeal lymph node metastasis to contralateral paratracheal lymph node metastasis, central lymph node metastasis, and lateral lymph node metastasis (3, 17, 18). The present study got similar results. One reason for not performing prophylactic central lymph node dissection for cT1-2N0 PTC in 2015 ATA Guidelines is that it increases the risk for temporary morbidity. Prelaryngeal lymph node dissection and pretracheal lymph node dissection could avoid this complication. What's more, they could be performed before thyroidectomy and then the tissues were checked by intraoperative frozen pathology, which could avoid the increase in surgery time. And the evidence that prelaryngeal lymph node metastasis was a poor prognostic factor in laryngeal and hypopharyngeal cancers gave enlightenment that it might affect the prognosis of PTC (19, 20). Based on those, the significance of prelaryngeal and/or pretracheal lymph node metastasis in PTC was studied (3, 10, 17).

A meta-analysis suggested that the sensitivities of prelaryngeal lymph node metastasis to predict central lymph node metastasis, contralateral central lymph node metastasis, and lateral lymph node

10.3389/fendo.2023.1156664

TABLE 5 The risk factors for more than 5 metastatic central lymph nodes.

Variables	Univariate Analysis			Multivariate Analysis (G=253.87, P<0.001)		
	Total number of metastatic lymph nodes		P	OR	95%CI	P
	>5 (n=84)	≤5 (n=653)				
Gender (F/M)	50/34	481/172	0.007			
Age (years)	38.0 ± 11.4	44.5 ± 12.4	<0.001			
≥55	8	131	0.02			
<55	76	522				
Hypertension	7	68	0.553			
Diabetes	0	19	0.152			
Hyperthyroidism	4	19	0.321			
Hypothyroidism	2	9	0.362			
Hashimoto's Thyroiditis	24	187	0.99			
Nodular goiter	45	341	0.815			
Multifocal tumors	11	71	0.542			
Capsular invasion	48	205	<0.001			
Largest tumor size (mm)	17.6 ± 8.3	11.2 ± 6.7	<0.001			
>10 (%)	68 (20.7)	261 (79.3)	<0.001	3.3	1.6 — 6.83	0.001
≤10 (%)	16 (3.9)	392 (96.1)				
Tumor location (upper/middle/lower)	17/33/34	180/292/181	0.02			
Surgical extent			<0.001			
LT+UCND	0	91				
TT+UCND	5	296				
TT+BCND	79	266				
PT-LNM (%)	73 (36.9)	125 (63.1)	<0.001	5.91	2.73 — 12.77	<0.001
PL-LNM (%)	30 (51.7)	28 (48.3)	<0.001	3.74	1.73 — 8.1	0.001
Ipa-LNM (%)	81 (23.1)	269 (76.9)	<0.001	12.22	3.43 — 43.48	<0.001
Cpa-LNM (%)	52 (64.2)	29 (35.8)	<0.001	7.68	3.86 — 15.3	<0.001

F, female; M, male; LT, lobe thyroidectomy; TT, total thyroidectomy; UCND, unilateral central lymph node dissection; BCND, bilateral central lymph node dissection; PT-LNM, pretracheal lymph node metastasis; PL-LNM, prelaryngeal lymph node metastasis; Ipa-LNM, ipsilateral paratracheal lymph node metastasis; Cpa-LNM, contralateral paratracheal lymph node metastasis.

metastasis were 32%, 46%, and 52%, respectively (21). A reason for the unsatisfactory sensitivities might be the not-high existing rate of prelaryngeal lymph nodes, which ranged from 23% to 38% (7, 8, 22, 23). The number of prelaryngeal lymph nodes ranged from 0 to 2, with a median number was 0 (24, 25). While the number of pretracheal lymph nodes varied from 0 to 35, with an average number was 12.4 (± 8.2) (24, 25). Several studies indicated that the sensitivities of prelaryngeal and/or pretracheal lymph node metastasis to predict ipsilateral central lymph node metastasis and contralateral central lymph node metastasis varied from 38.7% to 66% and from 32.3% to 56.1%, respectively (6, 11, 26, 27). In consideration of the difference in the number between prelaryngeal lymph nodes and pretracheal lymph nodes, and the lack of study of the significance of a different number of metastatic lymph nodes, the predictive values of a combination of prelaryngeal lymph node metastasis and a different number of metastatic pretracheal lymph nodes were studied in the study.

Due to the abundant intersecting lymph vessels and complex lymphatic drainage of the thyroid, there is no precise sentinel lymph node for thyroid carcinoma (10). As a part of perithyroidal lymph node metastasis, prelaryngeal and/or pretracheal lymph node metastasis was a reflection of ipsilateral central lymph node metastasis and a transfer station of contralateral central lymph node metastasis. In the present study, when patients suffered from 0 metastatic prelaryngeal lymph nodes and more than one metastatic pretracheal lymph node, approximately half of them were found more than 5 metastatic central lymph nodes, the predictive value of which was close to that of prelaryngeal lymph node metastasis. During patients with more than two metastatic prelaryngeal and/or pretracheal lymph nodes, 71.2% were found more than 5 metastatic

TABLE 6 The effect of different combinations of different statuses of prelaryngeal and pretracheal lymph nodes on paratracheal lymph node metastasis and more than 5 metastatic central lymph nodes.

Variables		Ipa-LNM			Cpa-LNM			Total number of metastatic lymph nodes		
		≥1	0	P	≥1	0	P	>5	≤5	P
PL-LNM (+)										
PT-LNM (-)	0	10 (58.8)	7 (41.2)	0.009	6 (35.3)	11 (64.7)	0.211	2 (11.8)	15 (88.2)	<0.001
PT-LNM (+)	1	12 (85.7)	2 (14.3)		7 (50)	7 (50)		5 (35.7)	9 (64.3)	
	≥2	25 (92.6)	2 (7.4)		15 (55.6)	12 (44.4)		23 (85.2)	4 (14.8)	
Total		47 (81.0)	11 (19.0)		28 (48.3)	30 (51.7)		30 (51.7)	28 (48.3)	
PL-LNM (-)										
PT-LNM (-)	0	180 (34.5)	342 (65.5)	<0.001	6 (1.1)	516 (98.9)	<0.001	9 (1.7)	513 (98.3)	<0.001
PT-LNM (+)	1	71 (74.0)	25 (26.0)		24 (25)	72 (75)		15 (15.6)	81 (84.4)	
	≥2	52 (85.2)	9 (14.8)		23 (37.7)	38 (62.3)		30 (49.2)	31 (50.8)	
Total		303 (44.6)	376 (55.4)	<0.001	53 (7.8)	626 (92.2)	<0.001	54 (8.0)	625 (92.0)	<0.001

Ipa-LNM ipsilateral paratracheal lymph node metastasis, Cpa-LNM contralateral paratracheal lymph node metastasis, PL-LNM prelaryngeal lymph node metastasis, PT-LNM pretracheal lymph node metastasis.

central lymph nodes. When the prelaryngeal lymph nodes metastasis and more than one metastatic pretracheal lymph node simultaneously occurred, the incidence of more than 5 metastatic central lymph nodes was 85.2%, and it even exceeded 90% in patients with the largest diameter more than 1 cm, the predictive value of which was far higher than that of prelaryngeal lymph node metastasis. For these patients, total thyroidectomy and prophylactic central lymph node dissection might be necessary.

According to the American Joint Committee on Cancer eighth edition cancer staging manual, the minor extrathyroidal extension detected only on histologic examination was removed from the definition of T3 disease (28, 29). While previous studies found that capsular invasion was a risk factor for prelaryngeal lymph node metastasis and contralateral paratracheal lymph node metastasis (7, 30). During the present study, capsular invasion was confirmed to increase the risk of prelaryngeal lymph node metastasis and pretracheal lymph node metastasis, but it did not convert to a risk factor for paratracheal lymph node metastasis and more than 5 metastatic central lymph nodes. The phenomenon might attribute to the fact that prelaryngeal lymph node metastasis and pretracheal lymph node metastasis included its' influence. Several studies also suggested that minor extrathyroidal extension was far less of an independent prognostic risk factor (31–33).

Male was found to be a risk factor for prelaryngeal lymph node metastasis and/or central lymph node metastasis for PTC in several studies (23, 34, 35). A similar result was obtained in the present study. Although female was more prone to suffer from PTC, the male might be an invasion factor. The pretracheal lymph node metastasis occurred more in the younger in the present study, which was consistent with the previous study (3). It might be a result of the guess that the carcinoma was more aggressive when it occurred in younger patients. The non-upper lesion was more closed to the pretracheal lymph node, so it might be more likely to lead to pretracheal lymph node metastasis. The present study suggested that unifocal lesion increased the risk of pretracheal lymph node metastasis, which was contrary to the previous studies (3, 23, 36). One reason for the phenomenon might be that previous studies included bilateral lobe lesions and/or isthmic lesion. Another reason might be that multifocal lesions was more actively and earlier treated in view of the higher invasive of which, so there was less chance for metastasis.

There are several limitations to the study. First, it is limited by its retrospective nature. Second, the study was conducted in a single center. Third, contralateral paratracheal lymph node dissection was not routinely performed, which was consistent with real-world clinical practice, while which might lead to data biases. Fourth, because of the lack of availability, molecular markers (such as BRAF V600E or TERT promoter mutations) were not included in the study.

Conclusion

In summary, patients with the larger size of the largest diameter of tumor (> 1cm), pretracheal lymph node metastasis, prelaryngeal lymph node metastasis, ipsilateral paratracheal lymph node metastasis, and contralateral paratracheal lymph node metastasis might be more likely to suffer from more than 5 metastatic central lymph nodes (intermediate-risk). And prelaryngeal and pretracheal lymph node metastasis could help to identify PTC with more than 5 metastatic central lymph nodes from unilateral lobe cT1-2N0 PTC. Based on the incidence of more than 5 metastatic central lymph nodes, total thyroidectomy and contralateral paratracheal lymph node dissection should be taken into consideration and ipsilateral central lymph node dissection might be necessary when the number of metastatic prelaryngeal and/or pretracheal lymph node was more than one; total thyroidectomy and ipsilateral central lymph node dissection should be performed and contralateral paratracheal lymph node dissection might be also necessary, especially for PTC with the largest diameter more than 1 cm, when more than

two metastatic prelaryngeal and/or pretracheal lymph nodes occurred. The larger the number of metastatic prelaryngeal and/or pretracheal lymph nodes was, the more likely paratracheal lymph node metastasis was to occur. More studies are necessary to validate the results of the retrospective study.

Data availability statement

The raw data supporting the conclusions of this article will be made available by the authors, without undue reservation.

Ethics statement

The studies involving human participants were reviewed and approved by Medical Ethics Committee of The Third People's Hospital of Chengdu. The patients/participants provided their written informed consent to participate in this study.

Author contributions

Conceptualization: BW, C-RZ, YF, HL, X-MY and JW. Methodology: BW, C-RZ and YF. Software: BW and YF. Validation: C-RZ, HL and X-MY. Formal analysis: BW and C-RZ. Data curation: BW and C-RZ. Writing—original draft preparation: BW and C-RZ. Writing—review and editing: YF and HL. Visualization: X-MY. Supervision: X-MY and JW. Project administration: X-MY and JW. Funding acquisition: BW and JW. All authors have read and agreed to the published version of the manuscript. All authors contributed to the article and approved the submitted version.

Funding

BW was supported by a nonprofit fund from CHINA HEALTH PROMOTION FOUNDATION. JW was supported by a grant from Scientific Research Fund of the Department of Science and Technology of Chengdu City (2015-HM01-00376-SF) and Science and Technology Program of Science & Technology Department of Sichuan Province (2015JY0190). The funding bodies had no role in the conception of the study, in the collection, analysis, and interpretation of data, in writing the manuscript and in the approval of the publication.

Acknowledgments

The authors thank the patients for their participation.

Conflict of interest

The authors declare that the research was conducted in the absence of any commercial or financial relationships that could be construed as a potential conflict of interest.

Publisher's note

References

1. Eun YG, Lee YC, Kwon KH. Predictive factors of contralateral paratracheal lymph node metastasis in papillary thyroid cancer: prospective multicenter study. *Otolaryngol Head Neck Surg* (2014) 150(2):210–5. doi: 10.1177/0194599813514726

2. Chen Q, Zou XH, Wei T, Huang QS, Sun YH, Zhu JQ. Prediction of ipsilateral and contralateral central lymph node metastasis in unilateral papillary thyroid carcinoma: a retrospective study. *Gland Surg* (2015) 4(4):288–94. doi: 10.3978/j.issn.2227-684X.2015.05.06

3. Zhu J, Zheng J, Li L, Huang R, Ren H, Wang D, et al. Application of machine learning algorithms to predict central lymph node metastasis in T1-T2, non-invasive, and clinically node negative papillary thyroid carcinoma. *Front Med (Lausanne)* (2021) 8:635771. doi: 10.3389/fmed.2021.635771

4. Haugen BR, Alexander EK, Bible KC, Doherty GM, Mandel SJ, Nikiforov YE, et al. 2015 American Thyroid association management guidelines for adult patients with thyroid nodules and differentiated thyroid cancer: The American thyroid association guidelines task force on thyroid nodules and differentiated thyroid cancer. *Thyroid* (2016) 26(1):1–133. doi: 10.1089/thy.2015.0020

5. Roh JL, Kim JM, Park CI. Central cervical nodal metastasis from papillary thyroid microcarcinoma: pattern and factors predictive of nodal metastasis. *Ann Surg Oncol* (2008) 15(9):2482–6. doi: 10.1245/s10434-008-0044-6

6. Zhou L, Li H, Liang W, Gao C, Chen B. Pretracheal-laryngeal lymph nodes in frozen section predicting contralateral paratracheal lymph nodes metastasis. *Eur J Surg Oncol* (2020) 46(10 Pt A):1829–34. doi: 10.1016/j.ejso.2020.06.048

7. Tan Z, Ge MH, Zheng CM, Wang QL, Nie XL, Jiang LH. The significance of delphian lymph node in papillary thyroid cancer. *Asia Pac J Clin Oncol* (2017) 13(5): e389–93. doi: 10.1111/ajco.12480

8. Yan Y, Wang Y, Liu N, Duan Y, Chen X, Ye B, et al. Predictive value of the delphian lymph node in cervical lymph node metastasis of papillary thyroid carcinoma. *Eur J Surg Oncol* (2021) 47(7):1727–33. doi: 10.1016/j.ejso.2021.02.010

9. Zhu J, Huang R, Yu P, Hu D, Ren H, Huang C, et al. Clinical implications of delphian lymph node metastasis in papillary thyroid carcinoma. *Gland Surg* (2021) 10 (1):73–82. doi: 10.21037/gs-20-521

10. Wang B, Zhu CR, Liu H, Yao XM, Wu J. Relationship between pretracheal and/or prelaryngeal lymph node metastasis and paratracheal and lateral lymph node metastasis of papillary thyroid carcinoma: A meta-analysis. *Front Oncol* (2022) 12:950047. doi: 10.3389/fonc.2022.950047

11. Kim WW, Yang SI, Kim JH, Choi YS, Park YH, Kwon SK. Experience and analysis of delphian lymph node metastasis in patients with papillary thyroid carcinoma. *World J Surg Oncol* (2012) 10:226. doi: 10.1186/1477-7819-10-226

12. Lee YC, Shin SY, Kwon KH, Eun YG. Incidence and clinical characteristics of prelaryngeal lymph node metastasis in papillary thyroid cancer. *Eur Arch Otorhinolaryngol* (2013) 270(9):2547–50. doi: 10.1007/s00405-013-2471-7

13. Zhao WJ, Luo H, Zhou YM, Dai WY, Zhu JQ. Evaluating the effectiveness of prophylactic central neck dissection with total thyroidectomy for cN0 papillary thyroid carcinoma: An updated meta-analysis. *Eur J Surg Oncol* (2017) 43(11):1989–2000. doi: 10.1016/j.ejso.2017.07.008

14. Zhao W, He L, Zhu J, Su A. A nomogram model based on the preoperative clinical characteristics of papillary thyroid carcinoma with hashimoto's thyroiditis to predict central lymph node metastasis. *Clin Endocrinol (Oxf)* (2021) 94(2):310–21. doi: 10.1111/cen.14302

15. Zheng H, Lai V, Lu J, Kang JK, Chou J, Burman KD, et al. Clinical factors predictive of lymph node metastasis in thyroid cancer patients: A multivariate analysis. *J Am Coll Surg* (2022) 234(4):691–700. doi: 10.1097/XCS.0000000000000107

16. Zhang K, Qian L, Chen J, Zhu Q, Chang C. Preoperative prediction of central cervical lymph node metastasis in fine-needle aspiration reporting suspicious papillary thyroid cancer or papillary thyroid cancer without lateral neck metastasis. *Front Oncol* (2022) 12:712723. doi: 10.3389/fonc.2022.712723

17. Chen W, Li Z, Zhu J, Lei J, Wei T. Unilateral papillary thyroid carcinoma treated with contralateral central lymph node dissection: A nomogram to aid in decision-making. *Med (Baltimore)* (2020) 99(38):e22200. doi: 10.1097/MD.0000000000022200

18. Liu N, Yang Y, Chen B, Li L, Zeng Q, Sheng L, et al. The extent of therapeutic central compartment neck dissection in unilateral cT1N1a or cT2N1a papillary thyroid carcinoma. *Cancer Manag Res* (2020) 12:12801–9. doi: 10.2147/CMAR.S273316

19. Resta L, Micheau C, Cimmino A. Prognostic value of the prelaryngeal node in laryngeal and hypopharyngeal carcinoma. *Tumori* (1985) 71(4):361–5. doi: 10.1177/030089168507100407

20. Tomik J, Skladzien J, Modrzejewski M. Evaluation of cervical lymph node metastasis of 1400 patients with cancer of the larynx. *Auris Nasus Larynx* (2001) 28 (3):233–40. doi: 10.1016/s0385-8146(00)00116-4

21. Kim DH, Kim SW, Hwang SH. Predictive value of delphian lymph node metastasis in the thyroid cancer. *Laryngoscope* (2021) 131(9):1990–6. doi: 10.1002/lary.29426

22. Iyer NG, Kumar A, Nixon IJ, Patel SG, Ganly I, Tuttle RM, et al. Incidence and significance of delphian node metastasis in papillary thyroid cancer. *Ann Surg* (2011) 253(5):988–91. doi: 10.1097/SLA.0b013e31821219ca

23. Qi Q, Xu P, Zhang C, Guo S, Huang X, Chen S, et al. Nomograms combining ultrasonic features with clinical and pathological features for estimation of delphian lymph node metastasis risk in papillary thyroid carcinoma. *Front Oncol* (2021) 11:792347. doi: 10.3389/fonc.2021.792347

24. Tavares MR, Cruz JA, Waisberg DR, Toledo SP, Takeda FR, Cernea CR, et al. Lymph node distribution in the central compartment of the neck: an anatomic study. *Head Neck* (2014) 36(10):1425–30. doi: 10.1002/hed.23469

25. Ofo E, Thavaraj S, Cope D, Barr J, Kapoor K, Jeannon JP, et al. Quantification of lymph nodes in the central compartment of the neck: a cadaveric study. *Eur Arch Otorhinolaryngol* (2016) 273(9):2773–8. doi: 10.1007/s00405-015-3827-y

26. Roh JL, Kim JM, Park CI. Central lymph node metastasis of unilateral papillary thyroid carcinoma: patterns and factors predictive of nodal metastasis, morbidity, and recurrence. *Ann Surg Oncol* (2011) 18(8):2245–50. doi: 10.1245/s10434-011-1600-z

27. Chen Q, Wei T, Wang XL, Li ZH, Du ZH, Zhu JQ. The total number of prelaryngeal and pretracheal lymph node metastases: is it a reliable predictor of contralateral central lymph node metastasis in papillary thyroid carcinoma? *J Surg Res* (2017) 214:162–7. doi: 10.1016/j.jss.2015.02.056

28. Tuttle RM, Morris LF, Haugen BR, Shah JP, Sosa JA, Rohren E, et al. *AJCC cancer staging manual, eighth edition*. New York: Springer International Publishing (2017).

29. Perrier ND, Brierley JD, Tuttle RM. Differentiated and anaplastic thyroid carcinoma: Major changes in the American joint committee on cancer eighth edition cancer staging manual. *CA Cancer J Clin* (2018) 68(1):55–63. doi: 10.3322/caac.21439

30. Wei T, Chen R, Zou X, Liu F, Li Z, Zhu J. Predictive factors of contralateral paratracheal lymph node metastasis in unilateral papillary thyroid carcinoma. *Eur J Surg Oncol* (2015) 41(6):746–50. doi: 10.1016/j.ejso.2015.02.013

31. Leboulleux S, Rubino C, Baudin E, Caillou B, Hartl DM, Bidart JM, et al. Prognostic factors for persistent or recurrent disease of papillary thyroid carcinoma with neck lymph node metastases and/or tumor extension beyond the thyroid capsule at initial diagnosis. *J Clin Endocrinol Metab* (2005) 90(10):5723–9. doi: 10.1210/jc.2005-0285

32. Shin JH, Ha TK, Park HK, Ahn MS, Kim KH, Bae KB, et al. Implication of minimal extrathyroidal extension as a prognostic factor in papillary thyroid carcinoma. *Int J Surg* (2013) 11(9):944–7. doi: 10.1016/j.ijsu.2013.06.015

33. Radowsky JS, Howard RS, Burch HB, Stojadinovic A. Impact of degree of extrathyroidal extension of disease on papillary thyroid cancer outcome. *Thyroid* (2014) 24(2):241–4. doi: 10.1089/thy.2012.0567

34. Li X, Duan Y, Liu D, Liu H, Zhou M, Yue K, et al. Diagnostic model incorporating clinicopathological characteristics of delphian lymph node metastasis risk profiles in papillary thyroid cancer. *Front Endocrinol (Lausanne)* (2021) 12:591015. doi: 10.3389/fendo.2021.591015

35. Zhu Y, Lin J, Yan Y, Zheng K, Zhang H, Wu K, et al. Delphian lymph node metastasis is a novel indicator of tumor aggressiveness and poor prognosis in papillary thyroid cancer. *J Surg Oncol* (2021) 123(7):1521–8. doi: 10.1002/jso.26380

36. Wang B, Wen XZ, Zhang W, Qiu M. Clinical implications of delphian lymph node metastasis in papillary thyroid carcinoma: a single-institution study, systemic review and meta-analysis. *J Otolaryngol Head Neck Surg* (2019) 48(1):42. doi: 10.1186/s40463-019-0362-7

frontiers | Frontiers in Endocrinology

TYPE Original Research
PUBLISHED 24 May 2023
DOI 10.3389/fendo.2023.1149826

OPEN ACCESS

EDITED BY
Emese Mezosi,
University of Pécs, Hungary

REVIEWED BY
Shi-Tong Yu,
Southern Medical University, China
Miklós Bodor,
University of Debrecen, Hungary

*CORRESPONDENCE
Tao Huang
huangtaowh@163.com
Jun Zhou
doctorzhoujun@163.com

†These authors share first authorship

RECEIVED 23 January 2023
ACCEPTED 10 May 2023
PUBLISHED 24 May 2023

CITATION
Xu M, Xi Z, Zhao Q, Yang W, Tan J, Yi P, Zhou J and Huang T (2023) Causal inference between aggressive extrathyroidal extension and survival in papillary thyroid cancer: a propensity score matching and weighting analysis. *Front. Endocrinol.* 14:1149826. doi: 10.3389/fendo.2023.1149826

Causal inference between aggressive extrathyroidal extension and survival in papillary thyroid cancer: a propensity score matching and weighting analysis

Ming Xu†, Zihan Xi†, Qiuyang Zhao, Wen Yang, Jie Tan, Pengfei Yi, Jun Zhou* and Tao Huang*

Department of Breast and Thyroid Surgery, Union Hospital, Tongji Medical College, Huazhong University of Science and Technology, Wuhan, China

Background: Extrathyroidal extension is a major risk factor for poor prognosis in papillary thyroid cancer. However, the effect of different degrees of extrathyroidal extension on prognosis remains controversial. We performed a retrospective study to elucidate how the extent of extrathyroidal extension in papillary thyroid cancer affected the clinical prognosis of patients and its covariates.

Methods: The study included 108,426 patients with papillary thyroid cancer. We categorized the extent of extension into none, capsule, strap muscles, and other organs. Three causal inference methods for retrospective studies, namely, inverse probability of treatment weighting, standardized mortality ratio weighting, and propensity score matching analysis, were used to minimize potential selection bias. Kaplan–Meier analysis and univariate Cox regression analyses were applied to analyze the precise effect of ETE on survival in papillary thyroid cancer patients.

Results: In the Kaplan–Meier survival analysis, only extrathyroidal extension into or beyond the strap muscles was statistically significant for both overall survival (OS) and thyroid cancer-specific survival (TCSS). In univariate Cox regression analyses before and after matching or weighting based on causal inference, extrathyroidal extension into soft tissues or other organs is a high-risk factor for both overall survival and thyroid cancer-specific survival. Sensitivity analysis revealed that lower overall survival was observed in patients with older age (≥55) and larger tumor size (>2 cm) of papillary thyroid cancer with extrathyroidal extension into or beyond the strap muscles.

Conclusions: Our study indicates that extrathyroidal extension into soft tissues or other organs is a high-risk factor in all papillary thyroid cancer. Even though invasion into the strap muscles did not seem to be a marker for poor prognosis, it still impaired the overall survival of patients with older age (≥55 years old) or larger tumor size (>2 cm). Further investigation is needed to confirm our results and to clarify further risk factors independent of extrathyroidal extension.

KEYWORDS

papillary thyroid cancer, extrathyroidal extension, survival analysis, Surveillance, Epidemiology, and End Results (SEER), causal inference analysis

Introduction

In papillary thyroid cancer (PTC), extrathyroidal extension (ETE) is an important risk factor for poor prognosis (1–7). ETE is defined as the primary tumor invading adjacent tissues beyond the thyroid gland (8–10). ETE has been one of the most important and controversial determinants of T stage in the AJCC staging system. In the seventh edition of AJCC staging, defined as microscopic tumor extension into skeletal muscles (i.e., strap muscles) or perithyroidal soft tissues (10), minimal ETE was considered a risk factor for prognosis. Patients with minimal ETE were classified as T3 and stage III. Gross ETE was categorized as T4 and stage IVa or IVb. These standards were revised in the eighth edition of the AJCC staging system (11–14). Minimal ETE has been removed from the staging system, demonstrating its limited impact on prognosis. Gross extension into the strap muscles only is considered T3b and stage II, while ETE into the perithyroidal soft tissues is ambiguous in the eighth edition (15). Further macroscopic extension into subcutaneous soft tissues or other organs is still marked as T4, but the stage is slightly downgraded to stage III or IVa. The change in the staging system will affect the extent of surgical resection and the decision of radioactive iodine (RAI) therapy (16, 17). Therefore, debates on the relationship between ETE and patient prognosis are necessary. It is accepted that ETE is associated with an increased risk of recurrence and death in PTC patients (3, 18–21). An analysis of more than 200,000 patients with differentiated thyroid cancer in the National Cancer Database has demonstrated that both minimal and extensive ETE are associated with adverse prognostic impact, while minimal ETE has a smaller hazard ratio (22). However, most of the studies have shown that minimal ETE does not significantly affect clinical outcomes (23–28). Gross invasion into the strap muscles and perithyroidal tissues also showed a variable influence on disease recurrence and outcome (4, 22, 29–31). Therefore, the extent of ETE still needs further investigation to help us classify patient prognosis and guide patient treatment.

Causal inference from observational studies has been a research difficulty due to the presence of covariates. In papillary thyroid cancer, extrathyroidal extension is an essential feature of poor prognosis. Researchers have explored how its extent influences patient recurrence, but extrathyroidal extension coexists with other features such as larger tumor size, multifocality, lymph node metastasis (32), etc. Their coexistence has been a confounding factor in the causal inference analysis of extrathyroidal extension. Therefore, we conducted various matching and weighting methods to investigate the true effect of ETE in papillary thyroid cancer.

In this retrospective study, we used clinical data from the Surveillance, Epidemiology, and End Results (SEER) program to investigate the effect of the extent of ETE on the survival of PTC patients. Multiple matching and weighting methods were used to control for potential covariates in the observational study to provide robust evidence for our findings. We attempted to elucidate how ETE affects patient survival and provide supportive evidence for the revision of the AJCC eighth edition on tumor staging.

Methods

Data source and selection

The National Cancer Institute's SEER program is one of the largest open cancer databases in the world (33). This retrospective study was based on data collected using SEER*Stat version 8.3.5 (http://seer.cancer.gov/seerstat/). We extracted patients diagnosed with PTC (8050/3, 8260/3, 8340/3, 8341/3, 8342/3, 8343/3, 8344/3) using the International Classification of Diseases for Oncology, Third Revision (ICD-O-3). Informed consent was not required for our work because the database is publicly available.

Patients with PTC were included according to the following inclusion criteria: 1) patients diagnosed with papillary thyroid carcinoma between 2004 and 2018, during which the extent of ETE is available; 2) papillary thyroid carcinoma was the first diagnosed primary tumor; 3) patients were followed up at least once and survival time was recorded; and 4) all covariates of interest were known and available. Patients who underwent non-specific surgery of the primary tumor or only lymph node biopsy were excluded.

Variables and outcomes

The patient characteristics we focused on were age at diagnosis, gender, tumor size, multifocality, extension, lymph node status, metastasis status, and surgical treatment including the primary tumor and lymph nodes. Age at diagnosis was divided into three groups: younger than 20 years, 20 to 54 years, and 55 years or older. Gender was dichotomized into male and female. Tumor size was classified into four groups, namely, ≤1 cm, >1 and ≤2 cm, >2 and ≤4 cm, and >4 cm, using the CS tumor size code. Multifocality was classified as solitary (code 10) or multifocal (code 20) according to CS site-specific factor 1 (solitary *vs.* multifocal tumor). Extension was classified as no extrathyroidal extension (no ETE) and extrathyroidal extension (ETE). ETE was further specified as ETE into capsule, strap muscles, soft tissues, and other organs including parathyroid gland, nerves, cartilage, sternocleidomastoid muscle, esophagus, larynx, trachea, blood vessels, and other extension into mediastinal tissues or prevertebral fascia according to the CS extension code. Lymph node status was reported as negative (N0) if no positive lymph nodes were found or positive (N1) if positive lymph nodes were found and reported in the CS lymph node code. Metastasis status was labeled as none, distant positive lymph nodes, or distant metastasis according to the CS Mets at DX code. Surgery on the primary tumor was divided into four categories, namely, no surgery, partial surgery, lobectomy, and near total/total thyroidectomy, as retrieved by the RX Summ–Surg Prim Site code. The lymph node surgery was marked as none or partial dissection as indicated by the RX Summ–Scope Reg LN Sur code. In our study, survival was defined as the time from diagnosis to the end event or last follow-up. Patients who were alive at the last follow-up were considered as right censored in the survival analysis.

Propensity scoring matching and weighting

The propensity scores, as formalized, are used to define the tendency of a patient to receive a certain treatment or characteristic, e.g., in our research, tumor extension. We calculated propensity scores using logistic regression (34). The confounders of our interest are age, gender, tumor size, multifocality, lymph node status, metastatic status, extent of surgery at the primary site, and central cervical lymph nodes. Using propensity scores, we performed propensity score matching (PSM) to reduce the influence of other covariates. Pairs of patients with or without ETE were matched using the "MatchIt" package in R. The matching method we used was the nearest method with a caliper width of 0.01 and a ratio of 1:1 without replacement. We assessed balance using standardized mean differences (SMDs) as previously reported (35).

In addition to matching, we considered alternative propensity adjustment approaches, such as inverse probability of treatment weighting (IPTW) and standardized mortality ratio weighting (SMRW). Unlike matching, these methods preserve the original sample characteristics without reducing the sample size. In IPTW, the entire population is taken as the reference population. We used stabilized weights in IPTW (36, 37) as follows:

$$We = \mathrm{Pt}/\mathrm{PS}$$

for patients with extension, and

$$Wc = (1 - \mathrm{Pt})/(1 - \mathrm{PS})$$

for the control population, where PS is the propensity score of an individual and Pt is the proportion of patients with extension in the whole population. On the contrary, in SMRW, treated patients are given a weight of 1, which means that the treated population is considered the standard population. The stabilized weights (38) we used for SMRW are as follows:

$$We = 1$$

and

$$Wc = [\mathrm{PS}(1 - \mathrm{Pt})/(1 - \mathrm{PS})\mathrm{Pt}],$$

where PS is the propensity score of an individual and Pt is the proportion of patients with extension in the whole population.

Statistical analysis

Clinicopathologic factors were compared by chi-squared test (χ^2). Survival curves were obtained by Kaplan–Meier analysis, and significance was tested by the log-rank test, except for the analysis after PSM, because the stratified log-rank test was used. Univariate Cox proportional hazards models were performed to analyze hazard ratios (HRs) and 95% confidence intervals (95% CIs) for different degrees of tumor extension. All analyses were performed using the survival and survminer packages in R (version 3.6.0). All p-values and 95% CIs were tested using two-tailed tests, and $p<0.05$ was considered statistically significant.

Results

Patients with ETE have aggressive characteristics

We identified 168,108 patients with PTC from the SEER database. According to the inclusion criteria, 108,426 patients were included in this study (Figure 1), with a median (range) follow-up of 53 months (0–143).

The patients were divided into two groups: PTC with ETE (n = 25,302, 23.3%) and PTC without ETE (n = 83,124, 76.6%). Patients with ETE were divided into four groups according to the extent of ETE: ETE in capsule, ETE in strap muscles, ETE in soft tissues, and ETE in other organs. The clinicopathologic characteristics are shown in Table 1. The results showed that patients with ETE had risk factors including older age, male over female, multifocality, larger tumor size, lymph node metastasis, distant metastasis, and more aggressive surgical treatment.

Because patients with ETE tended to have more invasive characteristics than those without, we performed additional analyses using three propensity adjustment approaches, namely,

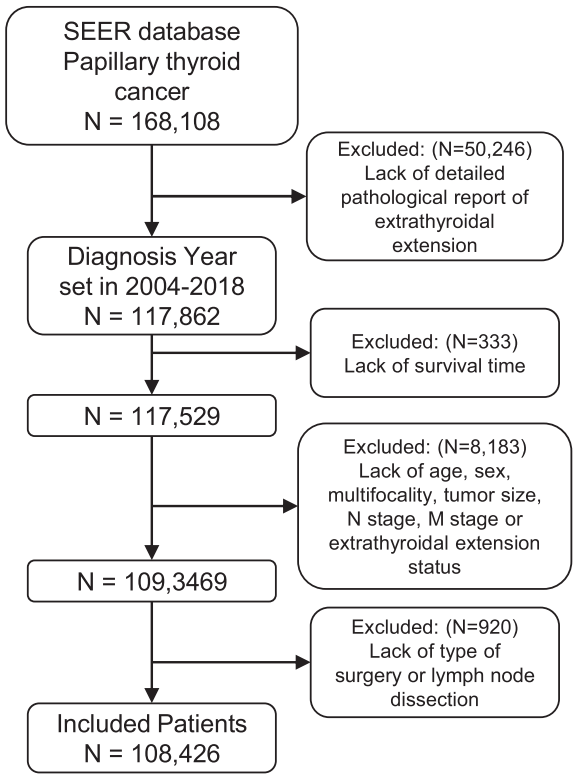

FIGURE 1
Flow diagram of patient selection for the study cohort. ICD-O-3 histology codes as follows: 8050/3 (papillary carcinoma), 8260/3 (papillary adenocarcinoma), 8340/3 (papillary carcinoma, follicular variant), 8341/3 (papillary microcarcinoma), 8342/3 (papillary carcinoma, oxyphilic cell), 8343/3 (papillary carcinoma, encapsulated), and 8344/3 (papillary carcinoma, columnar cell). SEER, Surveillance, Epidemiology, and End Results.

PSM, IPTW, and SMRW, to adjust for covariate factors. The SMD was calculated to assess the validity of the adjustment and weighting (Supplementary Figure 1). SMD<0.1 was considered to achieve a covariate balance between no ETE groups and ETE groups (34). After weighting, all covariates are balanced as shown in Table 2 and Supplementary Figure 1. The results showed that the three approaches tended to be consistent, further confirming the accuracy of these methods in reducing the influence of covariates.

Extension into the strap muscles, soft tissues, and other organs worsens patient's survival in Kaplan–Meier analysis

Kaplan–Meier survival analysis was performed to evaluate the prognostic value of different degrees of ETE in PTC patients. The OS rate of patients with ETE in the strap muscles, soft tissues, and other organs was significantly worse than that of patients without ETE (p = 0.001, p< 0.001, p< 0.001, p< 0.001), but there was no significant change in patients with ETE in the capsule (p = 0.573) (Figure 2A). Therefore, ETE into or beyond the strap muscles is a risk factor for the OS rate of thyroid cancer. At the same time, the thyroid cancer-specific survival rate of patients in the other four groups was worse than that of patients without ETE (p = 0.002, p< 0.001, p< 0.001, p< 0.001) (Figure 2B).

Survival analysis of patients after PSM showed that patients with ETE in the strap muscles and patients with ETE in soft tissues and other organs had a worse prognosis than patients without ETE in both OS (p = 0.026, p< 0.001, p< 0.001) and TCSS (p< 0.001, p< 0.001, p< 0.001, p< 0.001, Figures 2C, D). Capsular invasion was not a significant factor for patient survival in TCSS after PSM (p = 0.002 and p = 0.586 before and after PSM, respectively). These results further indicated that ETE into or beyond the strap muscles was a poor prognostic factor for both OS and TCSS using Kaplan–Meier survival analysis.

Invasion into the strap muscles shows varied effects on patients' overall and specific prognosis in univariate Cox regression analyses

We performed univariate Cox regression analysis on the four groups of patients, namely, all patients, filtered patients by PSM, weighted patients by IPTW, and weighted patients by SMRW, to calculate the hazard ratios. As shown in Figure 3, compared with patients without ETE, ETE in the capsule was not a risk factor for both OS (HR = 0.90, 95% CI = 0.79–1.04, p = 0.153, in patients after PSM; HR = 0.78, 95% CI = 0.69–0.88, p = 5.564, in patients after IPTW; HR = 0.80, 95% CI = 0.71–0.91, p< 0.001, in patients after SMRW) and TCSS (HR = 0.77, 95% CI = 0.52–1.16, p = 0.211, in patients after PSM; HR = 0.65, 95% CI = 0.43–0.98, p = 0.038, in patients after IPTW; HR = 0.58, 95% CI = 0.41–0.81, p = 0.002, in patients after SMRW). Similarly, ETE in the strap muscles was not a risk factor for OS (HR = 1.04, 95% CI = 0.91–1.18, p = 0.595, in patients after PSM; HR = 0.89, 95% CI = 0.78–1.00, p = 0.059, in patients after IPTW; HR = 1.00, 95% CI = 0.90–1.12, p = 0.998, in patients after SMRW). Compared with non-parametric analysis, Cox regression gives specific hazard ratios in the survival analysis. Therefore, we believe that strap muscle invasion was not a predictor of overall prognosis. However, ETE into the strap muscles was a high-risk factor in TCSS (HR = 1.53, 95% CI = 1.13–2.09, p = 0.007, in patients after PSM; HR = 1.43, 95% CI = 1.04–1.97, p = 0.027, in patients after IPTW; HR = 1.30, 95% CI = 1.04–1.63, p = 0.024, in patients after SMRW). ETE to soft tissues and ETE to other organs were always poor prognostic factors for both OS (HR > 1, p< 0.050) and TCSS (HR > 1, p< 0.050).

Extension into the strap muscles only affects patients' outcomes in elderly age (≥55 years old) and larger tumor size (>2 cm)

To determine the effect of the exact subgroup on the prognosis of ETE and to investigate why extension into the strap muscles had an inconsistent effect, we performed a

TABLE 1 Clinical characteristics of PTC patients with no extrathyroidal extension *versus* with extrathyroidal extensions.

Characteristics	No ETE	ETE					*p*-value*
		All ETE	Capsule	Strap muscles	Soft tissue	Other organs	
	n = 83,124	*n* = 25,302	*n* = 6,992	*n* = 8,196	*n* = 6,681	*n* = 3,433	
Age at diagnosis							<0.001
≤19 (%)	1,323 (1.6)	605 (2.4)	153 (2.2)	209 (2.6)	176 (2.6)	67 (2.0)	
20–54 (%)	51,539 (62.0)	14,756 (58.3)	4,492 (64.2)	4,830 (58.9)	3,948 (59.1)	1,486 (43.3)	
≥55 (%)	30,262 (36.4)	9,941 (39.3)	2,347 (33.6)	3,157 (38.5)	2,557 (38.3)	1,880 (54.8)	
Sex							<0.001
Female (%)	65,541 (78.8)	18,380 (72.6)	5,347 (76.5)	5,990 (73.1)	4,755 (71.2)	2,288 (66.6)	
Male (%)	17,583 (21.2)	6,922 (27.4)	1,645 (23.5)	2,206 (26.9)	1,926 (28.8)	1,145 (33.4)	
Multifocality							<0.001
Solitary (%)	50,998 (61.4)	11,918 (47.1)	3,772 (53.9)	3,575 (43.6)	2,906 (43.5)	1,665 (48.5)	
Multifocal (%)	32,126 (38.6)	13,384 (52.9)	3,220 (46.1)	4,621 (56.4)	3,775 (56.5)	1,768 (51.5)	
Tumor size							<0.001
≤1 cm (%)	41,326 (49.7)	4,375 (17.3)	1,579 (22.6)	1,437 (17.5)	1,098 (16.4)	261 (7.6)	
≤2 cm (%)	22,785 (27.4)	8,809 (34.8)	2,257 (32.3)	3,147 (38.4)	2,520 (37.7)	885 (25.8)	
≤4 cm (%)	14,673 (17.7)	8,284 (32.7)	2,205 (31.5)	2,638 (32.2)	2,131 (31.9)	1,310 (38.2)	
>4 cm (%)	4,340 (5.2)	3,834 (15.2)	951 (13.6)	974 (11.9)	932 (14.0)	977 (28.5)	
N category							<0.001
N0 (%)	69,877 (84.1)	13,524 (53.5)	5,353 (76.6)	3,907 (47.7)	3,058 (45.8)	1,206 (35.1)	
N1 (%)	13,247 (15.9)	11,778 (46.5)	1,639 (23.4)	4,289 (52.3)	3,623 (54.2)	2,227 (64.9)	
Metastasis							<0.001
None (%)	82,795 (99.6)	24,623 (97.3)	6,942 (99.3)	8,061 (98.4)	6,546 (98.0)	3,074 (89.5)	
Distant LN (%)	41 (0.0)	59 (0.2)	2 (0.0)	12 (0.1)	17 (0.3)	28 (0.8)	
Distant metastasis (%)	288 (0.3)	620 (2.5)	48 (0.7)	123 (1.5)	118 (1.8)	331 (9.6)	
Surgery							<0.001
Near TT/TT (%)	69,267 (83.3)	23,866 (94.3)	6,316 (90.3)	7,936 (96.8)	6,434 (96.3)	3,180 (92.6)	
Lobectomy (%)	12,052 (14.5)	1,206 (4.8)	640 (9.2)	232 (2.8)	226 (3.4)	108 (3.1)	
Partial (%)	686 (0.8)	105 (0.4)	29 (0.4)	21 (0.3)	14 (0.2)	41 (1.2)	
No surgery (%)	1,119 (1.3)	125 (0.5)	7 (0.1)	7 (0.1)	7 (0.1)	104 (3.0)	
LN surgery							<0.001
None (%)	44,177 (53.1)	7,869 (31.1)	3,194 (45.7)	2,099 (25.6)	1,734 (26.0)	842 (24.5)	
Partial (%)	38,947 (46.9)	17,433 (68.9)	3,798 (54.3)	6,097 (74.4)	4,947 (74.0)	2,591 (75.5)	

p-value* indicated the significance between no extrathyroidal extension and all extrathyroidal extensions.
PTC, papillary thyroid cancer; ETE, extrathyroidal extension; LN, lymph node; TT, total thyroidectomy; SMD, standardized mean difference.

subgroup analysis of all patients with respect to all factors, in which we found that age and tumor size were important factors influencing the effect of extension into the strap muscles. In the subgroup of age ≥55 years, the OS rate of patients with ETE into or beyond the strap muscles was statistically significant (p = 0.002) compared with patients without ETE (Figure 4). In contrast, extension into the strap muscles did not affect the prognosis of younger patients. Similarly, patients with ETE into or beyond the strap muscles had a lower OS rate (p< 0.001) than patients without ETE when the tumor size was greater than 2 cm, as shown in Figure 5. Extension into soft tissues did not significantly decrease the survival time of patients with papillary thyroid microcarcinoma. In conclusion, older age (≥55) and larger tumor size (>2 cm) were mainly unfavorable factors for the OS rate of PTC with ETE into or beyond the strap muscles.

TABLE 2 Propensity-matched clinical characteristics of PTC patients with no extrathyroidal extension *versus* with extrathyroidal extensions.

Characteristics	All data		SMD	After IPTW		SMD	After SMRW		SMD	After PSM		SMD
	No ETE	ETE		No ETE	ETE		No ETE	ETE		No ETE	ETE	
	n = 83,124	*n* = 25,302		*n* = 83,142	*n* = 24,953		*n* = 83,199	*n* = 25,302		*n* = 22,904	*n* = 22,904	
Age at diagnosis			0.195			0.04			0.024			0.011
≤19 (%)	1,323 (1.6)	605 (2.4)		1,476 (1.8)	447 (1.8)		1,979 (2.4)	605 (2.4)		535 (2.3)	507 (2.2)	
20–54 (%)	51,539 (62.0)	14,756 (58.3)		51,065 (61.4)	15,804 (63.3)		49,508 (59.5)	14,756 (58.3)		13,972 (61.0)	14,069 (61.4)	
≥55 (%)	30,262 (36.4)	9,941 (39.3)		30,601 (36.8)	8,702 (34.9)		31,712 (38.1)	9,941 (39.3)		8,397 (36.7)	8,328 (36.4)	
Sex			0.135			0.007			0.008			0.001
Female (%)	65,541 (78.8)	18,380 (72.6)		64,423 (77.5)	19,406 (77.8)		60,749 (73.0)	18,380 (72.6)		17,077 (74.6)	17,083 (74.6)	
Male (%)	17,583 (21.2)	6,922 (27.4)		18,719 (22.5)	5,547 (22.2)		22,450 (27.0)	6,922 (27.4)		5,827 (25.4)	5,821 (25.4)	
Multifocality			0.186			0.038			0.018			0.002
Solitary (%)	50,998 (61.4)	11,918 (47.1)		48,072 (57.8)	13,956 (55.9)		38,458 (46.2)	11,918 (47.1)		11,030 (48.2)	11,011 (48.1)	
Multifocal (%)	32,126 (38.6)	13,384 (52.9)		35,070 (42.2)	10,997 (44.1)		44,741 (53.8)	13,384 (52.9)		11,874 (51.8)	11,893 (51.9)	
Tumor size			0.535			0.026			0.011			0.007
≤1 cm (%)	41,326 (49.7)	4,375 (17.3)		35011 (42.1)	10,195 (40.9)		14,266 (17.1)	4,375 (17.3)		4,340 (18.9)	4,366 (19.1)	
≤2 cm (%)	22,785 (27.4)	8,809 (34.8)		24323 (29.3)	7,481 (30.0)		29,376 (35.3)	8,809 (34.8)		8,602 (37.6)	8,598 (37.5)	
≤4 cm (%)	14,673 (17.7)	8,284 (32.7)		17577 (21.1)	5,346 (21.4)		27,115 (32.6)	8,284 (32.7)		7,247 (31.6)	7,187 (31.4)	
>4 cm (%)	4,340 (5.2)	3,834 (15.2)		6231 (7.5)	1,931 (7.7)		12,442 (15.0)	3,834 (15.2)		2,715 (11.9)	2,753 (12.0)	
N category			0.577			0.014			0.001			0.006
N0 (%)	69,877 (84.1)	13,524 (53.5)		63,953 (76.9)	19,041 (76.3)		44,491 (53.5)	13,524 (53.5)		13,532 (59.1)	13,462 (58.8)	
N1 (%)	13,247 (15.9)	11,778 (46.5)		19,189 (23.1)	5,912 (23.7)		38,708 (46.5)	11,778 (46.5)		9,372 (40.9)	9,442 (41.2)	
Metastasis			0.218			0.004			0.006			0.011
None (%)	82,795 (99.6)	24,623 (97.3)		82,374 (99.1)	24,714 (99.0)		80,989 (97.3)	24,623 (97.3)		22,636 (98.8)	22,655 (98.9)	
Distant LN (%)	41 (0.0)	59 (0.2)		81 (0.1)	24 (0.1)		213 (0.3)	59 (0.2)		34 (0.1)	26 (0.1)	
Distant metastasis (%)	288 (0.3)	620 (2.5)		687 (0.8)	215 (0.9)		1,997 (2.4)	620 (2.5)		234 (1.0)	223 (1.0)	
Surgery			0.3			0.057			0.015			0.012
Near TT/TT (%)	69,267 (83.3)	23,866 (94.3)		71,469 (86.0)	21,871 (87.6)		78,705 (94.6)	23,866 (94.3)		21,553 (94.1)	21,515 (93.9)	
Lobectomy (%)	12,052 (14.5)	1,206 (4.8)		10,134 (12.2)	2,751 (11.0)		3,831 (4.6)	1,206 (4.8)		1,167 (5.1)	1,182 (5.2)	
Partial (%)	686 (0.8)	105 (0.4)		595 (0.7)	139 (0.6)		294 (0.4)	105 (0.4)		89 (0.4)	95 (0.4)	

(Continued)

TABLE 2 Continued

Characteristics	All data		SMD	After IPTW		SMD	After SMRW		SMD	After PSM		SMD
	No ETE	ETE		No ETE	ETE		No ETE	ETE		No ETE	ETE	
	n = 83,124	*n* = 25,302		*n* = 83,142	*n* = 24,953		*n* = 83,199	*n* = 25,302		*n* = 22,904	*n* = 22,904	
No surgery (%)	1,119 (1.3)	125 (0.5)		944 (1.1)	192 (0.8)		369 (0.4)	125 (0.5)		95 (0.4)	112 (0.5)	
LN surgery			0.33			0.028			0.001			0.005
None (%)	44,177 (53.1)	7,869 (31.1)		39,896 (48.0)	11,624 (46.6)		25,829 (31.0)	7,869 (31.1)		7,845 (34.3)	7,796 (34.0)	
Partial (%)	38,947 (46.9)	17,433 (68.9)		43,246 (52.0)	13,329 (53.4)		57,370 (69.0)	17,433 (68.9)		15,059 (65.7)	15,108 (66.0)	

SMD assessed the balance between no extrathyroidal extension and all extrathyroidal extensions.
PTC, papillary thyroid cancer; ETE, extrathyroidal extension; LN, lymph node; TT, total thyroidectomy; SMD, standardized mean difference.

Discussion

In observational studies focusing on risk characteristics of malignancy, Simpson's paradox could be a common phenomenon and severely compromise the robustness of the analysis. Several methods have been developed to eliminate the influence of covariates in causal inference. We used three statistical methods (IPTW, SMRW, PSM) to process the data in order to obtain more convincing results independent of ETE effects. During PSM, loss of analytic population is inevitable. Since ETE patients tend to have more risk factors, the matched sample from the non-ETE group tends to have similar adverse clinicopathologic features. Thus, negative effects could be inferred from the comparison between matched ETE and non-ETE samples. On the contrary, IPTW and

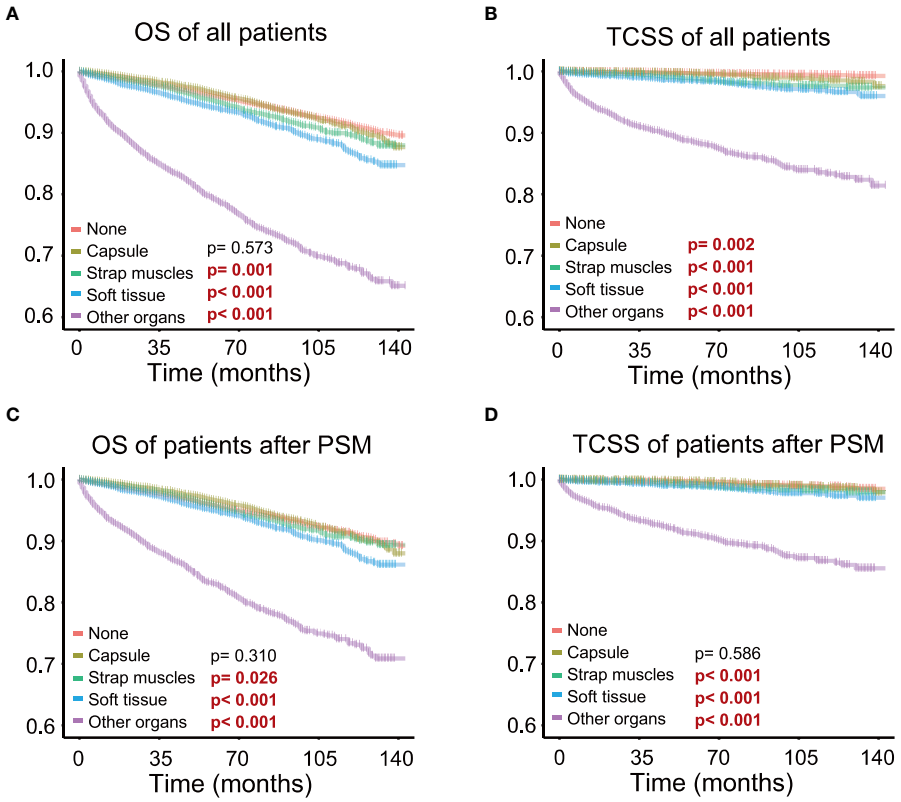

FIGURE 2
Different extents of extrathyroidal extension and survival; survival probability ranges from 0.6 to 1.0. **(A)** Extrathyroidal extension (ETE) into the strap muscles, soft tissues, and other organs all significantly impaired overall survival in all patients. **(B)** ETE into the strap muscles, soft tissues, and other organs all significantly impaired thyroid cancer-specific survival in all patients. **(C)** ETE into the strap muscles, soft tissues, and other organs all significantly impaired overall survival in patients after PSM. **(D)** ETE into the strap muscles, soft tissues, and other organs all significantly impaired thyroid cancer-specific survival in patients after PSM.

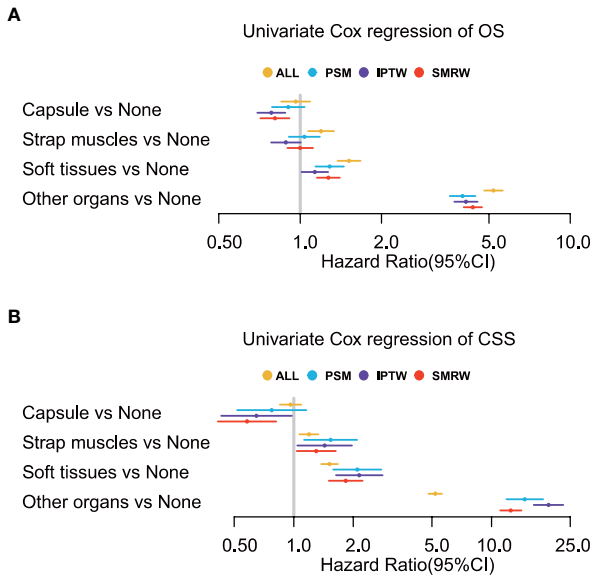

FIGURE 3
Univariate Cox regression analyses of **(A)** overall survival (OS) and **(B)** thyroid cancer-specific survival (TCSS) for the extension variables. Extension into the strap muscles is not a risk factor in OS but in TCSS.

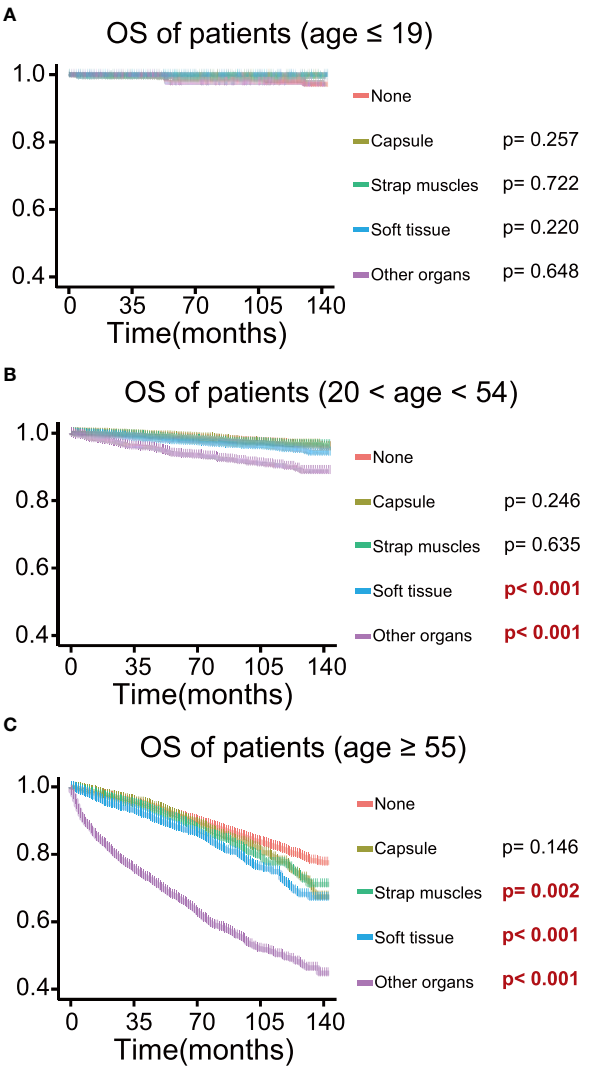

FIGURE 4
Kaplan–Meier survival curves of patients in different age groups for overall survival according to the extent of extrathyroidal extension; survival probability ranges from 0.4 to 1.0. **(A)** Age ≤ 19 group; **(B)** age 20–54 group; **(C)** age ≥ 55 group.

SMRW preserved all samples and details without a lack of representative characteristics of all thyroid cancer populations. Due to the calculation, IPTW gives the effect of the population average treatment effect (ATE), while SMRW presents the average treatment effect of the treated (ATT). In our analysis, we analyze the ETE in thyroid cancer instead of the treatment. The SMRW result better describes the potential adverse effect on the survival and prognosis of ETE patients. Importantly, the matching and weighting processes reduce bias from confounding factors, resulting in similar and robust results.

In our work, 23.3% (n = 25,302) of the patients have invasive thyroid cancer at least to the capsule. In the survival analysis before adjustment, capsular invasion is a risk factor for TCSS. After our matching and weighting process and sensitivity analysis, we clarified that capsular invasion alone could not be a prognostic marker for thyroid cancer in all subgroups.

ETE into the strap muscles was not a risk factor for OS but was still a risk factor for TCSS after adjustment. TCSS represents cancer-specific survival and better reflects the impact of thyroid cancer on individual patients. It is understandable that the small effect of strap muscles showed different effects on OS and TCSS. As shown in Figure 4, age was an important factor in the analysis of strap muscles. Age was also an essential element in the cause of death, which could lead to the different effects of strap muscles on OS and TCSS. Previous reports demonstrated that minimal ETE into the strap muscles only did not increase the risk of recurrence and death and was not considered a poor prognostic factor in PTC patients (24, 25, 30, 39–41). Regarding macroscopic extension into the strap muscles, Eyun Song et al. showed that tumor anterior extension into the strap muscles had no significant effect on disease-specific survival (4). Similarly, Genpeng Li et al. suggested that the extension of the strap muscles could not be considered as an independent predictor of recurrence in PTC patients (42). Based on these findings, some works have shown that low-dose radioiodine therapy is sufficient to treat patients with minimal or gross extension into the strap muscles (43–45). However, in a study of 596 PTC patients, both minimal and gross ETE into the strap muscles were independent risk factors for recurrence in PTC patients (46). The controversy about extension into the strap muscles may be due to the fact that the thyroid gland is only covered by an incomplete fibro-adipose connective tissue, which is histologically defined as a pseudo-capsule instead of a well-developed capsule (47). It could be explained by this phenomenon that capsular extension in thyroid cancer is not a well-defined concept nor has a significant impact on patient prognosis. The thyroid gland and strap muscles, sometimes soft tissues, migrate to each other and form a mixed area

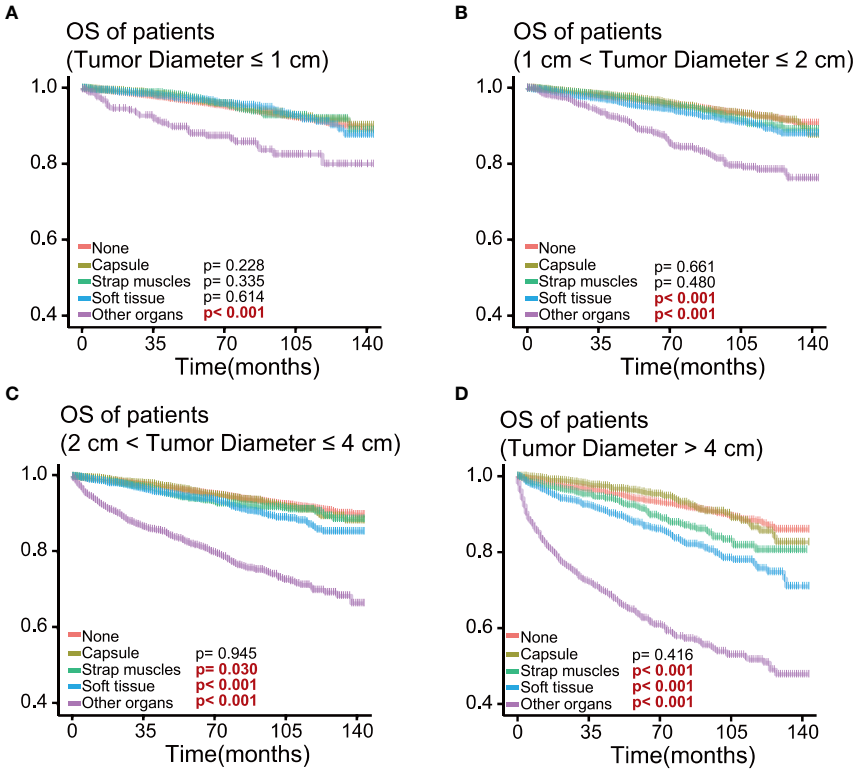

FIGURE 5
Kaplan–Meier survival curves of patients in different tumor size groups for overall survival according to the extent of extrathyroidal extension; survival probability ranges from 0.4 to 1.0. **(A)** Tumor size ≤ 1 cm group; **(B)** 1 cm< tumor size ≤ 2 cm group; **(C)** 2 cm< tumor size ≤ 4 cm group; **(D)** tumor size > 4 cm group.

microscopically (48). The mixed pathological pattern brings the difficulty of consistent diagnosis of ETE (49), which may be one reason why the research studies on strap muscles present so much diversity. However, the sensitivity analysis reminded us that older age (age ≥ 55) or larger tumor size (diameter > 2 cm) all played detrimental roles in the effect of strap muscle invasion on OS. This may suggest that patients with ETE in the strap muscles as well as older age (age ≥ 55) or larger tumor size (diameter > 2 cm) need more drastic treatment.

In our analysis, invasion into perithyroidal soft tissues or adjacent organs is a risk factor for OS and TCSS before and after adjustment. In another retrospective study involving 3,267 PTC patients, soft tissue invasion was also an aggressive phenomenon, even conferring worse survival in patients than those with lymph node metastasis (49). Taking into consideration the gross invasion of the strap muscles, we believe that the gross extension into the soft tissues should also be mentioned in the staging of thyroid cancer and should be considered as a signal for aggressive treatments, including surgery and radioiodine therapy. On the other hand, research on T4a tumors has shown that extensive ETE into adjacent organs is a significant predictor of poor prognosis (50). Our work has given supportive evidence that any extension into adjacent organs could substantially impair patient prognosis, which coordinated with other research that major neck structure invasion leads to early distant and locoregional recurrence (51). Although papillary thyroid microcarcinoma (PTMC) was considered to be less aggressive, extension to adjacent organs would still worsen the clinical survival of PTMC patients in our study and also indicated in other studies (8, 52–55). On the one hand, our work confirmed the negative effect of invasion into soft tissues and other organs on patient prognosis, and on the other hand, we proposed that age and tumor size could be taken into account when thyroid tumors only invaded the strap muscles. Specialized treatments should be carried out for different patients to promote precise and individualized treatment.

This retrospective analysis also has some limitations. We filtered out 8% of all patients (9,436 out of 117,862) because of missing values. Multiple imputations could be used to retain more samples but could introduce unknown bias. In addition, recurrence data and treatments (thyroid-stimulating hormone suppression or radioiodine therapy) were not analyzed in this work, so we are unable to report locoregional or distant recurrence or the effect of other treatments.

Conclusion

This is a retrospective study using data from the SEER database to evaluate the effect of different extents of ETE on survival in PTC patients. According to our results, ETE in soft tissues or other

organs is a high-risk factor in papillary thyroid cancer. As for PTC patients with ETE in the strap muscles, older age (≥55 years old) and larger tumor size (>2 cm) are of great importance in impaired prognosis and, thus, should be taken into consideration in the treatment option.

Data availability statement

The original contributions presented in the study are included in the article/Supplementary Material. Further inquiries can be directed to the corresponding authors.

Author contributions

MX: conceptualization, validation, formal analysis, data curation, and writing—original draft. ZX: conceptualization, visualization, data curation, and writing—original draft. QZ: investigation and writing—original draft. WY: formal analysis and data curation. PY: formal analysis and writing—review and editing. JT: methodology and visualization. JZ: validation, methodology, supervision, and writing—review and editing. TH: conceptualization, methodology, supervision, and writing—review and editing. All authors contributed to the article and approved the submitted version.

Funding

Grant No. 2021BCA142 of Key Program of Natural Science Foundation of Hubei Province. Grant No. 82002834 and Grant No. 82003207 of the National Natural Science Foundation of China.

Acknowledgments

We thank all the colleagues and tutors in Huang's team who helped us during the whole subject design. We thank Jinxin Cynthia Xi and Tong Wang for their help in the statistical analysis.

Conflict of interest

The authors declare that the research was conducted in the absence of any commercial or financial relationships that could be construed as a potential conflict of interest.

Publisher's note

Supplementary material

The Supplementary Material for this article can be found online at: https://www.frontiersin.org/articles/10.3389/fendo.2023.1149826/full#supplementary-material

SUPPLEMENTARY FIGURE 1
Standardized mean differences (SMD) comparison of propensity score matching (PSM), inverse probability of treatment weighting (IPTW) and standardized mortality ratio weighting (SMRW).

References

1. Hay ID, Bergstralh EJ, Goellner JR, Ebersold JR, Grant CS. Predicting outcome in papillary thyroid carcinoma: development of a reliable prognostic scoring system in a cohort of 1779 patients surgically treated at one institution during 1940 through 1989. *Surgery* (1993) 114(6):1050–7. doi: 10.5555/uri:pii:0039606093903214

2. McConahey WM, Hay ID, Woolner LB, van Heerden JA, Taylor WF. Papillary thyroid cancer treated at the Mayo clinic, 1946 through 1970: initial manifestations, pathologic findings, therapy, and outcome. *Mayo Clinic Proc* (1986) 61(12):978–96. doi: 10.1016/S0025-6196(12)62641-X

3. Ortiz S, Rodríguez JM, Soria T, Pérez-Flores D, Piñero A, Moreno J, et al. Extrathyroid spread in papillary carcinoma of the thyroid: clinicopathological and prognostic study. *Otolaryngology–head Neck Surg Off J Am Acad Otolaryngology-Head Neck Surg* (2001) 124(3):261–5. doi: 10.1067/mhn.2001.113141

4. Song E, Lee YM, Oh HS, Jeon MJ, Song DE, Kim TY, et al. A relook at the T stage of differentiated thyroid carcinoma with a focus on gross extrathyroidal extension. *Thyroid Off J Am Thyroid Assoc* (2019) 29(2):202–8. doi: 10.1089/thy.2018.0300

5. Russell MA, Gilbert EF, Jaeschke WF. Prognostic features of thyroid cancer. a long-term followup of 68 cases. *Cancer* (1975) 36(2):553–9. doi: 10.1002/1097-0142(197508)36:2<553::AID-CNCR2820360234>3.0.CO;2-%23

6. Carcangiu ML, Zampi G, Pupi A, Castagnoli A, Rosai J. Papillary carcinoma of the thyroid. a clinicopathologic study of 241 cases treated at the university of Florence, Italy. *Cancer* (1985) 55(4):805–28. doi: 10.1002/1097-0142(19850215)55:4<805::aid-cncr2820550419>3.0.co;2-z

7. Spires JR, Robbins KT, Luna MA, Byers RM. Metastatic papillary carcinoma of the thyroid: the significance of extranodal extension. *Head Neck* (1989) 11(3):242–6. doi: 10.1002/hed.2880110309

8. Liu L, Oh C, Heo JH, Park HS, Lee K, Chang JW, et al. Clinical significance of extrathyroidal extension according to primary tumor size in papillary thyroid carcinoma. *Eur J Surg Oncol J Eur Soc Surg Oncol Br Assoc Surg Oncol* (2018) 44 (11):1754–9. doi: 10.1016/j.ejso.2018.05.009

9. Hay ID, McConahey WM, Goellner JR. Managing patients with papillary thyroid carcinoma: insights gained from the Mayo clinic's experience of treating 2,512 consecutive patients during 1940 through 2000. *Trans Am Clin Climatol Assoc* (2002) 113:241–60.

10. Edge SB, Compton CC. The American joint committee on cancer: the 7th edition of the AJCC cancer staging manual and the future of TNM. *Ann Surg Oncol* (2010) 17(6):1471–4. doi: 10.1245/s10434-010-0985-4

11. Lamartina L, Grani G, Arvat E, Nervo A, Zatelli MC, Rossi R, et al. 8th edition of the AJCC/TNM staging system of thyroid cancer: what to expect (ITCO#2). *Endocrine-related Cancer* (2018) 25(3):L7–l11. doi: 10.1530/ERC-17-0453

12. Nam SH, Bae MR, Roh JL, Gong G, Cho KJ, Choi SH, et al. A comparison of the 7th and 8th editions of the AJCC staging system in terms of predicting recurrence and survival in patients with papillary thyroid carcinoma. *Oral Oncol* (2018) 87:158–64. doi: 10.1016/j.oraloncology.2018.11.003

13. Perrier ND, Brierley JD, Tuttle RM. Differentiated and anaplastic thyroid carcinoma: major changes in the American joint committee on cancer eighth edition cancer staging manual. *CA: Cancer J Clin* (2018) 68(1):55–63. doi: 10.3322/caac.21439

14. Tuttle RM, Haugen B, Perrier ND. Updated American joint committee on Cancer/Tumor-Node-Metastasis staging system for differentiated and anaplastic thyroid cancer (Eighth edition): what changed and why? *Thyroid Off J Am Thyroid Assoc* (2017) 27(6):751–6. doi: 10.1089/thy.2017.0102

15. Amin MB, Greene FL, Edge SB, Compton CC, Gershenwald JE, Brookland RK, et al. The eighth edition AJCC cancer staging manual: continuing to build a bridge from a population-based to a more "personalized" approach to cancer staging. *CA: Cancer J Clin* (2017) 67(2):93–9. doi: 10.3322/caac.21388

16. McHenry C, Jarosz H, Davis M, Barbato AL, Lawrence AM, Paloyan E. Selective postoperative radioactive iodine treatment of thyroid carcinoma. *Surgery* (1989) 106 (6):956–8. doi: 10.5555/uri:pii:0039606089902912

17. Jeon YW, Ahn YE, Chung WS, Choi HJ, Suh YJ. Radioactive iodine treatment for node negative papillary thyroid cancer with capsular invasion only: results of a large retrospective study. *Asia-Pacific J Clin Oncol* (2016) 12(1):e167–73. doi: 10.1111/ajco.12159

18. Bellantone R, Lombardi CP, Boscherini M, Ferrante A, Raffaelli M, Rubino F, et al. Prognostic factors in differentiated thyroid carcinoma: a multivariate analysis of 234 consecutive patients. *J Surg Oncol* (1998) 68(4):237–41. doi: 10.1002/(SICI)1096-9098(199808)68:4<237::AID-JSO6>3.0.CO;2-5

19. Siddiqui S, White MG, Antic T, Grogan RH, Angelos P, Kaplan EL, et al. Clinical and pathologic predictors of lymph node metastasis and recurrence in papillary thyroid microcarcinoma. *Thyroid Off J Am Thyroid Assoc* (2016) 26(6):807–15. doi: 10.1089/thy.2015.0429

20. Schindler AM, van Melle G, Evequoz B, Scazziga B. Prognostic factors in papillary carcinoma of the thyroid. *Cancer* (1991) 68(2):324–30. doi: 10.1002/1097-0142(19910715)68:2<324::AID-CNCR2820680220>3.0.CO;2-S

21. Akslen LA, Myking AO, Salvesen H, Varhaug JE. Prognostic importance of various clinicopathological features in papillary thyroid carcinoma. *Eur J Cancer (Oxford Engl 1990)* (1992) 29a(1):44–51. doi: 10.1016/0959-8049(93)90574-y

22. Youngwirth LM, Adam MA, Scheri RP, Roman SA, Sosa JA. Extrathyroidal extension is associated with compromised survival in patients with thyroid cancer. *Thyroid Off J Am Thyroid Assoc* (2017) 27(5):626–31. doi: 10.1089/thy.2016.0132

23. Tam S, Amit M, Boonsripitayanon M, Busaidy NL, Cabanillas ME, Waguespack SG, et al. Effect of tumor size and minimal extrathyroidal extension in patients with differentiated thyroid cancer. *Thyroid Off J Am Thyroid Assoc* (2018) 28(8):982–90. doi: 10.1089/thy.2017.0513

24. Al-Qurayshi Z, Shama MA, Randolph GW, Kandil E. Minimal extrathyroidal extension does not affect survival of well-differentiated thyroid cancer. *Endocrine-related Cancer* (2017) 24(5):221–6. doi: 10.1530/ERC-16-0509

25. Shin JH, Ha TK, Park HK, Ahn MS, Kim KH, Bae KB, et al. Implication of minimal extrathyroidal extension as a prognostic factor in papillary thyroid carcinoma. *Int J Surg (London England)* (2013) 11(9):944–7. doi: 10.1016/j.ijsu.2013.06.015

26. Moon HJ, Kim EK, Chung WY, Yoon JH, Kwak JY. Minimal extrathyroidal extension in patients with papillary thyroid microcarcinoma: is it a real prognostic factor? *Ann Surg Oncol* (2011) 18(7):1916–23. doi: 10.1245/s10434-011-1556-z

27. Woo CG, Sung CO, Choi YM, Kim WG, Kim TY, Shong YK, et al. Clinicopathological significance of minimal extrathyroid extension in solitary papillary thyroid carcinomas. *Ann Surg Oncol* (2015) 22 Suppl 3:S728–33. doi: 10.1245/s10434-015-4659-0

28. Diker-Cohen T, Hirsch D, Shimon I, Bachar G, Akirov A, Duskin-Bitan H, et al. Impact of minimal extra-thyroid extension in differentiated thyroid cancer: systematic review and meta-analysis. *J Clin Endocrinol Metab* (2018) 103(6):2100–6. doi: 10.1210/jc.2018-00081

29. Amit M, Boonsripitayanon M, Goepfert RP, Tam S, Busaidy NL, Cabanillas ME, et al. Extrathyroidal extension: does strap muscle invasion alone influence recurrence and survival in patients with differentiated thyroid cancer? *Ann Surg Oncol* (2018) 25 (11):3380–8. doi: 10.1245/s10434-018-6563-x

30. Jin BJ, Kim MK, Ji YB, Song CM, Park JH, Tae K. Characteristics and significance of minimal and maximal extrathyroidal extension in papillary thyroid carcinoma. *Oral Oncol* (2015) 51(8):759–63. doi: 10.1016/j.oraloncology.2015.05.010

31. Park SY, Kim HI, Kim JH, Kim JS, Oh YL, Kim SW, et al. Prognostic significance of gross extrathyroidal extension invading only strap muscles in differentiated thyroid carcinoma. *Br J Surg* (2018) 105(9):1155–62. doi: 10.1002/bjs.10830

32. Yu S-T, Ge J-N, Sun B-H, Wei Z-G, Xiao Z-Z, Zhang Z-C, et al. Lymph node yield in the initial central neck dissection (CND) associated with the risk of recurrence in papillary thyroid cancer: a reoperative CND cohort study. *Oral Oncol* (2021) 123:105567. doi: 10.1016/j.oraloncology.2021.105567

33. Xie J, Ying YY, Xu B, Li Y, Zhang X, Li C. Metastasis pattern and prognosis of male breast cancer patients in US: a population-based study from SEER database. *Ther Adv Med Oncol* (2019) 11:1758835919889003. doi: 10.1177/1758835919889003

34. Stürmer T, Joshi M, Glynn RJ, Avorn J, Rothman KJ, Schneeweiss S. A review of the application of propensity score methods yielded increasing use, advantages in specific settings, but not substantially different estimates compared with conventional multivariable methods. *J Clin Epidemiol* (2006) 59(5):437–47. doi: 10.1016/j.jclinepi.2005.07.004

35. Austin PC. The use of propensity score methods with survival or time-to-event outcomes: reporting measures of effect similar to those used in randomized experiments. *Stat Med* (2014) 33(7):1242–58. doi: 10.1002/sim.5984

36. Cole SR, Hernán MA. Constructing inverse probability weights for marginal structural models. *Am J Epidemiol* (2008) 168(6):656–64. doi: 10.1093/aje/kwn164

37. Hernán MA, Brumback B, Robins JM. Marginal structural models to estimate the causal effect of zidovudine on the survival of HIV-positive men. *Epidemiol (Cambridge Mass)* (2000) 11(5):561–70. doi: 10.1097/00001648-200009000-00012

38. Sato T, Matsuyama Y. Marginal structural models as a tool for standardization. *Epidemiol (Cambridge Mass)* (2003) 14(6):680–6. doi: 10.1097/01.EDE.0000081989.82616.7d

39. Ito Y, Tomoda C, Uruno T, Takamura Y, Miya A, Kobayashi K, et al. Prognostic significance of extrathyroid extension of papillary thyroid carcinoma: massive but not minimal extension affects the relapse-free survival. *World J Surg* (2006) 30(5):780–6. doi: 10.1007/s00268-005-0270-z

40. Ito Y, Tomoda C, Uruno T, Takamura Y, Miya A, Kobayashi K, et al. Minimal extrathyroid extension does not affect the relapse-free survival of patients with papillary thyroid carcinoma measuring 4 cm or less over the age of 45 years. *Surg Today* (2006) 36(1):12–8. doi: 10.1007/s00595-005-3090-8

41. Hay ID, Johnson TR, Thompson GB, Sebo TJ, Reinalda MS. Minimal extrathyroid extension in papillary thyroid carcinoma does not result in increased rates of either cause-specific mortality or postoperative tumor recurrence. *Surgery* (2016) 159(1):11–9. doi: 10.1016/j.surg.2015.05.046

42. Li G, Li R, Song L, Chen W, Jiang K, Tang H, et al. Implications of extrathyroidal extension invading only the strap muscles in papillary thyroid carcinomas. *Thyroid Off J Am Thyroid Assoc* (2020) 30(1):57–64. doi: 10.1089/thy.2018.0801

43. Park SY, Kim HI, Choi JY, Choe JH, Kim JH, Kim JS, et al. Low versus high activity radioiodine remnant ablation for differentiated thyroid carcinoma with gross extrathyroidal extension invading only strap muscles. *Oral Oncol* (2018) 84:41–5. doi: 10.1016/j.oraloncology.2018.07.002

44. Seo M, Kim YS, Lee JC, Han MW, Kim ES, Kim KB, et al. Low-dose radioactive iodine ablation is sufficient in patients with small papillary thyroid cancer having minor extrathyroidal extension and central lymph node metastasis (T3 N1a). *Clin Nucl Med* (2017) 42(11):842–6. doi: 10.1097/RLU.0000000000001812

45. Zhang Y, Liang J, Yang X, Yang K, Lin Y. Low-dose radioiodine ablation in differentiated thyroid cancer with macroscopic extrathyroidal extension and low level of preablative-stimulated thyroglobulin. *Nucl Med Commun* (2015) 36(6):553–9. doi: 10.1097/MNM.0000000000000296

46. Danilovic DLS, Castroneves LA, Suemoto CK, Elias LO, Soares IC, Camargo RY, et al. Is there a difference between minimal and gross extension into the strap muscles for the risk of recurrence in papillary thyroid carcinomas? *Thyroid Off J Am Thyroid Assoc* (2020) 30(7):1008–16. doi: 10.1089/thy.2019.0753

47. Mete O, Rotstein L, Asa SL. Controversies in thyroid pathology: thyroid capsule invasion and extrathyroidal extension. *Ann Surg Oncol* (2010) 17(2):386–91. doi: 10.1245/s10434-009-0832-7

48. Turk AT, Asa SL, Baloch ZW, Faquin WC, Fellegara G, Ghossein RA, et al. Interobserver variability in the histopathologic assessment of extrathyroidal extension of well differentiated thyroid carcinoma supports the new American joint committee on cancer eighth edition criteria for tumor staging. *Thyroid Off J Am Thyroid Assoc* (2019) 29(5):619–24. doi: 10.1089/thy.2018.0286

49. Lin JD, Hsueh C, Chao TC. Soft tissue invasion of papillary thyroid carcinoma. *Clin Exp metastas* (2016) 33(6):601–8. doi: 10.1007/s10585-016-9800-3

50. Abraham E, Roshan D, Tran B, Wykes J, Campbell P, Ebrahimi A. The extent of extrathyroidal extension is a key determinant of prognosis in T4a papillary thyroid cancer. *J Surg Oncol* (2019) 120(6):1016–22. doi: 10.1002/jso.25683

51. Moritani S. Impact of gross extrathyroidal extension into major neck structures on the prognosis of papillary thyroid carcinoma according to the American joint committee on cancer eighth edition. *Endoc J* (2020) 67(9):941–8. doi: 10.1507/endocrj.EJ19-0523

52. Ahn D, Sohn JH, Jeon JH, Jeong JY. Clinical impact of microscopic extrathyroidal extension in patients with papillary thyroid microcarcinoma treated with hemithyroidectomy. *J endocrinol Invest* (2014) 37(2):167–73. doi: 10.1007/s40618-013-0025-x

53. Lim DJ, Baek KH, Lee YS, Park WC, Kim MK, Kang MI, et al. Clinical, histopathological, and molecular characteristics of papillary thyroid microcarcinoma. *Thyroid Off J Am Thyroid Assoc* (2007) 17(9):883–8. doi: 10.1089/thy.2007.0001

54. So YK, Son YI, Hong SD, Seo MY, Baek CH, Jeong HS, et al. Subclinical lymph node metastasis in papillary thyroid microcarcinoma: a study of 551 resections. *Surgery* (2010) 148(3):526–31. doi: 10.1016/j.surg.2010.01.003

55. Kim WY, Kim HY, Son GS, Bae JW, Lee JB. Clinicopathological, immunohistochemical factors and recurrence associated with extrathyroidal extension in papillary thyroid microcarcinoma. *J Cancer Res Ther* (2014) 10(1):50–5. doi: 10.4103/0973-1482.131366

frontiers | Frontiers in Endocrinology

TYPE Original Research
PUBLISHED 26 May 2023
DOI 10.3389/fendo.2023.1140360

OPEN ACCESS

EDITED BY
Emese Mezosi,
University of Pécs, Hungary

REVIEWED BY
Yong Wang,
Chinese Academy of Medical Sciences and Peking Union Medical College, China
Zhixiang Wang,
Maastro Lab, Netherlands
Wenkun Bai,
Shanghai Jiao Tong University, China

*CORRESPONDENCE
Guo-Qing Sui
suiguoqing@jlu.edu.cn
Hui Wang
whui66@jlu.edu.cn

RECEIVED 08 January 2023
ACCEPTED 08 May 2023
PUBLISHED 26 May 2023

CITATION
Li W-H, Yu W-Y, Du J-R, Teng D-K, Lin Y-Q, Sui G-Q and Wang H (2023) Nomogram prediction for cervical lymph node metastasis in multifocal papillary thyroid microcarcinoma.
Front. Endocrinol. 14:1140360.
doi: 10.3389/fendo.2023.1140360

Nomogram prediction for cervical lymph node metastasis in multifocal papillary thyroid microcarcinoma

Wen-Hui Li, Wei-Ying Yu, Jia-Rui Du, Deng-Ke Teng, Yuan-Qiang Lin, Guo-Qing Sui* and Hui Wang*

Department of Ultrasound, China-Japan Union Hospital of Jilin University, Changchun, Jilin, China

Aim: Accurate preoperative prediction of cervical lymph node metastasis (LNM) in patients with mPTMC provides a basis for surgical decision making and the extent of tumor resection. This study aimed to develop and validate an ultrasound radiomics nomogram for the preoperative assessment of LN status.

Methods: A total of 450 patients pathologically diagnosed with mPTMC were enrolled, including 348 patients in the modeling group and 102 patients in the validation group. Univariate and multivariate logistic regression analyses were performed on the basic information, ultrasound characteristics, and American College of Radiology Thyroid Imaging Reporting and Data System (ACR TI-RADS) scores of the patients in the modeling group to identify independent risk factors for LNM in mPTMC and to construct a logistic regression equation and nomogram to predict the risk of LNM. The validation group data were used to evaluate the predictive performance of the nomogram.

Results: Male sex, age <40 years, a single lesion with a maximum diameter >0.5 cm, capsular invasion, a maximum ACR score >9 points, and a total ACR score >19 points were independent risk factors for the development of cervical LNM in mPTMC. Both the area under the curve (AUC) and concordance index (C-index) of the prediction model constructed from the above six factors were 0.838. The calibration curve of the nomogram was close to the ideal diagonal line. Furthermore, decision curve analysis (DCA) demonstrated a significantly greater net benefit of the model. The external validation demonstrated the reliability of the prediction nomogram.

Conclusions: The presented radiomics nomogram, which is based on ACR TI-RADS scores, shows favorable predictive value for the preoperative assessment of LNs in patients with mPTMC. These findings may provide a basis for surgical decision making and the extent of tumor resection.

KEYWORDS

nomogram, ultrasound radiomics, multifocal, papillary thyroid microcarcinoma, cervical lymph node metastasis

1 Introduction

According to the World Health Organization classification, papillary thyroid microcarcinoma (PTMC) is defined as papillary thyroid cancer (PTC) with a maximum diameter ≤1 cm. PTMC with ≥2 nodules is defined as multifocal papillary thyroid microcarcinoma (mPTMC), which accounts for 20-50% of PTMC.

Some studies have shown that the risk of lymph node metastasis (LNM), locoregional recurrence (LRR) or distant metastases is higher for mPTMC than for unifocal PTMC (uPTMC) (1–3), and some studies of low-risk mPTMC did not show clinical progression after long-term active surveillance (4). mPTMC has a wide variation in prognosis; therefore, its treatment is controversial (5, 6). Some studies have suggested that prophylactic central neck dissection (PCND) with total thyroidectomy (TT) is a significantly more efficient method to reduce the risk of LRR (7–10). However, some studies do not support the routine use of PCND in the treatment of patients with cN0 PTC10 because PCND + TT increased the incidence rate of temporary and permanent hypoparathyroidism and temporary laryngeal nerve injury (LNI) (5).

The 2015 American Thyroid Association (ATA) Practice Guidelines recommend that active monitoring can be implemented instead of surgical treatment for patients with low-risk mPTMC, while more aggressive surgical treatment should be adopted for patients with high-risk mPTMC (11). Cervical LNM is an important criterion for judging the risk of mPTMC and an important indicator for assessing the invasiveness and prognosis of mPTMC (1, 12).

Confronted with a disease such as mPTMC, which is highly controversial in terms of treatment modalities, physicians should focus on ways to better predict the natural history of disease (13). LNM is a breakthrough point in predicting disease regression. mPTMC with combined LNM is more aggressive than mPTMC without LNM.

LNM can be detected by auxiliary examinations, such as ultrasound and computed tomography (CT). However, due to the complexity of the neck structure, gas interference, and the small metastatic lymph node volume, the detection accuracy and sensitivity are low, and establishing a basis for clinical treatment is difficult (2, 14, 15).

In this study, mPTMC served as the study object. Univariate and multivariate logistic regression analyses were performed on the basic information, ultrasound characteristics, and American College of Radiology Thyroid Imaging Reporting and Data System (ACR TI-RADS) (16) scores of patients to Screen independent risk factors for cervical LNM in mPTMC patients. Nomograms are widely used for cancer prognosis, primarily because of their ability to reduce statistical predictive models into a single numerical estimate of the probability of an event, such as death or recurrence. Our study constructs a nomogram to predict cervical LNM in mPTMC patients through multivariate analysis results, providing guidance for clinical decision-making.

2 Materials and methods

2.1 Research subjects

This study used a single-center retrospective design, and data from all participating patients were anonymous. Therefore, this study was approved by the Research Ethics Committee, and the requirement for informed consent was waived.

Medical records from January 2019 to December 2019 were retrieved from the database of our hospital. A total of 450 eligible patients were enrolled, 348 of which were included in the modeling group, while 102 were included in the validation group.

Inclusion criteria: (1) preoperative ultrasound examination showing ≥2 suspected malignant nodules with postoperative pathological confirmation of mPTMC; (2) total thyroidectomy was performed in our hospital with central lymph node dissection (CLND) and/or lateral lymph node dissection (LLND); (3) postoperative pathological confirmation of the presence or absence of LNM; (4) no other treatment for thyroid diseases before surgery; (5) preoperative ultrasound examination results with complete images for each lesion meeting the assessment requirements; and (6) no history of head and neck radiation exposure.

Exclusion criteria: (1) a postoperative pathological type other than mPTMC or other types of thyroid cancer; (2) clinical and/or pathological detection of distant metastasis; (3) the presence of other malignant tumors; and (4) a family history of thyroid cancer or a history of other head and neck diseases.

2.2 Instruments and methods

The ultrasound examinations of all patients were independently performed by two physicians with more than 10 years of experience. A Mindray Resona 8 US unit (Mindray, China) with an L14-5 WU linear probe was used. The final diagnosis was established through consultation between the two physicians when discrepancies occurred.

Each patient was placed in the supine position, with the neck fully exposed, and thyroidectomy was performed transversely and longitudinally to avoid missing nodules. Suspicious nodules were examined by transverse and longitudinal section scanning.

In the modeling group, according to postoperative pathology and ACR TI-RADS, we recorded the following information of the PTMC which was diagnosed by postoperative pathology for each case: gender, age, number of PTMC nodules, number of thyroid lobes occupied by PTMCs, largest diameter of each PTMC, largest diameter of the case, TTD of all PTMCs, thyroid capsule invasion of each PTMC, highest ACR score and Total ACR scores and TDR. For example, the Case X is A 43-year-old male who has three nodules in both thyroid lobes. Postoperative pathology confirms that they are all PTMC. The preoperative ultrasound findings are as follows: nodule 1 (Figure 1A): Very hypoechoic echogenicity in the middle and lower left lobe, 0.40cm × 0.46cm in size, taller-than-wide in shape, irregular in margin and punctate echogenic foci is visible inside; nodule 2 (Figure 1B): Very hypoechoic echogenicity in the middle and lower left lobe, 0.62cm × 0.84cm in size (inner side adjacent to trachea), taller-than-wide in shape, irregular in margin and punctate echogenic foci visible inside; nodule 3 (Figure 1C): Very hypoechoic echogenicity at the upper pole of the right lobe, with a size of 0.34cm × 0.40cm, taller-than-wide in shape, irregular in margin and punctate echogenic foci visible inside.

The information recording process for this case is as follows: Male, 43 years old, with 3 lesions and 2 thyroid lobes were occupied

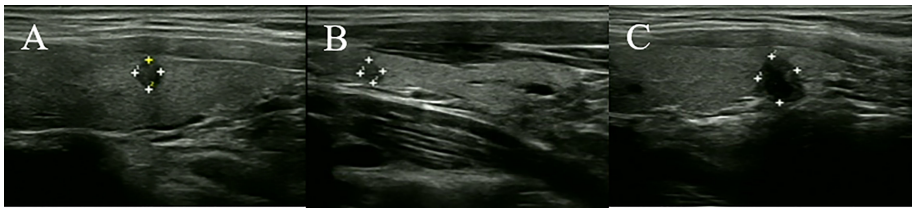

FIGURE 1
Ultrasound images of case X. **(A)** Nodule 1. **(B)** Nodule 2. **(C)** Nodule 3.

by thyroid nodules. The maximum diameter of each PTMC is 0.46cm, 0.84cm, and 0.40cm, respectively. The largest diameter of this case is 0.84cm, TTD=0.46 + 0.84 + 0.40 = 1.7cm, and there is no capsule invasion. Referring to ACR TI-RADS, the ACR scores of the three PTMCs are: 13 points, 13 points, and 13 points, respectively. Therefore, the Highest ACR score is 13 points, the Total ACR score is 13 + 13 + 36 points, and TDR=13/36 = 0.33 points. Finally, we recorded the following information for this case: male, 43 years old, 3 lesions, 2 lobes, largest diameter=0.84cm, TTD=1.7cm, no capsule invasion, highest ACR score=13 points, total ACR score=36 points, TDR=0.33. Other cases in the modeling group will collect the required information through this process and proceed to the next research and analysis.

In the validation group: First, we select TR4/TR5 nodules according to the ACR TI-RADS, and then record the following information: gender, age, number of PTMC nodules, number of thyroid lobes occurred by PTMCs, largest diameter of each PTMC, largest diameter of the case, TTD of all PTMCs, thyroid capsule invasion of each PTMC, highest ACR score, and Total ACR scores and TDR. The calculation methods such as largest diameter and TTD are the same as modeling group. The validation group information was substituted into NOMO to assess the risk of LNM and compared with postoperative pathology to evaluate the predictive efficacy of NOMO.

Receiver operating characteristic (ROC) curves were used to calculate the optimal cutoff points as the grouping basis.

According to postoperative paraffin pathology, patients without LNM were recorded as negative for LNM, and patients with LNM in the central and/or lateral cervical regions were recorded as positive for LNM.

2.3 Statistical analysis

Statistical analyses were performed using R software 4.2.0 and SPSS 27.0 software. Qualitative variables are expressed as frequencies and composition ratios. Univariate logistic regression analysis was performed on the clinical and ultrasound characteristics and ACR TI-RADS scores of the patients in the modeling group, and significant factors (P<0.1) were selected as independent variables (χ). Multivariate binary logistic regression analysis was performed, and whether the postoperative paraffin pathological results indicated LNM was used as the dependent variable (Y) to obtain independent risk factors for LNM in mPTMC. A value of P<0.05 was considered statistically significant. Based on the identified risk factors, a nomogram of risk factors associated with LNM in mPTMC was established.

The ROC curve, area under the ROC curve (AUC), concordance index (C-index), and calibration curve were used to evaluate the predictive accuracy and conformity of the model. Decision curve analysis (DCA) reflected the net benefit of the model for patients (Figure 2).

3 Results

3.1 Patient information

This study included 450 mPTMC patients with a pathological diagnosis, including a total of 1183 lesions, with 348 patients in the modeling group (901 lesions) and 102 patients in the validation group (282 lesions). The comparisons between the modeling group and validation group are summarized in Table 1.

Modeling group: The average age was 42.80 ± 9.456 years (16-68); the number of nodules ranged from 2 to 8, including 228 (65.5%) cases with 2 lesions, 68 (38%) cases with 3 lesions, 33 (9.5%) cases with 4 lesions, 10 (10%) cases with 5 lesions, 5 (1.4%) cases with 6 lesions, 3 (0.9%) cases with 7 lesions, and 1 (0.3%) case with 8 lesions; the maximum diameter range from 0.1 to 1.0cm; the average TTD was 1.0144 ± 0.47757 cm (0.2-3.3); the average Total ACR scores was 20.0 ± 8.797 points (8-67); the average TDR was 0.6162 ± 0.16813(0.13-1.00).

Validation group: The average age was 42.37 ± 9.581 years (23-68); the number of nodules ranged from 2 to 8, including 55 (53.9%) cases with 2 lesions, 24 (23.5%) cases with 3 lesions, 12 (11.8%) cases with 4 lesions, 5 (4.9%) cases with 5 lesions, 3 (2.9%) cases with 6 lesions, 2 (2.0%) cases with 7 lesions, and 1 (1.0%) case with 8 lesions; the maximum diameter range from 0.1 to 1.0cm; the average TTD was 0.9938 ± 0.46966 cm (0.2-3.3); the average Total ACR scores was 19.98 ± 9.386 points (8-61); the average TDR was 0.6087 ± 0.18346 (0.13-1.00).

We conduct a univariate analysis of the following factors: gender, age, number of PTMC nodules, number of thyroid lobes occupied by PTMCs, largest diameter of the case, TTD of all PTMCs, thyroid capsule invasion of each PTMC, highest ACR score and Total ACR scores and TDR.

10.3389/fendo.2023.1140360

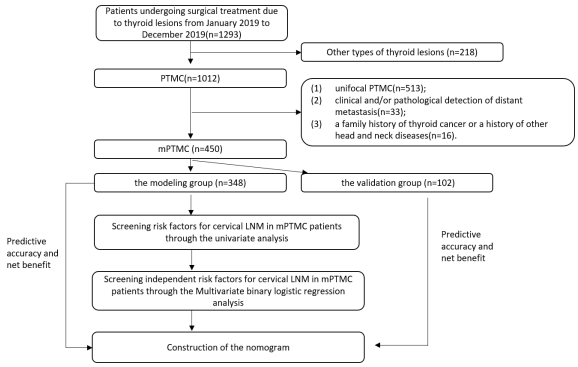

FIGURE 2
The flow chart of the whole experiment.

TABLE 1 Comparisons between modeling group and validation group.

Factor		Modeling group			Validation group			
		LNM+ (%)	LNM- (%)	Total number of cases (%)	LNM+ (%)	LNM- (%)	Total number of cases (%)	*p*
χ_1: Sex	Female	113 (38.2%)	183 (61.8%)	296(85.1%)	28 (32.6%)	58 (67.4%)	86(84.3%)	0.854
	Male	36 (69.2%)	16 (30.8%)	52(14.9%)	9(56.3%)	7 (43.8%)	16(15.7%)	
χ_2: Age	<40 years	67 (54.0%)	57 (46.0%)	124(35.6%)	23 (60.5%)	15 (39.5%)	38(37.3%)	0.696
	40-50 years	51 (33.6%)	101 (66.4%)	152(43.7%)	10 (25.0%)	30 (75.0%)	40(39.2%)	
	≥50 years	31 (43.1%)	41 (59.6%)	72(20.7%)	4(16.7%)	20 (83.3%)	24(23.5%)	
χ_3: Number of thyroid nodules	2	90 (39.5%)	138 (60.5%)	228(65.5%)	15 (27.3%)	40 (72.7%)	55(53.9%)	0.033
	>2	59 (49.2%)	61 (50.8%)	120(34.5%)	22 (46.8%)	25 (53.2%)	47(46.1%)	
χ_4: Number of thyroid lobes occupied by thyroid nodules	1	50 (44.6%)	62 (55.4%)	112(32.2%)	7(17.5%)	33 (82.5%)	40(39.2%)	<0.001
	2	95 (41.1%)	136 (58.9%)	231(66.4%)	23 (42.6%)	31 (57.4%)	54(52.9%)	
	3	4(80.0%)	1 (20.0%)	5(1.4%)	7(87.5%)	1 (12.5%)	8(7.9%)	
χ_5: Largest diameter	≤0.5 cm	43 (26.7%)	118 (73.3%)	161(46.3%)	9(19.6%)	37 (80.4%)	46(45.1%)	0.835
	>0.5 cm	106 (56.7%)	81 (43.3%)	187(53.7%)	28 (50.0%)	28 (50.0%)	56(54.9%)	
χ_6: TTD	≤0.8 cm	42 (27.6%)	110 (72.4%)	152(43.7%)	12 (25.5%)	35 (74.5%)	47(46.1%)	0.668
	>0.8 cm	107 (54.6%)	89 (45.4%)	196(56.3%)	25 (45.5%)	30 (54.5%)	55(53.9%)	
χ_7: Capsular invasion	No	74 (32.5%)	154 (67.5%)	228(65.5%)	21 (31.8%)	45 (68.2%)	66(64.7%)	0.880

(Continued)

TABLE 1 Continued

Factor		Modeling group			Validation group			
		LNM+ (%)	LNM- (%)	Total number of cases (%)	LNM+ (%)	LNM- (%)	Total number of cases (%)	*p*
	Yes	75 (62.5%)	45 (37.5%)	120(34.5%)	16 (44.4%)	20 (55.6%)	36(35.3%)	
χ_8: Highest ACR score	≤9	38 (23.5%)	124 (76.5%)	162(46.6%)	18 (36.7%)	31 (63.3%)	49(48.0%)	0.791
	>9	111 (59.7%)	75 (40.3%)	186(53.4%)	19 (35.8%)	34 (64.2%)	53(52.0%)	
χ_9: Total ACR scores	≤19	64 (31.5%)	139 (68.5%)	203(58.3%)	19 (31.7%)	41 (68.3%)	60(58.8%)	0.930
	>19	85 (58.6%)	60 (41.4%)	145(41.7%)	24 (57.1%)	18 (42.9%)	42(41.2%)	
χ_{10}: TDR	≤0.5	48 (47.1%)	54 (52.9%)	102(29.3%)	11 (35.5%)	20 (64.5%)	31(30.4%)	0.833
	>0.5	101 (41.1%)	145 (58.9%)	246(70.7%)	26 (36.6%)	45 (63.4%)	71(69.6%)	

3.2 Risk factors for cervical LNM in mPTMC patients

The univariate analysis results indicated that male sex ((χ_1) (P<0.001), age <40 years (χ_2) (P=0.004), the number of thyroid nodules (χ_3) (P=0.083), largest diameter in a single case >0.5 cm (χ_5) (P<0.001), TTD in a single case >0.8 cm (χ_6) (P<0.001), capsular invasion (χ_7) (P<0.001), total ACR score in a single case >19 points (χ_8) (P<0.001) and highest ACR score in a single case >9 points (χ_9) (P<0.001) were correlated with cervical LNM in mPTMC (P<0.1). The number of thyroid lobes occupied by thyroid nodules (χ_4) (P=0.264) and the tumor diameter ratio (TDR) (χ_{10}) (P=0.303) were not correlated with cervical LNM. The results of the univariate logistic regression analysis are shown in Table 2.

3.3 Independent risk factors for cervical LNM in mPTMC patients

Multivariate binary logistic regression analysis was performed on variables with significance in the univariate analysis, and the analysis results indicated that male sex (χ_1), age <40 years (χ_2), largest diameter >0.5 cm (χ_5), capsular invasion (χ_7), highest ACR score >9 points (χ_8), and total ACR score >19 points (χ_9) were independent risk factors for cervical LNM in mPTMC. The risk of cervical LNM in men was 3.808 times that of women (P<0.001), the risk in patients aged 40-50 years was 0.331 times that of patients aged <40 years (P<0.001), and the risk in patients aged ≥50 years was 0.451 times that of patients aged <40 years old (P=0.032), suggesting that age <40 years may be a risk factor for cervical LNM. The risk in patients whose largest tumor diameter was >0.5 cm was 4.665 times that in patients with a single lesion with a largest diameter ≤0.5 cm (P<0.001). The risk of cervical LNM in patients with capsular invasion (χ_7) was 3.773 times that in patients without capsular invasion (P<0.001). The risk in patients whose highest ACR score >9 points was 5.497 times that of patients whose highest ACR score ≤9 points (P<0.001). The risk in patients whose total ACR score >19 points (χ_9) was 1.916 times that in patients whose total ACR score ≤19 points (P=0.023). The multivariate logistic regression produced the following equation: $Y = -2.459 + 1.3371 - 1.1072(2) - 0.7972(3) + 1.5405 + 1.3287 + 1.7048 + 0.6509$. The multivariate logistic regression analysis results are shown in Table 3.

3.4 Construction of the nomogram

The nomogram was constructed based on the above six factors (R2 = 0.448, C-index=0.838) (Figure 3). For each patient, a greater number of total points indicated a higher risk of LNM. For example, if a 43-year-old man has three thyroid nodules, all with ACR TI-RADS scores of 13, with the largest diameter being 0.8 cm, and is negative for capsular invasion, then the corresponding scores would be approximately 46, 78, 100, 38, 90, and 0, respectively; for a total score of approximately 352, indicating an LNM risk of 83% for this patient. Postoperative pathological results suggesting LNM positivity would be consistent with the predicted results.

To use this nomogram in individual patients, the information for 7 (axes 2-8 axis) risk factors should be visualized as a point on the first axis. Then, the sum of these 7 points out of the total number of points should be plotted on axis 9. Then, a line is drawn downwards toward the risk axis (axis 10) to determine the likelihood of recurrence for an individual patient.

3.5 Predictive accuracy and net benefit of the nomogram

In the modeling group, the AUC was 0.838 (Figure 4A), and the calibration curve was close to the ideal diagonal line (Figure 5A). Furthermore, DCA showed a significantly greater net benefit of the

10.3389/fendo.2023.1140360

TABLE 2 Results of the univariate logistic regression analysis of risk factors for cervical LNM.

Risk factors	β	SE	χ^2	df	P	OR	95%CI	
							Lower limit	Upper limit
χ_1 Sex	1.293	0.323	15.985	1	<0.001	3.644	1.933	6.868
χ_2 Age			11.519	2	0.003			
<40 years						1		
40-50 years	-0.845	0.249	11.519	1	<0.001	0.430	0.264	0.700
≥50 years	-0.441	0.299	2.185	1	0.139	0.643	0.358	1.155
χ_3 Number of thyroid nodules	0.394	0.227	3.004	1	0.083	1.483	0.950	2.316
χ_4 Number of thyroid lobes occupied by thyroid nodules			2.666	2	0.264			
1						1		
2	-0.144	0.232	0.382	1	0.536	0.866	0.549	1.366
3	1.601	1.134	1.994	1	0.158	4.960	0.537	45.794
χ_5 Largest diameter >0.5cm	1.278	0.231	30.546	1	<0.001	3.591	2.282	5.651
χ_6 TTD >0.8cm	1.147	0.231	24.599	1	<0.001	3.149	2.001	4.954
χ_7 Capsular invasion	1.244	0.236	27.839	1	<0.001	3.468	2.185	5.505
χ_8 Highest ACR score >9 points	1.575	0.238	43.718	1	<0.001	4.829	3.028	7.702
χ_9 Total ACR scores >19 points	1.124	0.226	24.646	1	<0.001	3.077	1.974	4.795
χ_{10} TDR	-0.244	0.237	1.059	1	0.303	0.784	0.493	1.247

nomogram (Figure 6A). In addition, 102 patients from our hospital were used for external validation to test the nomogram. The AUC was 0.697 (Figure 4B), reflecting good accuracy of the nomogram. Meanwhile, the nomogram had good consistency, and the calibration curve of the validation group was also close to the ideal diagonal line (Figure 5B). Moreover, DCA also showed a significant net benefit of the nomogram in the validation group (Figure 6B). These data demonstrated that our nomogram had significant potential for clinical decision making. For example, the following results were obtained: female, 44 years old, largest diameter=0.70cm, TTD=1.1cm, no capsule invasion, highest ACR score=10 points, total ACR score=31 points. Then, the corresponding risk for LNM was 30%.

Physicians and patients can use the NOMO to predict the risk of LNM and individually assess patients more accurately to help them choose a more appropriate treatment plan.

TABLE 3 Results of multivariate logistic regression analysis of risk factors for cervical LNM.

Risk factors	β	SE	χ^2	df	P	OR	95%CI	
							Lower limit	Upper limit
χ_1 Sex	1.337	0.395	11.467	1	0.001	3.808	1.756	8.257
χ_2 Age			12.791	2	0.002			
<40 years						1		
40-50 years	-1.107	0.315	12.377	1	<0.001	0.331	0.178	0.613
≥50 years	-0.797	0.371	4.614	1	0.032	0.451	0.218	0.933
χ_5 Largest diameter>0.5cm	1.540	0.292	27.906	1	<0.001	4.665	2.634	8.261
χ_7 Capsular invasion	1.328	0.288	21.304	1	<0.001	3.773	2.147	6.631
χ_8 Highest ACR score>9 points	1.704	0.307	30.781	1	<0.001	5.497	3.010	10.036
χ_9 Total ACR scores>19 points	0.650	0.286	5.155	1	0.023	1.916	1.093	3.358
Constant	-2.459	0.371	43.847	1	<0.001	0.085		

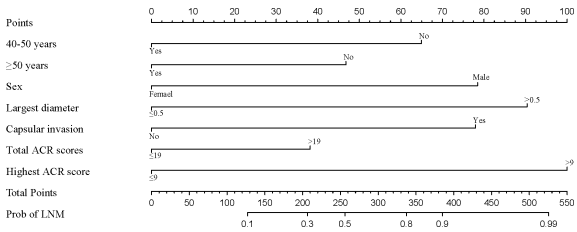

FIGURE 3
Nomogram for the prediction of LNM occurrence in mPTMC.

4 Discussion

In our study, univariate and multivariate logistic regression analyses were performed on factors that may be associated with the development of LNM in mPTMC. The analysis results indicated that male sex, age <40 years, largest diameter >0.5 cm, capsular invasion, highest ACR score >9 points, and total ACR score >19 points are independent risk factors for cervical LNM in mPTMC.

Previous studies on predictive models for the development of LNM in PTMC did not discuss uPTMC versus mPTMC separately, but their analyses also showed that male sex, age <40 years, largest diameter >0.5 cm, and capsular invasion were independent risk factors for the development of LNM in PTMC, which is consistent with the results of this study (17–22).

The TI-RADS from the ACR has been used since 2017 for the evaluation of thyroid nodules (16), which improves the diagnostic accuracy rate of thyroid nodules and has high rates of specificity (23–25). According to the ACR TI-RADS, thyroid nodules have multiple malignant features, and the assignment of different malignant features varies depending on their malignant potential. For example, if the peripheral(rim) calcifications are 2 points, and the extra-thyroidal extension is 3 points. Thyroid nodules with more suspicious features are given additional points. Those with a score greater than 7 points are classified as TR 5 and are likely to be more than 20% malignant. We consider that a higher score implies a higher malignant potential and a greater susceptibility to cervical LNM. Our study indicates that patients with highest ACR score >9 are more likely to develop cervical LNM, and this threshold value (9 points) is 2 points higher than the lower threshold value (7 points) of TR5 nodules, indicating that they have more suspicious features, have higher malignant potential, and have an increased risk of cervical LNM. This study also found that total ACR scores >19 points is associated with the risk of cervical LNM, which means that when there are more than 3 TR4 nodules in a case, the risk of cervical LNM increases. And there may also be another situation. According to ACR TI-RADS, a thyroid nodule can be rated as a maximum of 17 points. When there is a 17-point nodule in a case, adding any TR4 or TR5 nodule significantly increases the risk of cervical LNM. In summary, when the cumulative number of nodules or the cumulative suspicious features of the nodules reach the total ACR score >19, the patient has a greater susceptibility of cervical LNM.

No consensus has been established regarding whether the TTD (sum of the maximum diameter of each cancer nodule) is correlated with the incidence of central lymph node metastasis (CLNM) in PTMC (26, 27). Relevant studies have all used 10 mm as the cutoff value of TTD (28, 29). In our study, patients with multifocal cancer were divided into two groups based on whether the TTD was greater than 8 mm. This basis was selected by comparing the Youden index. The results showed no significant difference in LNM between the TTD > 0.8 cm group and TTD <0.8 cm group (P>0.005).Interestingly, in the univariate analysis, the number of

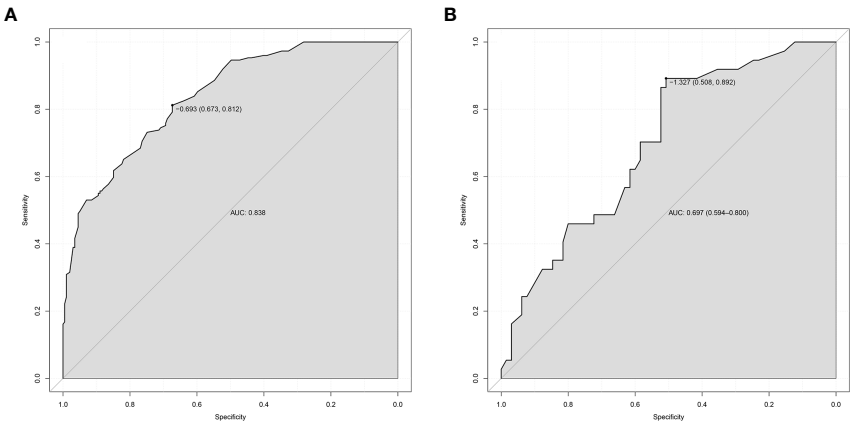

FIGURE 4
ROC curves. **(A)** Modeling group. **(B)** Validation group. ROC, receiver operating characteristic; AUC, area under the ROC curve.

10.3389/fendo.2023.1140360

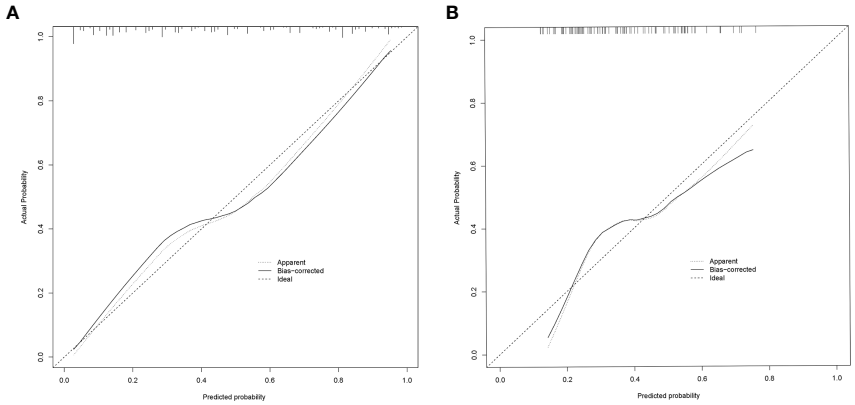

FIGURE 5
Calibration curve for predicting probability of LNM in mPTMC. **(A)** Modeling group. **(B)** Validation group; LNM, lymph node metastasis; mPTMC, multifocal papillary thyroid microcarcinoma.

thyroid nodules, number of thyroid lobes occupied by thyroid nodules and TTD >0.8 cm were significantly associated with LN status. However, they were not included in the final nomogram. We found that the strong discriminatory power of the ACR score diminished the value of those three factors in the final multivariate logistic regression analysis. The TTD is the sum of the maximum diameters of all nodules in a single case, and we suggest that it is correlated with the number of nodules in a single case. In our study, the number of nodules was also not an independent risk factor, which may explain the inconsistency between the results of this study and those of other studies. The results of this study may have occurred for the following reasons. (1) In this study, mPTMC with a TTD >8 mm had a relatively low composition ratio in the total mPTMC population (56.1%). The proportion of TTD >10 mm was only 37.9%, which was significantly lower than that in similar studies (26, 27, 30, 31). (2) In this study, after removing the primary nodules, only 9.5% of the secondary nodules had a maximum diameter >5 mm, and the remaining lesions were all <5 mm. Luo (20) suggested that cancer nodules with a maximum diameter of less than 5 mm were less likely to show enlargement or enhanced invasiveness, and related data also indicated that the incidence of CLNM was lower for cancer nodules with small diameters, which may also be one reason why no significant difference in CLNM was found between this patient type and patients with unifocal cancer.

This study shows that the number of nodules is a risk factor for LNM (P=0.083), but not an independent risk factor (P>0.05), indicating that it is associated with cervical LNM, but not an independent predictor, which is inconsistency with same type research. There are two main reasons, on the one hand, the relevant research did not separate unifocal PTMC (uPTMC) and mPTMC. However, this study excluded uPTMC and the only research object was mPTMC, which to some extent weakened the impact of the number of nodules. Another reason is that this study included features such as the total ACR scores, which is related to the number of nodules. For example, in case A, there are five PTMCs with highest ACR score of 7 points, 6 points, 7 points, 7 points, and 6 points, respectively, with a total ACR scores of 33 points; Case B has two PTMCs with highest ACR scores of 17 points and 16 points, respectively, and its total ACR scores is 33 points.

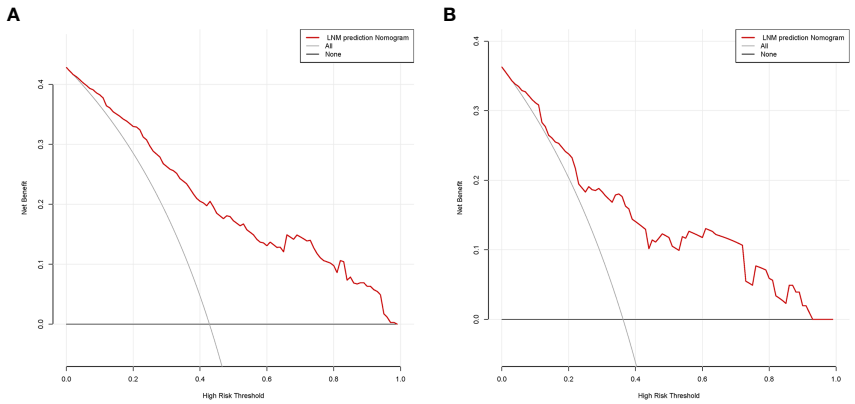

FIGURE 6
Decision curve analysis in prediction of LNM in mPTMC. **(A)** Modeling group. **(B)** Validation group. LNM, lymph node metastasis; mPTMC, multifocal papillary thyroid microcarcinoma.

According to the results of this study, the risk of LNM in both cases is consistent, but the number of lesions in case B is smaller than that in case A. The total ACR scores have weakened the impact of the number of nodules in the final model, leading to inconsistencies between the results of this study and other studies (17–22).

Our study developed and validated an ultrasound radiomics nomogram that had good accuracy and consistency, possibly because we reviewed a large amount of literature and selected risk factors that may be associated with the occurrence of LNM in mPTMC for the analysis, as much as possible, and because we constructed ROC curves for the risk factors and used the cutoff values as the basis for grouping each factor. For example, TTD was divided into >8 mm and ≤8 mm groups instead of using the 10 mm grouping criterion to avoid affecting the results of the subsequent regression analysis due to the uneven distribution of data between groups. Our nomogram can predict the risk of cervical LNM through basic patient information and ultrasound features before surgery, providing guidance for clinical treatment decisions. High risk patients receive early surgical treatment to obtain a good prognosis, while low risk patients can undergo active detection to avoid overtreatment.

Our study is innovative in several regards. First, our study distinguishes multifocal from unifocal cases. Second, our study is the first to examine mPTMC and to predict the occurrence of LNM in mPTMC. Moreover, our study introduced the ACR TI-RADS score as a risk factor.

The limitations of this study include the small number of included cases and its single-center design. The predictive performance of this model requires verification in studies with a large number of multicenter cases.

5 Conclusion

This study puts forward a radiomics nomogram, which is based on ACR TI-RADS scores, shows favorable predictive value for the preoperative assessment of LNs in patients with mPTMC. These findings may provide a basis for surgical decision making and the extent of tumor resection.

Data availability statement

The raw data supporting the conclusions of this article will be made available by the authors, without undue reservation.

Ethics statement

The studies involving human participants were reviewed and approved by Ethics Committee of the China-Japan Union Hospital of Jilin University. The patients/participants provided their written informed consent to participate in this study. Written informed consent was obtained from the individual(s) for the publication of any potentially identifiable images or data included in this article.

Author contributions

All authors listed have made a substantial, direct and intellectual contribution to the work, and approved it for publication.

Funding

This work was supported by the Finance Department of Jilin Province (Grant No. 2020SCZ08, Grant No.3D5206055430 and Grant No. 2021SCZ026).

Acknowledgments

The authors would like to thank Yan-Liu for her encouragement and support of this study.

Conflict of interest

The authors declare that the research was conducted in the absence of any commercial or financial relationships that could be construed as a potential conflict of interest.

Publisher's note

References

1. Al Afif A, Williams BA, Rigby MH, Bullock MJ, Taylor SM, Trites J, et al. Multifocal papillary thyroid cancer increases the risk of central lymph node metastasis. *Thyroid* (2015) 25(9):1008–12. doi: 10.1089/thy.2015.0130

2. Alabousi M, Alabousi A, Adham S, Pozdnyakov A, Ramadan S, Chaudhari H, et al. Diagnostic test accuracy of ultrasonography vs computed tomography for papillary thyroid cancer cervical lymph node metastasis: a systematic review and meta-analysis. *JAMA otolaryngology– Head Neck Surg* (2022) 148(2):107–18. doi: 10.1001/jamaoto.2021.3387

3. Joseph KR, Edirimanne S, Eslick GD. Multifocality as a prognostic factor in thyroid cancer: a meta-analysis. *Int J Surg (London England)* (2018) 50:121–5. doi: 10.1016/j.ijsu.2017.12.035

4. Nagaoka R, Ebina A, Toda K, Jikuzono T, Saitou M, Sen M, et al. Multifocality and progression of papillary thyroid microcarcinoma during active surveillance. *World J Surg* (2021) 45(9):2769–76. doi: 10.1007/s00268-021-06185-2

5. Kim KJ, Kim SM, Lee YS, Chung WY, Chang HS, Park CS. Prognostic significance of tumor multifocality in papillary thyroid carcinoma and its

relationship with primary tumor size: a retrospective study of 2,309 consecutive patients. *Ann Surg Oncol* (2015) 22(1):125–31. doi: 10.1245/s10434-014-3899-8

6. Sugitani I, Ito Y, Takeuchi D, Nakayama H, Masaki C, Shindo H, et al. Indications and strategy for active surveillance of adult low-risk papillary thyroid microcarcinoma: consensus statements from the Japan association of endocrine surgery task force on management for papillary thyroid microcarcinoma. *Thyroid* (2021) 31(2):183–92. doi: 10.1089/thy.2020.0330

7. Zhao WJ, Luo H, Zhou YM, Dai WY, Zhu JQ. Evaluating the effectiveness of prophylactic central neck dissection with total thyroidectomy for cN0 papillary thyroid carcinoma: an updated meta-analysis. *Eur J Surg Oncol J Eur Soc Surg Oncol Br Assoc Surg Oncol* (2017) 43(11):1989–2000. doi: 10.1016/j.ejso.2017.07.008

8. Chen L, Wu YH, Lee CH, Chen HA, Loh EW, Tam KW. Prophylactic central neck dissection for papillary thyroid carcinoma with clinically uninvolved central neck lymph nodes: a systematic review and meta-analysis. *World J Surg* (2018) 42(9):2846–57. doi: 10.1007/s00268-018-4547-4

9. Zhao W, You L, Hou X, Chen S, Ren X, Chen G, et al. The effect of prophylactic central neck dissection on locoregional recurrence in papillary thyroid cancer after total thyroidectomy: a systematic review and meta-analysis: pCND for the locoregional recurrence of papillary thyroid cancer. *Ann Surg Oncol* (2017) 24(8):2189–98. doi: 10.1245/s10434-016-5691-4

10. Dobrinja C, Troian M, Cipolat Mis T, Rebez G, Bernardi S, Fabris B, et al. Rationality in prophylactic central neck dissection in clinically node-negative (cN0) papillary thyroid carcinoma: is there anything more to say? a decade experience in a single-center. *Int J Surg (London England)* (2017) 41(Suppl 1):S40–s7. doi: 10.1016/j.ijsu.2017.01.113

11. Haugen BR, Alexander EK, Bible KC, Doherty GM, Mandel SJ, Nikiforov YE, et al. 2015 American Thyroid association management guidelines for adult patients with thyroid nodules and differentiated thyroid cancer: the American thyroid association guidelines task force on thyroid nodules and differentiated thyroid cancer. *Thyroid* (2016) 26(1):1–133. doi: 10.1089/thy.2015.0020

12. Lee X, Gao M, Ji Y, Yu Y, Feng Y, Li Y, et al. Analysis of differential BRAF (V600E) mutational status in high aggressive papillary thyroid microcarcinoma. *Ann Surg Oncol* (2009) 16(2):240–5. doi: 10.1245/s10434-008-0233-3

13. Mechanic RE, Galvin RS. Self-insured employers - the payment-reform wild card. *N Engl J Med* (2018) 379(4):308–10. doi: 10.1056/NEJMp1801544

14. Ahn JE, Lee JH, Yi JS, Shong YK, Hong SJ, Lee DH, et al. Diagnostic accuracy of CT and ultrasonography for evaluating metastatic cervical lymph nodes in patients with thyroid cancer. *World J Surg* (2008) 32(7):1552–8. doi: 10.1007/s00268-008-9588-7

15. Hwang HS, Orloff LA. Efficacy of preoperative neck ultrasound in the detection of cervical lymph node metastasis from thyroid cancer. *Laryngoscope* (2011) 121 (3):487–91. doi: 10.1002/lary.21227

16. Zhao L, Sun X, Luo Y, Wang F, Lyu Z. Clinical and pathologic predictors of lymph node metastasis in papillary thyroid microcarcinomas. *Ann Diagn Pathol* (2020) 49:151647. doi: 10.1016/j.anndiagpath.2020.151647

17. Goran M, Markovic I, Buta M, Gavrilovic D, Cvetkovic A, Santrac N, et al. The influence of papillary thyroid microcarcinomas size on the occurrence of lymph node metastases. *J BUON Off J Balkan Union Oncol* (2019) 24(5):2120–6.

18. Ito Y, Miyauchi A, Kihara M, Higashiyama T, Kobayashi K, Miya A. Patient age is significantly related to the progression of papillary microcarcinoma of the thyroid under observation. *Thyroid* (2014) 24(1):27–34. doi: 10.1089/thy.2013.0367

19. Song J, Yan T, Qiu W, Fan Y, Yang Z. Clinical analysis of risk factors for cervical lymph node metastasis in papillary thyroid microcarcinoma: a retrospective study of 3686 patients. *Cancer Manage Res* (2020) 12:2523–30. doi: 10.2147/CMAR.S250163

20. Luo Y, Zhao Y, Chen K, Shen J, Shi J, Lu S, et al. Clinical analysis of cervical lymph node metastasis risk factors in patients with papillary thyroid microcarcinoma. *J endocrinological Invest* (2019) 42(2):227–36. doi: 10.1007/s40618-018-0908-y

21. Huang Y, Yin Y, Zhou W. Risk factors for central and lateral lymph node metastases in patients with papillary thyroid micro-carcinoma: retrospective analysis on 484 cases. *Front Endocrinol* (2021) 12:640565. doi: 10.3389/fendo.2021.640565

22. Tessler FN, Middleton WD, Grant EG, Teefey SA, Abinanti N, Boschini FJ, et al. ACR thyroid imaging, reporting and data system (TI-RADS): white paper of the ACR TI-RADS committee. *J Am Coll Radiol JACR* (2017) 14(5):587–95. doi: 10.1016/j.jacr.2017.01.046

23. Griffin AS, Mitsky J, Rawal U, Bronner AJ, Tessler FN, Hoang JK. Improved quality of thyroid ultrasound reports after implementation of the ACR thyroid imaging reporting and data system nodule lexicon and risk stratification system. *J Am Coll Radiol JACR* (2018) 15(5):743–8. doi: 10.1016/j.jacr.2018.01.024

24. Hoang JK, Middleton WD, Farjat AE, Teefey SA, Abinanti N, Boschini FJ, et al. Interobserver variability of sonographic features used in the American college of radiology thyroid imaging reporting and data system. *AJR Am J Roentgenol* (2018) 211 (1):162–7. doi: 10.2214/AJR.17.19192

25. Ha EJ, Na DG, Baek JH, Sung JY, Kim JH, Kang SY. US Fine-needle aspiration biopsy for thyroid malignancy: diagnostic performance of seven society guidelines applied to 2000 thyroid nodules. *Radiology* (2018) 287(3):893–900. doi: 10.1148/radiol.2018171074

26. Zhao Q, Ming J, Liu C, Shi L, Xu X, Nie X, et al. Multifocality and total tumor diameter predict central neck lymph node metastases in papillary thyroid microcarcinoma. *Ann Surg Oncol* (2013) 20(3):746–52. doi: 10.1245/s10434-012-2654-2

27. Liu C, Wang S, Zeng W, Guo Y, Liu Z, Huang T. Total tumour diameter is superior to unifocal diameter as a predictor of papillary thyroid microcarcinoma prognosis. *Sci Rep* (2017) 7(1):1846. doi: 10.1038/s41598-017-02165-6

28. Feng JW, Pan H, Wang L, Ye J, Jiang Y, Qu Z. Total tumor diameter: the neglected value in papillary thyroid microcarcinoma. *J Endocrinol Invest* (2020) 43 (5):601–13. doi: 10.1007/s40618-019-01147-x

29. Tam AA, Ozdemir D, Ogmen BE, Fakı S, Dumlu EG, Yazgan AK, et al. Should multifocal papillary thyroid carcinomas classified as t1a with a tumor diameter sum of 1 to 2 centimeters be reclassified as T1B? *Endocr Pract* (2017) 23(5):526–35. doi: 10.4158/EP161488.OR

30. Jiang KC, Lin B, Zhang Y, Zhao LQ, Luo DC. Total tumor diameter is a better indicator of multifocal papillary thyroid microcarcinoma: a propensity score matching analysis. *Front Endocrinol* (2022) 13:974755. doi: 10.3389/fendo.2022.974755

31. Hîțu L, Ştefan PA, Piciu D. Total tumor diameter and unilateral multifocality as independent predictor factors for metastatic papillary thyroid microcarcinoma. *J Clin Med* (2021) 10(16):3707. doi: 10.3390/jcm10163707

frontiers | Frontiers in Endocrinology

TYPE Original Research
PUBLISHED 20 June 2023
DOI 10.3389/fendo.2023.1186381

OPEN ACCESS

EDITED BY
Emese Mezosi,
University of Pécs, Hungary

REVIEWED BY
Anupam Kotwal,
University of Nebraska Medical Center, United States
Ludovico Docimo,
University of Campania Luigi Vanvitelli, Italy

*CORRESPONDENCE
Xiangdong Hu
huxd2005@126.com

RECEIVED 14 March 2023
ACCEPTED 05 June 2023
PUBLISHED 20 June 2023

CITATION
Chen Q, Liu Y, Liu J, Su Y, Qian L and Hu X (2023) Development and validation of a dynamic nomogram based on conventional ultrasound and contrast-enhanced ultrasound for stratifying the risk of central lymph node metastasis in papillary thyroid carcinoma preoperatively. *Front. Endocrinol.* 14:1186381. doi: 10.3389/fendo.2023.1186381

Development and validation of a dynamic nomogram based on conventional ultrasound and contrast-enhanced ultrasound for stratifying the risk of central lymph node metastasis in papillary thyroid carcinoma preoperatively

Qiyang Chen, Yujiang Liu, Jinping Liu, Yuan Su, Linxue Qian and Xiangdong Hu*

Department of Ultrasound, Beijing Friendship Hospital, Capital Medical University, Beijing, China

Purpose: The aim of this study was to develop and validate a dynamic nomogram by combining conventional ultrasound (US) and contrast-enhanced US (CEUS) to preoperatively evaluate the probability of central lymph node metastases (CLNMs) for patients with papillary thyroid carcinoma (PTC).

Methods: A total of 216 patients with PTC confirmed pathologically were included in this retrospective and prospective study, and they were divided into the training and validation cohorts, respectively. Each cohort was divided into the CLNM (+) and CLNM (–) groups. The least absolute shrinkage and selection operator (LASSO) regression method was applied to select the most useful predictive features for CLNM in the training cohort, and these features were incorporated into a multivariate logistic regression analysis to develop the nomogram. The nomogram's discrimination, calibration, and clinical usefulness were assessed in the training and validation cohorts.

Results: In the training and validation cohorts, the dynamic nomogram (https://clnmpredictionmodel.shinyapps.io/PTCCLNM/) had an area under the receiver operator characteristic curve (AUC) of 0.844 (95% CI, 0.755–0.905) and 0.827 (95% CI, 0.747–0.906), respectively. The Hosmer–Lemeshow test and calibration curve showed that the nomogram had good calibration (p = 0.385, p = 0.285). Decision curve analysis (DCA) showed that the nomogram has more predictive value of CLNM than US or CEUS features alone in a wide range of high-

risk threshold. A Nomo-score of 0.428 as the cutoff value had a good performance to stratify high-risk and low-risk groups.

Conclusion: A dynamic nomogram combining US and CEUS features can be applied to risk stratification of CLNM in patients with PTC in clinical practice.

KEYWORDS

contrast-enhanced ultrasound (CEUS), papillary thyroid carcinoma, central lymph node metastasis, risk assessment, dynamic nomogram

1 Introduction

Papillary thyroid carcinoma (PTC) is the most common type of thyroid cancer, accounting for 80%–90% of all thyroid carcinomas (1, 2). PTC is a lymphotropic tumor, and 20%–90% of patients with PTC develop cervical lymph node metastasis (LNM), and approximately 70% of these cases involve central lymph node metastasis (CLNM) (3, 4). For patients with PTC, CLNM is an important risk factor for distant metastasis or tumor recurrence and an indicator for surgical strategy (5–8); in these cases, central compartment lymph node dissection (CLND) is recommended (9). However, preoperative identification of CLNM has been a challenge. Approximately 45% of PTC patients with clinically negative central ventricular LNs (cN0) were reported to have CLNM pathologically confirmed after surgery (10). Whether prophylactic CLND should be performed in cN0 PTC patients is still under debate, possibly raising risks of nerve injury and hypoparathyroidism (11). Therefore, accurate and noninvasive preoperative prediction of CLNM has been of increasing importance in clinical practice to optimize treatment decisions.

Conventional ultrasound (US) is the first-line modality for evaluating thyroid nodules and cervical lymph nodes (9). However, US is limited in detecting CLNM because of interference of the thyroid gland and adjacent organs. As reported, just 30.0%–53.2% of cases with CLNM could be detected by US (2, 12, 13). In recent years, some US-based imaging modalities were proposed to enhance the capability of identifying CLNM. A radiomics nomogram based on the shear wave elastography (SWE) was established by Jiang et al. (7). However, SWE has not been widely used in clinical practice.

Contrast-enhanced US (CEUS) is an imaging modality that reveals tumor microvascular perfusion through the accumulation of contrast agent microbubbles in blood vessels (14). CEUS has been widely applied to distinguish benign and malignant thyroid nodules (15, 16). Several studies reported that CEUS may be a potential tool to predict CLNM in patients with PTC (14, 17). However, most studies focused on CEUS features alone and failed to provide a feasible and generalizable prediction model.

In this study, we aimed to develop and validate a nomogram by combining US and CEUS features to facilitate preoperative risk stratification for individualizing treatment decision.

2 Materials and methods

2.1 Patients

This two-way cohort study was approved by the Ethics Committee of our hospital. The requirement for individual consent for retrospective data was waived. All patients with prospective data signed informed consent.

Patients who underwent total or partial (lobectomy or near-total thyroidectomy) thyroidectomy for PTC between January 2017 and December 2019 were retrospectively evaluated from the institutional database. From February 2021 to October 2021, we prospectively recruited PTC patients who were diagnosed by ultrasound-guided fine needle aspiration and prepared to receive surgery in our institution. Patients were enrolled according to the following inclusion criteria (1): solitary PTC was determined pathologically; (2) CLND was performed; and (3) US and CEUS were performed preoperatively. The exclusion criteria were as follows: (1) maximum tumor diameter was <5 mm (CEUS is limited by respiratory motion and volume effect); (2) US or CEUS image was incomplete or unclear; (3) skip metastases were found; and (4) history of secondary malignancy.

A total of 216 patients with pathologically confirmed PTC were included. The patients were divided into the training and validation cohorts, with a patient ratio in the training to validation cohorts of 1:1. The training cohort consisted of 108 patients (33 male and 75 female patients; mean age, 43.72 ± 12.44 years), and the validation cohort enrolled 108 patients (20 male and 88 female patients; mean age, 44.4 ± 11.48 years) who were randomly selected from the prospective data. Each cohort was divided into CLNM (+) and CLNM (−) groups according to the pathology results. Figure 1 shows the patient selection.

2.2 US and CEUS image acquisition

Training cohort images were acquired with an EPIQ5 (Philips Ultrasound, Inc., Bothell, Washington, USA) system equipped with a 5- to 12-MHz linear probe, and validation cohort images were acquired with a Resona7 (Shenzhen Mindray Bio-Medical Electronics Co., Ltd., Shenzhen, China) system equipped with a 5- to 12-MHz linear probe. US and CEUS images for individuals were

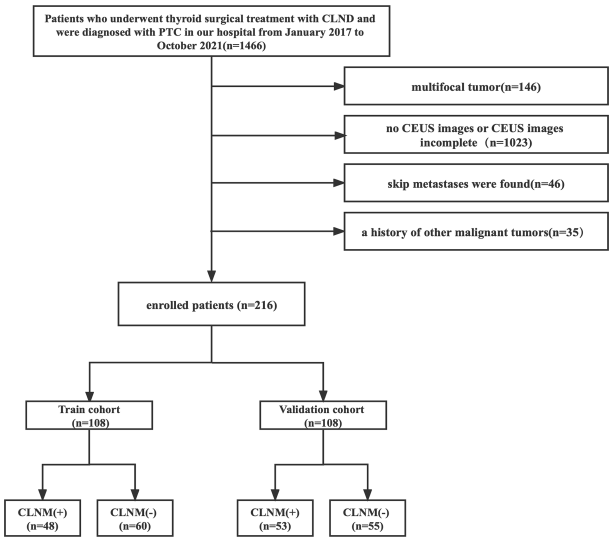

FIGURE 1
Flowchart of patient enrollment in the study.

obtained from the same instruments. SonoVue (Bracco, SpA, Milan, Italy) was used for all patients as a contrast agent with a mechanical index of 0.08 and a volume of 1.2–2.4 ml (2.4 ml in the validation cohort) when CEUS was performed. The US features of the lesion were carefully evaluated, including size, location, margin, echogenicity, aspect ratio, calcification, and contact with the capsule. The longitudinal plane with the clear lesion was selected for CEUS. The contrast agent was injected intravenously as a bolus, followed by a 5-ml saline flush (0.9% sodium chloride). All CEUS images were observed for 3 min and stored on the hard disk for further analysis.

The US and CEUS features were independently analyzed by two experienced radiologists (with more than 10 years of experience in thyroid imaging) blinded to pathological outcomes. If the radiologists disagreed, a consensus was obtained by discussion.

2.3 Conventional US image analysis

US features were characterized as follows. Size refers to the maximum tumor diameter. The location was classified into the left lobe, right lobe, and isthmus. The margin was divided into regular or irregular. Echogenicity was classified into hypoechoic, isoechoic, or hyperechoic relative to surrounding thyroid parenchyma. The aspect ratio was classified as ≤1 or >1. Contact with the capsule was described as yes or no according to whether more than 20% of the tumor was touching the thyroid capsule or an absence of echogenicity of the thyroid capsule on US.

2.4 CEUS image analysis

The CEUS qualitative parameters were defined as follows: (1) enhancement patterns (centripetal or hybrid enhancement), (2) homogeneity of enhancement (homogeneous or heterogeneous), (3) enhancement intensity (hypo-enhancement, iso-, or hyperenhancement compared with surrounding thyroid parenchyma), (4) time of wash-in (earlier or concurrent and later), (5) time of wash-out time (earlier or concurrent and later), and (6) discontinuous capsular enhancement (anterior and/or posterior hyperechoic thyroid capsular was discontinued).

The CEUS quantitative parameters were obtained by QLAB or Resona7 system software. The region of interest (ROI) was first outlined along the outer margin of the tumor, defined as ROI1. ROI2 was copied from ROI1 and outlined in the surrounding thyroid parenchyma at the same tumor depth. Two time–intensity curves (TIC) were obtained. The analysis time was the first 60 s of the dynamic CEUS images. TIC parameters included the following: (1) wash in slope (WIS), (2) time to peak (TP), (3) peak intensity (PI), and (4) area under the curve (AUC). These values were measured three times for each tumor and averaged as P_{ROI1} and P_{ROI2}. The ratio of P_{ROI1} to P_{ROI2} ($P_{ROI1}/_{ROI2}$) was used for comparison to reduce the potential effect of differences from the imaging system, image analysis software, and contrast agent doses.

2.5 Feature selection and model construction

The least absolute shrinkage and selection operator (LASSO) regression with penalty parameter tuning conducted by 10-fold cross-validation was applied in the training cohort to select useful predictive features for CLNM. Univariate and multivariate logistic analyses were performed to identify the risk factors of CLNM. The prediction model was established by combining LASSO and multivariate logistic regression analysis and presented in the form of a nomogram.

2.6 Evaluation and validation of the model

The prediction model's performance was evaluated by receiver operating characteristic (ROC) curves in the training and validation cohorts. AUC was calculated to assess the discrimination performance of the prediction model in the training and validation cohorts. Calibration of the nomogram was evaluated using the calibration curve and Hosmer–Lemeshow test.

2.7 Clinical utility of the prediction model

To estimate the predictive value of the prediction model, decision curve analysis (DCA) was performed by quantifying the net benefits at different threshold probabilities in the validation cohort.

The Nomo-score, that is, the nomogram-predicted probability, was calculated in each patient. The cutoff value of the Nomo-score was obtained through the maximum Youden index, and patients were classified as high risk and low risk using this value.

10.3389/fendo.2023.1186381

2.8 Statistical analysis

Statistical analysis was conducted with SPSS Statistics version 26.0 (IBM Corp.), R software version 4.1.0 (The R Foundation for Statistical Computing), and GraphPad Prism 9.0. Quantitative data were presented as mean ± standard deviation, and Mann–Whitney *U* tests were used for comparison. Categorical data were presented as numbers and percentages, and the chi-square test was used for comparison. The Delong test was used in ROC. The two-sided $p < 0.05$ was considered as significant difference.

3 Results

3.1 Patient characteristics

Clinical characteristics, US, and CEUS features of all patients are summarized in Table 1. Except for margin, aspect ratio, and time of wash-in, there were no differences in characteristics between the two cohorts ($p > 0.05$). The rates of CLNM were 44.4% (48/108) and 49.1% (53/108) in the training and validation cohorts, respectively, with no significant difference found between the cohorts ($p = 0.495$).

3.2 Correlation between clinical characteristics and CLNM

As shown in Table 2, sex, age, tumor size, enhancement intensity, and homogeneity of enhancement were significantly different between CLNM (+) and CLNM (−) subgroups of patients with PTC in both the training and validation cohorts ($p < 0.05$). The ROC curve showed that the best cutoff values of age and tumor size were 42 years with an AUC of 0.675 and 0.95 cm with an AUC of 0.709, respectively.

Contact with the capsule was associated with CLNM only in the training cohort ($p = 0.033$). Differences of WIS ($p = 0.001$) and PI ($p = 0.010$) between CLNM (+) and CLNM (−) groups were only observed in the validation cohort. There was no significant difference in other clinical characteristics. There were no differences of US and CEUS features between CLNM (+) and CLNM (−) patients with PTC ($p > 0.05$).

3.3 Feature selection and model construction

In the training cohort, LASSO regression analysis was performed to select the useful predictive features for CLNM, including sex, age (≤42 years), size, and enhancement intensity (Figure 2). Multivariate logistic regression analysis revealed that sex, age (≤ 42 years), size, enhancement intensity, and homogeneity of enhancement were independent risk factors for CLNM (Table 3). All these risk factors were incorporated into the prediction model

TABLE 1 Characteristics of patients in the training and validation cohorts.

Characteristics	Training cohort (*N* = 108)	Validation cohort (*N* = 108)	*p*-value
CLNM			0.495
CLNM (+)	48 (44.4%)	53 (49.1%)	
CLNM (−)	60 (55.6%)	55 (50.9%)	
Sex			0.946
Male	22 (20.4%)	20 (18.5%)	
Female	86 (79.6%)	88 (81.5%)	
Age (years)	43.6 ± 12.3	44.4 ± 11.48	0.554
>42	51 (47.2%)	55 (50.9%)	0.586
≤42	57 (52.8%)	53 (49.0%)	
Size (cm)	1.09 ± 0.53	1.04 ± 0.54	0.558
≥0.95	61 (56.5%)	48 (44.4%)	0.077
<0.95	47 (43.5%)	60 (55.6%)	
Location			0.118
Left lobe	49 (45.3%)	61 (56.5%)	
Right lobe	57 (45.3%)	47 (43.5%)	
Isthmus	2 (45.3%)	0	
Margin			<0.001
Regular	40 (37.0%)	14 (13.0%)	
Irregular	68 (63.0%)	94 (87.0%)	
Aspect ratio			0.021
>1	63 (58.3%)	46 (42.6%)	
≤1	45 (41.7%)	62 (57.4%)	
Calcification			0.111
Yes	87 (80.6%)	77 (71.3%)	
No	21 (19.4%)	31 (28.7%)	
Echogenicity			0.358
Hypoechoic	99 (91.7%)	104 (96.3%)	
Isoechoic	7 (6.5%)	3 (2.8%)	
Hyperechoic	2 (1.9%)	1 (0.9%)	
Contact with the capsule			0.761
Yes	79 (73.1%)	77 (71.3%)	
No	29 (26.9%)	31 (28.7%)	
Enhancement intensity			1.000
Hypo-enhancement	61 (56.5%)	61 (56.5%)	
Iso- or hyperenhancement	47 (43.5%)	47 (43.5%)	
Enhancement patterns			0.575

(Continued)

10.3389/fendo.2023.1186381

TABLE 1 Continued

Characteristics	Training cohort (*N* = 108)	Validation cohort (*N* = 108)	*p*-value
Centripetal enhancement	65 (60.2%)	69 (63.9%)	
Hybrid enhancement	43 (39.8%)	39 (36.1%)	
Homogeneity of enhancement			0.390
Homogeneous	34 (31.5%)	40 (37.0%)	
Heterogeneous	74 (68.5%)	68 (63.0%)	
Discontinuous capsular enhancement			0.118
Yes	33 (30.6%)	44 (40.7%)	
No	75 (69.4%)	64 (59.3%)	
Time of wash-in			<0.001
Earlier	78 (72.2%)	13 (12.0%)	
Meantime and later	30 (27.8%)	95 (88.0%)	
Time of wash-out time			0.122
Earlier	35 (32.4%)	46 (42.6%)	
Meantime and later	73 (67.6%)	62 (57.4%)	
WIS	1.05 ± 0.97	0.87 ± 0.43	0.341
TP	1.10 ± 0.43	1.16 ± 1.16	0.698
PI	0.82 ± 0.29	0.77 ± 0.33	0.176
AUC	0.82 ± 0.33	0.75 ± 0.36	0.115

(Figure 3). This prediction model is displayed as a dynamic nomogram (https://clnmpredictionmodel.shinyapps.io/PTCCLNM/).

3.4 Evaluation and validation of the prediction models

The ROC curves of the prediction model and the single ultrasonic features in the training and validation cohorts are shown in Figure 3. There was good discrimination of the prediction model in the training (AUC: 0.844, 0.773–0.915) or validation (AUC: 0.827, 0.747–0.906) cohorts (Table 4). The AUC value of the prediction model was higher compared with any single US or CEUS feature ($p < 0.05$) (Figure 4).

The calibration curve and Hosmer–Lemeshow test showed that the prediction model had good concordance in the training ($p = 0.385$) and validation ($p = 0.285$) cohorts (Figure 5).

3.5 Clinical use

The DCA results of the prediction and clinical models are presented in Figure 6. Based on the DCA results, the prediction model has a higher clinical net benefit rate than the US or CEUS features alone in predicting CLNM when the threshold probability is between 7% and 82%.

The cutoff value of the Nomo-score for the diagnosis of CLNM was ≥0.428. We divided patients into low-risk (100 patients) and high-risk groups (116 patients) using this cutoff value. Patients in the high-risk group were more likely to have CLNM ($p < 0.001$). CLNM (+) and CLNM (−) were discriminated well with a cutoff value of 0.428 in both the training and validation cohorts (Figure 7).

4 Discussion

In this study, we developed and validated a prediction model by combining US and CEUS features for evaluating the risk of CLNM in PTC patients. The prediction model presented as a dynamic nomogram was more convenient for clinical use, and it showed good diagnostic performance in both training and validation cohorts. A cutoff value derived from Nomo-score can be used for CLNM risk stratification in patients with PTC.

Only half of CLNM cases can be accurately detected by the conventional US (18–20). Some studies reported that the US features of PTC, such as calcification, taller than wide, and contact with the capsule, are related to CLNM (21, 22). However, these US features were not correlated with the CLNM in our study, likely owing to different definitions of US features among prior studies. For example, Tian et al. (23) reported that microcalcification within PTC was the strongest predictor for CLNM, and the type of microcalcification depended on its size. In contrast, we classified the microcalcification pattern as present or absent. Previous studies showed that larger tumor size was associated with an increased risk of CLNM (24). In our study, the binary variable of tumor size according to 0.95 cm was not related to CLNM in the LASSO logistic regression and multivariate logistic regression ($p = 0.175$). Considering that tumor size was associated with CLNM in both the training and validation cohorts, we incorporated tumor size into the prediction model as a continuous variable, and multivariate regression revealed a strong correlation with CLNM (OR: 4.118, $p = 0.009$).

Previous studies have shown that some US features were valuable for predicting CLNM in PTC patients, but the results were not consistent. In addition, it is difficult to predict CLNM with US alone. Therefore, we explored the value of multimodal US in the diagnosis of CLNM.

In this study, regarding the CEUS features of PTC, heterogeneous enhancement and iso- or hyperenhancement were associated with CLNM, which is consistent with some previous studies. PTC may destroy neovascular tissue when tumorous infiltration and metastasis occur, and it may cause perfusion defects as presented in heterogeneous enhancement (25). Of note, iso- or hyperenhancement is the strongest risk factor in the prediction model. Angiogenesis plays an important role in the process of tumor invasion and underlies the development, growth, and metastasis of tumor. Hyperenhancement indicates an abundant blood supply in the tumor microenvironment, which is associated with an increased risk for CLNM. Similar findings were

10.3389/fendo.2023.1186381

TABLE 2 Associations between the lymph node status and characteristics of patients in the training and validation cohorts.

Characteristics	Training cohort (*N* = 108)		*p*-value	Validation cohort (*N* = 108)		*p*-value
	CLNM (+)	CLNM (–)		CLNM (+)	CLNM (–)	
Sex			<0.001			0.038
Male	18 (37.5%)	4 (6.70%)		14 (26.4%)	6 (10.9%)	
Female	30 (62.5%)	56 (93.3%)		39 (73.6%)	49 (89.1%)	
Age (years)	39.63 ± 11.89	47.00 ± 11.99	0.002	39.85 ± 11.03	48.82 ± 10.18	<0.001
>42	13 (27.1%)	38 (63.3%)	<0.001	17 (32.1%)	38 (69.1%)	<0.001
≤42	35 (72.9%)	22 (36.7%)		36 (67.9%)	17 (30.9%)	
Size (cm)	1.33 ± 0.65	0.91 ± 0.37	<0.001	1.23 ± 0.59	0.86 ± 0.41	<0.001
≥0.95	32 (66.7%)	19 (31.7%)	<0.001	31 (58.5%)	17 (30.9%)	0.004
<0.95	16 (33.3%)	41 (68.3%)		22 (41.5%)	38 (69.1%)	
Location			0.948			0.679
Left lobe	21 (43.8%)	28 (46.7%)		22 (41.5%)	25 (45.5%)	
Right lobe	26 (54.2%)	31 (51.7%)		31 (58.5%)	30 (54.5%)	
Isthmus	1 (2.1%)	1 (1.7%)		0	0	
Margin			0.265			0.073
Regular	15 (31.3%)	25 (41.7%)		10 (18.9%)	4 (7.3%)	
Irregular	33 (68.8%)	35 (58.3%)		43 (81.1%)	51 (92.7%)	
Aspect ratio			0.116			0.823
>1	24 (50%)	39 (65.0%)		22 (41.5%)	24 (43.6%)	
≤1	24 (50%)	21 (35.0%)		31 (58.5%)	31 (56.4%)	
Calcification			0.174			0.172
Yes	43 (89.6%)	48 (80.0%)		41 (77.4%)	36 (65.5%)	
No	5 (10.4%)	12 (20.0%)		12 (22.6%)	19 (34.5%)	
Echogenicity			0.324			0.484
Hypoechoic	42 (87.5%)	57 (95.0%)		50 (94.3%)	54 (98.2%)	
Isoechoic	5 (10.4%)	2 (3.3%)		2 (3.8%)	1 (1.8%)	
Hyperechoic	1 (2.1%)	1 (1.7%)		1 (1.9%)	0	
Contact with the capsule			0.033			0.606
Yes	40 (83.3%)	39 (65.0%)		39 (73.6%)	38 (69.1%)	
No	8 (16.7%)	21 (35.0%)		14 (26.4%)	17 (30.9%)	
Enhancement intensity			0.002			0.004
Hypo-enhancement	19 (39.6%)	42 (70.0%)		20 (37.7%)	36 (65.5%)	
Iso-or hyperenhancement	29 (60.4%)	18 (30.0%)		33 (62.3%)	19 (34.5%)	
Enhancement patterns			0.455			0.956
Centripetal enhancement	27 (56.3%)	38 (63.3%)		34 (64.2%)	35 (63.6%)	
Hybrid enhancement	21 (43.8%)	22 (36.7%)		19 (35.85)	20 (36.4%)	
Homogeneity of enhancement			0.033			0.065
Homogeneous	10 (20.8%)	24 (40.0%)		15 (28.3%)	25 (45.5%)	

(Continued)

TABLE 2 Continued

Characteristics	Training cohort (*N* = 108)		*p*-value	Validation cohort (*N* = 108)		*p*-value
	CLNM (+)	CLNM (–)		CLNM (+)	CLNM (–)	
Heterogeneous	38 (79.2%)	36 (60.0%)		38 (71.7%)	30 (54.5%)	
Discontinuous capsular enhancement			0.161			0.250
Yes	18 (37.5%)	15 (25.0%)		29 (54.7%)	24 (43.6%)	
No	30 (62.5%)	45 (75.0%)		24 (45.2%)	31 (56.4%)	
Time of wash-in			0.547			0.032
Earlier	22 (45.8%)	31 (51.7%)		10 (18.9%)	3 (5.5%)	
Meantime and later	26 (54.2%)	29 (48.3%)		43 (81.1%)	52 (94.5%)	
Time of wash-out time			0.29			0.035
Earlier	13 (27.1%)	22 (36.7%)		28 (52.8%)	18 (21.8%)	
Meantime and later	35 (72.9%)	38 (63.3%)		25 (47.2%)	37 (67.3%)	
WIS	1.059 ± 0.976	1.037 ± 0.966	0.956	1.00 ± 0.50	0.74 ± 0.31	0.001
TP	1.072 ± 0.317	1.123 ± 0.509	0.466	1.29 ± 1.88	1.03 ± 0.42	0.799
PI	0.850 ± 0.325	0.802 ± 0.255	0.214	0.86 ± 0.37	0.69 ± 0.28	0.010
AUC	0.819 ± 0.329	0.825 ± 0.341	0.625	0.82 ± 0.40	0.68 ± 0.31	0.089

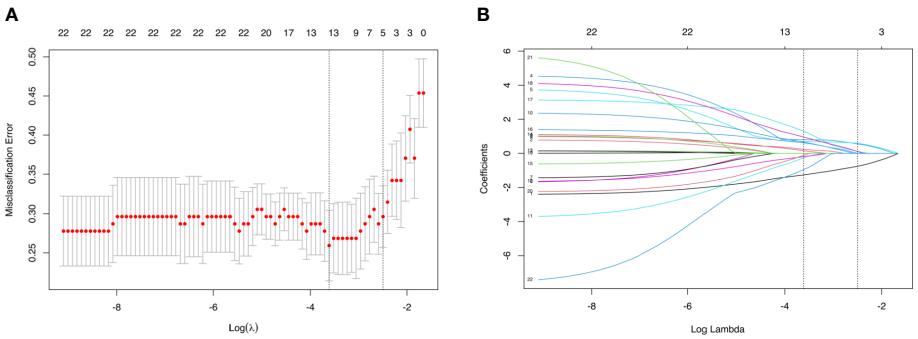

FIGURE 2
Parameters of prediction model selection using the LASSO logistic regression model in the training cohort. **(A)** The area under the receiver operating characteristic curve was plotted versus log (λ). **(B)** The features were profiled by the LASSO coefficient.

TABLE 3 Risk factors for cervical lymph node metastasis in the prediction model.

Intercept and variables	β	OR	95% CI	*p*-value
Sex	1.720	0.179	1.531–20.377	0.009
Age	1.102	3.010	1.097–8.263	0.032
Size	1.415	4.118	1.421–11.932	0.009
Peak Intensity	1.138	3.119	1.031–9.434	0.044
Degree of homogeneity	1.507	4.511	1.309–15.550	0.017
Intercept	−4.260	0.014	——	0.000

CI, confidence interval; β, regression coefficient; OR, odds ratio.

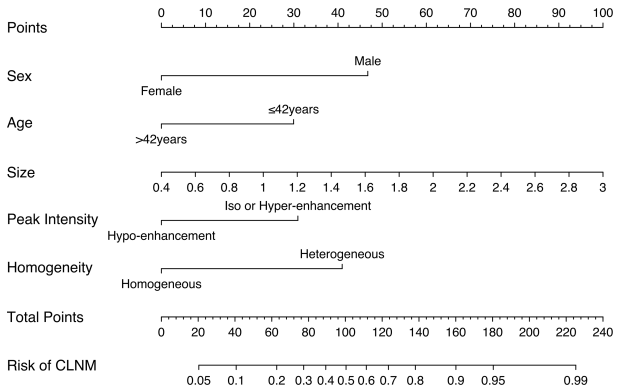

FIGURE 3
Nomogram of the prediction model to assess the risk of CLNM in patients with PTC.

TABLE 4 Performance of prediction model and the single US and CEUS features in the training and validation cohorts.

	Training cohort			Validation cohort		
	Sensitivity	Specificity	vAUC (95% CI)	Sensitivity	Specificity	AUC (95% CI)
Prediction model	81.3%	75.0%	0.844 (0.755–0.905)	77.4%	78.2%	0.827 (0.747–0.906)
Size	66.7%	68.3%	0.709 (0.609–0.810)	54.7%	78.2%	0.720 (0.625–0.814)
Peak INTENSITY	60.4%	70.0%	0.652 (0.547–0.757)	62.3%	65.5%	0.639 (0.533–0.744)
Degree of homogeneity	79.2%	40.0%	0.596 (0.489–0.703)	71.7%	45.5%	0.586 (0.478–0.693)

AUC, area under the curve; CI, confidence interval.

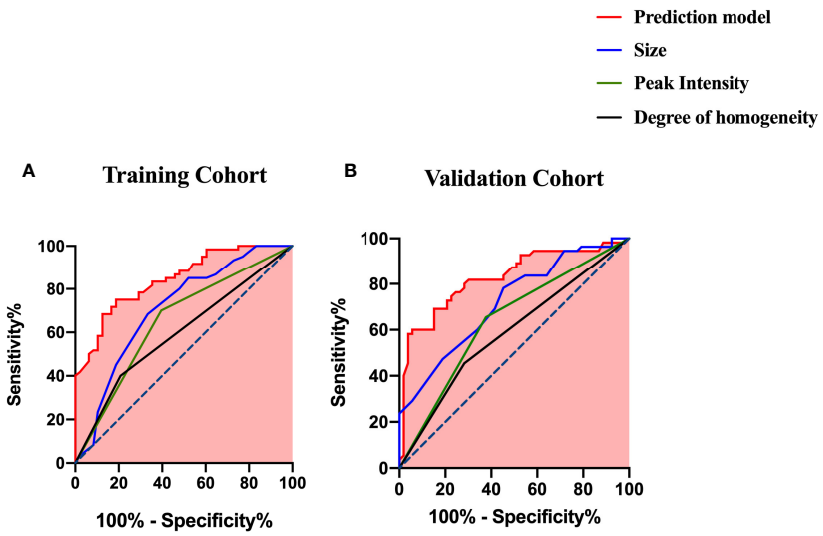

FIGURE 4
ROC curves of the prediction model and the single US and CEUS features for predicting CLNM **(A)** in the training cohort and **(B)** in the validation cohort.

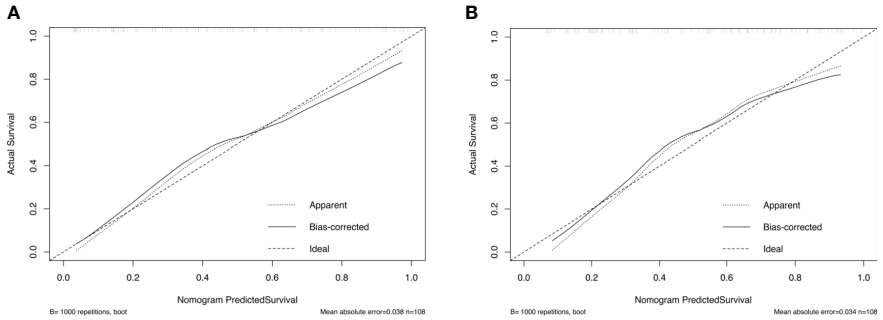

FIGURE 5
Calibration curves of the nomogram in the training **(A)** and validation **(B)** cohorts.

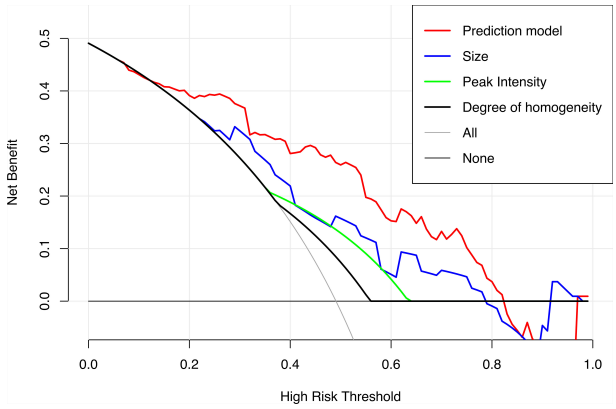

FIGURE 6
Decision curves of the prediction model and the single US and CEUS features in predicting CLNM for papillary thyroid carcinoma.

found in high-grade breast tumors (26). As previously reported, some CEUS quantitative parameters can be applied to predict the risk of CLNM in PTC patients. We also analyzed quantitative parameters such as WIS, TP, PI, and AUC. In the training cohort, the PI and WIS were higher in patients with PTC who had CLNM than in patients without CLNM, but the difference was not statistically significant ($p > 0.05$). Tao et al. (14) reported that PI was an independent risk factor of CLNM. Considering PI value is likely related to tumor microvessel density, further showing angiogenesis' important role in the development and metastases of tumors (27). However, limited sample in this study leads to the cautious interpretation of the results; thus, further study is required.

In the present study, younger age and male were related to a higher risk of CLNM in PTC patients, consistent with other studies (28, 29). Ning et al. (30) suggested that younger age may indicate a higher biological aggressiveness of tumor. Our study concluded that PTC patients who are less than 42 years old are prone to have CLNM, with an age cutoff value close to the value suggested by Tian et al. (≤40 years old). Accumulating evidence has shown an association between being male and a poor prognosis of PTC, but the results have been inconsistent (31–33).

We used LASSO and multivariate logistic regression in this study to select features. Our prediction model combining US, CEUS features, and clinical factors showed better diagnostic efficiency compared with the single ultrasonic imaging features in both training and validation cohorts. According to the DCA curve, the application of the prediction model could benefit patients more than a treat-none or treat-all strategy when the threshold probability was between 7% and 82%. We also established a risk stratification criterion based on the Nomo-score and showed that patients with a Nomo-score ≥ 0.428 were likely to have a higher incidence of CLNM. Therefore, this prediction model can be used to evaluate individuals preoperatively, and CLND was recommended for patients with a Nomo-score ≥ 0.428.

Our study has several limitations. First, the training cohort in this study was retrospective, and some bias inevitably exists. Second, the data might be affected by the different machines and probes used in the training and validation cohorts, but a ratio was used to reduce

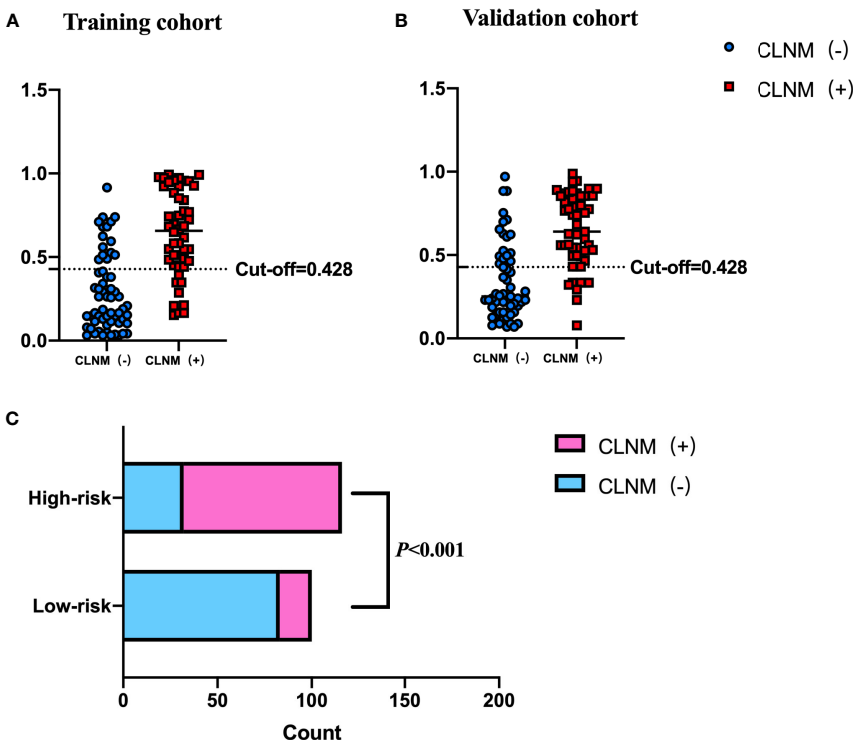

FIGURE 7
Performance of the cutoff value for predicting CLNM in patients with PTC. In **(A, B)**, the cutoff value of the Nomo-score performed well in the differential diagnosis of pN1 from pN0 in the training and validation cohorts, respectively. **(C)** The risk classification performance of the cutoff value is shown.

this effect. Third, this study needs to be further validated using a study with a larger sample size. Finally, all data were obtained from a single institution; thus, external validation in multicenter clinical trials is warranted.

In conclusion, a web-based dynamic nomogram based on US and CEUS features was constructed and showed a good performance in predicting the CLNM risk in PTC patients. This may be instrumental in refining surgery strategy in PTC patients.

Data availability statement

The original contributions presented in the study are included in the article/supplementary material. Further inquiries can be directed to the corresponding author.

Author contributions

QC performed the statistical work and wrote the first draft of the manuscript. YL, JL, and YS completed the data collection work. LQ and XH edited and revised the manuscript. All authors revised the manuscript critically and approved the final version of the manuscript.

Funding

This work was supported by the Ministry of Industry and Information Technology of the People's Republic of China (2018MND102015) and Beijing key Clinical Discipline Funding (2021-135).

Conflict of interest

The authors declare that the research was conducted in the absence of any commercial or financial relationships that could be construed as a potential conflict of interest.

Publisher's note

References

1. Giordano TJ. Genomic hallmarks of thyroid neoplasia. *Annu Rev Pathol* (2018) 13:141–62. doi: 10.1146/annurev-pathol-121808-102139

2. Huang C, Cong S, Liang T, Feng Z, Gan K, Zhou R, et al. Development and validation of an ultrasound-based nomogram for preoperative prediction of cervical central lymph node metastasis in papillary thyroid carcinoma. *Gland Surg* (2020) 9 (4):956–67. doi: 10.21037/gs-20-75

3. Al Afif A, Williams BA, Rigby MH, Bullock MJ, Taylor SM, Trites J, et al. Multifocal papillary thyroid cancer increases the risk of central lymph node metastasis. *Thyroid* (2015) 25(9):1008–12. doi: 10.1089/thy.2015.0130

4. Kim SK, Chai YJ, Park I, Woo JW, Lee JH, Lee KE, et al. Nomogram for predicting central node metastasis in papillary thyroid carcinoma. *J Surg Oncol* (2017) 115(3):266–72. doi: 10.1002/jso.24512

5. Zheng CM, Ji YB, Song CM, Ge MH, Tae K. Number of metastatic lymph nodes and ratio of metastatic lymph nodes to total number of retrieved lymph nodes are risk factors for recurrence in patients with clinically node negative papillary thyroid carcinoma. *Clin Exp Otorhinolaryngol* (2018) 11(1):58–64. doi: 10.21053/ceo.2017.00472

6. Maksimovic S, Jakovljevic B, Gojkovic Z. Lymph node metastases papillary thyroid carcinoma and their importance in recurrence of disease. *Med Arch* (2018) 72(2):108–11. doi: 10.5455/medarh.2018.72.108-111

7. Jiang M, Li C, Tang S, Lv W, Yi A, Wang B, et al. Nomogram based on shear-wave elastography radiomics can improve preoperative cervical lymph node staging for papillary thyroid carcinoma. *Thyroid* (2020) 30(6):885–97. doi: 10.1089/thy.2019.0780

8. Li F, Pan D, He Y, Wu Y, Peng J, Li J, et al. Using ultrasound features and radiomics analysis to predict lymph node metastasis in patients with thyroid cancer. *BMC Surg* (2020) 20(1):315. doi: 10.1186/s12893-020-00974-7

9. Haugen BR, Alexander EK, Bible KC, Doherty GM, Mandel SJ, Nikiforov YE, et al. 2015 American Thyroid association management guidelines for adult patients with thyroid nodules and differentiated thyroid cancer: the American thyroid association guidelines task force on thyroid nodules and differentiated thyroid cancer. *Thyroid* (2016) 26(1):1–133. doi: 10.1089/thy.2015.0020

10. Liang K, He L, Dong W, Zhang H. Risk factors of central lymph node metastasis in Cn0 papillary thyroid carcinoma: a study of 529 patients. *Med Sci Monit* (2014) 20:807–11. doi: 10.12659/msm.890182

11. Zhao WJ, Luo H, Zhou YM, Dai WY, Zhu JQ. Evaluating the effectiveness of prophylactic central neck dissection with total thyroidectomy for Cn0 papillary thyroid carcinoma: an updated meta-analysis. *Eur J Surg Oncol* (2017) 43(11):1989–2000. doi: 10.1016/j.ejso.2017.07.008

12. Choi JS, Kim J, Kwak JY, Kim MJ, Chang HS, Kim EK. Preoperative staging of papillary thyroid carcinoma: comparison of ultrasound imaging and ct. *AJR Am J Roentgenol* (2009) 193(3):871–8. doi: 10.2214/ajr.09.2386

13. Choi YJ, Yun JS, Kook SH, Jung EC, Park YL. Clinical and imaging assessment of cervical lymph node metastasis in papillary thyroid carcinomas. *World J Surg* (2010) 34(7):1494–9. doi: 10.1007/s00268-010-0541-1

14. Tao L, Zhou W, Zhan W, Li W, Wang Y, Fan J. Preoperative prediction of cervical lymph node metastasis in papillary thyroid carcinoma Via conventional and contrast-enhanced ultrasound. *J Ultrasound Med* (2020) 39(10):2071–80. doi: 10.1002/jum.15315

15. Liu Q, Cheng J, Li J, Gao X, Li H. The diagnostic accuracy of contrast-enhanced ultrasound for the differentiation of benign and malignant thyroid nodules: a prisma compliant meta-analysis. *Med (Baltimore)* (2018) 97(49):e13325. doi: 10.1097/md.0000000000013325

16. Zhan J, Diao X, Chen Y, Wang W, Ding H. Predicting cervical lymph node metastasis in patients with papillary thyroid cancer (Ptc) - why contrast-enhanced ultrasound (Ceus) was performed before thyroidectomy. *Clin Hemorheol Microcirc* (2019) 72(1):61–73. doi: 10.3233/ch-180454

17. Zhan J, Zhang LH, Yu Q, Li CL, Chen Y, Wang WP, et al. Prediction of cervical lymph node metastasis with contrast-enhanced ultrasound and association between presence of Braf(V600e) and extrathyroidal extension in papillary thyroid carcinoma. *Ther Adv Med Oncol* (2020) 12:1758835920942367. doi: 10.1177/1758835920942367

18. Goto K, Watanabe S. Large-Billed crows (Corvus macrorhynchos) have retrospective but not prospective metamemory. *Anim Cognit* (2012) 15(1):27–35. doi: 10.1007/s10071-011-0428-z

19. Baek SK, Jung KY, Kang SM, Kwon SY, Woo JS, Cho SH, et al. Clinical risk factors associated with cervical lymph node recurrence in papillary thyroid carcinoma. *Thyroid* (2010) 20(2):147–52. doi: 10.1089/thy.2008.0243

20. O'Connell K, Yen TW, Quiroz F, Evans DB, Wang TS. The utility of routine preoperative cervical ultrasonography in patients undergoing thyroidectomy for differentiated thyroid cancer. *Surgery* (2013) 154(4):697–701. doi: 10.1016/j.surg.2013.06.040

21. Guo L, Ma YQ, Yao Y, Wu M, Deng ZH, Zhu FW, et al. Role of ultrasonographic features and quantified Brafv600e mutation in lymph node metastasis in Chinese patients with papillary thyroid carcinoma. *Sci Rep* (2019) 9(1):75. doi: 10.1038/s41598-018-36171-z

22. Wang QC, Cheng W, Wen X, Li JB, Jing H, Nie CL. Shorter distance between the nodule and capsule has greater risk of cervical lymph node metastasis in papillary thyroid carcinoma. *Asian Pac J Cancer Prev* (2014) 15(2):855–60. doi: 10.7314/apjcp.2014.15.2.855

23. Tian X, Song Q, Xie F, Ren L, Zhang Y, Tang J, et al. Papillary thyroid carcinoma: an ultrasound-based nomogram improves the prediction of lymph node metastases in the central compartment. *Eur Radiol* (2020) 30(11):5881–93. doi: 10.1007/s00330-020-06906-6

24. Andrioli M, Valcavi R. Sonography of normal and abnormal thyroid and parathyroid glands. *Front Horm Res* (2016) 45:1–15. doi: 10.1159/000442273

25. Zhang Y, Luo YK, Zhang MB, Li J, Li CT, Tang J, et al. Values of ultrasound features and mmp-9 of papillary thyroid carcinoma in predicting cervical lymph node metastases. *Sci Rep* (2017) 7(1):6670. doi: 10.1038/s41598-017-07118-7

26. Szabó BK, Saracco A, Tánczos E, Aspelin P, Leifland K, Wilczek B, et al. Correlation of contrast-enhanced ultrasound kinetics with prognostic factors in invasive breast cancer. *Eur Radiol* (2013) 23(12):3228–36. doi: 10.1007/s00330-013-2960-5

27. Lee SH, Lee SJ, Jin SM, Lee NH, Kim DH, Chae SW, et al. Relationships between lymph node metastasis and expression of Cd31, D2-40, and vascular endothelial growth factors a and c in papillary thyroid cancer. *Clin Exp Otorhinolaryngol* (2012) 5(3):150–5. doi: 10.3342/ceo.2012.5.3.150

28. Liu W, Cheng R, Ma Y, Wang D, Su Y, Diao C, et al. Establishment and validation of the scoring system for preoperative prediction of central lymph node metastasis in papillary thyroid carcinoma. *Sci Rep* (2018) 8(1):6962. doi: 10.1038/s41598-018-24668-6

29. Kwak JY, Han KH, Yoon JH, Moon HJ, Son EJ, Park SH, et al. Thyroid imaging reporting and data system for us features of nodules: a step in establishing better stratification of cancer risk. *Radiology* (2011) 260(3):892–9. doi: 10.1148/radiol.11110206

30. Qu N, Zhang L, Ji QH, Zhu YX, Wang ZY, Shen Q, et al. Number of tumor foci predicts prognosis in papillary thyroid cancer. *BMC Cancer* (2014) 14:914. doi: 10.1186/1471-2407-14-914

31. Wang F, Zhao S, Shen X, Zhu G, Liu R, Viola D, et al. Braf V600e confers Male sex disease-specific mortality risk in patients with papillary thyroid cancer. *J Clin Oncol* (2018) 36(27):2787–95. doi: 10.1200/jco.2018.78.5097

32. Suman P, Wang CH, Abadin SS, Moo-Young TA, Prinz RA, Winchester DJ. Risk factors for central lymph node metastasis in papillary thyroid carcinoma: a national cancer data base (Ncdb) study. *Surgery* (2016) 159(1):31–9. doi: 10.1016/j.surg.2015.08.032

33. Sun W, Lan X, Zhang H, Dong W, Wang Z, He L, et al. Risk factors for central lymph node metastasis in Cn0 papillary thyroid carcinoma: a systematic review and meta-analysis. *PloS One* (2015) 10(10):e0139021. doi: 10.1371/journal.pone.0139021

frontiers | Frontiers in Endocrinology

TYPE Original Research
PUBLISHED 12 July 2023
DOI 10.3389/fendo.2023.1187825

OPEN ACCESS

EDITED BY
Eleonora Lori,
Sapienza University of Rome, Italy

REVIEWED BY
Giovanni Succo,
San Giovanni Bosco Hospital, Italy
Pietro Giorgio Calo',
University of Cagliari, Italy

*CORRESPONDENCE
Chengcheng Niu
niuchengcheng@csu.edu.cn

RECEIVED 16 March 2023
ACCEPTED 27 June 2023
PUBLISHED 12 July 2023

CITATION
Gong Y, Zuo Z, Tang K, Xu Y, Zhang R, Peng Q and Niu C (2023) Multimodal predictive factors of metastasis in lymph nodes posterior to the right recurrent laryngeal nerve in papillary thyroid carcinoma.
Front. Endocrinol. 14:1187825.
doi: 10.3389/fendo.2023.1187825

Multimodal predictive factors of metastasis in lymph nodes posterior to the right recurrent laryngeal nerve in papillary thyroid carcinoma

Yi Gong[1], Zhongkun Zuo[1], Kui Tang[2], Yan Xu[2], Rongsen Zhang[2], Qiang Peng[2] and Chengcheng Niu[2]*

[1]Department of General Surgery, The Second Xiangya Hospital, Central South University, Changsha, Hunan, China, [2]Department of Ultrasound Diagnosis, The Second Xiangya Hospital, Central South University, Changsha, Hunan, China

Objective: The lymph node posterior to the right recurrent laryngeal nerve (LN-prRLN) is a crucial component of the central lymph nodes (LNs). We aimed to evaluate multimodal predictive factors of LN-prRLN metastasis in patients with papillary thyroid carcinomas (PTCs), including the clinical data, pathologic data, and preoperative sonographic characteristics of PTCs.

Methods: A total of 403 diagnosed PTC patients who underwent unilateral, subtotal, or total thyroidectomy with central neck dissection were enrolled in this retrospective study. The clinical data, pathologic data, conventional ultrasound (US) and contrast-enhanced ultrasound (CEUS) characteristics of PTCs were collected and evaluated for predicting LN-prRLN metastasis.

Results: In this study, 96 PTC patients with LN-prRLN metastasis and 307 PTC patients without LN-prRLN metastasis were included. Univariate analysis demonstrated that PTC patients with LN-prRLN metastasis more often had younger age, larger size, multifocal cancers, A/T < 1, well-margins, microcalcification, petal-like calcification, internal vascularity, centripetal perfusion pattern and surrounding ring enhancement. Multivariate logistic regression analysis revealed that the CEUS centripetal perfusion pattern, central LN detected by ultrasound and LN-arRLN metastasis were independent characteristics for predicting LN-prRLN metastasis in PTC patients.

Conclusion: According to our research, it is essential for clinicians to thoroughly dissect central LNs, particularly LN-prRLNs.

KEYWORDS

contrast-enhanced ultrasound (CEUS), conventional Ultrasound, central cervical lymph node metastasis, papillary thyroid carcinomas (PTCs), lymph nodes posterior to the right recurrent laryngeal nerve metastasis

Introduction

PTCs are one of the most prevalent thyroid cancer histological subtypes, with rising incidence and substantial lymph node metastatic rates (1, 2). According to studies, PTC lymph node metastasis cases range from 20% to 90% of total PTC cases, with central lymph node (level VI) metastasis constituting the majority of cases (3). Thyroidectomy and lymph node dissection are the two basic treatments for PTCs (4). Prelaryngeal LNs, pretracheal LNs, left paratracheal LNs, and right paratracheal LNs are the four groups that typically make up cervical central LNs. Due to the anatomical variations of the recurrent laryngeal nerves on both sides, the right paratracheal LNs are divided into those that are anterior to the right recurrent laryngeal nerve (LN-arRLN) and those that are posterior to the right recurrent laryngeal nerve (LN-prRLN) (5, 6).

Due to the difficult surgical technique and the high rate of complications as a result of the deep position with confined exposure, some researchers contend that routine LN-prRLN removal is not necessary. Furthermore, it can be difficult to assess metastases before surgery, and even experienced surgeons are likely to ignore this location. However, the LN-prRLN metastasis rate in PTC patients has been reported to be as high as 2.7–30.4% (3, 5, 7). The first surgical treatment strategy for LN-prRLN is crucial for the patient's prognosis. Inadequate cervical LN dissection may increase the risk of recurrence and complications due to repeated operations, so some researchers have suggested routine removal of LN-prRLNs to maximize treatment success (8). These disagreements demonstrate that LN-prRLN merits consideration and additional study. Hence, it is critical to appropriately estimate the probability of LN-prRLN metastasis, which could aid in determining the scope of surgery and lowering the recurrence rates.

Some studies have reported the clinicopathologic risk factors for LN-prRLN metastasis for PTCs. Zhang et al. reported that tumor size larger than 1 cm, multifocality, and extrathyroidal extension were independent predictors of LN-prRLN metastasis in right-sided PTC (3). Zhou et al. proved that tumor size larger than 1. 5cm, extrathyroidal extension, and LN-arRLN metastasis were independent predictors of LN-prRLN metastasis in cN0 PTC (5). However, the research solely included clinicopathologic features, limiting their clinical application; thus, the preoperative sonographic features of primary tumors are essential for evaluating the risk factors for LN-prRLN metastasis in PTCs. US is an incredibly sensitive tool for evaluating initial PTC lesions, providing ultrasonographic signs of PTCs that can be utilized to predict cervical LN metastases in PTC patients and offer a basis for the selection of surgical techniques (9, 10). Unfortunately, few similar studies have been conducted in LN-prRLN metastasis (11).

CEUS, which provides more information about vascularity than conventional US, could reveal the thyroid nodule's microvasculature and increase the diagnostic accuracy of thyroid nodules (12, 13). Our previous studies found that preoperative CEUS characteristics could offer help in predicting central lymph node metastasis in PTCs with coexistent Hashimoto's thyroiditis and identifying malignant cervical LNs from benign cervical LNs (14–16).

By analyzing the preoperative US characteristics of PTCs and the postoperative pathological data in 403 PTC patients, this study seeks to identify potential predictors for the preoperative clinical evaluation of LN-prRLN metastases.

Methods and materials

Patients

The study was approved by the Ethical Committee of the Second Xiangya Hospital of Central South University in China and performed in accordance with the Declaration of Helsinki for human study. The requirement of informed consent from human subjects was waived by IRBs due to the retrospective nature of the review of images acquired for clinical diagnostic purposes. From May 2021 to August 2022, 1253 consecutive patients with thyroid nodules who received conventional US and CEUS examinations were prospectively enrolled in this single-center study. The inclusion criteria were as follows: (i) patients with thyroid nodules who underwent conventional US and CEUS examinations and (ii) pathological examination confirming PTCs after surgery. Patients with the following criteria were excluded: (i) a history of neck surgery or neck radiotherapy; (ii) central cervical lymph node dissection not performed; and (iii) LN-prRLN without clear pathological diagnosis. The final diagnosis of malignant thyroid nodules and metastatic lymph nodes was confirmed by histopathology after surgery. For patients with multifocal PTCs, the largest one was selected for CEUS examination. Finally, 403 PTC patients (96 patients with LN-prRLN metastasis and 307 patients without LN-prRLN metastasis proven by pathological examination) were included in this study. In addition, TSH, thyroid peroxidase antibody (A-TPO), and thyroglobulin antibody (A-TG) levels were evaluated in all patients within one week before surgery.

Conventional US and CEUS examination

A GE E11 US scanner with a 3-12L (3-12 MHz) linear array transducer or Siemens Acuson S3000 US scanner with a 9L4 (4–9 MHz) linear array transducer was used for conventional US and CEUS examination. All examinations were performed by operators with more than ten years of experience in thyroid ultrasound diagnosis and five years of experience in performing CEUS examinations. Two other investigators with 5 years of experience in thyroid ultrasound diagnosis analyzed the US images independently. Disagreements were solved by consensus. Two-milliliters of SonoVue (Bracco, Italy) or 0.4 mL of Sonozoid (GE, USA) was injected intravenously, followed by a saline flush of 5 mL. Thyroid nodule imaging lasted at least 30 seconds.

Conventional US features of the thyroid nodules were classified as follows (13): shape (taller than wide, A/T >1; or wider than tall,

A/T< 1); margins (well-defined or ill-defined); echogenicity (marked hypo-, hypo-, iso- or hyper-echoic); calcification (no calcification, microcalcification<1 mm in diameter, macrocalcification >1 mm in diameter); petal-like calcification (defined as microcalcification displayed around the thyroid nodule like a petal) (17) and internal vascularity (present or absent).

The following categories describe the thyroid nodules' CEUS characteristics (14): enhancement type (hyper-, iso- or hypo-enhancement); enhancement uniformity (heterogeneous or homogeneous enhancement); perfusion pattern (centripetal perfusion, the perfusion of microbubbles from the periphery to the center; centrifugal perfusion, the perfusion of microbubbles from the center to the periphery); and surrounding ring enhancement (presence or absence).

Surgical treatment proposal

Three surgical options (unilateral, sub-total, or total thyroidectomy with central neck dissection) are available, according to the Chinese Thyroid Association's guidelines. The procedure was chosen based on the surgeon's desire and a comprehensive analysis of the patient's condition. Prelaryngeal LN, pretracheal LN, left paratracheal LN, LN-arRLN, and LN-prRLN were the five subgroups of the central LNs and sent for individual pathological evaluation. If the lateral cervical LNs were diagnosed as metastatic LNs from PTCs, lateral cervical lymph node dissection was performed.

Reference standard

The histopathological results after surgery were used as the only reference standard for the final diagnosis of malignant thyroid nodules and metastatic lymph nodes.

Statistical analysis

The statistical analysis was carried out using SPSS version 21.0. (SPSS, Chicago, IL, USA). The mean and standard deviation (SD) of continuous data were displayed, and they were compared using an independent t test. Categorical data were evaluated using the chi-square test and are shown as percentages. To evaluate multimodal factors and their independent associations with LN-prRLN metastasis, binary logistic regression was performed. $P < 0.05$ was used to evaluate whether differences were statistically significant.

Results

This study comprised a total of 403 PTC patients, including 307 individuals without LN-prRLN metastasis and 96 patients with LN-prRLN metastasis. Table 1 displays the clinical and pathologic characteristics of the patients. Among the 403 patients with PTCs,

TABLE 1 Clinical and pathologic data of the enrolled 403 patients.

Variables	Numbers (%)
Age (year)	41.69 ± 12.01
< 45	233 (57.8%)
≥ 45	170 (42.2%)
Gender	
Male	99 (24.6%)
Female	304 (75.4%)
Tumor size (mm)	12.56 ± 8.65
≤ 5 mm	62 (15.4%)
>5 and ≤10 mm	163 (40.4%)
>10 and ≤20 mm	114 (28.3%)
>20 and ≤40 mm	56 (13.9%)
> 40 mm	8 (2.0%)
Coexistent Hashimoto's thyroiditis	
Yes	130 (32.3%)
No	273 (67.7%)
Multifocality	
Yes	186 (46.2%)
No	217 (53.8%)
Tumor location	
Right lobe	209 (51.9%)
Left lobe	40 (9.9%)
Isthmus	10 (2.5%)
Bilateral lobe	144 (35.7%)
Central LN detected by Ultrasound**	176 (43.7%)
Operation type##	
TT or ST + central neck dissection	367 (91.1%)
UL + central neck dissection	36 (8.9%)
LN metastatic sites	
Left paratracheal LN	115 (28.5%)
Prelaryngeal LN	53 (13.2%)
Pretracheal LN	121 (30.0%)
LN-arRLN&	145 (36.0%)
LN-prRLN#	96 (23.8%)
Lateral LN	99 (24.6%)
Hypoparathyroidism	
Transient	55 (13.6%)
Permanent	2 (0.5%)
Vocal cord paralysis	

(Continued)

TABLE 1 Continued

Variables	Numbers (%)
Transient	10 (2.5%)
Permanent	0 (0.0%)

**LN, lymph node.
##TT, total thyroidectomy; ST, sub-total thyroidectomy; UL, unilateral lobectomy.
&LN-arRLN, lymph node anterior to the right recurrent laryngeal nerve.
#LN-prRLN, lymph node posterior to the right recurrent laryngeal nerve.

the mean age was 41.69 ± 12.01 years (range 18-73 years), 57.8% (233/403) were younger than 45 years, and 75.4% (304/403) were female patients. The mean tumor size was 12.56 ± 8.65 mm (range 2–51 mm). In total, 32.3% (130/403) of patients had Hashimoto's thyroiditis, 46.2% (186/403) had multifocal PTCs, 51.9% (209/403) had lesions in the right lobe, 9.9% (40/403) had lesions in the left lobe, 2.5% (10/403) had lesions in the isthmus, and 35.7% (144/403) had lesions in the bilateral lobe. Level VI lymph nodes were detected in 176 (43.7%) patients on preoperative conventional US examination. Sub-total and total thyroidectomy with central neck dissection were performed in 367 (91.1%) patients, and unilateral thyroidectomy with central neck dissection was performed in 36 (8.9%). Histopathological examination showed that the rates of left paratracheal LN, prelaryngeal LN, pretracheal LN, LN-arRLN, LN-prRLN and lateral LN metastasis were 28.5% (115/403), 13.2% (53/403), 30.0% (121/403), 36.0% (145/403), 23.8% (96/403) and 24.6% (99/403), respectively. In addition, among patients without any other cervical lymph node metastasis, the rate of LN-prRLN metastasis was 8.2% (8/96). Transient and permanent hypoparathyroidism were noted in 55 (13.6%) and 2 (0.5%) patients, respectively. Voice change developed in 10 (2.5%) patients, but all patients recovered during follow-up, and no patient had consistent dysfunction with vocal cord paralysis.

The univariate analysis of predictors for LN-prRLN is reported in Table 2. The average age of PTC patients with or without LN-prRLN metastasis was 36.65 ± 12.19 years (range: 18-71 years) or 43.27 ± 11.52 years (range: 18-73 years), respectively. Seventy-two (75.0%) patients with LN-prRLN metastasis were younger than 45 years, and 161 (52.4%) patients without LN-prRLN metastasis were younger than 45 years (p = 0.000), showing that the patients with LN-prRLN metastasis were more inclined to be younger. The mean diameters of PTCs with or without LN-prRLN metastasis were 18.23 ± 10.94 mm (range: 3-51 mm) and 10.79 ± 6.93 mm (range: 2-42 mm), respectively, showing that the former had considerably higher mean diameters than the latter (p = 0.000). A size > 10 mm was present in 68 (70.8%) of the patients with LN-prRLN metastasis and 110 (35.8%) of the patients without LN-prRLN metastasis (p = 0.000). Multifocal malignancies were present in 53 (55.2%) individuals with LN-prRLN metastases and in 133 (43.3%) patients without this occurrence (p = 0.041). Only the largest PTC was selected in patients with multifocal PTCs. LN-prRLN metastasis did not appear to be correlated with any other variables (all p>0.05).

Compared with PTCs without LN-prRLN metastasis, PTCs with LN-prRLN metastasis had more A/T < 1 and well-defined margins, microcalcification, petal-like calcification and internal vascularity on conventional US images. For CEUS images, the PTCs with LN-prRLN metastasis showed a more centrifugal perfusion pattern and the presence of surrounding ring enhancement than the PTCs without LN-prRLN metastasis (Figures 1, 2).

Level VI lymph nodes were detected in 74 (77.1%) patients in the PTC with LN-prRLN metastasis group compared with 102 (33.2%) patients in the PTC without LN-prRLN metastasis group on preoperative conventional US examination. In addition, all metastatic rates of left paratracheal LNs, prelaryngeal LNs, pretracheal LNs, LN-arRLNs, LN-prRLNs and lateral LNs were higher than those of the PTCs without LN-prRLN metastasis group on histopathological examination.

All of the statistically significant factors (p < 0.05) underwent multivariate logistic regression analysis. The outcomes showed that the CEUS centrifugal perfusion pattern (B= 1.314, OR = 3.720, 95% CI = 1.808-7.654, p=0.000), central LN detected by ultrasound (B= 1.027, OR = 2.792, 95% CI = 1.440-5.415, p=0.002), and LN-arRLN metastasis (B =0.753, OR =2.123, 95% CI = 1.083-4.163, p=0.028) were independent characteristics for predicting LN-prRLN metastasis (Table 3).

Discussion

Currently, there is still controversy about whether to dissect the LN-prRLN in the absence of certain LNs that are positive. Dissection of the LN-prRLN requires patience and experience and could lead to nerve damage and parathyroid injury, affecting the patient's quality of life (18). According to some researchers, PTCs are a kind of tumor; hence, LN-prRLN dissection is not needed, thus reducing surgical risks to patients after surgery. Hypoparathyroidism and vocal cord paralysis were the two serious complications after thyroid surgery. Transient and permanent hypoparathyroidism occurred in 4.1-51.9% and 0-1.1% of patients, respectively (6, 18–20). Postoperative voice change was found in 4.9-7.4% of patients, while consistent voice change with vocal cord immobility was found in 0-4.0% of patients (6, 18–20).

Although PTCs have a favorable prognosis, other scholars contend that the central LNs are the most frequent sites for lymph node metastasis with a high incidence of 13.7%-72.2% (14, 16, 21). Thorough initial dissection with simultaneous dissection of the LN-prRLN is essential to reduce local recurrence and metastasis and avoid significant complication rates by secondary surgery. Secondary thyroid surgery is difficult for young and inexperienced surgeons, but even skilled and experienced surgeons can have difficulty in mapping the recurrent laryngeal nerve and preventing inadvertent recurrent laryngeal nerve injury, particularly in nonanatomical fields with many scars from the first operations (22, 23). In accordance with the recommendations of the American Thyroid Association (ATA), cervical LNs should be evaluated using preoperative neck US to determine the surgical approach, particularly for lymph node dissection (4). However, conventional US only has a sensitivity of less than 30% for central LNs (24, 25). The risk factors for LN-prRLN metastases in PTCs

10.3389/fendo.2023.1187825

TABLE 2 Univariate analysis of predictor for lymph node posterior to the right recurrent nerve metastasis (LN-prRLN).

Variables	LN-prRLN status		P valve
	Positive (n=96)	Negative (n=307)	
Age (year)	36.65 ± 12.19	43.27 ± 11.52	0.000*
< 45	72 (75.0%)	161 (52.4%)	0.000*
≥ 45	24 (25.0%)	146 (47.6%)	
Gender			0.141
Male	29 (30.2%)	70 (22.8%)	
Female	67 (69.8%)	237 (77.2%)	
Tumor size (mm)	18.23 ± 10.94	10.79 ± 6.93	0.000*
≤ 10 mm	28 (29.2%)	197 (64.2%)	0.000*
> 10 mm	68 (70.8%)	110 (35.8%)	
Coexistent Hashimoto's thyroiditis			0.135
Yes	25 (26.0%)	105 (34.2%)	
No	71 (74.0%)	202 (65.8%)	
Multifocality			0.041*
Yes	53 (55.2%)	133 (43.3%)	
No	43 (44.8%)	174 (56.7%)	
Tumor location			0.081
Right lobe	52 (54.2%)	157 (51.1%)	
Left lobe	3 (3.1%)	37 (12.1%)	
Isthmus	2 (2.1%)	8 (2.6%)	
Bilateral lobe	39 (40.6%)	105 (34.2%)	
A/T			0.000*
> 1	45 (46.9%)	207 (67.4%)	
< 1	51 (53.1%)	100 (32.6%)	
Margin			0.009*
Well-defined	13 (13.5%)	17 (5.5%)	
Ill-defined	83 (86.5%)	290 (94.5%)	
Echogenicity			0.359
Marked hypoechoic or hypoechoic	93 (96.9%)	302 (98.4%)	
Iso- or hyperechoic	3 (3.1%)	5 (1.6%)	
Calcification			0.001*
Absent or macrocalcification	6 (6.2%)	65 (21.2%)	
Microcalcification	90 (93.8%)	242 (78.8%)	
Petal-like calcification			0.000*
Present	19 (19.8%)	22 (7.2%)	
Absent	77 (80.2%)	285 (92.8%)	
Internal vascularity			0.000*
Yes	26 (27.1%)	29 (9.4%)	
No	70 (72.9%)	278 (90.6%)	

(Continued)

TABLE 2 Continued

Variables	LN-prRLN status		P valve
	Positive (n=96)	Negative (n=307)	
Enhancement type			0.060
Hyper- or iso-enhancement	26 (27.1%)	56 (18.2%)	
Hypo-enhancement	70 (72.9%)	251 (81.8%)	
Perfusion pattern			0.000*
Centrifugal	34 (35.4%)	32 (10.4%)	
Centripetal	62 (64.6%)	275 (89.6%)	
Enhancement uniformity			0.703
Heterogeneous enhancement	85 (88.5%)	276 (89.9%)	
Homogeneous enhancement	11 (11.5%)	31 (10.1%)	
Surrounding ring enhancement			0.014*
Present	9 (9.4%)	10 (3.3%)	
Absent	87 (90.6%)	297 (96.7%)	
Central LN detected by Ultrasound**			0.000*
Yes	74 (77.1%)	102 (33.2%)	
No	22 (22.9%)	205 (66.8%)	
LN metastatic sites			
Left paratracheal LN	51 (53.1%)	64 (20.8%)	0.000*
Prelaryngeal LN	28 (29.2%)	25 (8.1%)	0.000*
Pretracheal LN	53 (55.2%)	68 (22.1%)	0.000*
LN-arRLN&	80 (83.3%)	65 (21.2%)	0.000*
Lateral LN	57 (59.4%)	42 (13.7%)	0.000*

**LN, lymph node.
&LN-arRLN, lymph node anterior to the right recurrent laryngeal nerve.
*$p < 0.05$ was considered a significant difference.

must be identified for surgeons to choose the best surgical procedures. The variables that predict LN-prRLN metastases in PTC patients, however, are not well known.

Univariate analysis in this study demonstrated that age < 45 years was a clinical risk factor related to LN-prRLN metastasis in PTC patients, demonstrating that patients with LN-prRLN metastasis were more likely to be young people, which was consistent with other previous studies (11, 26). In addition, tumor size > 10 mm was also a clinical risk factor associated with LN-prRLN metastasis, indicating that tumor size was closely linked to an elevated risk of LN-prRLN metastasis, which was also consistent with other previous reports (11, 19).

Recent studies have shown that US characteristics could help predict cervical central LN metastasis in PTC patients (9, 10, 27). Xu et al. reported that a virtual touch tissue imaging area ratio >1, abnormal cervical LNs, microcalcification and multiple nodules were risk factors for the prediction of cervical central LN metastasis in PTC patients (10). Liu et al. found that microcalcification, resistance index >0.7 and multiple nodules have predictive value in central LN metastasis of PTCs (27). However, few studies have been reported for LN-prRLN metastasis prediction by ultrasonographic features. In this study, we found that multiple nodules, calcification, petal-like calcification and internal vascularity were significantly associated with LN-prRLN metastasis in PTC patients. However, the suspicious ultrasonographic features for malignant thyroid nodules, including a taller-than-wider shape (A/T <1) and an ill-defined margin were protective factors for LN-prRLN metastasis in PTC patients, which may contribute to the tumor size of thyroid nodules. The smaller thyroid nodules in PTC patients without LN-prRLN metastasis were more likely to have an ill-defined margin and a taller-than-wider shape of PTCs, which was also reported in our previous study on PTCs with HT patients with coexisting central LN metastasis (14).

Compared to color Doppler technology, the accuracy of thyroid nodule diagnosis may improve with the use of CEUS, which can detect more tumor microvessels. However, to the best of our knowledge, these CEUS parameters for predicting LN-prRLN metastasis in PTC patients have not been explored to date. In our study, we found that the centrifugal perfusion pattern and presence of surrounding ring enhancement were significantly associated with

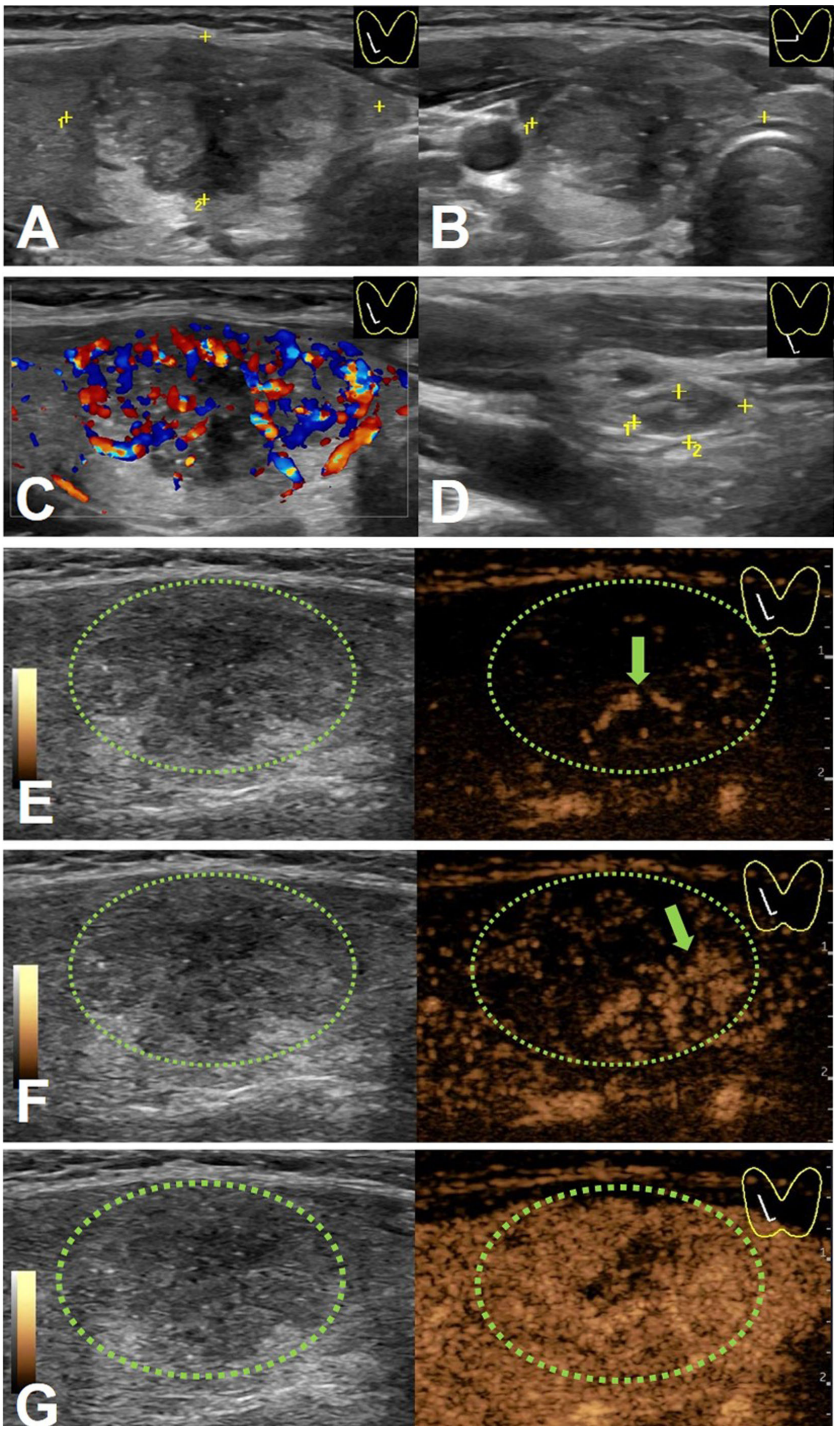

FIGURE 1
An 18-y-old female PTC patient with LN-prRLN metastasis. Initial longitudinal scan **(A)** and transverse scan **(B)** showing a 30-mm thyroid nodule with hypo-echogenicity, ill-defined margins, and petal calcification. **(C)** Doppler image revealing abundant signals in the nodule. **(D)** A level VI lymph node (yellow cross) identified on conventional US. **(E)** CEUS image 6 s after injection of contrast-enhanced agent, the thyroid nodule enhanced from the center to the periphery (green arrow). **(F)** CEUS image 7 s after injection of contrast-enhanced agent, the thyroid nodule showed heterogeneous enhancement (green arrow). **(G)** CEUS image 8 s after injection of contrast-enhanced agent, the thyroid nodule showed heterogeneous iso-enhancement.

LN-prRLN metastasis in PTC patients. Multivariate analysis demonstrated that the centrifugal perfusion pattern was one of the independent characteristics for the presence of LN-prRLN metastasis.

Although central LNs have a low display rate on preoperative conventional US examination, the present study found central LNs in 176 (43.7%) patients. Moreover, the display rate of central LNs in the PTC with LN-prRLN metastasis group was as high as 77.1%,

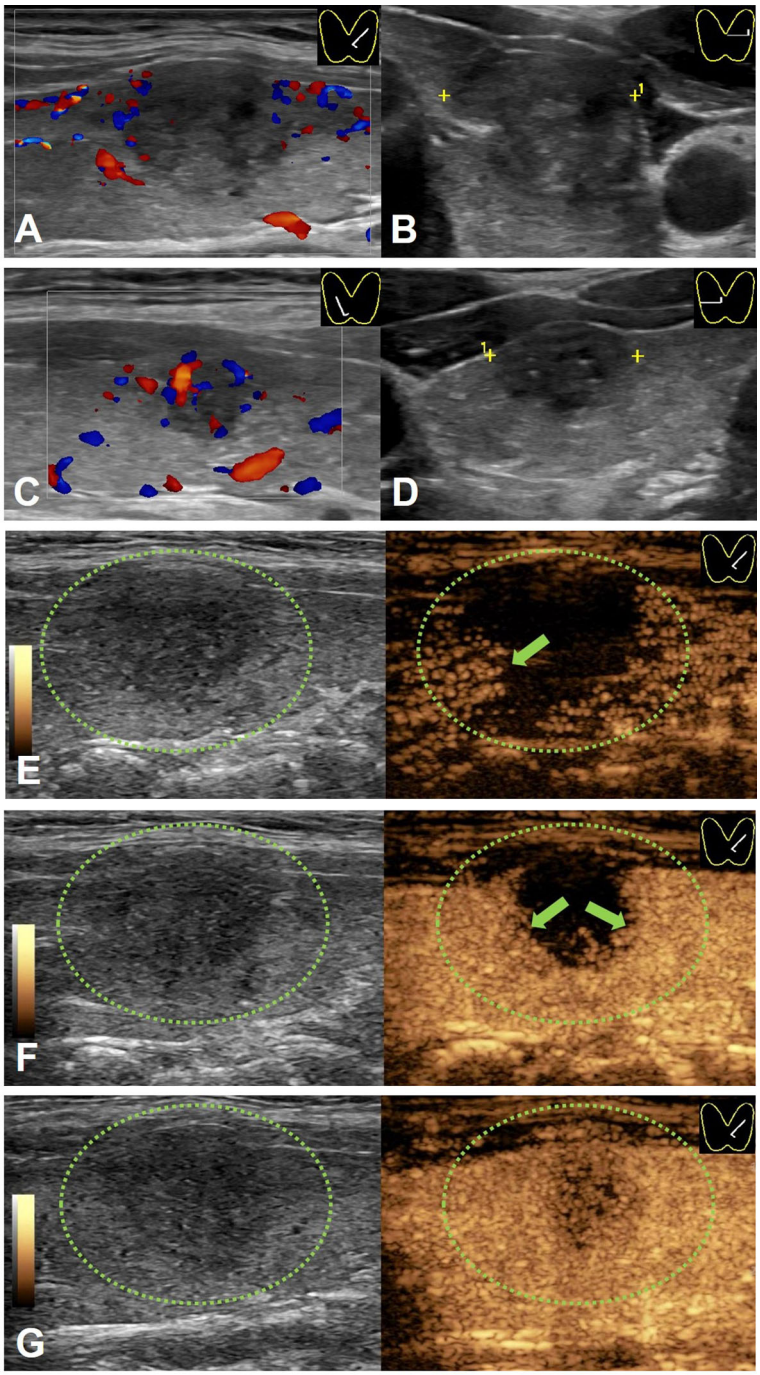

FIGURE 2
A 41-y-old male PTC patient without LN-prRLN metastasis. **(A)** Longitudinal Doppler image and **(B)** transverse scan image showing a 17-mm thyroid nodule with hypo-echogenicity, ill-defined margins, microcalcification and poor signals in the nodule in the left lobe. **(C)** Longitudinal Doppler image and **(D)** transverse scan image showing a 11-mm thyroid nodule with hypo-echogenicity, ill-defined margins, microcalcification and few signals in the nodule in the right lobe. **(E)** CEUS image 10 s after injection of contrast-enhanced agent, the thyroid nodule enhanced from the periphery to the center (green arrow). **(F)** CEUS image 12 s after injection of contrast-enhanced agent, the thyroid nodule showed heterogeneous enhancement (green arrow). **(G)** CEUS image 14 s after injection of contrast-enhanced agent, the thyroid nodule showed heterogeneous hypo-enhancement.

which was significantly higher than that of 33.2% in PTC without LN-prRLN metastasis group. Multivariate analysis demonstrated that central LN detected by US was another independent characteristic for the prediction of LN-prRLN metastasis, indicating that the centrifugal perfusion pattern on CEUS and central LN detected by US could serve as preoperative factors for predicting LN-prRLN metastasis. In addition, all histopathological metastatic rates of left paratracheal LNs, prelaryngeal LNs, pretracheal LNs, LN-arRLNs, LN-prRLNs and lateral LNs were significantly higher than those of PTCs without LN-prRLN metastasis. In this study, individuals who had LN-arRLN metastases had a nearly fourfold increased probability of LN-

TABLE 3 Multivariate analysis of the predictors of lymph node posterior to the right recurrent laryngeal nerve metastasis (LN-prRLN).

Variables	B	SE	Odd ratio	P valve	95% CI
Centrifugal perfusion	1.314	0.368	3.720	0.000*	1.808-7.654
Central LN detected by Ultrasound**	1.027	0.338	2.792	0.002*	1.440-5.415
LN-arRLN metastasis&	0.753	0.344	2.123	0.028*	1.083-4.163
Constant	-3.452	0.330	0.032	0.000*	

**LN, lymph node.
&LN-arRLN, lymph node anterior to the right recurrent laryngeal nerve.
*$p < 0.05$ was considered a significant difference.

prRLN metastasis than patients who did not. According to the multivariate analysis, LN-arRLN metastasis in PTC patients was a significant risk factor for LN-prRLN metastasis, suggesting that the LN-arRLN compartment may be used intraoperatively to predict LN-prRLN metastasis.

According to the findings of univariate and multivariate analyses, the centrifugal perfusion pattern on CEUS, central LN detected by US, and LN-arRLN metastasis were independent predictors of LN-prRLN metastasis in these patients. In that case, suggesting that the LN-prRLN should be removed with thorough neck dissection to prevent metastasis.

There are several limitations to our study. First, it was a single institutional retrospective analysis, hence the findings may not have been applicable to other PTC patient populations. Second, selection bias was also present. To further explain these findings, a large-scale prospective multicenter investigation is needed.

Conclusions

In summary, complete central LN dissection should be taken into consideration given the rate of LN-prRLN metastasis and the challenges and complications of reoperation. Centrifugal perfusion patterns on CEUS, central LN detected by US and LN-arRLN metastasis are helpful in predicting metastasis to LN-prRLNs. Thus, preoperative conventional US and CEUS may serve as useful tools in predicting LN-prRLN metastasis in PTC patients.

Data availability statement

The original contributions presented in the study are included in the article/supplementary material. Further inquiries can be directed to the corresponding author.

Ethics statement

The studies involving human participants were reviewed and approved by the Ethics Committee of Second Xiangya Hospital, Central South University, China. The patients/participants provided their written informed consent to participate in this study. Written informed consent was obtained from the individual(s) for the publication of any potentially identifiable images or data included in this article.

Author contributions

CN contributed to the conception and design of the work. YG participated to data analysis and manuscript writing. ZZ, KT, YX, RZ and QP participated to data collection and patients' follow-up. All authors contributed to the article and approved the submitted version.

Funding

This project was funded by the National Natural Science Foundation of China (81974267), the Science and Technology Innovation Program of Hunan Province (2021RC3033), the Hunan Provincial Natural Science Foundation of China (2022JJ30827 and 2022JJ30806) and Natural Science Foundation of Hunan Provincial Health Commission (A202309026329).

Conflict of interest

The authors declare that the research was conducted in the absence of any commercial or financial relationships that could be construed as a potential conflict of interest.

Publisher's note

References

1. Lim H, Devesa SS, Sosa JA, Check D, Kitahara CM. Trends in thyroid cancer incidence and mortality in the United States, 1974-2013. *JAMA* (2017) 317(13):1338–48. doi: 10.1001/jama.2017.2719

2. Sung H, Ferlay J, Siegel RL, Laversanne M, Soerjomataram I, Jemal A, et al. Global cancer statistics 2020: GLOBOCAN estimates of incidence and mortality worldwide for 36 cancers in 185 countries. *CA Cancer J Clin* (2021) 71(3):209–49. doi: 10.3322/caac.21660

3. Eun YG, Lee YC, Kwon KH. Predictive factors of contralateral paratracheal lymph node metastasis in papillary thyroid cancer: prospective multicenter study. *Otolaryngol Head Neck Surg* (2014) 150(2):210–5. doi: 10.1177/0194599813514726

4. Haugen BR, Alexander EK, Bible KC, Doherty GM, Mandel SJ, Nikiforov YE, et al. 2015 American Thyroid association management guidelines for adult patients with thyroid nodules and differentiated thyroid cancer: the American thyroid association guidelines task force on thyroid nodules and differentiated thyroid cancer. *Thyroid* (2016) 26(1):1–133. doi: 10.1089/thy.2015.0020

5. Zhou M, Duan Y, Ye B, Wang Y, Li H, Wu Y, et al. Pattern and predictive factors of metastasis in lymph nodes posterior to the right recurrent laryngeal nerve in papillary thyroid carcinoma. *Front Endocrinol (Lausanne)* (2022) 13:914946. doi: 10.3389/fendo.2022.914946

6. Zhang S, Zhang R, Wang C, Gong W, Zheng C, Fang Q, et al. Unnecessity of routine dissection of right central lymph nodes in cN0 papillary thyroid carcinoma located at the left thyroid lobe. *Front Oncol* (2021) 11:685708. doi: 10.3389/fonc.2021.685708

7. Chang H, Yoo RN, Kim SM, Kim BW, Lee YS, Lee SC, et al. The clinical significance of the right para-oesophageal lymph nodes in papillary thyroid cancer. *Yonsei Med J* (2015) 56(6):1632–7. doi: 10.3349/ymj.2015.56.6.1632

8. Liu C, Xiao C, Chen J, Li X, Feng Z, Gao Q, et al. Risk factor analysis for predicting cervical lymph node metastasis in papillary thyroid carcinoma: a study of 966 patients. *BMC Cancer* (2019) 19(1):622. doi: 10.1186/s12885-019-5835-6

9. Chen J, Li XL, Zhao CK, Wang D, Wang Q, Li MX, et al. Conventional ultrasound, immunohistochemical factors and BRAF(V600E) mutation in predicting central cervical lymph node metastasis of papillary thyroid carcinoma. *Ultrasound Med Biol* (2018) 44(11):2296–306. doi: 10.1016/j.ultrasmedbio.2018.06.020

10. Xu JM, Xu XH, Xu HX, Zhang YF, Guo LH, Liu LN, et al. Prediction of cervical lymph node metastasis in patients with papillary thyroid cancer using combined conventional ultrasound, strain elastography, and acoustic radiation force impulse (ARFI) elastography. *Eur Radiol* (2016) 26(8):2611–22. doi: 10.1007/s00330-015-4088-2

11. Zou M, Wang YH, Dong YF, Lai XJ, Li JC. Clinical and sonographic features for the preoperative prediction of lymph nodes posterior to the right recurrent laryngeal nerve metastasis in patients with papillary thyroid carcinoma. *J Endocrinol Invest* (2020) 43(10):1511–7. doi: 10.1007/s40618-020-01238-0

12. Gao L, Xi X, Gao Q, Tang J, Yang X, Zhu S, et al. Blood-rich enhancement in ultrasonography predicts worse prognosis in patients with papillary thyroid cancer. *Front Oncol* (2021) 10:546378. doi: 10.3389/fonc.2020.546378

13. Peng Q, Niu C, Zhang M, Chen S. Sonographic characteristics of papillary thyroid carcinoma with coexistent hashimoto's thyroiditis: conventional ultrasound, acoustic radiation force impulse imaging and contrast-enhanced ultrasound. *Ultrasound Med Biol* (2019) 45(2):471–80. doi: 10.1016/j.ultrasmedbio.2018.10.020

14. Chen S, Niu C, Peng Q, Tang K. Sonographic characteristics of papillary thyroid carcinoma with coexistent hashimoto's thyroiditis in the preoperative prediction of central lymph node metastasis. *Front Endocrinol (Lausanne)* (2021) 12:556851. doi: 10.3389/fendo.2021.556851

15. Fang F, Gong Y, Liao L, Ye F, Zuo Z, Li X, et al. Value of contrast-enhanced ultrasound for evaluation of cervical lymph node metastasis in papillary thyroid carcinoma. *Front Endocrinol* (2022) 13:812475. doi: 10.3389/fendo.2022.812475

16. Ye F, Gong Y, Tang K, Xu Y, Zhang R, Chen S, et al. Contrast-enhanced ultrasound characteristics of preoperative central cervical lymph node metastasis in papillary thyroid carcinoma. *Front Endocrinol* (2022) 13:941905. doi: 10.3389/fendo.2022.941905

17. Peng Q, Zhang Q, Chen S, Niu C. Petal-like calcifications in thyroid nodules on ultrasonography: a rare morphologic characteristic of calcification associated with aggressive biological behavior. *Front Endocrinol (Lausanne)* (2020) 11:271. doi: 10.3389/fendo.2020.00271

18. Du W, Fang Q, Zhang X, Dai L. Metastasis of cN0 papillary thyroid carcinoma of the isthmus to the lymph node posterior to the right recurrent laryngeal nerve. *Front Endocrinol (Lausanne)* (2021) 12:677986. doi: 10.3389/fendo.2021.677986

19. Liu Z, Sun M, Xiao Y, Yang J, Zhang T, Zhao Y. Predictors of metastasis to lymph nodes posterior to the right recurrent laryngeal nerve in differentiated thyroid carcinoma: a prospective study. *Asian J Surg* (2017) 40(4):270–7. doi: 10.1016/j.asjsur.2015.12.003

20. Yuan J, Li J, Chen X, Zhong Z, Chen Z, Yin Y, et al. Predictors of lymph nodes posterior to the right recurrent laryngeal nerve metastasis in patients with papillary thyroid carcinoma: a retrospective study. *Med (Baltimore)* (2017) 96(35):e7908. doi: 10.1097/MD.0000000000007908

21. Medas F, Canu GL, Cappellacci F, Boi F, Lai ML, Erdas E, et al. Predictive factors of lymph node metastasis in patients with papillary microcarcinoma of the thyroid: retrospective analysis on 293 cases. *Front Endocrinol (Lausanne)* (2020) 11:551. doi: 10.3389/fendo.2020.00551

22. Wojtczak B, Sutkowski K, Kaliszewski K, Barczynski M, Bolanowski M. Thyroid reoperation using intraoperative neuromonitoring. *Endocrine* (2017) 58(3):458–66. doi: 10.1007/s12020-017-1443-x

23. Pai SI, Tufano RP. Reoperation for recurrent/persistent well-differentiated thyroid cancer. *Otolaryngol Clin North Am* (2010) 43(2):353–63. doi: 10.1016/j.otc.2010.02.004

24. Khokhar MT, Day KM, Sangal RB, Ahmedli NN, Pisharodi LR, Beland MD, et al. Preoperative high-resolution ultrasound for the assessment of malignant central compartment lymph nodes in papillary thyroid cancer. *Thyroid* (2015) 25(12):1351–4. doi: 10.1089/thy.2015.0176

25. Hwang HS, Orloff LA. Efficacy of preoperative neck ultrasound in the detection of cervical lymph node metastasis from thyroid cancer. *Laryngoscope* (2011) 121 (3):487–91. doi: 10.1002/lary.21227

26. Sun J, Jiang Q, Wang X, Liu W, Wang X. Nomogram for preoperative estimation of cervical lymph node metastasis risk in papillary thyroid microcarcinoma. *Front Endocrinol (Lausanne)* (2021) 12:613974. doi: 10.3389/fendo.2021.613974

27. Liu W, Cheng R, Ma Y, Wang D, Su Y, Diao C, et al. Establishment and validation of the scoring system for preoperative prediction of central lymph node metastasis in papillary thyroid carcinoma. *Sci Rep* (2018) 8(1):6962. doi: 10.1038/s41598-018-24668-6

frontiers | Frontiers in Endocrinology

TYPE Original Research
PUBLISHED 14 September 2023
DOI 10.3389/fendo.2023.1158826

OPEN ACCESS

EDITED BY
Emese Mezosi,
University of Pécs, Hungary

REVIEWED BY
Pietro Locantore,
Catholic University of the Sacred Heart, Italy
Anupam Kotwal,
University of Nebraska Medical Center, United States

*CORRESPONDENCE
Yafei Shi
jysyf@mail.jnmc.edu.cn

RECEIVED 04 February 2023
ACCEPTED 23 August 2023
PUBLISHED 14 September 2023

CITATION
Ma T, Cui J, Shi P, Liang M, Song W, Zhang X, Wang L and Shi Y (2023) Assessing the role of central lymph node ratio in predicting recurrence in N1a low-to-intermediate risk papillary thyroid carcinoma.
Front. Endocrinol. 14:1158826.
doi: 10.3389/fendo.2023.1158826

Assessing the role of central lymph node ratio in predicting recurrence in N1a low-to-intermediate risk papillary thyroid carcinoma

Teng Ma[1,2], Jian Cui[2], Peng Shi[1], Mei Liang[1], Wenxiao Song[1], Xueyan Zhang[3], Lulu Wang[4] and Yafei Shi[1]*

[1]Department of Thyroid Surgery, Affiliated Hospital of Jining Medical University, Jining, Shandong, China, [2]Breast Disease Center, Affiliated Hospital of Qingdao University, Qingdao, Shandong, China, [3]Qingdao Medical College, Qingdao University, Qingdao, Shandong, China, [4]Department of Cardiovascular Surgery, Affiliated Hospital of Qingdao University, Qingdao, Shandong, China

Introduction: Lymph node metastasis in patients with papillary thyroid carcinoma (PTC) is associated with postoperative recurrence. Recently, most studies have focused on the evaluation of recurrence in patients with late-stage PTC, with limited data on those with early-stage PTC. We aimed to assess the relationship between lymph node ratio (LNR) and recurrence in low-to-intermediate-risk patients and validate its diagnostic efficiency in both structural (STR) and biochemical recurrence (BIR).

Methods: Clinical data of patients with PTC diagnosed at the Affiliated Hospital of Jining Medical University were retrospectively collected. The optimal LNR cut-off values for disease-free survival (DFS) were determined using X-tile software. Predictors were validated using univariate and multivariate Cox regression analyses.

Results: LNR had a higher diagnostic effectiveness than metastatic lymph nodes in patients with low-to-intermediate recurrence risk N1a PTC. The optimal LNR cutoff values for STR and BIR were 0.75 and 0.80, respectively. Multivariate Cox regression analysis showed that LNR≥0.75 and LNR≥0.80 were independent factors for STR and BIR, respectively. The 5-year DFS was 90.5% in the high LNR (≥0.75) and 96.8% in low LNR (<0.75) groups for STR. Regarding BIR, the 5-year DFS was 75.7% in the high LNR (≥0.80) and 86.9% in low LNR (<0.80) groups. The high and low LNR survival curves exhibited significant differences on the log-rank test.

Conclusion: LNR was associated with recurrence in patients with low-to-intermediate recurrence risk N1a PTC. We recommend those with LNR≥0.75 require a comprehensive evaluation of lateral neck lymphadenopathy and consideration for lateral neck dissection and RAI treatment.

KEYWORDS

papillary thyroid carcinoma, lymph node ratio, structural recurrence, biochemical recurrence, total thyroidectomy

1 Introduction

Papillary thyroid carcinoma (PTC) accounts for approximately 90% of thyroid cancers and has a favorable prognosis, with a 10-year disease-specific mortality of approximately 4% (1, 2). However, the high incidence of its recurrence is nonnegligible. Although the majority of PTC recurrences are not fatal (3), they can cause significant suffering, particularly in countries such as China, where PTC is common (4).

To determine the risk of recurrence and establish a corresponding follow-up strategy and postoperative treatment plan, three risk categories have been recommended by the American Thyroid Association (ATA): low, intermediate, and high risk (5). Some studies have reported that radioactive iodine (RAI) ablation or prophylactic lateral neck dissection is required to reduce the risk of recurrence in high-risk patients with PTC (6–9). Nevertheless, patients in the low-to-intermediate-risk group also show a certain risk of recurrence (10). Patients with less than five metastatic lymph nodes (MLNs) are classified as low risk, but the number of MLNs varies according to the degree of lymph node (LN) dissection scope and pathological sampling extent (11). Some patients still exhibit a significant probability of recurrence under this system, even with fewer than five MLNs (12).

According to the American Joint Committee on Cancer (AJCC) 8th TNM classification of Differentiated Thyroid Carcinoma, N1a and N1b are categorized into the same stage (13). Therefore, the N staging of TNM classification is inadequate to assess the probability of recurrence in patients with positive LNs (14–16). Furthermore, it is unclear which patients with pN1a should undergo prophylactic lateral neck dissection to prevent lateral lymph node recurrence (17). To differentiate between "lower risk characteristics" and "higher risk characteristics" in these patients, a new risk stratification system is required in order to provide individualized therapy for each patient, reducing hazards and optimizing benefits.

The number of MLNs divided by the total number of lymph nodes (TLNs) is known as the lymph node ratio (LNR). This ratio has been utilized to assess oncological prognoses of solid tumors, including those of the lung (18), stomach (19), and colon (20). This study aimed to identify an optimal cutoff value for LNR and explore the relationship between LNR and patients with low-to-intermediate recurrence risk N1a PTC. Furthermore, we aimed to validate the value of LNR as an indicator of tumor structural recurrence (STR) and biochemical recurrence (BIR).

2 Materials and methods

2.1 Patient selection

Data from patients with PTC who were diagnosed at the Affiliated Hospital of Jining Medical University between December 2012 and December 2017 were retrospectively collected and analyzed. Of 2861 patients who underwent surgical treatment during the study period, 617 met the inclusion criteria.

The inclusion criteria were: having undergone total thyroidectomy and central lymph node dissection; being aged at least 18 years; being classified as pathological T1-3N1aM0 according to the AJCC 8th TNM Classification of Differentiated Thyroid Carcinoma system; being classified as low-to-intermediate risk according to the 2015 ATA management guidelines; having achieved excellent responses after initial surgery (suppressed thyroglobulin (Tg) < 0.2 ng/mL or thyroid-stimulating hormone [TSH]-stimulated Tg < 1 ng/mL and negative imaging); and not having undergone radioactive iodine (RAI) ablation postoperatively.

The exclusion criteria were postoperative persistent disease; other significant malignant tumors; serious medical record deficiency or loss during follow-up; and a TLN number less than 4.

This study was conducted in compliance with the 2013 revision of the Helsinki Declaration. The Ethics Committee of the Affiliated Hospital of Jining Medical University approved the study (2022C092). All participants provided written informed consent before participation.

2.2 Post-operative follow-up

All patients were followed up with and treated based on the ATA management guidelines (2009 or 2015 version) (5, 21). Outpatient reviews were recommended every 3–6 months for the first 2 years, and annually thereafter. Physical examination and thyroid ultrasonography were performed to evaluate the surgical area. Additionally, thyroid function was evaluated by testing serum thyroglobulin (Tg), anti-thyroglobulin antibodies (TgAb), and TSH levels. Data collected from medical records included age; sex; BMI; Hashimoto's thyroiditis (HT) status; TNM staging; tumor number; tumor size; extrathyroidal extension (ETE); TLNs; MLNs; BRAF status; ultrasound and RAI scanning results; and Tg, TgAb, and TSH levels.

Based on evaluations at each follow-up visit after surgery, the disease outcomes of STR and BIR were diagnosed. STR was diagnosed based on cytological or histological proof, as well as clear results of ultrasound, computerized tomography (CT), RAI whole-body scans, or positron emission tomography-CT. BIR was defined as suppressed Tg levels of ≥1 ng/mL, TSH-stimulated Tg levels ≥10 ng/mL, or progressive rise in TgAb, without evidence of structural disease on imaging modality (22). Disease-free survival (DFS) was defined as the period without disease recurrence after initial treatment, including structural recurrence-free survival (STRFS) and biochemical recurrence-free survival (BIRFS). RAI ablation or follow-up was recommended for patients with BIR. However, RAI ablation, a second surgery, or further follow-up was recommended for patients with STR.

2.3 Statistical analysis

The Student's t-test (normally distributed data) and Mann-Whitney test (non-normally distributed data) were used to compare continuous data. The chi-square test was used to compare categorical data. Continuous variables are presented as means ± standard deviations, whereas categorical variables are presented as numbers with percentages. The optimal cut-off values of LNR

relevant to the STRFS and BIRFS were determined using X-tile software. The patients were allocated into groups according to the optimal cutoff values for LNR. The Kaplan–Meier method was used to evaluate survival rates, and the results were compared using the log-rank test. Predictors were validated using univariate and multivariate Cox regression analyses. Statistical significance was defined as a *p*-value of less than 0.05. X-tile and SPSS version 26.0 software were used for all statistical assessments.

3 Results

3.1 Patient characteristics and follow-up

This study included 617 patients (181 men and 436 women). Table 1 presents the patient and tumor characteristics. The average age was 42.94 ± 14.35 years, and the average tumor size was 1.77 ± 0.75 cm. The ETE rate was 16.21%, the Hashimoto's thyroiditisrate was 36.47%, and BRAF mutations rate was 52.19%. In addition, the median numbers of MLNs and TLNs were 4.17 ± 1.98 and 8.08 ± 3.02 in this study, respectively.

Structural recurrence was found in 31 cases (5.02%): six in the initial thyroidectomy bed, seven in the cervical lymph nodes, and 18 in the lateral lymph nodes. Of these 31 patients, 24 were treated with secondary surgery and five with RAI ablation, while two chose to continue their follow-up (Figure 1).

Biochemical recurrence was found in 94 cases (15.24%): 37 patients were treated with RAI ablation and the others were followed up. Of these 94 patients, 12 were also diagnosed with STR. After diagnosis, the remaining 82 patients were monitored. The results showed that 16 patients developed STR in the following 1–35 months, including 10 patients who had undergone RAI. Twenty-four patients had a disease-free state at the last follow-up, 10 of whom had undergone RAI. Forty-two patients continued to have a biochemical incomplete response status, including 17 patients who had received RAI. Additional RAI ablation did not have a significant impact on the outcomes of the patients with BIR (Table 2).

The median follow-up period for the group as a whole was 69.69 ± 17.07 months (range, 6–108 months). Nine patients died during follow-up due to PTC-unrelated events. At the last follow-up, 511 (82.82%) patients were alive and disease free.

TABLE 1 Demographics and tumor characteristics.

	N	P(%)
Sex (Female)	436	70.66
Age,years (Mean ± SD)	42.94 ± 14.35	
Age, number (≥55)	173	28.04
Body Mass Index (mean ± SD)	25.47 ± 3.35	
Hashimoto's thyroiditis, number	225	36.47
Bilateral tumors, number	54	8.75
Size, cm (mean ± SD)	1.77 ± 0.75	
Multifocality, number	110	17.83
Extrathyroidal extension	100	16.21
BRAF mutation, number	322	52.19
Metastasized lymph nodes (mean ± SD)	4.17 ± 1.98	
Total lymph nodes (mean ± SD)	8.18 ± 3.02	
Lymph node ratio	0.53 ± 0.23	
Follow-up time,months (mean ± SD)	69.69 ± 17.07	
Structural recurrence, number	31	5.02
Biochemical recurrence, number	94	15.24

3.2 Optimal LNR cut-off values

ROC curve analysis was performed to assess the diagnostic effectiveness of LNR and MLNs in STRFS and BIRFS. The results showed that the area under the curve (AUC) of the LNR was larger than that of the MLNs for both STRFS (0.669 versus 0.600) and BIRFS (0.558 versus 0.535) (Figures 2A, B). X-tile software was used to determine the ideal LNR cut-off value. The results indicated that, for STR and BIR, 0.75 and 0.80 were the optimal cut-off values, respectively. Baseline clinicopathological features were compared according to optimal LNR cut off values (Tables 3 and 4).

Considering STR, the high LNR (≥0.75) group had a higher recurrence rate than did the low LNR (<0.75) group (9.46% versus 3.63%, p=0.044). BIR was greater in the high LNR (≥0.80) group than in the low LNR (<0.80) group (24.58% versus 13.03%, p=0.002) group.

3.3 Risk factors for recurrence

Univariate analyses revealed that old age (≥55 years), tumor size, ETE, BRAF mutation, MLN number, and high LNR (≥0.75) were the main factors that influenced STRFS (p<0.10). Multivariate analyses showed that tumor size, ETE, BRAF mutation, MLN number, and high LNR (≥0.75) were independent influencing factors for STRFS (p < 0.05) (Table 5).

As regards BIRFS, univariate analyses demonstrated that old age (≥ 55 years), tumor size, multifocality, ETE, and high LNR (≥0.80) were relative influencing factors (p<0.10). Multivariate analyses showed that tumor size, ETE, and high LNR (≥0.80) were independent influencing factors (p<0.05) (Table 6).

Figures 3 and 4 show Kaplan–Meier curves grouped by the optimal LNR cut-off value. The high and low LNR survival curves exhibited significant differences in the log-rank test for both STRFS and BIRFS (p=0.003 and p=0.001, respectively). With regard to structural recurrence, the 5-year STRFS was 90.5% in the high LNR (≥0.75) and 96.8% in low LNR (<0.75) groups. However, in terms of biochemical recurrence, the 5-year BIRFS was 75.7% in the high LNR (≥0.80) and 86.9% in low LNR (<0.80) groups.

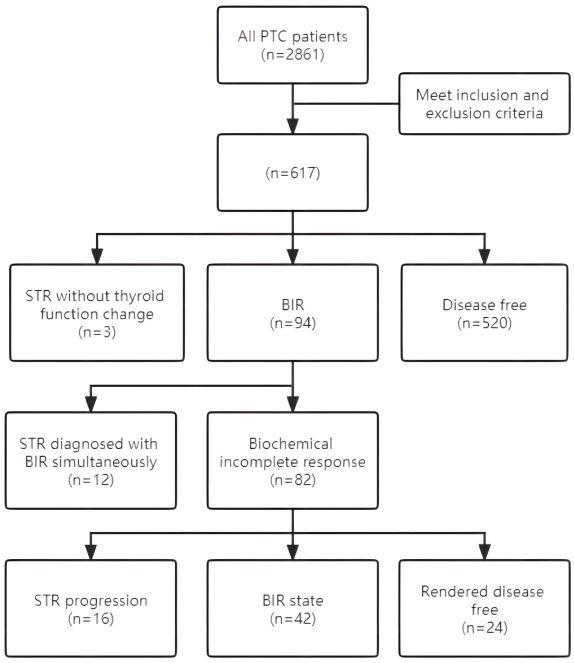

FIGURE 1
Flowchart for study sample.

4 Discussion

PTC has a rather favorable prognosis, with a 10-year disease-specific mortality rate of approximately 4%. However, the high incidence of recurrence is nonnegligible. Although the majority of PTC recurrences are not deadly, they can be quite painful for patients.

Age, tumor size, pathological subtype, MLNs, ETE, and multifocality are risk variables that have been established as independent predictors of PTC recurrence. Various methods have been developed to determine the likelihood of recurrence based on these factors (23–25).

The 2015 ATA management guidelines classified recurrence risk as low, intermediate, and high, according to pathological features. These features included degree of residual lesion, tumor size, pathological subtype, envelope infiltration, vascular invasion, lymph node metastasis features, molecular pathological features, stimulated Tg level, and post-treatment whole-body scan (5). Local recurrence has been observed in 3–13% of patients with low-risk tumors, 21–36% of those with intermediate-risk tumors, and 68% of those with high-risk tumours (5). In this study, the median follow-up period was 69.69 ± 17.07 months, and total structural recurrence rate was 5.02%.

Lymph node metastasis in patients with PTC is associated with high recurrence rate. The number of MLNs varies with the degree of LNs dissection scope and pathological sampling ability. Some patients with fewer MLNs still have a high risk of recurrence. Are there other diagnostic indicators that, in combination with the existing ATA criteria, would be good predictors of recurrence in patients. According to the AJCC 8th TNM classification, N1a and N1b were categorized into the same stage. Therefore, the N staging of TNM classification is inadequate for assessing recurrence risk (26). Furthermore, it is unclear which patients with pN1a should undergo RAI ablation and which, prophylactic lateral neck dissection, to prevent recurrence. To differentiate between "lower risk characteristics" and "higher risk characteristics" in these patients, a new risk stratification strategy is required to provide individualized therapy for each patient, reducing hazards and optimizing benefits.

LNR has been widely used to assess oncological prognosis such as lungs, stomach, and colon cancer. In terms of PTC, after collecting data from 10, 955 patients, Schneider et al. (27) showed

TABLE 2 Clinical outcome of BIR patients.

	RAI	Non-RAI	Total	P-value
STR progression	10	6	16	
BIR keep	17	25	42	
Rendered disease-free	10	14	24	
Total	37	45	82	0.296

STR, structural recurrence; BIR, biochemical recurrence.

10.3389/fendo.2023.1158826

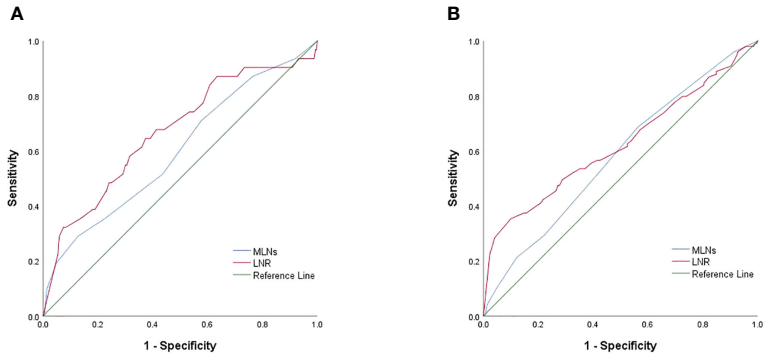

FIGURE 2
(A) ROC curves for LNR and MLNs in STR. **(B)** ROC curves for LNR and MLNs in BIR.

TABLE 3 Comparison of demographics and tumor characteristics according to optimal LNR cut off values of structural recurrence.

	LNR <0.75 N=469	HNR ≥0.75 N=148	P-value
Sex			0.044
Male	142	39	
Female	327	109	
Age (Mean ± SD)(y)	42.28 ± 14.12	45.01 ± 14.92	0.009
Age55			0.382
≥55	119	54	
<55	350	94	
BMI	25.54 ± 3.32	25.26 ± 3.47	0.598
HT			0.052
Absence	304	88	
Presence	165	60	
Bilaterral			0.483
Absence	422	141	
Presence	47	7	
Tumor size	1.784 ± 0.75	1.73 ± 0.75	0.557
Multifocality			0.201
Absence	383	124	
Presence	86	24	
Infiltration			0.478
Absence	398	119	
Presence	71	29	
BRAF mutation			0.000
Absence	228	67	
Presence	241	81	
MLN	3.83 ± 1.99	5.22 ± 1.54	0.000
TLN	8.84 ± 3.04	6.07 ± 1.72	0.006

(Continued)

TABLE 3 Continued

	LNR <0.75 N=469	HNR ≥0.75 N=148	P-value
Structural recurrence			0.044
Absence	452	134	
Presence	17	14	

STR, structural recurrence; BIR, biochemical recurrence; HT, Hashimoto's thyroiditis;
MLN, metastatic lymph nodes; TLN, total lymph nodes.

TABLE 4 Comparison of demographics and tumor characteristics according to optimal LNR cut off values of biochemical recurrence.

	LNR <0.80 n=499	HNR ≥0.80 n=118	P-value
Sex			0.557
Male	149	32	
Female	350	86	
Age (Mean ± SD) (y)	42.40 ± 14.11	45.21 ± 15.17	0.056
Age55			0.004
≥55	127	46	
<55	372	72	
BMI	25.50 ± 3.32	25.38 ± 3.51	0.724
HT			0.867
Absence	320	72	
Presence	179	46	
Bilaterral			0.124
Absence	451	112	
Presence	48	6	
Tumor size	1.79 ± 0.74	1.70 ± 0.77	0.239
Multifocality			0.992
Absence	410	97	
Presence	89	21	
Infiltration			0.104
Absence	424	93	
Presence	75	25	
BRAF mutation			0.267
Absence	244	51	
Presence	255	67	
MLN	3.89 ± 1.20	5.34 ± 1.43	0.000
TLN	8.69 ± 3.07	6.02 ± 1.49	0.000
Biochemical recurrence			0.002
Absence	434	89	
Presence	65	29	

STR, structural recurrence; BIR, biochemical recurrence; HT, Hashimoto's thyroiditis;
MLN, metastatic lymph nodes; TLN, total lymph nodes.

10.3389/fendo.2023.1158826

TABLE 5 Cox regression analysis of structural recurrence.

	Univariate Logistic Regression		Multivariate Logistic Regression	
	OR (95% CI)	P Value	OR (95% CI)	P Value
Sex	1.522(0.738-3.135)	0.255		
Age55	1.903(0.933-3.885)	0.077	1.564(0.761-3.214)	0.224
BMI	1.061(0.953-1.181)	0.281	NA	NA
HT	1.014(0.612-1.681)	0.957	NA	NA
Bilaterral	2.004(0.769-5.224)	0.155	NA	NA
Size	2.179(1.360-3.490)	0.001	1.798(1.134-2.851)	0.013
Multifocality	1.891(0.871-4.106)	0.107	NA	NA
Infiltration	4.660(2.296-9.457)	0.000	3.855(1.840-8.076)	0.000
BRAF mutation	2.216(1.020-4.815)	0.044	2.402(1.092-5.283)	0.029
MLN	1.232(1.039-1.461)	0.016	1.203(1.000-1.446)	0.050
TLN	0.979(0.869-1.103)	0.732	NA	NA
LNR	2.811(1.385-5.706)	0.004	2.130(1.018-4.456)	0.045

HT, Hashimoto's thyroiditis; MLN, metastatic lymph nodes; TLN, total lymph nodes; LNR, lymph node ratio; NA, not applicable.

that LNR was associated with disease-related mortality. Parvathareddy et al. (28), in a retrospective study of 1407 cases, reported that TNM classification in combination with LNR had a stronger diagnostic capability for recurrence than did TNM alone. Lee et al. (29) claimed that the 2015 ATA risk stratification and 8th AJCC staging system provided greater predictive value for recurrence in patients with PTC once integrated with LNR. Kang et al. (30) reported that LNR was more accurate in predicting recurrence than N stage, after an analysis of a group of 307 patients with N1b PTC. Despite numerous findings on the use of LNR to assess PTC prognosis, no studies have assessed the clinical significance of LNR in patients with low-to-intermediate recurrence risk N1a PTC.

Our results showed that the diagnostic efficiency of LNR was higher than that of MLNs for STRFS (AUC of 0.669 versus 0.600). X-tile analysis showed that 0.75 was the optimal cut-off value for STR. Patients with LNRs of ≥0.75 had a significantly greater incidence of STR than did those with LNRs of <0.75 (9.46% versus 3.63%, p=0.044). Regarding STRFS, multivariate analyses showed that tumor size, ETE, BRAF mutation, MLN number, and high LNR (≥0.75) were independent influencing factors (p<0.05). Significant differences between the survival curves for high and low

TABLE 6 Cox regression analysis of biochemical recurrence.

	Univariate Logistic Regression		Multivariate Logistic Regression	
	OR (95% CI)	P Value	OR (95% CI)	P Value
Sex	1.386(0.910-2.111)	0.129	NA	NA
Age55	1.434(0.939-2.190)	0.095	1.241(0.805-1.912)	0.328
BMI	0.985(0.929-1.045)	0.620	NA	NA
HT	1.011(0.750-1.364)	0.940	NA	NA
Bilaterral	1.406(0.750-2.637)	0.288	NA	NA
Size	1.754(1.344-2.289)	0.000	1.519(1.162_1.986)	.002
Multifocality	1.535(0.959-2.456)	0.074	1.213(0.746-1.972)	0.436
Infiltration	3.680(2.427-5.582)	0.000	2.932(1.899-4.525)	0.000
BRAF mutation	1.226(0.815-1.845)	0.329	NA	NA
MLN	1.075(0.971-1.190)	0.166	NA	NA
TLN	1.012(0.946-1.082)	0.734	NA	NA
LNR	2.037(1.315-3.156)	0.001	1.953(1.254-3.043)	0.003

HT, Hashimoto's thyroiditis; MLN, metastatic lymph nodes; TLN, total lymph nodes; LNR, lymph node ratio; NA, not applicable.

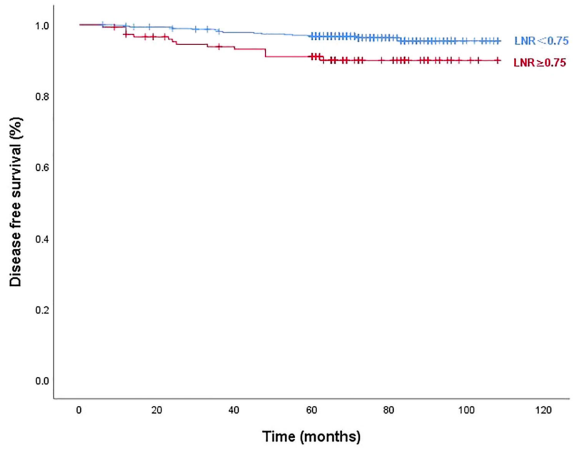

FIGURE 3
Disease-free survival curves according to optimal LNR cut off values of structural recurrence (log-rank p=0.003).

LNR were observed using the log-rank test (p=0.003). Five-year STRFS was 90.5% in the high and 96.8% in the low LNR groups. It is worth mentioning that the best cut-off value of LNR for predicting STR in this study was 0.8, which is higher than that reported in the relevant reports. We speculate that this is related to the different inclusion criteria, the patients included in this study were all low-to-intermediate risk patients (T1-3N1aM0), who had a better prognosis and a higher LNR cut-off value for the STR.

The majority of research evaluating long-term results frequently focuses on STR rather than BIR. A biochemical incomplete response is diagnosed based on increased serum levels of Tg or TgAb without any signs of structural abnormalities. In addition, if a patient achieved an excellent response after primary total thyroidectomy, this kind of biochemical incomplete response may be labelled BIR. According to the ATA, BIR is seen in 11–19% of low-risk, 2–22% of intermediate-risk, and 16–18% of high-risk patients (31, 32). However, the BIR rate of patients with N1a has not been assessed thus far. Our assessment revealed a 15.24% chance of BIR in patients with low-to-intermediate N1a. Since the long-term prognosis in these patients is not well understood, and some may develop structural illness, close follow-up is required. In this study, we also found that 0.80 was the optimal cutoff value for BIR. Patients with LNRs of ≥0.80 had significantly greater BIR incidences than did those with LNRs of <0.80 (9.46% vs. 3.63%, p=0.044). Multivariate analyses showed that tumor size, ETE, and high LNR (≥0.80) were independent factors influencing BIRFS (p<0.05). Significant differences between the survival curves for the high and low LNR groups were observed using the log-rank test (p=0.001). Five-year BIRFS was 75.7% for high LNR and 86.9% for low LNR. It is notable that, unlike the findings of other studies, performing RAI ablation after BIR had no significant effect on the progression to STR in our trial, which may have result from a high lymph node recurrence rate of STR in our cohort (33).

This retrospective study has several limitations that should be considered. Due to the possibility of selection bias in single-center studies, our findings may not be applicable to a larger population.

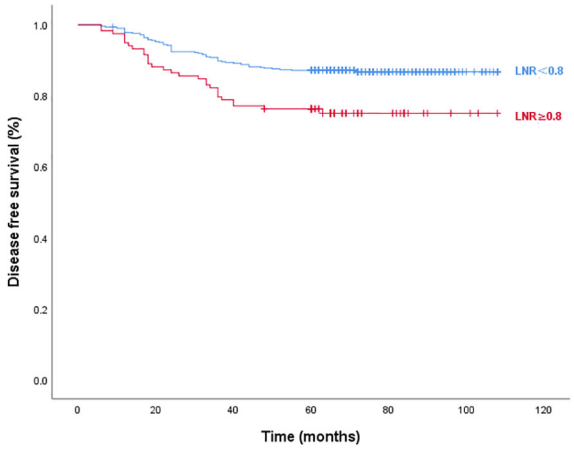

FIGURE 4
Disease-free survival curves according to optimal LNR cut off values of biochemical recurrence (log-rank p=0.001).

Since we only included patients with pathologic N1a PTC, it might be challenging to extrapolate our findings to all patients with PTC. Furthermore, although certain patient data, such as histological subtypes, diameters of the biggest MLNs, extra-nodal extension and micrometastases of MLNs, did not appear in pathology reports 10 years ago, they were reported to have prognostic value (34–36). To overcome these restrictions, we intend to conduct prospective research in the future that also takes LN-related parameters into consideration. Our study also has a number of advantages. Every patient was diagnosed, treated, and followed up by the same medical team, in accordance with the same standardized procedure. In addition, our study had a longer follow-up period compared to that in similar studies. We also assessed factors influencing biochemical recurrence.

5 Conclusions

According to our findings, LNR was associated with recurrence in patients with N1a PTC. LNR≥0.75 and LNR≥0.80 were independent predictors of STRFS and BIRFS, respectively. We recommend those low-risk and intermediate-risk patients with a high LNR (≥0.75), even with limited MLNs, require a comprehensive evaluation of lateral neck lymphadenopathy and consideration for lateral neck dissection and RAI treatment. These findings may help physicians identify patients who are at risk and aid them in choosing the best postsurgical therapy and monitoring. The results of this research may help develop more effective staging standards.

Data availability statement

The original contributions presented in the study are included in the article/supplementary material. Further inquiries can be directed to the corresponding author.

Ethics statement

The experimental protocol was established, according to the ethical guidelines of the Helsinki Declaration and was approved by the Human Ethics Committee of Affiliated Hospital of Jining Medical University (2022C092).

Author contributions

TM designed the study, analyzed the data and commented on the manuscript at all stages. WS and LW collected the data. JC,PS, XZ, ML revised the manuscript. YS provided the research direction. All authors contributed to the article and approved the submitted version.

Funding

Academician He Lin Research Foundation of Affiliated Hospital of Jining Medical University (JYHL2022FMS10).

Conflict of interest

The authors declare that the research was conducted in the absence of any commercial or financial relationships that could be construed as a potential conflict of interest.

Publisher's note

All claims expressed in this article are solely those of the authors and do not necessarily represent those of their affiliated organizations, or those of the publisher, the editors and the reviewers. Any product that may be evaluated in this article, or claim that may be made by its manufacturer, is not guaranteed or endorsed by the publisher.

References

1. Megwalu UC, Moon PK. Thyroid cancer incidence and mortality trends in the United States: 2000-2018. *Thyroid* (2022) 32(5):560–70. doi: 10.1089/thy.2021.0662

2. La Vecchia C, Malvezzi M, Bosetti C, Garavello W, Bertuccio P, Levi F, et al. Thyroid cancer mortality and incidence: a global overview. *Int J Cancer* (2015) 136 (9):2187–95. doi: 10.1002/ijc.29251

3. Conzo G, Mauriello C, Docimo G, Gambardella C, Thomas G, Cavallo F, et al. Clinicopathological pattern of lymph node recurrence of papillary thyroid cancer. Implications for surgery. *Int J Surg* (2014) 12 Suppl 1:S194–7. doi: 10.1016/j.ijsu.2014.05.010

4. Wang J, Yu F, Shang Y, Ping Z, Liu L. Thyroid cancer: incidence and mortality trends in China, 2005-2015. *Endocrine* (2020) 68(1):163–73. doi: 10.1007/s12020-020-02207-6

5. Haugen BR. 2015 American thyroid association management guidelines for adult patients with thyroid nodules and differentiated thyroid cancer: the american thyroid association guidelines task force on thyroid nodules and differentiated thyroid cancer. *Thyroid* (2016) 26(1):1–133. doi: 10.1089/thy.2015.0020

6. Marti JL, Morris L, Ho AS. Selective use of radioactive iodine (RAI) in thyroid cancer: No longer "one size fits all". *Eur J Surg Oncol* (2018) 44(3):348–56. doi: 10.1016/j.ejso.2017.04.002

7. Zambeli-Ljepovic A, Wang F, Dinan MA, Hyslop T, Roman SA, Sosa JA, et al. Low-risk thyroid cancer in elderly: total thyroidectomy/RAI predominates but lacks survival advantage. *J Surg Res* (2019) 243:189–97. doi: 10.1016/j.jss.2019.05.029

8. Yang P, Li J, Jing H, Chen Q, Song X, Qian L. Effect of prophylactic central lymph node dissection on locoregional recurrence in patients with papillary thyroid microcarcinoma. *Int J Endocrinol* (2021) 2021:8270622. doi: 10.1155/2021/8270622

9. Sterpetti AV. Optimization of staging of the neck with prophylactic central and lateral neck dissection for papillary thyroid carcinoma. *Ann Surg* (2015) 261(1):e30. doi: 10.1097/SLA.0000000000000510

10. Shen FC, Hsieh CJ, Huang IC, Chang YH, Wang PW. Dynamic risk estimates of outcome in Chinese patients with well-differentiated thyroid cancer after total thyroidectomy and radioactive iodine remnant ablation. *Thyroid* (2017) 27(4):531–6. doi: 10.1089/thy.2016.0479

11. Yu ST, Ge JN, Sun BH, Wei ZG, Xiao ZZ, Zhang ZC, et al. Lymph node yield in the initial central neck dissection (CND) associated with the risk of recurrence in papillary thyroid cancer: A reoperative CND cohort study. *Oral Oncol* (2021) 123:105567. doi: 10.1016/j.oraloncology.2021.105567

12. Feng JW, Ye J, Wu WX, Qu Z, Qin A-C, Jiang Y. Management of cN0 papillary thyroid microcarcinoma patients according to risk-scoring model for central lymph

node metastasis and predictors of recurrence. *J Endocrinol Invest* (2020) 43(12):1807–17. doi: 10.1007/s40618-020-01326-1

13. Amin MB, Greene FL, Edge SB, Compton CC, Gershenwald JE, Brookland RK, et al. The Eighth Edition AJCC Cancer Staging Manual: Continuing to build a bridge from a population-based to a more "personalized" approach to cancer staging. *CA Cancer J Clin* (2017) 67(2):93–9. doi: 10.3322/caac.21388

14. Shaha AR. TNM classification of thyroid carcinoma. *World J Surg* (2007) 31 (5):879–87. doi: 10.1007/s00268-006-0864-0

15. Xiang J, Wang Z, Sun W, Zhang H. A relook at the 8th edition of the AJCC TNM staging system of anaplastic thyroid carcinoma: A SEER-based study. *Clin Endocrinol (Oxf)* (2021) 94(4):700–10. doi: 10.1111/cen.14371

16. Kim TH, Kim YN, Kim HI, Park SY, Choe JH, Kim JH, et al. Prognostic value of the eighth edition AJCC TNM classification for differentiated thyroid carcinoma. *Oral Oncol* (2017) 71:81–6. doi: 10.1016/j.oraloncology.2017.06.004

17. Lim YC, Liu L, Chang JW, Koo BS. Lateral lymph node recurrence after total thyroidectomy and central neck dissection in patients with papillary thyroid cancer without clinical evidence of lateral neck metastasis. *Oral Oncol* (2016) 62:109–13. doi: 10.1016/j.oraloncology.2016.10.010

18. Chiappetta M, Leuzzi G, Sperduti I, Bria E, Mucilli F, Lococo F, et al. Lymph-node ratio predicts survival among the different stages of non-small-cell lung cancer: a multicentre analysisdagger. *Eur J Cardiothorac Surg* (2019) 55(3):405–12. doi: 10.1093/ejcts/ezy311

19. Wang H, Qi H, Liu X, Gao Z, Hidasa I, Aikebaier A, et al. Positive lymph node ratio is an index in predicting prognosis for remnant gastric cancer with insufficient retrieved lymph node in R0 resection. *Sci Rep* (2021) 11(1):2022. doi: 10.1038/s41598-021-81663-0

20. Chen SL, Steele SR, Eberhardt J, Zhu K, Bilchik A, Stojadinovic A. Lymph node ratio as a quality and prognostic indicator in stage III colon cancer. *Ann Surg* (2011) 253(1):82–7. doi: 10.1097/SLA.0b013e3181ffa780

21. Cooper DS, Doherty GM, Haugen BR, Kloos RT, Lee SL, Mandel SJ, et al. Revised American Thyroid Association management guidelines for patients with thyroid nodules and differentiated thyroid cancer. *Thyroid* (2009) 19(11):1167–214. doi: 10.1089/thy.2009.0110

22. Llamas-Olier AE, Cuellar DI, Buitrago G. Intermediate-risk papillary thyroid cancer: risk factors for early recurrence in patients with excellent response to initial therapy. *Thyroid* (2018) 28(10):1311–7. doi: 10.1089/thy.2017.0578

23. Siddiqui S, White MG, Antic T, Grogan RH, Angelos P, Kaplan E, et al. Clinical and pathologic predictors of lymph node metastasis and recurrence in papillary thyroid microcarcinoma. *Thyroid* (2016) 26(6):807–15. doi: 10.1089/thy.2015.0429

24. Heng Y, Feng S, Yang Z, Cai W, Qiu W, Tao L. Features of lymph node metastasis and structural recurrence in papillary thyroid carcinoma located in the upper portion of the thyroid: A retrospective cohort study. *Front Endocrinol (Lausanne)* (2021) 12:793997. doi: 10.3389/fendo.2021.793997

25. Jiang LH, Yin KX, Wen QL, Chen C, Ge MH, Tan Z. Predictive risk-scoring model for central lymph node metastasis and predictors of recurrence in papillary thyroid carcinoma. *Sci Rep* (2020) 10(1):710. doi: 10.1038/s41598-019-55991-1

26. Tam S, Boonsripitayanon M, Amit M, Fellman BM, Li Y, Busaidy NL, et al. Survival in differentiated thyroid cancer: comparing the AJCC cancer staging seventh and eighth editions. *Thyroid* (2018) 28(10):1301–10. doi: 10.1089/thy.2017.0572

27. Schneider DF, Chen H, Sippel RS. Impact of lymph node ratio on survival in papillary thyroid cancer. *Ann Surg Oncol* (2013) 20(6):1906–11. doi: 10.1245/s10434-012-2802-8

28. Parvathareddy SK, Siraj AK, Qadri Z, Ahmed SO, DeVera F, Al-Sobhi S, et al. Lymph node ratio is superior to AJCC N stage for predicting recurrence in papillary thyroid carcinoma. *Endocr Connect* (2022) 11(2). doi: 10.1530/EC-21-0518

29. Lee J, Lee SG, Kim K, Yim S, Ryu H, Lee CR, et al. Clinical value of lymph node ratio integration with the 8(th) edition of the UICC TNM classification and 2015 ATA risk stratification systems for recurrence prediction in papillary thyroid cancer. *Sci Rep* (2019) 9(1):13361. doi: 10.1038/s41598-019-50069-4

30. Kang IK, Kim K, Park J, Bae JS, Kim JS. Central lymph node ratio predicts recurrence in patients with N1b papillary thyroid carcinoma. *Cancers (Basel)* (2022) 14 (15). doi: 10.3390/cancers14153677

31. Tuttle RM, Tala H, Shah J, Leboeuf R, Ghossein R, Gonen M, et al. Estimating risk of recurrence in differentiated thyroid cancer after total thyroidectomy and radioactive iodine remnant ablation: using response to therapy variables to modify the initial risk estimates predicted by the new American Thyroid Association staging system. *Thyroid* (2010) 20(12):1341–9. doi: 10.1089/thy.2010.0178

32. Pitoia F, Bueno F, Urciuoli C, Abelleira E, Cross G, Tuttle RM. Outcomes of patients with differentiated thyroid cancer risk-stratified according to the American thyroid association and Latin American thyroid society risk of recurrence classification systems. *Thyroid* (2013) 23(11):1401–7. doi: 10.1089/thy.2013.0011

33. Haddad RI, Bischoff L, Ball D, Bernet D, Blomain D, Busaidy D, et al. Thyroid carcinoma, version 2.2022, NCCN clinical practice guidelines in oncology. *J Natl Compr Canc Netw* (2022) 20(8):925–51. doi: 10.6004/jnccn.2022.0040

34. Sun Y, Liu X, Ouyang W, Feng H, Wu J, Chen P, et al. Lymph node characteristics for predicting locoregional recurrence of papillary thyroid cancer in adolescents and young adults. *Oral Oncol* (2017) 66:22–7. doi: 10.1016/j.oraloncology.2016.12.028

35. Ricarte-Filho J, Ganly I, Rivera M, Katabi N, Fu W, Shaha A, et al. Papillary thyroid carcinomas with cervical lymph node metastases can be stratified into clinically relevant prognostic categories using oncogenic BRAF, the number of nodal metastases, and extra-nodal extension. *Thyroid* (2012) 22(6):575–84. doi: 10.1089/thy.2011.0431

36. Park J, Kim D, Lee JO, Park HC, Ryu BY, Kim JH, et al. Dissection of molecular and histological subtypes of papillary thyroid cancer using alternative splicing profiles. *Exp Mol Med* (2022) 54(3):263–72. doi: 10.1038/s12276-022-00740-0

frontiers | Frontiers in Endocrinology

TYPE Original Research
PUBLISHED 15 September 2023
DOI 10.3389/fendo.2023.1185327

OPEN ACCESS

EDITED BY
Eleonora Lori,
Sapienza University of Rome, Italy

REVIEWED BY
Anupam Kotwal,
University of Nebraska Medical Center, United States
Ludovico Docimo,
University of Campania Luigi Vanvitelli, Italy

*CORRESPONDENCE
Shuai Xue
xueshuai@jlu.edu.cn

RECEIVED 13 March 2023
ACCEPTED 21 August 2023
PUBLISHED 15 September 2023

CITATION
Zhang L, Wang P, Li K and Xue S (2023) A novel nomogram for identifying high-risk patients among active surveillance candidates with papillary thyroid microcarcinoma. *Front. Endocrinol.* 14:1185327. doi: 10.3389/fendo.2023.1185327

A novel nomogram for identifying high-risk patients among active surveillance candidates with papillary thyroid microcarcinoma

Li Zhang[1], Peisong Wang[2], Kaixuan Li[2] and Shuai Xue[2]*

[1]Department of Nephrology, The First Hospital of Jilin University, Changchun, China, [2]General Surgery Center, Department of Thyroid Surgery, The First Hospital of Jilin University, Changchun, China

Objective: Active surveillance (AS) has been recommended as the first-line treatment strategy for low-risk (LR) papillary thyroid microcarcinoma (PTMC) according to the guidelines. However, preoperative imaging and fine-needle aspiration could not rule out a small group of patients with aggressive PTMC with large-volume lymph node micro-metastasis, extrathryoidal invasion to surrounding soft tissue, or high-grade malignancy from the AS candidates.

Methods: Among 2,809 PTMC patients, 2,473 patients were enrolled in this study according to the inclusion criteria. Backward stepwise multivariate logistic regression analysis was used to filter clinical characteristics and ultrasound features to identify independent predictors of high-risk (HR) patients. A nomogram was developed and validated according to selected risk factors for the identification of an HR subgroup among "LR" PTMC patients before operation.

Results: For identifying independent risk factors, multivariable logistic regression analysis was performed using the backward stepwise method and revealed that male sex [3.91 (2.58–5.92)], older age [0.94 (0.92–0.96)], largest tumor diameter [26.7 (10.57–69.22)], bilaterality [1.44 (1.01–2.3)], and multifocality [1.14 (1.01–2.26)] were independent predictors of the HR group. Based on these independent risk factors, a nomogram model was developed for predicting the probability of HR. The C index was 0.806 (95% CI, 0.765–0.847), which indicated satisfactory accuracy of the nomogram in predicting the probability of HR.

Conclusion: Taken together, we developed and validated a nomogram model to predict HR of PTMC, which could be useful for patient counseling and facilitating treatment-related decision-making.

KEYWORDS

active surveillance, papillary thyroid microcarcinoma, high risk, high-volume lymph node metastasis, extrathyroidal invasion, aggressive variant, predictive model, nomogram

1 Introduction

In the past few decades, the incidence of papillary thyroid microcarcinoma (PTMC) has increased noticeably but with excellent prognosis (1). Despite its increasing incidence, the relatively stable and considerably low disease-specific mortality of PTMC in recent years has raised concerns about overdiagnosis and overtreatment (2, 3). Thus, active surveillance (AS) was recommended as an alternative disease management option for low-risk (LR) PTMC (4). According to a prospective trial of 1,235 PTMC patients in Kuma hospital in Japan, 8% of the patients had tumor enlargement ≥ 3 mm, and 3.8% demonstrated novel lymph node metastases during AS at the 10-year follow-up (5). Moreover, there were considerably fewer medical costs and unfavorable events in the AS group patients, although both immediate surgery and the AS cohorts had excellent prognosis (6). Thus, AS was chosen as the initial treatment strategy by increasing LR PTMC patients in Kuma hospital (7). Moreover, studies from other countries have also validated these results, resulting in AS being recommended as the first-line treatment strategy for LR PTMC according to the guidelines (4, 8).

Based on the patient selection criteria, LR PTMC was defined as a lack of high-grade malignancy in cytology, absence of symptoms or signs of invasion to the recurrent laryngeal nerve (RLN) or trachea, and no N1 and M1 (9). These criteria for determining AS candidature rely heavily on imaging, particularly ultrasound (US). However, preoperative imaging and fine-needle aspiration (FNA) could not rule out a small group of patients with aggressive PTMC with large-volume lymph node micro-metastasis, extrathryoidal extension (ETE) invasion to surrounding soft tissue, or high-grade malignancy from the AS candidates (10). If aggressive PTMC is considered as an "LR" category, AS would delay surgery for such patients, causing more harm than benefit. Therefore, this retrospective study was conducted to identify the preoperative predictors of high risk (HR) among "LR" PTMC patients. Then, a nomogram was developed and validated to predict the probability of HR among PTMC AS patients to facilitate preoperative decision-making.

2 Materials and methods

2.1 Study design and population

A nomogram was developed and validated according to the clinical characteristics and US features for the identification of an HR subgroup among "LR" PTMC patients before operation.

We retrospectively reviewed a total of 2,809 consecutive PTMC patients, who had undergone surgery at the Department of Thyroid Surgery, General Surgery Center at the First Hospital of Jilin University, between January 2021 and January 2022. The study was approved by the ethics committee of the First Hospital of Jilin University. The inclusion criteria were (1) PTMC confirmed by pathologic examination; (2) lobectomy (LT) with ipsilateral or total thyroidectomy (TT) with bilateral central lymph node dissection (CLND); (3) patients who were considered "LR" according to the AS selection criteria; (4) no history of neck radiation; (5) no history of thyroid surgery; and (6) the availability of complete medical records.

Among 2,809 PTMC patients, 2,473 patients were enrolled in this study and 336 patients were excluded as shown in Figure 1. According to the chronological order of enrollment, the included participants were divided into two groups in a ratio of 7:3—a training set consisting of 1,728 consecutive patients between January 2021 and August 2021 and a validation set consisting of 745 consecutive patients between September 2021 and January 2022.

2.2 Surgery and variable assessment

Routine US examination with a high-resolution US scanner was performed for thyroid nodules and cervical lymph nodes in all patients. The US images were reviewed independently by three experienced US physicians. In case of disagreement, the final decision was made after discussion with another US physician with more than 10 years of experience in neck US. As previously described (11), FNA of the thyroid was recommended if the

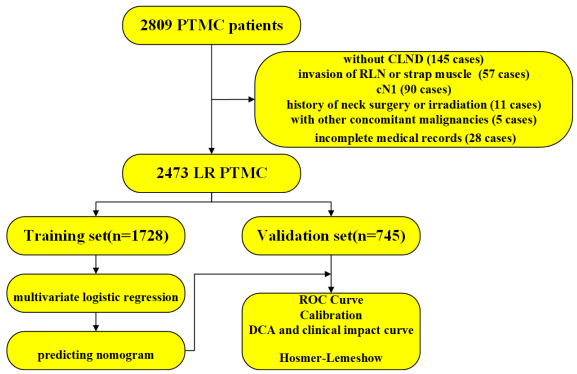

FIGURE 1
The workflow diagram of this study. PTMC, papillary thyroid microcarcinoma; CLND, central lymph node dissection; RLN, recurrent laryngeal nerve; LR, low risk; ROC, receiver operating characteristic curve; DCA, decision curve analysis.

maximum diameter of a nodule was larger than 5 mm and the results of ultrasonography were suspicious. If the thyroid nodule was <5 mm in diameter, the doctor explained the risks and benefits of surgery and a decision was made according to the patient's preference. For US-suspicious thyroid nodules or lymph nodes, FNA with or without thyroglobulin (Tg) washout was recommended for further assessment. Pathologic specimens were reviewed independently by two pathologists, and a few discordant cases were discussed with the third experienced pathologist. Regarding the surgical methods, LT was suggested for PTMC patients without any other HR factors such as gross ETE, vascular invasion, aggressive histology, and clinical N1. Otherwise, TT was performed. Patients with bilateral thyroid microcarcinoma underwent routine TT and bilateral CLND operations; CLND was performed as previously described (11).

Clinical characteristics and US features were analyzed to identify the predictive factors for HR patients: age, gender, largest tumor diameter (LTD), tumor location, echogenicity, boundary, shape, aspect ratio, calcification, CDFI, multifocality, bilaterality, and Hashimoto's thyroiditis (HT). US features were confirmed by ultrasound for solitary tumors or the largest tumor in multifocal cases prior to surgery. Multifocality meant more than one foci of a tumor in a single lobe. Echogenicity implied both hypoechoic and nonhypoechoic masses (including isoechoic and hyperechoic). Calcification could mean no, microcalcification, macrocalcification, or both microcalcification and macrocalcification in one tumor at the same time. Blood flow features of tumors detected through Color Doppler US were divided into no (avascularity), rare (limited vascularity), and abundant (peripheral or strip-like vascularity). The diagnosis of HT was based on thyroid function examination and US: positivity for antithyroid peroxidase antibody and/or antiTg antibody and a diffusely enlarged thyroid gland with a heterogeneous echotexture on US.

2.3 Statistical analysis

Categorical variables were expressed as frequency and percentage (%), and continuous variables were shown as median and interquartile range. The chi-squared test was used for comparing categorical variables and the nonparametric rank sum test for comparing continuous variables. Backward stepwise multivariate logistic regression analysis was used to filter all variables to identify independent predictors of HR. Then, the nomogram was developed according to the independent predictors. Finally, a calibration curve, a concordance index (C-index), and a receiver operating characteristic (ROC) curve were constructed to assess the predictive performance of the nomogram. Moreover, decision curve analysis (DCA) and clinical impact curves were drawn to evaluate the clinical usefulness of the predictive model. The Hosmer–Lemeshow test was performed for assessing the goodness-of-fit of the model. Two-sided p-values < 0.05 were considered statistically significant. Statistical analyses were performed using R software (version 4.2.2).

3 Results

3.1 Patient characteristics

The study population in the training set consisted of 1,728 PTMC candidates for AS. These included 303 (17.5%) men and 1,425 (82.5%) women; the median age was 46 (38–52) years. The median tumor diameter was 0.5 (0.4–0.7) cm. All patients were considered to be in the LR group according to imaging and FNA preoperatively, while 115 (6.7%) patients were confirmed to be HR. The baseline clinical characteristics and US features in the training set are summarized in Table 1 and show significant differences in age, sex, LTD, multifocality, and bilaterality between the LR and HR groups.

3.2 Development of the nomogram model

For identifying independent risk factors, multivariable logistic regression analysis was performed using the backward stepwise method and revealed that male sex [3.91 (2.58–5.92)], older age [0.94 (0.92–0.96)], LTD [26.7 (10.57–69.22)], bilaterality [1.44 (1.01–2.3)], and multifocality [1.14 (1.01–2.26)] were independent predictors of the HR group (Table 2). Based on these independent risk factors, a nomogram model was developed for predicting the probability of HR (Figure 2). The baseline characteristics and predictors for HR in the validation cohort are given in Supplementary Appendix SA1.

3.3 Validation of the nomogram model

Bootstrap validation was performed for the internal validation of the nomogram. The C index was 0.806 (95% CI, 0.765–0.847), which indicated satisfactory accuracy of the nomogram in predicting the probability of HR, also shown as the ROC curve (Figure 3A). The calibration curve demonstrated good agreement between the probability predicted by the model and the actual incidence of HR (mean absolute error: 0.016) (Figure 3B). Moreover, both DCA and clinical impact curves were used to assess the clinical utility of the nomogram. The DCA curve indicated that preoperative "LR" PTMC patients would benefit more if this model was used to predict the risk of HR when the threshold probability is between >1% and <20% (Figure 3C). The clinical impact curve (Figure 3D) indicated that the patients categorized as HR by the nomogram were more likely to be truly HR when the threshold probability < 40%. Additionally, the good calibration of the model was evaluated by the Hosmer–Lemeshow test (p = 0.243). The Brier score of 0.056 showed a good overall performance.

In the validation cohort, the calibration, ROC curve, Hosmer–Lemeshow test, DCA curve, and clinical impact curve, given in Supplementary Appendix SA2, also showed good overall performance.

10.3389/fendo.2023.1185327

TABLE 1 Baseline characteristics and risk factors of the high-risk group in the derivation cohort.

Characteristics	Total	LR	HR	*p*-value
Total, *n* (%)	1,728 (100)	1,613 (93.3)	115 (6.7)	
Age, median [IQR]	46.00 [38.00, 52.00]	46.00 [38.00, 52.00]	39.00 [32.00, 47.50]	<0.001
Gender, *n* (%)				<0.001
Male Female	303 (17.5) 1,425 (82.5)	253 (15.7) 1,360 (84.3)	50 (43.5) 65 (56.5)	
LTD, median [IQR]	0.50 [0.40, 0.70]	0.50 [0.40, 0.70]	0.70 [0.55, 0.80]	<0.001
Tumor location, *n* (%)				0.044
Upper Middle Lower Isthmus	422 (24.4) 622 (36.0) 615 (35.6) 69 (4.0)	406 (25.2) 571 (35.4) 572 (35.5) 64 (4.0)	16 (13.9) 51 (44.3) 43 (37.4) 5 (4.3)	
Echogenicity, *n* (%)				1.000
Nonhypoechoic Hypoechoic	29 (1.7) 1,699 (98.3)	27 (1.7) 1,586 (98.3)	2 (1.7) 113 (98.3)	
Boundary, *n* (%)				0.728
Not clear Clear	1,633 (94.5) 95 (5.5)	90 (5.6) 1,523 (94.4)	5 (4.3) 110 (95.7)	
Shape, *n* (%)				0.804
Not regular Regular	1,581 (91.5) 147 (8.5)	1,477 (91.6) 136 (8.4)	104 (90.4) 11 (9.6)	
Aspect ratio, *n* (%)				0.129
≤1 >1	630 (36.5) 1,098 (63.5)	580 (36.0) 1,033 (64.0)	50 (43.5) 65 (56.5)	
Calcification, *n* (%)				<0.001
No Micro Macro Both	883 (51.1) 731 (42.3) 99 (5.7) 15 (0.9)	849 (52.6) 658 (40.8) 93 (5.8) 13 (0.8)	34 (29.6) 73 (63.5) 6 (5.2) 2 (1.7)	
CDFI, *n* (%)				0.022
No Rare Abundant	850 (49.2) 573 (33.2) 305 (17.7)	807 (50.0) 523 (32.4) 283 (17.5)	43 (37.4) 50 (43.5) 22 (19.1)	
Multifocality, *n* (%)				0.011
No Yes	1,128 (65.3) 600 (34.7)	1,066 (66.1) 547 (33.9)	62 (53.9) 53 (46.1)	
Bilateral, *n* (%)				0.010
No Yes	1,280 (74.1) 448 (25.9)	1,207 (74.8) 406 (25.2)	73 (63.5) 42 (36.5)	
HT, *n* (%)				0.239
No Yes	1,169 (67.7) 559 (32.3)	1,085 (67.3) 528 (32.7)	84 (73.0) 31 (27.0)	

LR, low risk; MHR, medium-high risk; LTD, largest tumor diameter; HT, Hashimoto's thyroiditis.

4 Discussion

To our knowledge, this is the first study to identify factors predicting HR in "LR" PTMC patients based on preoperative examination. In our "LR" PTMC cohort, 170 of the 2,473 (6.9%) patients were reclassified into the HR group after surgery based on the results of the pathologic examination. Overall, 170 PTMCs were categorized into the HR group based on the presence of the following: more than five micro-lymph node metastases (95 cases), soft tissue invasion (64 cases), vascular invasion (2 cases),

10.3389/fendo.2023.1185327

TABLE 2 Multivariable logistic regression analysis for predictive factors of the medium- to high-risk group in the derivation cohort.

	Odds ratio [95% CI]	p-value
Gender: Male	3.91 [2.58, 5.92]	<0.001
Age	0.94 [0.92, 0.96]	<0.001
LTD	26.7 [10.57, 69.22]	<0.001
Bilateral: Yes	1.44 [1.01, 2.30]	0.03
Multifocal: Yes	1.14 [1.01, 2.26]	0.04

LTD, largest tumor diameter.

RLN invasion (2 cases), aggressive variant (1 case), and two more risk factors (6 cases). Multivariant regression analysis found male sex, younger age, larger tumor size, bilaterality, and multifocality to be independent predictors for the HR group. Moreover, the nomogram model was constructed and validated using the training and validation sets.

Gross ETE, or macroscopic ETE, was a risk factor for recurrence and disease-specific mortality (12). Thus, PTMCs with gross ETE should be excluded from the AS cohort at the time of patient selection, rendering the imaging of PTMC, especially US, extremely important for the diagnosis of gross ETE. As shown in Figure 1, 32 cases of gross ETE to strap muscle were all diagnosed correctly, and 23 cases (23/25, 92%) of gross ETE to RLN were confirmed before surgery. Strap muscle invasion is much easier to diagnose because of the obviously different echogenicity between thyroid cancer and muscle (13). There are few reports of RLN invasion by PTMC because of the low incidence. In Ito's study, only 9 of 1,143 PTMC patients were diagnosed with RLN invasion (14). As all tumor diameters with RLN invasion were 7 mm or larger, it can be concluded that tumors of <7 mm are not likely to invade the RLN (14). According to data from Memorial Sloan Kettering Cancer Center, gross invasion of the RLN was not observed for tumors of <9 mm in diameter, regardless of tumor location (15). In our study, only 25 of 2,809 patients were diagnosed with RLN invasion, an incidence similar to that reported by Ito et al. However, the tumor diameters of two patients with RLN invasion were lower than 7 mm (5 mm and 6 mm), and two cases with RLN invasion were not differentiated correctly because the coarse calcification of the tumor hindered boundary evaluation. Microscopic invasion of the soft tissue of the tumor was also considered a risk factor for recurrence, although reports of PTMC with microscopic invasion to soft tissue are rare (16). Whether minimal invasion into the soft tissue plays an important role in the prognosis of PTMC is still unknown. In 2019, in a BRAFV600E-mutated multifocal PTMC cohort, we had found that the recurrence rate of ETE to soft tissue was 6.6% while that of intrathyroidal PTMC was 3.8% (11). These patients were probably not differentiated before surgery due to the greater difficulty in diagnosing microscopic invasion to soft tissue using US. Moon et al. established a sonographic T staging method to predict the ETE degree of PTMC and found that it had high sensitivity and specificity (17); however, this method was not validated in other studies.

Although preoperative diagnosis is very difficult for high-volume central lymph node metastasis (CLNM) in cN0 PTMC, the incidence is low, ranging from 3.8% to 9.5% (18–20). In our "LR" PTMC patients, 3.8% (95/2,473) of the patients were diagnosed as high-volume CLNM. Moreover, studies have shown that younger age, male sex, tumor size > 5 mm, ETE, multifocality, microcalcification, capsular invasion, and abundant blood flow are independent clinicopathological risk factors for high-volume CLNM in cN0 PTMC patients (21–23), which in agreement with our results. Furthermore, the incidence of aggressive variants is low. According to the American National Cancer Database from 2004 to 2015, among 83,198 cases of PTMC, the classic variant accounted for 98.6%, the tall-cell variant (TCV) accounted for 1.1%, and diffuse sclerosis accounted for 0.3% of all PTMC cases (24). In another study of 745 cases of PTMC, only 1 (0.13%) patient was diagnosed with the hobnail variant (25). Although the aggressive

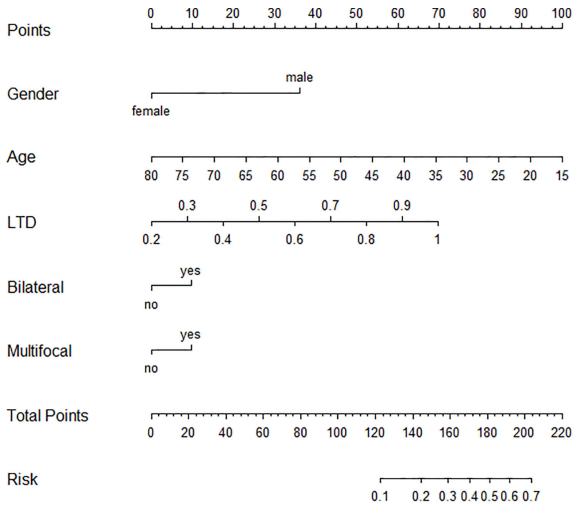

FIGURE 2
Graphic nomogram based on a multivariable logistic regression model for prediction of HR patients among AS candidates. HR, high risk; AS, active surveillance.

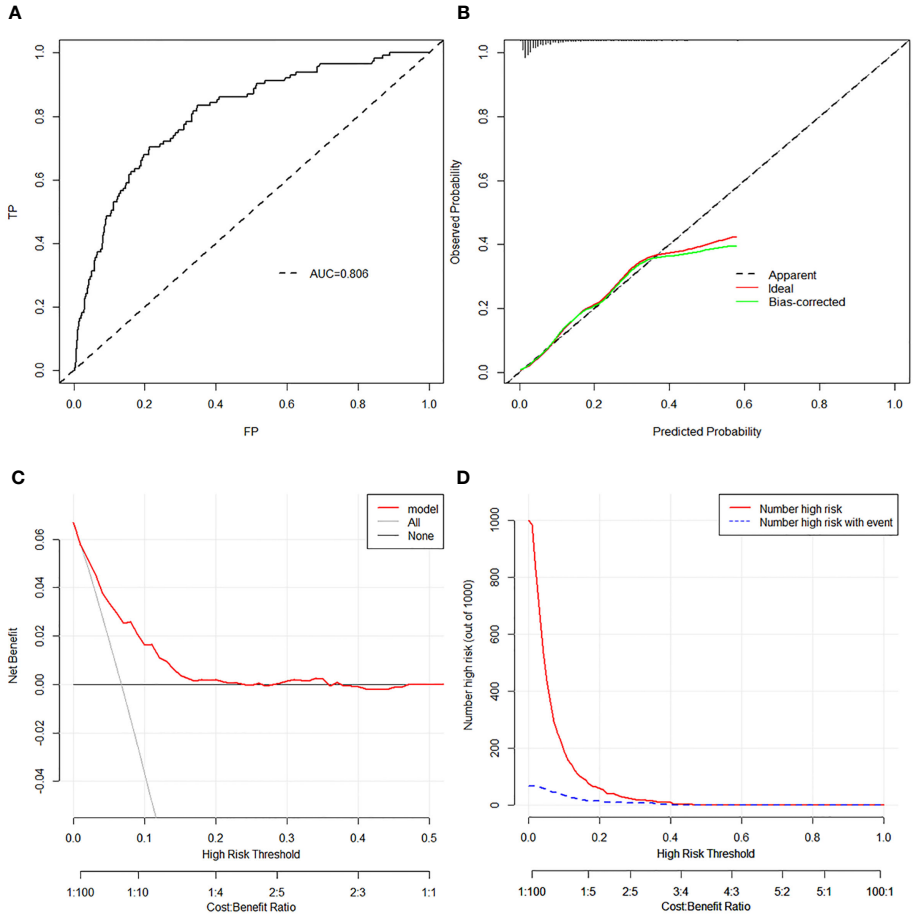

FIGURE 3
(A) The ROC analysis with AUC for training set. **(B)** Discrimination plot for training set. **(C)** DCA revealed that preoperative "LR" PTMC patients would benefit more if this model was used to predict the risk of HR when the threshold probability is between >1% and <20% in the training set. **(D)** The clinical impact curve of the training set revealed that the patients categorized as HR by the nomogram were more likely to be truly HR when the threshold probability < 40%. ROC, receiver operating characteristic curve; AUC, area under curve; DCA, decision curve analysis; LR, low risk; PTMC, papillary thyroid microcarcinoma; HR, high risk.

variant is associated with pathologic features exhibiting greater invasion, there were no differences in overall survival of patients with this variant compared with that of patients with classical PTMC after treatment (25–27). Additionally, studies have shown some US features in TCV-PTMC, for example, a hypoechoic halo around nodules and hypoechoic nodules with a localized central isoechoic lesion were much more common in TCV-PTMC (28). Moreover, TCV-PTMC showed nodules with a more regular margin and less microcalcification than classical PTMC (29). In our study, only one patient was diagnosed with the TCV after surgery. Vascular invasion of the tumor is typically associated with a poor prognosis. However, studies on vascular invasion of PTMC are scarce, and only two patients showed vascular invasion in this study, indicating that the incidence of vascular invasion in PTMC is probably low.

When PTMC patients choose between AS and surgery, they would like to know the possibility of HR after surgery. Without reliable molecular markers and an accurate imaging method, a small group of HR PTMC patients will be misdiagnosed as "LR", which will be harmful for the patients. To avoid this, we identified preoperative factors, such as younger age, male sex, larger tumors, bilaterality, and multifocality, to establish a nomogram for predicting the possibility of HR in our study. Younger age has been proven to be an important factor for disease progression during AS (30). Mounting evidence also confirmed that younger age, male sex, larger tumors, bilaterality, and multifocality were related to a greater degree of CLNM and a higher recurrence rate (18, 19, 21). Studies have provided strong evidence that bilateral multifocality, rather than unilateral multifocality, should be considered an aggressive marker of PTMC (31, 32). In another study, when unilateral multifocality and bilaterality coexisted in PTMC, patients had the highest risk of CLNM and possibly of local recurrence compared with those with either risk factor alone (31). Based on these factors, we could differentiate some HR PTMC patients from "LR" patients and recommend surgery as soon as possible.

There are several limitations in our study. First, this is a retrospective single-center study, which could have probably given rise to selection biases despite the large sample size. Furthermore, molecular markers, such as BRAF and TERT, were

not considered in our study, which might affect the risk category. Finally, only the internal validation method was used for developing the nomogram in this study. Therefore, prospective multi-center studies, especially considering molecular markers, should be conducted to obtain more objective conclusions.

In summary, the predictors of the HR subgroup in the AS candidates of PTMC patients were male sex, younger age, larger tumor size, bilaterality, and multifocality. Based on preoperative clinical and US factors, we developed and validated a nomogram model to predict HR of PTMC, which could be useful for patient counseling and facilitating treatment-related decision-making.

Data availability statement

The raw data supporting the conclusions of this article will be made available by the authors, without undue reservation.

Ethics statement

The studies involving human participants were reviewed and approved by the ethics committee of the First Hospital of Jilin University. Written informed consent to participate in this study was provided by the participants' legal guardian/next of kin.

Author contributions

All authors listed have made a substantial, direct, and intellectual contribution to the work, and approved it for publication.

Funding

This research was supported by the Natural Science Funding of Jilin Province (YDZJ202201ZYTS109 and YDZJ202301ZYTS458) and the Interdiscipline Subject Foundation of the First Hospital of Jilin University (04033990001).

Conflict of interest

The authors declare that the research was conducted in the absence of any commercial or financial relationships that could be construed as a potential conflict of interest.

Publisher's note

All claims expressed in this article are solely those of the authors and do not necessarily represent those of their affiliated organizations, or those of the publisher, the editors and the reviewers. Any product that may be evaluated in this article, or claim that may be made by its manufacturer, is not guaranteed or endorsed by the publisher.

Supplementary material

The Supplementary Material for this article can be found online at: https://www.frontiersin.org/articles/10.3389/fendo.2023.1185327/full#supplementary-material

References

1. La Vecchia C, Malvezzi M, Bosetti C, Garavello W, Bertuccio P, Levi F, et al. Thyroid cancer mortality and incidence: a global overview. *Int J Cancer* (2015) 136 (9):2187–95. doi: 10.1002/ijc.29251

2. Megwalu UC, Moon PK. Thyroid cancer incidence and mortality trends in the United States: 20 00-2018. *Thyroid* (2022) 32(5):560–70. doi: 10.1089/thy.2021.0662

3. Ahn HS, Kim HJ, Welch HG. Korea's thyroid-cancer "epidemic"–screening and overdiagnosis. *N Engl J Med* (2014) 371(19):1765–7. doi: 10.1056/NEJMp1409841

4. Haugen BR, Alexander EK, Bible KC, Doherty GM, Mandel SJ, Nikiforov YE, et al. American thyroid association management guidelines for adult pati ents with thyroid nodules and differentiated thyroid cancer: the ameri can thyroid association guidelines task force on thyroid nodules and d ifferentiated thyroid cancer. *Thyroid* (2016) 26(1):1–133. doi: 10.1089/thy.2015.0020

5. Ito Y, Miyauchi A. Active surveillance as first-line management of papillary microcarcino ma. *Annu Rev Med* (2019) 70:369–79. doi: 10.1146/annurev-med-051517-125510

6. Miyauchi A, Ito Y, Oda H. Insights into the Management of Papillary Microcarcinoma of the Thyroi d. *Thyroid* (2018) 28(1):23–31. doi: 10.1089/thy.2017.0227

7. Ito Y, Miyauchi A, Kudo T, Oda H, Yamamoto M, Sasai H, et al. Trends in the implementation of active surveillance for low-risk papillary thyroid microcarcinomas at kuma hospital: gradual increase and heterogeneity in the acceptance of this new management option. *Thyroid* (2018) 28(4):488–95. doi: 10.1089/thy.2017.0448

8. Sugitani I, Ito Y, Takeuchi D, Nakayama H, Masaki C, Shindo H, et al. Indications and strategy for active surveillance of adult low-risk papillary thyroid microcarcinoma: consensus statements from the japan association of endocrine surgery task force on management for papillaryt hyroid microcarcinoma. *Thyroid* (2021) 31(2):183–92. doi: 10.1089/thy.2020.0330

9. Ito Y, Miyauchi A, Oda H. Low-risk papillary microcarcinoma of the thyroid: A review of active surveillance trials. *Eur J Surg Oncol* (2018) 44(3):307–15. doi: 10.1016/j.ejso.2017.03.004

10. Xue S, Wang P, Hurst ZA, Chang YS, Chen G. Active surveillance for papillary thyroid microcarcinoma: challenges a nd prospects. *Front Endocrinol (Lausanne)* (2018) 9:736. doi: 10.3389/fendo.2018.00736

11. Xue S, Zhang L, Wang P, Liu J, Yin Y, Jin M, et al. Predictive factors of recurrence for multifocal papillary thyroid microcarcinoma with $braf^{v600e}$ mutation: a single center study of 1,207 chinese patients. *Front Endocrinol (Lausanne)* (2019) 10:407. doi: 10.3389/fendo.2019.00407

12. Jin BJ, Kim MK, Ji YB, Song CM, Park JH, Tae K. Characteristics and significance of minimal and maximal extrathyroidal extension in papillary thyroid carcinoma. *Oral Oncol* (2015) 51(8):759–63. doi: 10.1016/j.oraloncology.2015.05.010

13. Zhang L, Liu J, Wang P, Xue S, Li J, Chen G. Impact of gross strap muscle invasion on outcome of differentiated thyroid cancer: systematic review and meta-analysis. *Front Oncol* (2020) 10:1687. doi: 10.3389/fonc.2020.01687

14. Ito Y, Miyauchi A, Oda H, Kobayashi K, Kihara M, Miya A. Revisiting low-risk thyroid papillary microcarcinomas resected without observation: was immediate surgery necessary? *World J Surgery* (2016) 40(3):523–8. doi: 10.1007/s00268-015-3184-4

15. Newman SK, Harries V, Wang L, McGill M, Ganly I, Girshman J, et al. Invasion of a recurrent laryngeal nerve from small well-differentiated papillary thyroid cancers: patient selection implications for active surveillance. *Thyroid* (2022) 32(2):164–9. doi: 10.1089/thy.2021.0310

16. Lin J-D, Hsueh C, Chao T-C. Soft tissue invasion of papillary thyroid carcinoma. *Clin Exp Metastasis* (2016) 33(6):601–8. doi: 10.1007/s10585-016-9800-3

17. Moon SJ, Kim DW, Kim SJ, Ha TK, Park HK, Jung SJ. Ultrasound assessment of degrees of extrathyroidal extension in papill ary thyroid microcarcinoma. *Endocr Pract* (2014) 20(10):1037–43. doi: 10.4158/EP14016.OR

18. Wang Z, Gui Z, Wang Z, Huang J, He L, Dong W, et al. Clinical and ultrasonic risk factors for high-volume central lymph node metastasis in cN0 papillary thyroid microcarcinoma: A retrospective study and meta-analysis. *Clin Endocrinol* (2022) 98 (4):609–621. doi: 10.1111/cen.14834

19. Liu C, Liu Y, Zhang L, Dong Y, Hu S, Xia Y, et al. Risk factors for high-volume lymph node metastases in cN0 papillary thyroid microcarcinoma. *Gland Surgery* (2019) 8(5):550–6. doi: 10.21037/gs.2019.10.04

20. Wei X, Min Y, Feng Y, He D, Zeng X, Huang Y, et al. Development and validation of an individualized nomogram for predicting the high-volume (> 5) central lymph node metastasis in papillary thyroid microcarcinoma. *J Endocrinol Invest* (2022) 45(3):507–15. doi: 10.1007/s40618-021-01675-5

21. Zhang L, Yang J, Sun Q, Liu Y, Liang F, Liu Z, et al. Risk factors for lymph node metastasis in papillary thyroid microcarcinoma: Older patients with fewer lymph node metastases. *Eur J Surg Oncol* (2016) 42(10):1478–82. doi: 10.1016/j.ejso.2016.07.002

22. Huang X-P, Ye T-T, Zhang L, Liu R-F, Lai X-J, Wang L, et al. Sonographic features of papillary thyroid microcarcinoma predicting high-volume central neck lymph node metastasis. *Surg Oncol* (2018) 27(2):172–6. doi: 10.1016/j.suronc.2018.03.004

23. Liu C, Zhang L, Liu Y, Xia Y, Cao Y, Liu Z, et al. Ultrasonography for the prediction of high-volume lymph node metastases in papillary thyroid carcinoma: should surgeons believe ultrasound results? *World J Surgery* (2020) 44(12):4142–8. doi: 10.1007/s00268-020-05755-0

24. Holoubek SA, Yan H, Khokar AH, Kuchta KM, Winchester DJ, Prinz RA, et al. Aggressive variants of papillary thyroid microcarcinoma are associated with high-risk features, but not decreased survival. *Surgery* (2020) 167(1):19–27. doi: 10.1016/j.surg.2019.03.030

25. Gubbiotti MA, Livolsi V, Montone K, Baloch Z. Papillary thyroid microcarcinomas: does subtyping predict aggressive clinical behavior? *Hum Pathol* (2021) 114:28–35. doi: 10.1016/j.humpath.2021.04.015

26. Kuo EJ, Goffredo P, Sosa JA, ROman SA. Aggressive variants of papillary thyroid microcarcinoma are associated with extrathyroidal spread and lymph-node metastases: a population-level analysis. *Thyroid* (2013) 23(10):1305–11. doi: 10.1089/thy.2012.0563

27. Bernstein J, Virk RK, Hui P, Prasad A, Westra WH, Tallini G, et al. Tall cell variant of papillary thyroid microcarcinoma: clinicopathologic features with BRAF (V600E) mutational analysis. *Thyroid* (2013) 23(12):1525–31. doi: 10.1089/thy.2013.0154

28. Zhang Y, Mei F, He X, Ma J, Wang S. Reconceptualize tall-cell variant papillary thyroid microcarcinoma: From a "sonographic histology" perspective. *Front Endocrinol (Lausanne)* (2022) 13:1001477. doi: 10.3389/fendo.2022.1001477

29. Oh WJ, Lee YS, Cho U, Bae JS, Lee S, Kim MH, et al. Classic papillary thyroid carcinoma with tall cell features and tall cell variant have similar clinicopathologic features. *Korean J Pathol* (2014) 48(3):201–8. doi: 10.4132/KoreanJPathol.2014.48.3.201

30. Koshkina A, Fazelzad R, Sugitani I, Miyauchi A, Thabane L, Goldstein DP, et al. Association of patient age with progression of low-risk papillary thyroid carcinoma under active surveillance: A systematic review and meta-analysis. *JAMA Otolaryngol Head Neck Surg* (2020) 146(6):552–60. doi: 10.1001/jamaoto.2020.0368

31. Cai J, Fang F, Chen J, Xiang D. Unilateral multifocality and bilaterality could be two different multifocal entities in patients with papillary thyroid microcarcinoma. *BioMed Res Int* (2020) 2020:1–7. doi: 10.1155/2020/9854964

32. Yan T, Qiu W, Song J, Ying T, Fan Y, Yang Z. Bilateral multifocality, a marker for aggressive disease, is not an independent prognostic factor for papillary thyroid microcarcinoma: A propensity score matching analysis. *Clin Endocrinol* (2021) 95 (1):209–16. doi: 10.1111/cen.14455

Frontiers in Endocrinology

Explores the endocrine system to find new therapies for key health issues

The second most-cited endocrinology and metabolism journal, which advances our understanding of the endocrine system. It uncovers new therapies for prevalent health issues such as obesity, diabetes, reproduction, and aging.

Discover the latest Research Topics

See more →

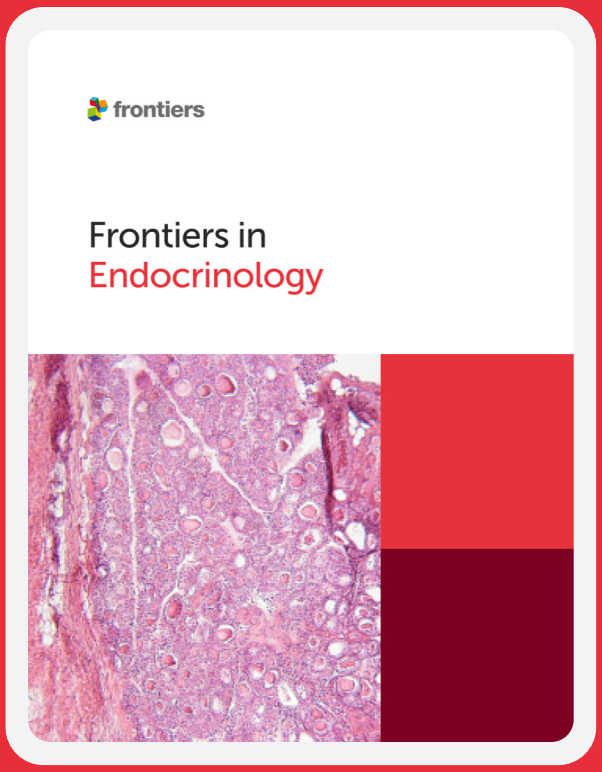

Frontiers

Avenue du Tribunal-Fédéral 34
1005 Lausanne, Switzerland
frontiersin.org

Contact us

+41 (0)21 510 17 00
frontiersin.org/about/contact